2012

Syntheses and characterization of water-soluble phythalocyanines for diagnosis and treatment of cancer

Benson Getenga Ongarora
Louisiana State University and Agricultural and Mechanical College

SYNTHESES AND CHARACTERIZATION OF WATER-SOLUBLE PHTHALOCYANINES FOR DIAGNOSIS AND TREATMENT OF CANCER

A Dissertation

Submitted to the Graduate Faculty of the
Louisiana State University and
Agricultural and Mechanical College
in partial fulfillment of the
requirement for the degree of
Doctor of Philosophy

in

The Department of Chemistry

by
Benson Getenga Ongarora
B.Sc., Moi University, 2005
December 2012

Dedicated to my dear wife (Nancy Kemunto), my son (Braden Getenga) and my parents (Margaret Bitutu and Peter Ongarora). This is a sign of my gratitude since I can never thank you as much as necessary for your love, guidance, encouragement and constant prayers.

ACKNOWLEDGEMENTS

I earnestly thank my advisor, Prof. M. Graça H. Vicente, for endlessly mentoring, inspiring, supporting and encouraging me since I joined the group four years ago. I appreciate your caring, considerate and optimistic approach to issues that gave me an opportunity to tap the best concepts from you. Our countless discussions helped me appreciate the importance of the project and thus its direction.

I would like to thank Prof. Steve Soper, Prof. Carol M. Taylor, Prof. George G. Stanley and Prof. Jin-Woo Choi for being my advisory committee members. Thank you all for your time, constant guidance and encouragement throughout the research period. Thanks for the patience as you read my thesis.

Appreciation also goes to my lab mates: Haijun Wang and Elizabeth A. Okoth. Thanks a lot to Daniel and Igor, who helped me with the purification work as undergraduate research students. Thank you for your relentless efforts to make this work a success. I thank the past and the current group members of Prof. Vicente and Prof. Kevin Smith: Hairong Li, Moses Ihachi, Haijun Li, Raja Waruna, Timsy Uppal, Alecia McCall, Krystal Fontenot, Hillay Tanui, Edith Amuhaya, Dinesh Bhupathiraju, and all for the team-work during my research.

I thank Dr. Frank R. Fronczek for the great job done on crystal structure resolution of the compounds synthesized during my research work. I am also thankful to Dr. Dale Treleaven and Dr. Thomas Weldegheorghis for lending a hand in NMR studies of the samples synthesized during this course. Your efforts made it possible to publish this piece of work in recognizable journals such as *MedChemComm.*, *J. Med. Chem.* and *Theranostics* among others.

I am especially indebted to Dr. Robert Cook for allowing me to use the instruments in his laboratory for photophysical studies. Special thanks to Prof. Carol Taylor for laboratory

equipment and space. Similarly, appreciation goes to Dr. Inder Sehgal, Dr. Krystal Fontenot, Dr. Xiaoke and Zehua Zhou for helping me with biological studies. Thanks too to Prof. Chang Kwang Poo and Sujoy Dutta for helping me with biological experiments.

I would like to thank all my friends at LSU, and elsewhere, for your support and encouragement. Your positive criticism in all aspects propelled me to greater heights every day. In the criticisms, I found energy to conquer most of the challenges that I encountered.

The financial support of this research by the National Institutes of Health (NIH) grant number R21 CA139385 is greatly acknowledged.

I would like to thank Dr. Samuel Lutta, Dr. Maurice Okoth, and Dr. Fredrick Segor, who some years back recommended me to seek admission at LSU. Their strong commendation is exceedingly valued. I also thank my brother, Vincent Ongarora, and my sister, Aska Ongarora, for their continued support throughout the course. Your unconditional love and care is incalculable.

I give my thanks to my wife, Nancy Kemunto and my son, Braden Getenga, for their resolute love. Thank you for your support and encouragement. Even when challenges seemed excruciating, your resilience kept me going. Without your shoulders, my effort could have been futile and this work may not have been accomplished.

Most importantly, I thank God for this generous opportunity to study at LSU. Everything was availed at the allotted time and the transition was smooth. The working environment was wonderful and I have enjoyed good health all through. Thanks be to God, the Almighty.

TABLE OF CONTENTS

LIST OF ABBREVIATIONS

σ	Chemical shift
λ_{ex}	Excitation wavelength
br	Broad
BBr_3	Boron tribromide
Boc	*tert*-Butyl carbamate
°C	Degrees Celsius
CEA	Carcinoembryonic antigen
$CHCl_3$	Chloroform
CH_3OH	Methanol
CLE	Confocal laser endomicroscopy
^{13}C NMR	Carbon 13 nuclear magnetic resonance
CRC	Colorectal cancer
d	Doublet
DBN	1,5-Diazobicyclo[4.3.0]non-ene
DCM	Dichloromethane
DIEA	N,N-Diisopropylethylamine
DIPA	*N,N*-diisopropylamine
DMAE	N,N-Dimethylaminoethanol
DMEM	Dulbecco's modified eagle's medium
DMSO	Dimethyl sulfoxide
DMF	Dimethylformamide
EDCI	1-Ethyl-3-(3-dimethylaminopropyl)-carbodiimide hydrochloride
EGFR	Epidermal growth factor receptor
ER	Endoplasmic reticulum

ESI	Electrospray ionization
FBS	Fetal bovine serum
FDA	United States Food and Drug Administration
FT-IR	Fourier transform infrared
h	Hours
HATU	2-(1H-Azabenzotriazol-1-yl)-1,1,3,3-tetramethyluronium hexafluorophosphate
HOBt	N-Hydroxybenzotriazole
H_2Pc	Metal-free phthalocyanine
HPLC	High Performance Liquid Chromatography
HRMS	High resolution mass spectrometry
Hz	Hertz
IC_{50}	Inhibitory concentration 50%
IR	Infrared
J/cm^2	Joule per square centimeters
MALDI	Matrix assisted laser desorption/ionization
MeI	Methyl iodide
MeOH	Methanol
MS	Mass spectrometry
m/z	Mass to charge ratio
nm	Nanometer
nM	Nanomolar
NMR	Nuclear Magnetic resonance
OH	Hydroxyl
ppm	Parts per million

PBS	Phosphate buffered saline
Pc	Phthalocyanine
PDB	Protein databank
PDT	Photodynamic therapy
PEG	Polyethylene glycol
PS	Photosensitizer
rt	Room temperature
RES	Reticulo-endothelial-system
ROS	Reactive oxygen species
s	Singlet
SPS	Solid-phase synthesis
t	Triplet
TBTU	2-(1H-Benzotriazol-1-yl)-1,1,3,3-tetramethyluronium tetrafluoroborate
TEA	Triethylamine
TFA	Trifluoroacetic acid
THF	Tetrahydrofuran
TIS	Triisopropylsilane
TLC	Thin layer chromatography
µL	Microliter
µM	Micromolar
UV-Vis	Ultraviolet visible
ZnPc	Zinc phthalocyanine

ABSTRACT

Chapter 1 describes the general properties of phthalocyanines, synthesis of metallo-phthalocyanines, their photophysical features and their uses. The concepts of PDT and targeted therapeutics are also introduced.

Chapter 2 describes the syntheses, characterization, photophysical studies and biological evaluation of cationic phthalocyanines. The trimethylaminophenoxy substituted phthalocyanines were synthesized through statistical condensation method, which gave a statistical mixture of isomers. Di-cationic phthalocyanines were found to be more cytotoxic. The amphiphilicity of the phthalocyanines played an important role.

Chapter 3 covers the conjugation of phthalocyanines to peptides and is in pursuit of targeted therapeutics. The conjugation of two peptides, EGFR L1 (six amino acid residues) and EGFR L2 (twelve amino acid residues), gave conjugates with different charge, length, and hydrophobicity. The bioconjugates were synthesized via SPS method using typical peptide coupling agents. Cellular and animal studies are described for the conjugates.

Chapter 4 is a description of the syntheses and characterization of pure regiomeric phthalocyanines. Previous chapters described, mostly, statistical mixture of Pcs. In this chapter, strategy to the synthesis of monomeric isomers and their characterization is presented.

Chapter 5 describes the syntheses, characterization and cellular studies of a series of di-cationic and pegylated phthalocyanines. Statistical condensation was used in the synthesis of macrocycles. Phthalocyanines with cationic charge at close proximity and on α-substitution position of the macrocycle were found to be more cytotoxic. In addition, Pc-antibody bioconjugates are discussed. The biological studies are described for both cationic Pcs and Pc-conjugates. Just like Chapter 3, this chapter is also in pursuit of targeted therapeutics.

CHAPTER 1

INTRODUCTION

1.1. Overview of Phthalocyanines

Phthalocyanines (Pcs), also known as azaporphyrin derivatives, are a class of synthetic tetrapyrrolic compounds which are closely related to the naturally occurring porphyrin.[1] The structural difference between the Pc and porphyrin macrocycles is that Pc has four extended benzo subunits and four nitrogen atoms at the *meso* position on the macrocycle; hence Pcs are often referred to as tetra-benzotetraazaporphyrins.[2] The Pcs are a unique set of organic pigments that provide stable and strongly chromatic blues and greens. Pcs have strong absorbance at longer wavelengths than porphyrins and often have improved photophysical and photochemical properties.[3] The first Pc was reported as a dark blue insoluble byproduct during the preparation of *o*-cyanobenzamide from phthalimide and acetic acid by Braun and Tcherniac in 1907.[4] Von der Weid and Diesbach of Fribourg University, twenty years later, isolated Pc as an unexpected stable blue material in reactions of *o*-dibromobenzene with copper cyanide in refluxing pyridine.[5]

Since their discovery and identification (1900s), Pcs have been extensively used as dyes and pigments in paint, printing, textile and paper industries, due to their intense blue-green color.[6] Owing to their increased stability, improved spectroscopic characteristics, diverse coordination properties, and architectural flexibility, Pcs have surpassed porphyrins in a number of applications.[7] Most recently, Pcs have found high-tech applications in electrophotography and ink-jet printing and as photoconducting agents in photocopying devices.[8] In addition, their novelty is rapidly growing in other fields where they are used as chemical sensors, liquid crystals, semiconductors, functional polymers and molecular metals, among others.[9] They have

also found use in photodynamic therapy (PDT). Most of the photosensitizers used in PDT are tetrapyrrolic in nature; chlorin, porphyrin and bacteriochlorin. These cyclic tetrapyrrolic derivatives have an inherent similarity to naturally occurring porphyrins present in living matter; this probably gives them little or no toxicity in the absence of light.[10,11]

1.2. Structure of Phthalocyanines

The structure, charge and hydrophobicity of a photosensitizer determines its interactions with its biological surroundings and in turn determines its cellular uptake, subcellular localization and cytotoxicity.[12] For instance, amphiphilic photosensitizers are often more photodynamically active than hydrophobic or hydrophilic molecules.[13] Amphiphilicity, the element of having both hydrophobic and hydrophilic characteristics in different segments within the same molecule, permits distinct portions to interact differently with their biological environment and tend to enhance solubility, improve cellular uptake and intracellular targeting, and modulate aggregation. Though, it should be noted that strong amphiphilic photochemical internalization (PCI)-photosensitizers, including porphyrin, chlorin and phthalocyanine derivatives are not substrates for breast cancer Resistance Protein (ABCG2) in multi-drug resistance chemotherapeutic agents.[14]

A number of functional groups have been added to Pc framework via the benzene rings to increase their utility. Functional groups such as alkyl chains, ethers, amines and thiols among others, have been introduced to enhance solubility.[15] Instituting quaternized and sulfonated groups as substituents promotes solubility in aqueous media[16,17] while organic functional groups such as thio and aryloxo promotes solubility in organic solvents.[18,19] The substitutions can be made directly onto the Pc framework (Method S) or on the phthalonitrile precursor before condensation to form the Pc ring.[20] The use of substituted precursors leads to cleaner reactions in

terms of degree of substitution; for example, a mono-substituted precursor leads to a tetrasubstituted Pc. Such substitutions can be carried out at any of the 16 available positions on the Pc framework (Figure 1.1). While the number and position of the substituents obtained by condensation is known, still constitutional isomers are obtained. Nevertheless, this method is preferred for adding substituents to the framework, giving Pcs with improved properties and desired chemical structures.[5] The positions 1,4,8,11,15,18,22,25 are referred to as non-peripheral or α- positions, while 2,3,9,10,16,17,23,24 are known as peripheral or *β*- positions.[21]

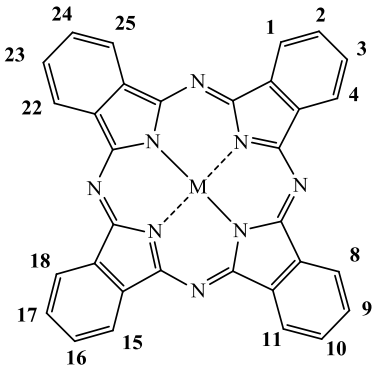

Figure 1.1: Potential sites for Pc substitution (numbering used traditionally for Pc nomenclature).[21]

1.3. Synthesis of Phthalocyanines

1.3.1. Synthesis via Tetramerization of a Single Precursor

A number of derivatives of *ortho*-substituted benzene can serve as precursors in the synthesis of Pc macrocycles (Figure 1.1). The precursors include phthalic anhydride, phthalic acid, phthalonitrile, phthalimide, diiminoisoindoline, *o*-cyanobenzamide, *o*-dibromobenzene and cyclohex-1-ene-1,2-dicarboxylic anhydride, among others. Phthalonitriles are popular for laboratory syntheses due to better yields, while phthalic anhydride is used in mass production, as it is relatively cheap.[22] Phthalonitriles mostly require heating with a metal template in a high boiling point solvent such as quinoline or N,N-dimethylaminoethanol (DMAE). The advantage

of phthalonitrile as a precursor is that it readily gives good yields of Pc complexes with most metals except mercury and silver, while other precursors such as phthalimide and other phthalic acid derivatives often give unreliable results.[23]

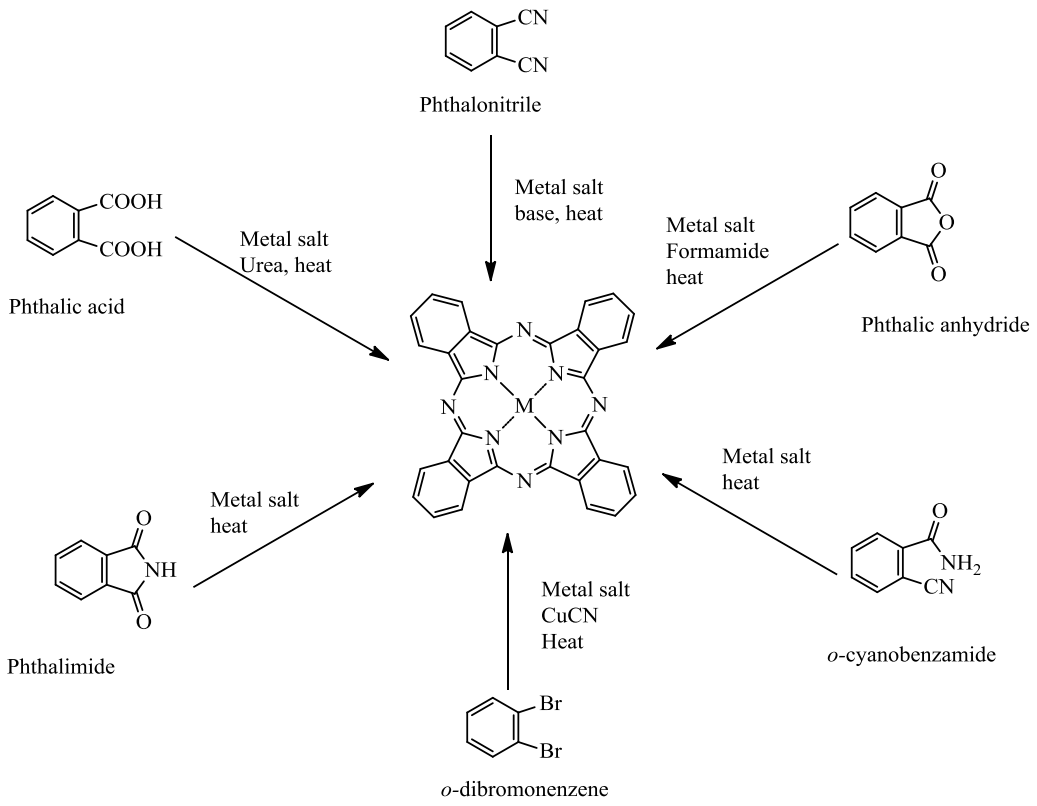

Scheme 1.1: Synthetic routes to metallophthalocyanines (MPcs) from various precursors.

Unsubstituted metal-free Pcs (H_2Pcs) can be prepared using the Linstead method[24] from phthalonitrile in refluxing lithium, sodium or magnesium alkoxide solution. The Pc can then be demetallated by adding a dilute acid to obtain H_2Pc. Tomoda method, a simple route to the synthesis of Pcs by heating phthalonitrile with catalytic amount of DBU or DBN, was reported in the 1980s.[25,26] This route may yield up to 70% metal-free and 80% metallated Pcs. Strong organic bases such as DBU and DBN (Figure 1.2) generally promote the formation of Pcs in higher yields, while weaker ones such as TEA and pyridine do not favor the formation of Pcs.

The use of these bases allows the reaction to proceed under milder conditions by promoting the formation of the alkoxide ion (Scheme 1.2).

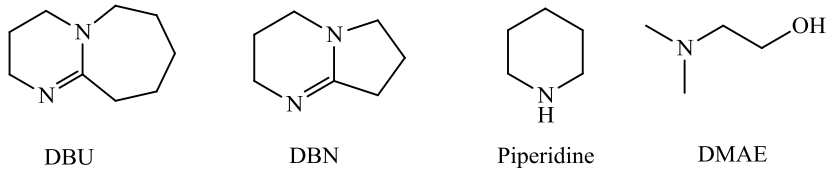

Figure 1.2: Structures of common organic bases used in Pc synthesis.

Tomoda *et al.* proposed that the strong base is a proton acceptor, therefore, generating an alkoxide in the process (Scheme 1.2).[25] The resulting alkoxide then acts both as the nucleophile and reducing agent as shown in Scheme 1.3.[27] The alkoxide reacts with cyano group of a phthalonitrile, forming an alkoxyisoindoline intermediate, which rapidly tetracyclizes to form a Pc.

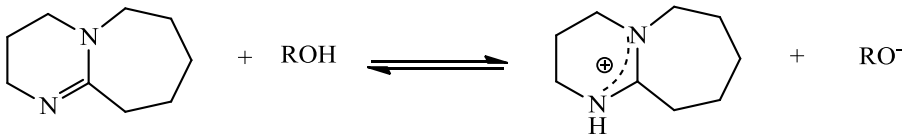

Scheme 1.2: Formation of alkoxide anion (RO^-) in preparation of Pcs.[25]

The mechanism for the condensation of phthalonitriles to form Pcs (Scheme 1.3) probably involves a stepwise polymerization of the precursors or reactive intermediates, followed by coordination of the central metal ion (in case of MPcs) and finally ring closure to form the macrocycle.[28,29] The ring closure is driven by aromatization, thermodynamic stability and inherent stabilization caused by metal coordination.

Metallated Pcs may also be prepared from metal-free Pcs through the addition of a metal salt into a reaction. The only limitation of this method is that large metals cannot be added into the cavity.[30] Therefore, the metal salt must be added into a refluxing solution of the Pc or Pc precursor (phthalonitrile) for successful insertion of the metal ion. The industrial manufacture of

Pc colorants is based on the methodology developed by Max Wyler at the ICI research center at Blackley, Manchester.[21] The method involves heating inexpensive phthalic anhydride in the presence of a nitrogen source, such as urea and a catalyst such, as ammonium molybdate to obtain a Pc macrocycle.

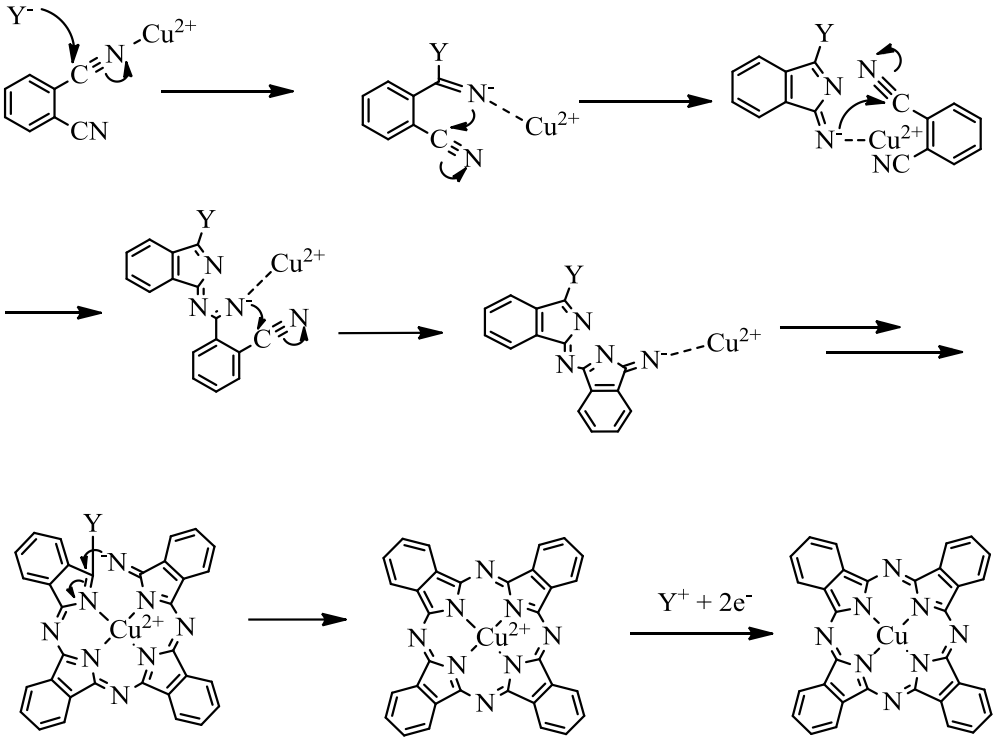

Scheme 1.3: Mechanism of formation of metallo-Pc initiated by alkoxide anion (Y^-).[27]

During cyclotetramerization of a 3-substituted phthalonitrile, a mixture of four isomers of C_{4h}, C_{2v}, C_s and D_{2h} symmetry is obtained (Figure 1.3).[21] In this case, due to the close proximity of the substituent to the core Pc ring, steric bulkiness of the substituents may be exploited to direct the regioselectivity of the products formed. For example, Pcs with C_{4h} symmetry can be selectively[31] or exclusively[32,33] synthesized. The enrichment of the C_{4h} isomer reduces the D_{2h} isomer.[31] Electronic effects may also play a role in the formation of C_{4h} isomer as the sterically undemanding 3-methoxyphthalonitrile forms this isomer exclusively at room temperature.[34] The

methoxy group (strong electron donor) may deactivate the '*ortho*' nitrile towards nucleophilic attack, leading to '*meta*' nitrile selectivity.

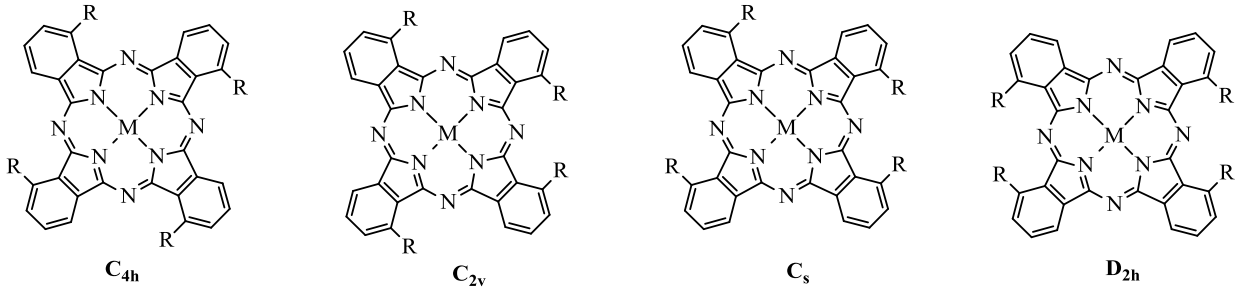

Figure 1.3: Structures and symmetries of different Pc constitutional isomers resulting from 3-substituted phthalonitriles.[35]

Similarly, statistical condensation of a 4-substituted phthalonitrile can lead to four constitutional isomers: C_{4h}, C_{2v}, C_s and D_{2h} (Figure 1.4). Modification of the properties of substituents on the phthalonitrile and optimization of the reaction conditions can improve the formation of one or two of the major isomers. Unlike the 3-substituted phthalonitriles, there is no steric influence over the tetramerization reactions. Nonetheless, one case has been reported in which mild conditions gave a non-statistical mixture of Pc at room temperature;[36] the electronic effect of the electron-rich alkoxy substituent may reduce the reactivity of the '*para*' nitrile and not the '*meta*' nitrile, so that nucleophilic attack takes place regioselectively. The major challenge in this case is the tedious chromatographic procedures.[37-41]

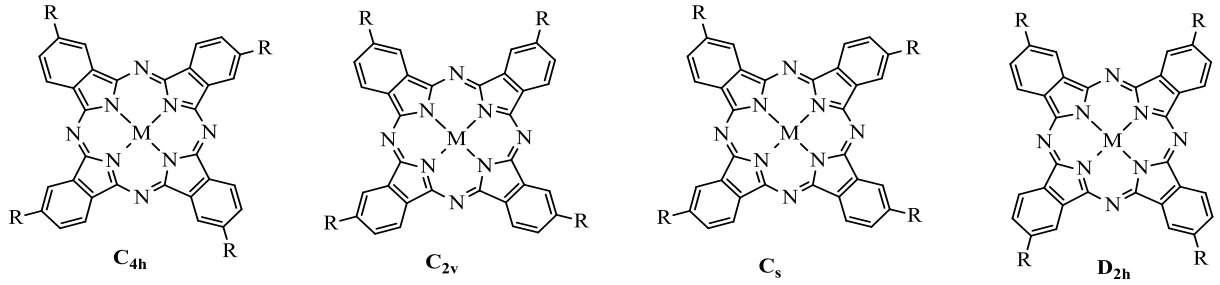

Figure 1.4: Structures and symmetries of different Pc constitutional isomers from 4-substituted phthalonitriles.[35]

Bridged-Pcs or side-strapped Pcs, which may be obtained via bis-phthalonitriles, have been synthesized previously. Suitable bis(3-phthalonitriles) are prepared from 2,2-dialkyl propane-1,3-diols or chiral bis-naphthols, although many other bis(3-phthalonitriles) do not form side-strapped Pcs.[42] The synthesis of these Pcs require highly dilute conditions for the cyclotetramerization of bis(3-phthalonitriles) or bis(4-phthalonitriles). This route results in D_{2h} symmetry Pcs.[42-44] A chiral side-strapped Pc with D_{2h} symmetry has also been synthesized from bis(4-phthalonitrile) containing flexible linker (Scheme 1.4).[45] A recent example is the synthesis of 1,2-bis(3,4-dicyanophenoxymethyl)benzene from 1,2-bis(hydroxymethyl)benzene and 4-nitrophthalonitrile.[46]

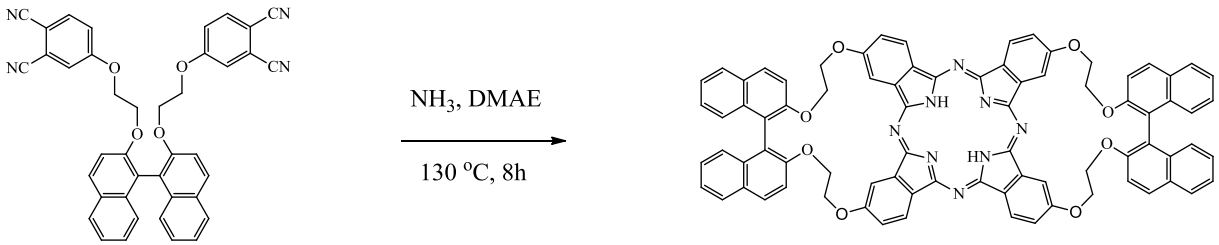

Scheme 1.4: Chiral side-strapped Pc with D_{2h} symmetry containing flexible linker.[45]

Non-peripherally substituted Pcs (with substituents on 1,4,8,11,15,18,22,25 positions) and peripheral Pcs (with substituents on 2,3,9,10,16,17,23,24 positions) have also been synthesized from appropriate single precursors. Octa-substituted non-peripheral Pcs are attractive because the substituents on the ring make them more soluble in organic solvents and the Pcs are obtained as single isomers.[47,48] In addition, alkoxy groups at non-peripheral positions cause a large bathochromic shift of the Q-band into the IR region (above 750 nm).[49,50] The octa-substituted peripheral Pcs can be obtained by reacting 4,5-di-substituted phthalonitriles. If the two substituents are identical, then regiomerically pure Pcs are produced. Pre-formed Pc reactions may also be used to obtain the desired products. For example, aromatic methyl ether

cleavage can give octahydroxy-substituted Pcs.[51,52] The free hydroxyl groups on Pcs can then undergo alkylation[51] or silylation[52]. Other Pcs in which substituents form a bridge between 2:3, 9:10, 16:17, and 23:24 positions have been reported (Figure 1.5).[45] Such Pcs form cyclic or macrocyclic units, with macrocyclic ones acting as ligands for metal cations and may form multiple metal ion arrays.[53] Hexadeca-substituted Pcs (with substituents both at peripheral and non-peripheral positions) have also been synthesized.[48] Others have been synthesized by means of introducing further functionality by reaction of substituents.[54]

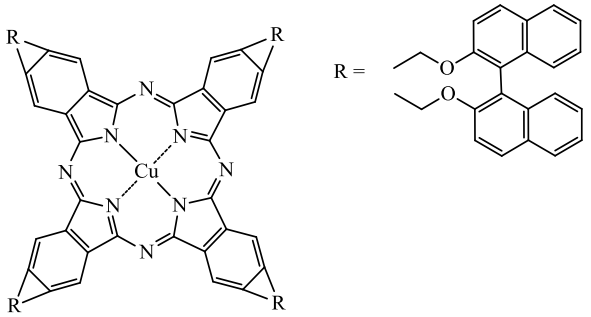

Figure 1.5: Pc with substituents forming a bridge between 2:3, 9:10, 16:17, and 23:24 positions.[45]

1.3.2. Synthesis via Tetramerization of Two or More Precursors

The unsubstituted and many of the substituted Pcs reported in literature are symmetrical compounds. However, the inherent symmetry is a limitation for many purposes.[37] The aim of the synthesis of Pcs with different substituents is to introduce different functional groups, which will provide coexistent features such as improved solubility and reactivity at the same time.[29,55-57] Many of the Pcs resulting from two or more different phthalonitriles is a statistical mixture of Pcs. However, if the precursors are symmetrical, then product ratios may change significantly.

Various protocols for the tetramerization of two or more phthalonitriles have been reported in the past. Kobayashi and coworkers, in the late 1980s, developed a method to synthesize A_3B-type Pcs, through ring expansion of a subphthalocyanine in the presence of

succinamide or diiminoisoindoline derivatives (Scheme 1.5).[35] The ring expansion depends highly on the reactants' properties and reaction conditions. The best yield could be achieved when a metal template is used and by selectively choosing the substituents on the precursors. For example, subphthalocyanines without substituents or with electron-withdrawing groups, and diiminoisoindoline derivatives with electron donating groups resulted in better yields.[6,58] The only disadvantage of this approach, in many cases, is the fragmentation of the subphthalocyanine ring followed by statistical ring closure to form a mixture of all possible Pcs.[59,60]

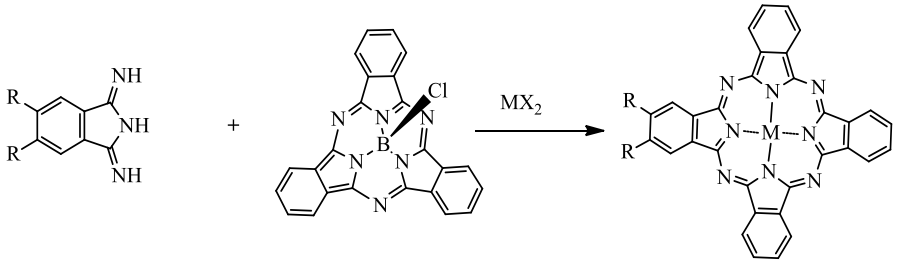

Scheme 1.5: Selective synthesis of A_3B-type Pc.[60]

Polymeric support in the synthesis of A_3B-type Pcs (Scheme 1.6) was developed by Leznoff and coworkers in 1982, where a mono-functionalized diiminoisoindoline precursor (B) bound to solid polymer (P) reacts with another precursor (A).[61-63] The soluble A_4-type Pc and unreacted precursor-A are washed off and the desired Pc is cleaved under mild conditions. However, this is limited to easy on-off properties of the precursor bound to the solid support.

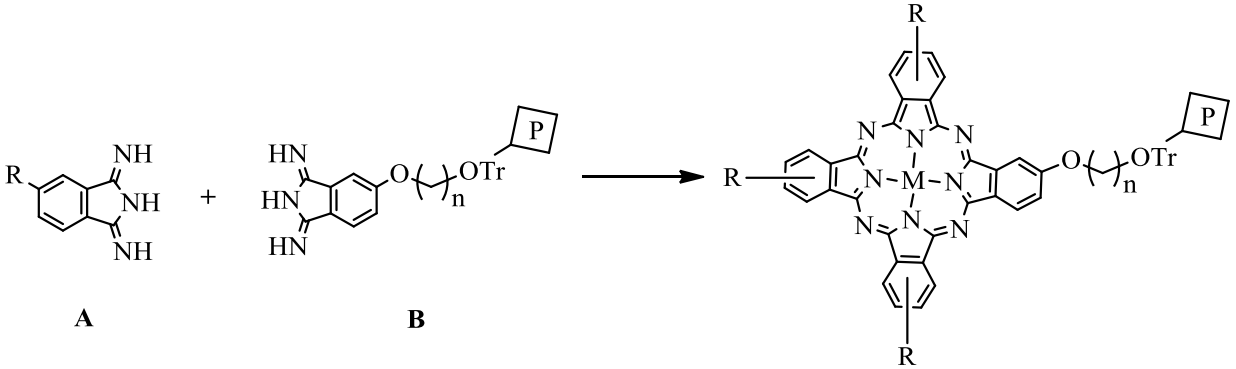

Scheme 1.6: Synthesis of A_3B-type Pc on polymer support.[61]

Substituted Pcs (both symmetrical and unsymmetrical) resulting from two or more phthalonitriles can also be synthesized by statistical condensation of appropriate precursors, followed by chromatographic separation of the desired products. This may be achieved via Tomoda synthesis, just as those obtained from single phthalonitriles. This method, by optimization of reactant ratios and reaction conditions, may yield the desired compound in reasonable amounts, but still gives six (Figure 1.6) differently substituted Pcs, not including constitutional isomers.[35] Modification of the properties of substituents on the phthalonitriles and optimization of the reaction conditions can improve the formation of one or two of the major isomers. The use of one of the phthalonitriles in excess is one such modification that may favor the formation A_3B Pcs. In other cases, half Pcs have been used in the preparation of A_2B_2 Pcs.[64] Nevertheless, separation of constitutional isomers is often difficult, and involves tedious chromatographic procedures.[38-41]

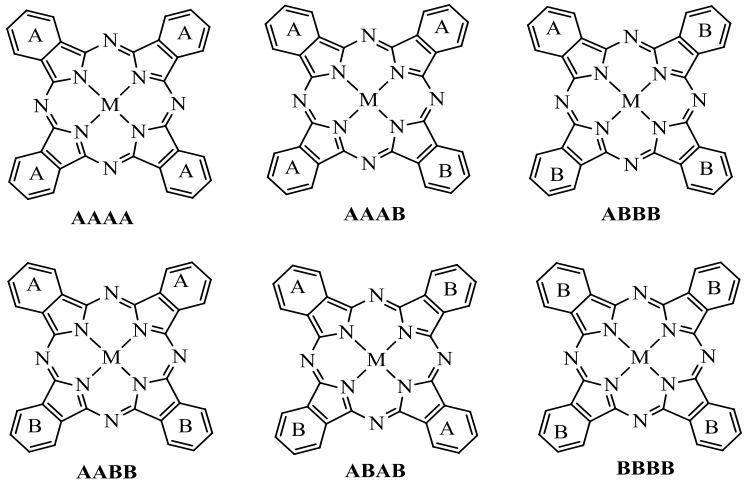

Figure 1.6: Six differently substituted Pcs formed during mixed condensation of two differently substituted precursors, A and B.[35]

1.4. Photophysical Properties of Phthalocyanines

Photophysical processes are changes in the electronic states of a molecule and can affect its chemical nature. The energy transfer process, which occurs when light of a specific

wavelength is absorbed, may result in a variety of physical changes, but the chemical integrity of the molecule is retained. The absorbed light excites an electron from a lower (stable state) to a higher molecular quantum state (unstable with respect to the ground). The simplified Jablonski diagram (Figure 1.7) represents pathways of losing the energy to return to the ground state.[65-67]

Absorption occurs from singlet ground state, S_0, to a vibrationally excited level of first singlet excited state, S_1, or sometimes to a second electronically excited state, S_2. Through collisions with solvent molecules, vibrational relaxation occurs and the S_2-excited molecules return to the first vibration level of S_1, from which there are several possibilities: fluorescence, phosphorescence or heat generation. Fluorescence is a radiative process, which occurs when S_1-excited molecules lose energy and return to ground state directly. The $S_1 \rightarrow S_0$ transition which leads to fluorescence (F) has a very short time interval (10^{-8} to 10^{-5} sec).

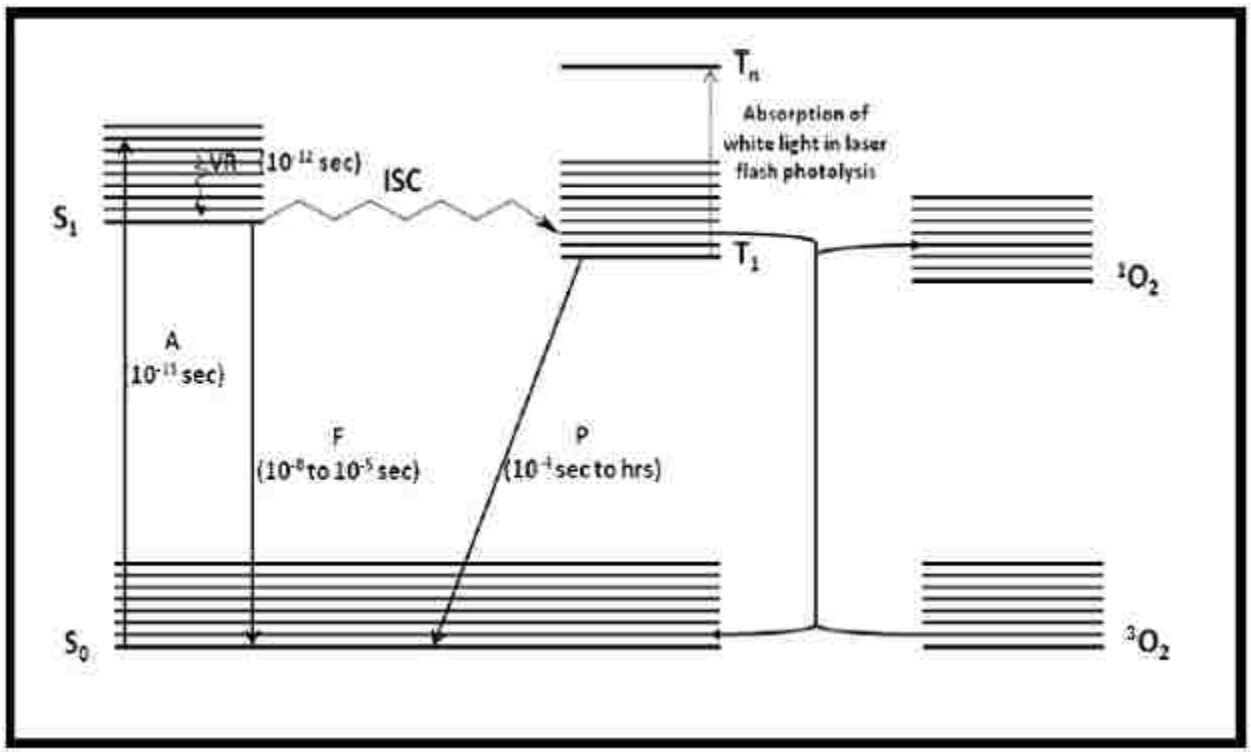

Figure 1.7: Jablonski Diagram illustrating electronic states of a molecule and transitions between the excited states and the ground state.[65]

Phosphorescence process is preceded by internal conversion (IC) and intersystem crossing (ISC), which are non-radiative processes. Phosphorescence decay is comparable to fluorescence, except for the electron spin transition into a "forbidden" triplet state ($\mathbf{T_1}$) instead of the lowest singlet excited state. This transition is referred to as intersystem crossing. The decay from electronic level $\mathbf{T_1}$ occurs with lower energy relative to fluorescence. If this transition occurs within tissues, involved molecules may transfer energy to ground state molecular oxygen (in triplet state) to generate singlet oxygen, as one of the reactive oxygen species (ROS), that is capable of initiating oxidation of tissue. The concept of photodynamic therapy (PDT) is founded on this feature.

1.4.1. Fluorescence Quantum Yield (Φ_f)

The fluorescence quantum yield (Φ_f) of a compound is a measure of the efficiency of its molecules in the fluorescence process. It is the expression of the number of fluorescing molecules to the number of absorbed photons. It can be determined using a comparative method,[39] and compared with ZnPc as reference in DMF solvent ($\Phi_f = 0.17$).[68-70] Other solvents, such as DMSO and THF can also be used in fluorescence experiments, depending on the solubility of the Pcs under study. Fluorescence measurements in this project, gave fluorescence quantum yields ranging between 0.1 and 0.3 (in DMF solvent), which is in agreement with the literature for this type of Pc macrocycle.[69,70]

1.4.2. Singlet Oxygen Quantum Yield (Φ_Δ)

The singlet oxygen quantum yield is the measure of the efficiency of Pcs in the generation of singlet oxygen. The singlet oxygen quantum yield, Φ_Δ, value may be determined by means of photochemical or photophysical methods. A photochemical method was used in this study, in which a solution containing oxygen, a Pc and a singlet oxygen scavenger were used. A

scavenger is a sensitive compound that reacts quickly with singlet oxygen as soon as it is produced. The Pc is irradiated with light and the decay of the scavenger is measured spectroscopically. Some of the scavengers that may be used include guanine, furan and 1,3-diphenylisobenzofuran (DPBF). In this study, the singlet oxygen quantum yields (Φ_Δ) were determined in DMF solvent through a relative method, using ZnPc (Φ_f = 0.56) as reference and DPBF as a scavanger.[71]

1.4.3. UV-vis Absorption Spectra

All monomeric H_2Pcs and MPcs exhibit a characteristic UV-vis absorption spectrum, which includes a Soret-band in the visible region at approximately 350 nm, and a major strong Q-band in the near-IR region (670 – 750 nm), as shown in Figure 1.8.[72] The Pcs with four substituents at the α-position usually exhibit a bathochromic shift in their UV-vis absorption spectra.[73] They exhibit approximately a 15 nm red-shift of their Q-bands, and 20 nm red-shift of their Soret-bands compared with the mono-substituted Pcs. Even within mono-substituted Pcs, those which have the substituent at α-position, show approximately 3 nm red-shift in their Soret-bands, and approximately 3 nm hypsochromic shift in their Q-bands compared with β-substituted Pcs. This shows that both the number and the position of the substituents on the macrocycle affect the absorption spectra of Pcs.

In addition, for the Pcs exhibiting narrow and intense Q-bands, and follow Beer-Lambert law for both the Q-band and Soret-band in the concentration range 10^{-6} - 10^{-4} mol/L, it is usually believed that no aggregation has occurred within this range.[74] The typical molar extinction coefficient of the Q-band of a Pc is in ca. 10^5 $M^{-1}cm^{-1}$. In this work, similar features were observed, in addition to the Stokes Shifts in the range 2 – 10 nm, which is in agreement with those reported in the literature.[75,76]

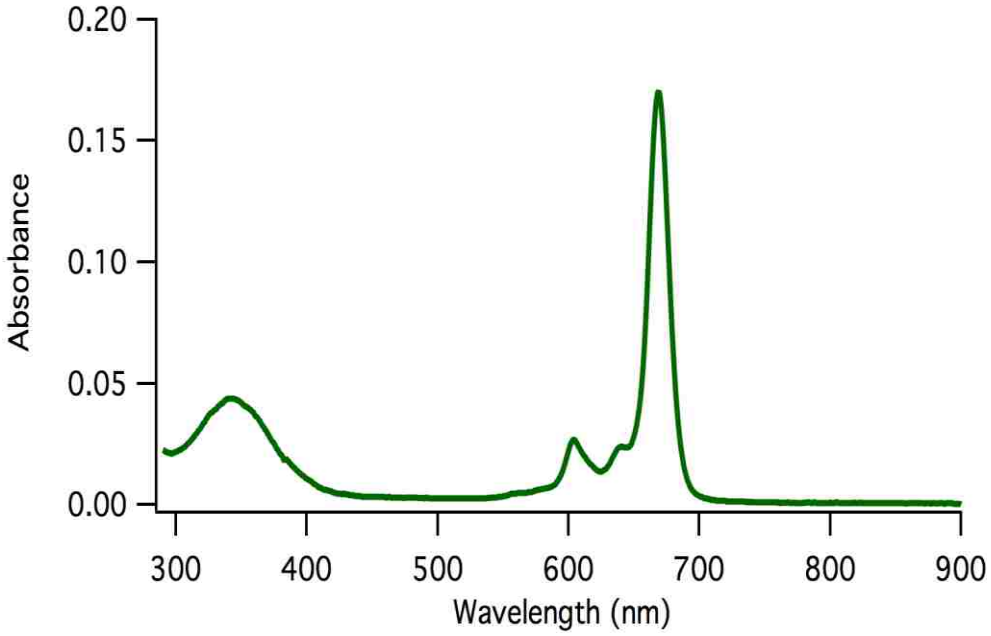

Figure 1.8: A typical absorption spectrum of a ZnPc in HPLC grade DMF solvent.

1.5. Applications of Phthalocyanine

Since their discovery and identification, Pcs have been extensively used as dyes and pigments in paint, printing, textile and paper industries due to their intense blue-green color.[72,77,78] Most recently, Pcs have found high-tech applications in electrophotography and ink-jet printing and as photoconducting agents in photocopying devices.[29] In addition, their novelty is rapidly growing in other fields where they are used as chemical sensors,[79] liquid crystals,[80] semiconductors,[79,81] functional polymers,[82] and molecular metals,[83] among others.

1.5.1. Applications in Photodynamic Therapy

Pcs have also found use in the field of PDT, a therapeutic modality in which a dye used as a photosensitizer is administered to the patient. Following a time interval during which the dye localizes in the diseased tissue, the latter is exposed to light of appropriate wavelength and destroyed. The destruction of the tissues is caused by the excitation of the dye in the presence of oxygen molecules, which produces reactive oxygen species (ROS) (Figure 1.9).[84-86]

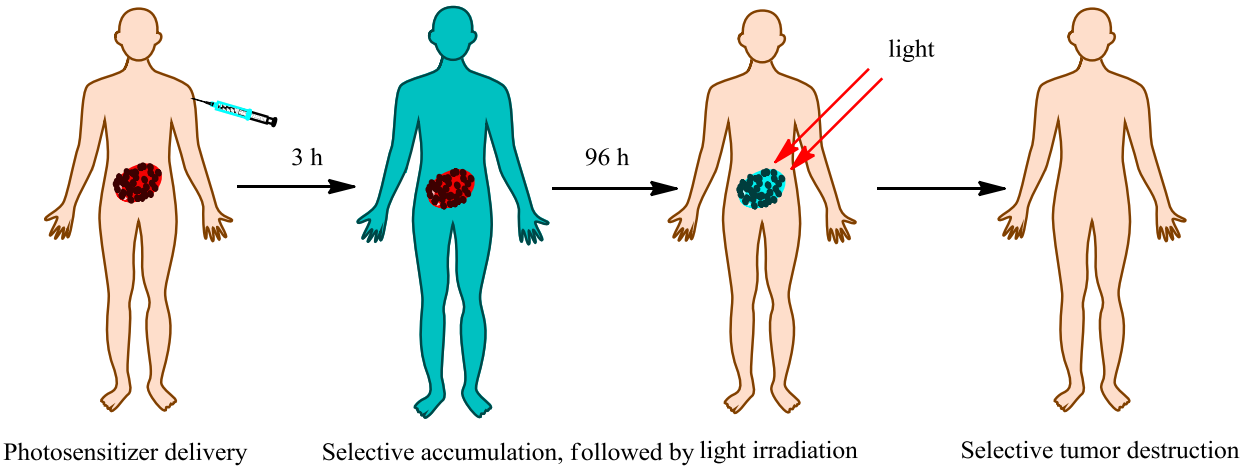

Figure 1.9: Treatment of cancer using PDT.[86]

In 1995, FDA approved Photofrin®, a porphyrin derivative, as a PDT photosensitizer. However, it has synthetic reproducibility problems, long half-life in patients and low selectivity for tumors.[87,88] Therefore, benzoporphyrin derivatives, chlorins, purpurins and Pcs have emerged as second generation photosensitizers, with Pcs having the most promising PDT applications in the treatment of cancer due to their strong absorptions at wavelengths > 660 nm and generally low dark toxicity and high stability.

Pcs have been used in photobiology and PDT since 1985,[89] with derivatives such as ZnPc (CGP55847), $AlPcS_4$ (Photosense®) and Pc4 currently being used in clinical trials.[88,90,91] The di-substituted silicon-Pc, Pc4, with an axial alkylsilyl ligand bearing a terminal amine (Figure 1.10) is in Phase I clinical trials for cancer treatment.[92]

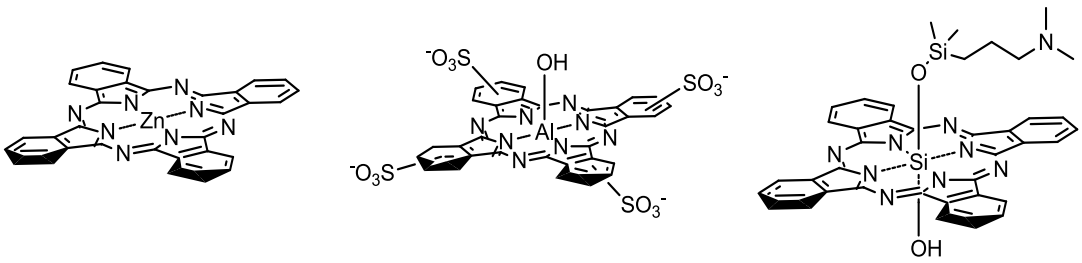

Figure 1.10: Molecular structures of current Pcs under clinical investigation for PDT.

An ideal photosensitizer should be chemically pure and maintain a stable composition throughout the treatment. It should have preference for tumor cells. Its dark toxicity should be minimal but should have high phototoxicity. It should have a high $^1O_2$ quantum yield and a large absorption coefficient in the range 600 – 800 nm wavelength. It is also important that the photosensitizer is rapidly cleared from the normal cells after treatment. The drugs should be amphiphilic.[10,12,88] Various hydrophilic groups such as carboxylic acids, phosphonic acid, sulfonic acid, hydroxyl and quaternary ammonium salts have been added to the hydrophobic Pc ring to achieve this.

In addition, cell-targeted therapeutics has received significant attention and seems to define the future of PDT of cancers. Sibrian-Vasquez *et al.* recently reported the synthesis and biological evaluation of cancer cell-targeted Pc-peptide conjugates with high phototoxicity towards human carcinoma HEp2 cells.[93] Positively charged macrocycles have also demonstrated a potential to interact with negatively charged tumor cell plasma membranes and bacterial surfaces, thus enhancing their cellular targeting ability.[94,95] Cationic PS have been observed to localize subcellularly within the mitochondria,[96,97] lysosomes,[98,76] ER[9] and nuclei.[99] They also bind to anionic DNA and RNA,[100,101] which can enhance their overall PDT efficacy. In Chapters 2 and 5, the syntheses of cationic Pcs as potential candidates for PDT is described.

1.5.2. Applications in Bioimaging

Pcs have also been used as colorants or dyes.[29,72,78] Nevertheless, till recently, not many Pcs have been reported as fluorescent agents, appropriate for bioconjugation applications.[102] Most Pcs are hydrophobic, and are inclined to aggregate in aqueous medium, or they do not have a reactive group for bioconjugation purposes. La Jolla Blue (Figure 1.11) was the first

commercially available Pc dye. It has two axial polyethylene glycol moieties and two free carboxylic acids for bioconjugation.[103] The axial glycol moieties make the dye water soluble and therefore, attractive as a biomarker. Different biomolecules such as peptides and proteins can bind to Pc dyes; the dyes are, therefore, applied in bioimaging and bioanalytical fields.[104-107] Another group of MPcs, which was synthesized by Renzoni, *et al.*,[108] lacks the water soluble axial groups described in La Jolla blue, but contains both water soluble groups and another reactive group that is bound to the benzo-ring (Figure 1.11). The copper in this structure may also be replaced by another metal, such as silicon, which will allow it to bear two axial ligands.

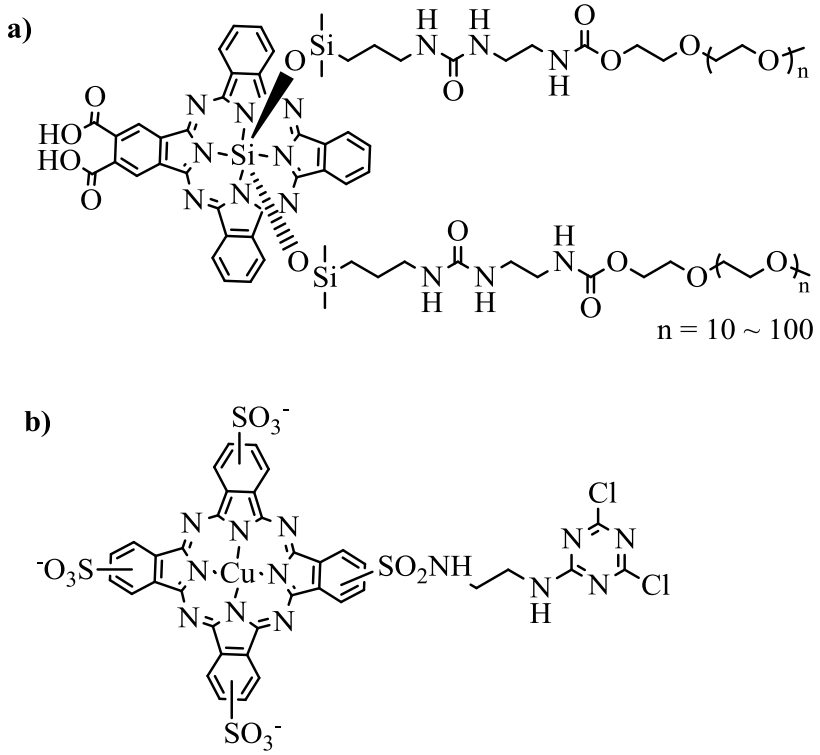

Figure 1.11: Structure of a) La Jolla Blue dye™ [109] and b) Copper sulfophthalocyanine dye.[108]

The conjugation of Pcs with peptide ligands or antibodies directed at specific receptors over-expressed in cancer cells, such as the human epidermal growth factor receptor (EGFR), is a remarkable strategy for increasing their biological efficacy.[110-114] EGFR is over-expressed in various cancers, including small cancers (< 5 mm) and the flat, dysplastic and aberrant crypt foci,

which are believed to precede the development of cancer.[115-117] In the development of selective delivery of cytotoxic drugs to the tumor sites,[118-124] two small peptides with sequences LARLLT[123] and YHWYGYTPQNVI[124] have proved attractive due to their ready-availability, low immunogenicity, ease of conjugation to other molecules, and a relatively superior EGFR-targeting ability. Pcs conjugated to peptides via various linkers for colorectal cancer (CRC) diagnostic applications have been evaluated *in vitro* and *in vivo*.[125] Chapters 3 and 5 of this work reports the syntheses, photophysical, and biological evaluation of Pc conjugates to either peptide ligands or a monoclonal antibody, which can serve as bioimaging agents.

Polyethylene glycols (PEG) have been used as delivery vehicles[126,127] and, in other cases, may be covalently-bound[128,129] to Pcs for improved delivery to target tissues. Pegylation of photosensitizers increases their water-solubility, serum life, tumor accumulation, and also reduces their uptake by the reticuloendothelial system.[130,131] Investigations were carried out to identify potential ZnPcs that may serve as photosensitizers with enhanced biological effectiveness. In Chapter 4, the syntheses, characterization and biological evaluation of a new series of regiomerically pure Pcs, containing at least a PEG group are described.

1.6. References

1. Allen, C. M.; Langlois, R.; Sharman, W. M.; La Madeleine, C.; van Lier, J. E. *Photochem. Photobiol.* **2002,** *76* (2), 208-216.
2. Dent, C. E.; Linstead, R. P.; Lowe, A. R. *J. Chem. Soc.*, **1934**, 1033-1039.
3. Leznoff, C.C.; Lever, A.B.P., Eds., *Phthalocyanines: Properties and Applications, VCH Publishing, New York* **1996**.
4. Byrne, G. T.; Linstead, R. P.; Lowe, A. R. *J. Chem. Soc. (Resumed)* **1934**, 1017-1022.
5. de Diesbach, H.; von der Weid, E. *Helv. Chim. Acta* **1927**, *10* (1), 886-888.
6. Sharman, W. M.; van Lier, J. E. *Bioconj. Chem.* **2005**, *16* (5), 1166-1175.
7. Gelir, A.; Yılmaz, İ.; Yılmaz, Y. *J. Phys. Chem. B* **2006**, *111* (2), 478-484.

8. Gregory, P. *J. Porphyr. Phthalocyan.* **2000**, *4* (4), 432-437.

9. Şen, Z.; Gümüş, G.; Gürol, I.; Musluoğlu, E.; Öztürk, Z. Z. *Sensors and Actuators B: Chemical* **2011**, *160* (1), 1203-1209.

10. Sharman, W. M.; Allen, C. M.; van Lier, J. E. *Drug Discovery Today* **1999**, *4* (11), 507-517

11. Castano, A. P.; Demidova, T. N.; Hamblin, M. R. *Photodiagnosis and Photodynamic Therapy* **2004**, *1* (4), 279-293.

12. Macdonald, I. J.; Dougherty, T. J. *J. Porphyr. Phthalocyan.* **2001**, *5* (2), 105-129.

13. Boyle, R. W.; Dolphin, D. *Photochem. Photobiol.* **1996**, *64* (3), 469-485.

14. Selbo, P. K.; Weyergang, A.; Eng, M. S.; Bostad, M.; Mælandsmo, G. M.; Høgset, A.; Berg, K. *Journal of Controlled Release* **2012**, *159* (2), 197-203.

15. Dumoulin, F.; Durmuş, M.; Ahsen, V.; Nyokong, T. *Coordination Chemistry Reviews* **2010**, *254* (23–24), 2792-2847.

16. Booysen, I.; Matemadombo, F.; Durmus, M.; Nyokong, T. *Dyes Pigm.* 2011, *89*, 111-119.

17. Masilela, N.; Nyokong, T. *Dyes Pigm.* 2010, *84*, 242-248.

18. Nombona, N.; Nyokong, T. *Dyes Pigm.* **2009**, *80*, 130-135.

19. Modibane, D. K.; Nyokong, T. *Polyhedron* **2009**, *28*, 1475-1480.

20. Causey, P. W.; Dubovyk, I.; Leznoff, C. C. *Can. J. Chem.* **2006**, *84* (10), 1380-1387.

21. Mckeown, N. B. *The Porphyrin Handbook (Kadish, K. M.; Smith, K. M.; Guilard, R., Eds.), Academic Press: Boston* **2003**, *15*, 61-124.

22. Yiru, P.; Fenghua, H.; Zhipeng, L.; Naisheng, C.; Jinling, H.; *Inorg. Chem. Commum.* **2004**, *7*, 967-970.

23. Bezerin, B.D. *Coordination Compounds of Porphyrins and Phthalocyanines*, *Wiley, J.* & *Sons*, *New York*, *NY*, **1981**.

24. Barrett, P. A.; Linstead, R. P.; Tuey, G. A. P. *J. Chem. Soc.* **1939**, 1809-1820.

25. Tomoda, H.; Saito, S.; Ogawa, S.; Shiraishi, S. *Chem. Lett.* **1980**, 1277-1280.

26. Tomoda, H.; Saito, S.; Shiraishi, S. *Chem. Lett.* **1983**, 313-316.

27. Christie, R. M.; Deans, D. D. *J. Chem. Soc., Perkins Trans.* **1989**, *2*, 193-198.

28. Hurley, T. J.; Robinson, M.A.; Trotz, S, I. *Inorg. Chem.* 1967, *6*, 389-392.

29. Leznoff, C. C. *Phthalocyanines: Properties and Applications*. Leznoff, C. C.; Lever, A. B. P. Eds.; *VCH Publishers (LSK) Ltd.: Cambridge* **1989**, *1*, 1-54.

30. Britton, J.; Litwinski, C.; Durmuş, M.; Chauke, V.; Nyokong, T. *J. Porphyr. Phthalocyanines* **2011,** *15* (11,12), 1239-1249.

31. Hanack, M.; Schmid, G.; Sommerauer, M. *Angew. Chem.* **1993**, 105, 1540; *Angew. Chem. Int. Ed. Engl*. **1993**, 32, 1422.

32. Leznoff, C. C.; Hu, M.; McArthur, C. R.; Qin, Y.; van Lier, J. *Can. J. Chem.* **1994**, *72*, 1990-1998.

33. Hu, M.; Brasseur, N.; Yildiz, S. Z.; van Lier, J. E.; Leznoff, C. C. *J. Med. Chem.* **1998**, *41*, 1789-1802.

34. Leznoff, C. C.; Hu, M. G.; Nolan, K. J. M. *J. Chem. Soc*., *Chem. Commun.* **1996**, 1245-1246.

35. Sharmam, W. M.; Van Lier, J. E. *The Porphyrin Handbook (Kadish, K. M.; Smith, K. M.; Guilard, R., Eds.), Academic Press: Boston* **2003**, *15*, 1-60.

36. Leznoff, C. C.; D'Ascanio, A. M.; Yildiz, S. Z. *J. Porphyr. Phthalocyan.* **2000**, *4* (1), 103-111.

37. Rodriguez-Morgade, M. S.; de la Torre, G.; Torres, T. *The Porphyrin Handbook (Kadish, K. M.; Smith, K. M.; Guilard, R., Eds.), Academic Press: Boston* **2003**, *15*, 125-160.

38. Giuntini, F.; Nistri, D.; Chiti, G.; Fantetti, L.; Jori, G.; Roncucci, G. *Tetra. Lett.* **2003**, *44*, 515-517.

39. Brykina, G. D.; Uvarova, M. I.; Koval, Y. N.; Shpigun, O. A. *J. Anal. Chem.* **2001**, *56*, 940-944.

40. Uvarova, M. I.; Brykina, G. D.; Shpigun, O. A. *J. Anal. Chem.* **2000**, *55*, 910-925.

41. Wang, J.; Liu, H.; Xue, J. P.; Jiang, Z.; Chen, N. S.; Huang, J. L. *Chinese Sci. Bull.* **2008**, *53*, 1657-1664.

42. Leznoff, C. C.; Drew, D. M. *Can J. Chem.* **1996**, *74*, 307-318.

43. Drew, D. M.; Leznoff, C. C. *Synlett.* **1994**, 623-624.

44. Kobayashi, N. *J. Chem. Soc*., *Chem. Commun.* **1998**, 487.

45. Kobayashi, N.; Kobayashi, Y; Osa, T. *J. Am. Chem. Soc.* **1993**, *115*, 10994-10995.

46. Tolbin, A. Y.; Ivanov, A. V.; Tomilova, L. G.; Sefirov, N. S. *Mendeleev Commun.* **2002**, *3*, 96-97.

47. Mckeown, N. B.; Chambrier, I.; Cook, M. J. *J. Chem. Soc., Perkin Trans. 1* **1990**, 1169-1177.

48. Cook, M. J.; Dunn, A. J.; Howe, S. D.; Thomson, A. J.; Harrison, K. J. *J. Chem. Soc., Perkin Trans. 1* **1988**, 2453-2458.

49. Cook, M. J.; Daniel, M. F.; Harrison, K. J.; Mckeown, N. B.; Thomson, A. J. *J. Chem. Soc., Chem. Commun. 1* **1987**, 1086-1088.

50. Kobayashi, N.; Sasaki, N.; Higashi, Y.; Ossa, T. *Inorg. Chem.* **1995**, *34*, 1636-1637.

51. Ruf, M.; Lawrence, A. M.; Noll, B. C.; Pierpont, C. G. *Inorg. Chem.* **1998**, *37*, 1992-1999.

52. van der Pol, J. F.; Neeleman, E.; van Miltenburg, J. C.; Zwikker, J. W.; Nolte, R. J. M.; Drenth, W. *Macromolecules* **1990**, *23*, 155-162.

53. Toupance, T.; Ahsen, V.; Simon, J. *J. Am. Chem. Soc., Commun.* **1994**, *116*, 5352-5361.

54. Kobayashi, N.; Sudo, K.; Osa, T. *Bull. Chem. Soc. Jpn* **1990**, *63*, 571.

55. Fernandez-Lazaro, F.; Maya, E. M.; Nicolau, M.; Torres, T. *Advances in Porphrin Chemistry*. *Golubtchikov, O. A., Ed.; ISUCT Press: St. Petersburg* **1999**, 279-299.

56. Torres, T. *J. Porphyrins Phthalocyanines* **2000**, *4*, 325-330.

57. de la Torre, G.; Claessens, C. g.; Torres, T. *Eur. J. Org. Chem*. **2000**, 2821-2830.

58. Weitemeyer, A.; Kliesch, H.; Wohrle, D. *J. Org. Chem.* **1995**, *60*, 4900-4904.

59. Sastre, A.; delRey, B.; Torres, T. *J. Org. Chem.* **1996**, *61*, 8591-8597.

60. Sastre, A.; Torres, T.; Hanack, M. *Tetra. Lett.* **1995**, *36*, 8501-8504.

61. Leznoff, C. C. *Can. J. Chem.* **2000**, *78*, 167-183.

62. Hall, T. W.; Greenberg, S.; McArthur, C. R.; Khouw, B.; Leznoff, C. C. *J. Chem.* **1982**, *6*, 653-658.

63. Leznoff, C. C.; Hall, T. W. *Tetra. Lett.* **1982**, *23*, 3023-3026.

64. Oliver, S. W.; Smith, T. D. *J.Chem. Soc., Perkin Trans. II* **1987**, (11), 1579-1582.

65. Jablonski, A. *Z. Phys.* (*Zeitschrift für Physik A Hadrons and Nuclei)* **1935**, *94* (1), 38-48.

66. Atkins, P. W. *Physical Chemistry (Atkins, P. W., 6th Eds) Oxford*: *Oxford University Press* **1998**, 17.

67. Ishii, K.; Kobayashi, N. *The Porphyrin handbook (Guilard, R.; Smith, K. M., Eds.) New York: Elsevier Science* **2003**, *16*, 102.

68. Zorlu, Y.; Dumoulin, F.; Durmus, M. Ahsen, V. *Tetrahedron* **2010**, *66*, 3248–3258.

69. Saka, E. T.; Durmus, M.; Kantekin, H. *J. Organomet. Chem.* **2011**, *696*, 913–924.

70. Fery-Forgues, S.; Lavabre, D. *J. Chem. Educ.* **1999**, *76*, 1260–1264.

71. Maree, M. D.; Kuznetsova, N.; Nyokong, T. *J. Photochem. Photobiol. A*. **2001**, *140*, 117–125.

72. Robertson, J. M. *J. Chem. Soc.* **1936**, 1195-1209.

73. Li, Y.; Pritchett, T. M.; Huang, J.; Ke, M.; Shao, P.; Sun, W. *J. Phys. Chem. A.* **2008**, *112* (31), 7200-7207.

74. Stillman, M. J.; Nyokong, T. *The Porphyrin handbook (Leznoff, C. C., Lever, A. B. P., Eds.) VCH: New York* **1989**, *1*, 139-247.

75. Li, H.; Jensen, T. J.; Fronczek, F. R.; Vicente, M. G. H. *J. Med. Chem.* **2008**, *51* (3), 502-511.

76. Jiang, X.-J.; Yeung, S.-L.; Lo, P.-C.; Fong, W.-P.; Ng, D. K. P. *J. Med. Chem.* **2010**, *54* (1), 320-330.

77. Robertson, J. M.; Woodward, I. *J. Chem. Soc.* **1937**, 219-230.

78. Robertson, J. M.; Woodward, I. *J. Chem. Soc.* **1940**, 36-48.

79. Guillaud, G.; Simon, J.; Germain, J. P. *Coord. Chem. Rev.* **1998**, *178-180*, 1433-1484.

80. Mckeown, N. B. *Chem. & Industry* **1999**, 92-98.

81. Zhou, R; Josse, F.; Gopel, W.; Oztuk, Z. Z.; Bekaroglu, ö. *Appl. Organomet. Chem.* **1996**, *10*, 557-577.

82. Mckeown, N. B. *J. Mater. Chem.* **1999**, *10*, 1979-1995.

83. Achar, B. N.; Jayasree, P. K. *Can. J. Chem.* **1999**, *77*, 1690-1696.

84. Henderson, B. W.; Dougherty, T. J. *Photochem. Photobiol.* **1992**, *55* (1), 145-157.

85. Dolmans, D. E. J. G. J.; Ananth, K.; John, S. H.; Kevin, R. F.; Joseph, N. G.; Jeffrey, P. W.; Inne, H. M. B. R.; Rakesh, K. J.; Dai, F. *Cancer Research* **2002**, *62*, 4289–4294.

86. Josefsen, L. B.; Boyle, R. W. *Metal-Based Drugs* **2008**, 1 - 24.

87. Berg, K.; Selbo, P. K.; Weyergang, A.; Dietze, A.; Prasmickaite, L.; Bonsted, A.; Engesaeter, B. O.; Angell-Petersen, E.; Warloe, T.; Frandsen, N.; Hogset, A. *J. Microsc.* **2005**, *218*, 133 – 147.

88. Allison, R. R.; Downie, G. H.; Cuenca, R.; Hu, X. H.; Childs, C. J.; Sibata, C. H. *Photodiag. Photodyn. Ther.* **2004**, *1*, 27 – 42.

89. Ben-Hur, E.; Rosenthal, I. *Int. J. Radiat. Biol.* **1985**, *47*, 145-147.

90. Huang, Z. *Tech. Res. Treat.* **2005**, *4*, 283 – 293.

91. Detty, M. R.; Gibson, S. L.; Wagner, S. J. *J. Med. Chem.* **2004**, *47*, 3897 – 3915.

92. Baron, E. D.; Malbasa, C. L.; Santo-Domingo, D.; Fu, P.; Miller, J. D.; Hanneman, K. K.; Hsia, A. H.; Oleinick, N. L.; Colussi, V. C.; Cooper, K. D. *Lasers in Surgery and Medicine* **2010**, *42* (10), 728-735.

93. Sibrian-Vazquez, M.; Ortiz, J.; Nesterova, I. V.; Fernandez-Lazaro, F.; Sastre-Santos, A.; Soper, S. A.; Vicente, M. G. H. *Bioconjugate Chem.* **2007**, *18*, 410 – 420.

94. Reddi, E.; Ceccon, M.; Valduga, G.; Jori, G.; Bommer, J. C.; Elisei, F.; Latterini, L.; Mazzucato, U. *Photochem. Photobiol.* **2002**, *75*, 462-470.

95. Sol, V.; Branland, P.; Chaleix, V.; Granet, R.; Guilloton, M.; Lamarche, F.; Verneuil, B.; Krausz, P. *Bioorg. Med. Chem. Lett.* **2004**, *14*, 4207-4211.

96. Jensen, T. J.; Vicente, M. G. H.; Luguya, R.; Norton, J.; Fronczek, F. R.; Smith, K. M. *J. Photochem. Photobiol. B: Biol.* **2010**, *100*, 100-111.

97. Duan, W. B.; Lo, P. C.; Duan, L.; Fong, W. P.; Ng, D. K. P. *Bioorg. Med. Chem.* **2010**, *18*, 2672-2677.

98. Ricchelli, F.; Franchi, L.; Miotto, G.; Borsetto, L.; Gobbo, S.; Nikolov, P.; Bommer, J. C. Reddi, E. *Int. J. Biochem. Cell Biol.* **2005**, *37*, 306-319.

99. Villanueva, A. *J. Photochem. Photobiol. B: Biol.* **1993**, *18*, 295-298.

100. Caminos, D. A.; Durantini, E. N. *J. Photochem. Photobiol. A: Chem.* **2008**, *198*, 274-281.

101. Fu, B. Q.; Zhang, D.; Weng, X. C.; Zhang, M.; Ma, H.; Ma, Y. Z.; Zhou, X. *Chem. Eur. J.* **2008**, *14*, 9431-9441.

102. Luo, S.; Zhang, E.; Su, Y.; Cheng, T.; Shi, C. *Biomaterials* **2011**, *32* (29), 7127-7138.

103. Devlin, R. F.; Dandliker, W. B.; Arrhenius, P. O. G. *U.S. Patent* 6,060,598, **2000**.

104. Li, X. Y.; Ng, D. K. P. *Tetra. Lett.* **2001**, *42*, 305-309.

105. Hammer, R. P.; Owens, C. V.; Hwang, S. H.; Sayes, C. M.; Soper, S. A. *Bioconj. Chem.* **2002**, *13*, 1244-1252.

106. Ogunsipe, A.; Nyokong, T. *J. Porphyr. Phthalocyanines* **2005**, *9*, 121-129.

107. Walker, G. T.; Nadeau, J. G.; Linn, C. P.; Devlin, R. F.; Dandliker, W. B. *Clin. Chem.* **1996**, *42*, 9-13.

108. Schindele, D. C.; Pepich, B. V.; Renzoni, G. E.; Fearon, K. L.; Andersen, N. H.; Stanton, T. H. *U.S. Patent* 5,494,793, **1996**.

109. Devlin, R.; Studholme, R. M.; Dandliker, W. B.; Fahy, E.; Blumeyer, K.; Ghosh, S. S. *Clin. Chem.* **1993**, *39*, 1939-1943.

110. Sharman, W. M.; van Lier, J. E.; Allen, C. M. *Adv. Drug Delivery Rev.* **2004**, *56*, 53-76

111. Savellano, M. D.; Hasan, T. *Clin. Cancer Res.* **2005**, *11*, 1658-1668

112. Hudson, R.; Boyle, R. W. *J. Porphyrins Phthalocyanines* **2004**, *8*, 954-975.

113. Pérez-Soler, R. HER1/EGFR *The Oncologist* **2004**, *9*, 58-67.

114. Meric-Bernstam, F.; Hung, M.-C. *Clin. Cancer Res.* **2006**, *12*, 6326-6330.

115. Spano, J.–P.; Lagorce, C.; Atlan, D.; Milano, G.; Domont, J.; Bnamouzig, R.; Attar, A.; Benichou, J.; Martin, A.; Morere, J. –F.; Raphael, M.; Penault-Llorca, F.; Breau, J.–L.; Fagard, R.; Khayat, D.; Wind, P. *Ann. of Oncol.* **2005**, *16*, 102-108.

116. Galizia, G.; Iieto, E.; Ferraraccio, F.; De Vita, F.; Castellano, P.; Orditura, M.; Imperatore, V.; La Mura, A.; La Manna, G.; Pinto, M.; Catalano, G.; Pignatelli, C.; Ciardiello, F. *Ann. of Surg. Oncol.* **2006**, *13*, 823-835.

117. Dougherty, U.; Sehdev, A.; Cerda, S.; Mustafi, R.; Little, N.; Yuan, W.; Jagadeeswaran, S.; Chumsangsri, A.; Delgado, J.; Tretiakova, M.; Joseph, L.; Hart, J.; Cohen, E. E.; Aluri, L.; Fichera, A.; Bissonnette, M. *Clin. Cancer Res.* **2008**, *14*, 2253-2262.

118. Loeffler-Ragg, J.; Schwentner, I.; Sprinzl, G. M.; Zwierzina, H. *Expert Opin. Investig. Drugs* **2008**, *17*, 1517-1531.

119. Molema, G. *Acta Biochim. Polonica* **2005**, *52*, 301-310.

120. Dane, K. Y.; Chan, L. A.; Rice, J. J.; Daugherty, P. S. *J. Immun. Meth.* **2006**, *309*, 120-129.

121. Frochot, C.; Stasio, B. D.; Vanderesse, R.; Belgy, M.-J.; Dodeller, M.; Guillemin, F.; Viriot, M.-L.; Barberi-Heyob, M. *Bioorganic Chem.* **2007**, *35*, 205-220.

122. Song, S. X.; Liu, D.; Peng, J. L.; Sun, Y.; Li, Z. H.; Gu, J. R.; Xu, Y. H. *Int. J. Pharmac.* **2008**, *363*, 155-161.

123. Song, S.; Liu, D.; Peng, J.; Deng, H.; Guo, Y.; Xu, L. X.; Miller, A. D.; Xu, Y. *FASEB J.* **2009**, *23*, 1396-1404.

124. Li, Z.; Zhao, R.; Wu, X.; Sun, Y.; Yao, M.; Li, J.; Xu, Y.; Gu, J. *FASEB J.* **2005**, *19*, 1978-1985.

125. Ongarora, B. G.; Fontenot, K. R.; Hu, X.; Sehgal, I.; Satyanarayana-Jois, S. D.; Vicente, d. G. H. *J. Med. Chem.* **2012**, *55* (8), 3725-3738.

126. Arnida; Nishiyama, N.; Kanayama, N.; Jang, W-D.; Yamasaki, Y.; Kataoka, K. *J. Controlled Release* **2006**, 115, *2*, 208-215.

127. Suzuki, T.; Oishi, M.; Nagasaki, Y. *J. Photopoyml. Sci. and Technol.* **2009**, 22, *4*, 547-550.

128. Bai, M.; Lo, P-C.; Ye, J.; Wu, C.; Fong, W-P.; Ng Dennis, K. P. *Org. & Biomol. Chem.* 2011, 9, *20*, 7028-7032.

129. Li, H.; Fronczek, F. R.; Vicente, M. G. H. *Tetra. Lett.* **2011**, 52, 6675-6678.

130. Fang, J.; Sawa, T.; Akaike, T.; Greish, K.; Maeda, H. *Int. J. Cancer*. **2004**, 109, 1-8.

131. Ichikawa, K.; Hikita, T.; Maeda, N.; Takeuchi, Y.; Namba, Y.; Oku, N. *Biol. Pharm. Bull.* **2004**, 27, 443-444.

CHAPTER 2

SYNTHESES AND BIOLOGICAL EVALUATION OF CATIONIC TRIMETHYLAMINOPHENOXY-SUBSTITUTED ZINC(II)-PHTHALOCYANINES*

2.1. Background

Photofrin was the first PDT drug approved for the treatment of thousands of patients worldwide since 1995. Nonetheless, it has some shortcomings ranging from being a complex mixture of compounds to having a limited tissue selectivity and absorbing only weakly in the red region of the spectrum (λ_{max} = 630 nm),[1] where light penetrates deeper into tissues.[2,3] Therefore, intense research in the last 20 years, has focused on the developing PS with improved tumor-tissue selectivity and overall PDT efficiency. Pcs are predominantly promising PS owing to their long wavelength absorptions in the infra-red region of the spectrum (670 – 750 nm) with high extinction coefficients, high photochemical stability and superior ability to generate singlet oxygen.[4-7] The major challenge in the use of the Pcs is the insolubility of the macrocycle in common organic solvents.

Different water-solubilizing and/or bulky groups have been attached to either the macrocycle periphery of Pcs or their central core, in order to improve their photophysical features such as their quantum yields and biological interactions or photodynamic efficacy.[7] Of all the substituted Pcs, positively charged ones have received special attention due to their strong interactions with negatively charged tumor cell plasma membranes, thus enhancing their cellular targeting ability.[8-11] Equally, cationic PS have been observed to target vulnerable subcellular units such as the mitochondria,[12-16]

* This chapter originally appeared in the *Journal of MedChemComm.*[17] Reproduced with permission of The Royal Society of Chemistry.

lysosomes,[12,18,19] ER[14,15] and nuclei.[20] The photosensitizers can bind to anionic DNA and RNA,[21-24] therefore, largely boosting their PDT efficacy.

Substantial variations in the cytotoxicity, cellular uptake and photodynamic capability of a series of porphyrins with similar cationic groups ($-N(CH_3)_3^+$) have been reported recently.[15] The features of a series of octa-cationic pyridyloxy-Pcs bearing different metal ions and axial ligands in human HEp2 cells have also been reported before.[19] In addition, a Pc bearing a single quaternary ammonium group ($-NH_3^+$) was found to be ~20-fold more phototoxic than its corresponding tetra-ammonium Pc toward HEp2 cells.[25] Although all the cationic porphyrins in this series targeted cell mitochondria, the mono-cationic was the most phototoxic, while the di-cationic accumulated the most within HEp2 cells.

In this chapter, the synthesis of cationic Pcs which will add to the library of photosensitizers with a potential to act as biomarkers or photosensitizing agents is reported. Lowery reported a simple synthesis of silicon-dichlorophthalocyanine in 1965.[26] He used diiminoisoindoline as a starting material, which was reacted with silicon tetrachloride to obtain 71% yield of the silicon Pc. A similar synthesis has been reported by Li, H. *et al.*[19] A direct way of synthesizing ZnPcs has also been reported, where zinc acetate acts as the source of metal.[16,19] The starting phthalonitrile was refluxed in n-pentanol using a small amount of DBU as a catalyst to obtain 88% yield.

Throughout this chapter, statistical condensation of phthalonitriles to Pcs is the main method of synthesis. Phthalonitriles were refluxed in DMAE using catalytic amounts of DBN to obtain Pcs in reasonable yields. This method of synthesis is known as 'Tomoda method' and was discussed in chapter one. Apart from the octaamino-Pc, which was obtained as a pure

regiomeric Pc, all the other Pcs were mixtures of isomers. The cationic Pcs were achieved via trimethylation of the 4-aminophenoxy-substituents on the Pc core. In general, the mono-, di-, tetra- and octa-amino Pcs were synthesized and then trimethylated them to obtain corresponding positively charged analogues. As part of the continued investigation of cationic Pcs as potential photosensitizers, the quaternized Pcs were evaluated *in vitro* and the preliminary results are described.

2.2. Synthesis

2.2.1. Synthesis of Phthalonitriles

The phthalonitriles used in the synthesis of Pcs were prepared according to the procedures established in literature, with slight modifications.[14,19] The mono-, di-, tetra- and octa-cationic Pcs **2.5**, **2.7**, **2.12**, **2.14**, **2.16**, **2.20**, **2.22**, **2.25** and **2.27** were synthesized according to strategies shown in Schemes 2.1 – 2.5. The key precursors: 3(4)-(p-N-Boc-aminophenoxy)phthalonitrile **2.3** and **2.10** (Scheme 2.1 and 2.2) and 4,5-di(p-N-Boc-aminophenoxy)phthalonitrile **2.10** (Scheme 2.3) were all obtained in >80% yields from commercially accessible 3-nitrophthalonitrile and 4-nitrophthalonitrile, or 4,5-dichlorophthalonitrile and *p*-N-Boc-aminophenol in DMF at 80 ºC, in the presence of K_2CO_3, following known methodology.[27,28] Another important precursor 2,2-bis(2,3-dicyanophenoxy) biphenyl **2.23** (Scheme 2.4 and 2.5), was obtained in 66% yield according to a known literature procedure.[29] The use of unprotected *p*-aminophenol in these reactions, gave lower yields (60 – 70%) of the corresponding aminophenoxyphthalonitriles. This is due to the fact that the unprotected amino groups are more polar and thus, the Pcs got stuck in the column. The aminophenoxyphthalonitriles **2.2** and **2.9** were synthesized using unprotected *p*-

aminophenol, which was reacted with either 3-nitrophthalonitrile or 4-nitrophthalonitrile to obtain the desire precursors.

These phthalonitriles, alongside commercially accessible 4-*tert*-butylphthalonitrile, were used in the synthesis of cationic Pcs. The synthesis of mixture of isomers of Pcs, *via* statistical condensation, was accomplished using 4-*tert*-butylphthalonitrile or 2,2-bis(2,3-dicyanophenoxy) biphenyl **2.23**. In order to enhance the solubility of Pcs – which are infamous for their insolubility – 4-*tert*-butylphthalonitrile was used. The bulky *tert*-butyl groups on the Pc macrocycle, boosts the hydrophilicity and decrease the aggregation affinity of the Pc core. Notably, reduced aggregation may improve the uptake of the Pcs by the cells, causing higher photodynamic activities.[30]

The molecular structures of four phthalonitriles crystals, which were grown from dichloromethane for X-ray analyses, are shown in Figure 2.1. The dicyanophenyl group in phthalonitrile **2.3** was essentially orthogonal to the central phenyl group and formed a dihedral angle of 89.83(3)º with it. Its CO_2N plane was tilted considerably less from the central ring and formed a dihedral angle of 28.47(6)º with it. In phthalonitrile **2.10**, the conformation was similar, with the dicyanophenyl and central phenyl rings formed a dihedral angle of 86.23(4)º. Its CO_2N plane was almost coplanar with the central phenyl and had a dihedral angle 3(1)º. The dicyanophenyl plane was nearly orthogonal to both phenyl rings connected to it through O in phthalonitrile **2.18**, with the dihedral angles being 79.22(2)º and 85.25(2)º. The tips of the two CO_2N planes out of the phenyl groups to which they were bonded were midway between those seen in **2.3** and **2.10**; 14.7(1)º and 14.9(1)º for this phthalonitrile. The tips of the carbonyl O were in opposite directions in **2.18**; one toward the Ph $(CN)_2$ and the other away from it. The central diphenyl group in diphthalonitrile **2.23** had a torsion angle of

74.5(4)º about the bond connecting the two rings. Its dicyanophenyl groups were tilted by comparable amounts out of the phenyl groups they are bonded to, and formed dihedral angles of 70.68(7)º and 67.60(7)º with them. The dicyanophenyl groups formed a dihedral angle of 7.7(4)º and the molecule had nearly a C_2 symmetry.

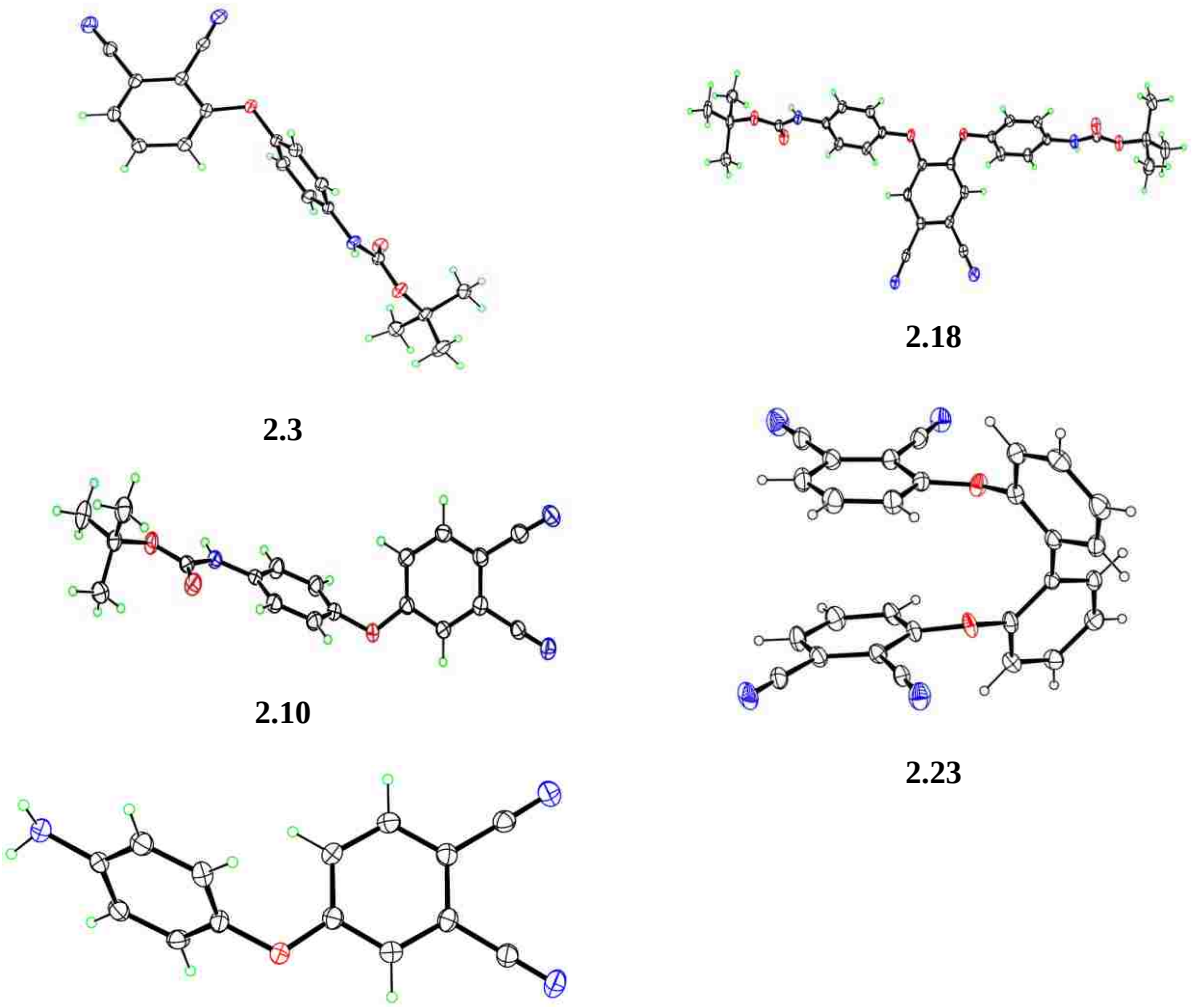

Figure 2.1. X-ray structures of phthalonitriles **2.3**, **2.9**, **2.10**, **2.18** and **2.23** obtained from single crystals (N atoms are blue, O atoms red and H atoms green; H atoms are white in **2.23**). Ellipsoids are drawn at the 50% probability level.

2.2.2. Synthesis of Cationic ZnPcs

In order to enhance the solubility of the precursor Pcs and the target cationic ZnPcs, 4-*tert*-butylphthalonitrile was selected for use in the statistical condensation[28,29,31]

with the appropriate p-N-Boc-aminophenoxyphthalonitrile. A mixture of N-Boc-protected phthalonitrile **2.3** and 3 equiv. 4-*tert*-butylphthalonitrile was reacted in the presence of Zn(II) acetate and a catalytic amount of DBN in DMAE (Schemes 2.1). After refluxing the reaction mixture for 5 h, a number of ZnPcs were obtained. The A_4-type Pc was the major product, followed by the A_3B- and A_2B_2-types ZnPcs, as confirmed by TLC and MS analyses. In order to purify the mixture, column chromatography using mixtures of hexane and ethyl acetate for elution gave the subsequent N-Boc-protected A_3B-type ZnPcs in 15-20% yields and the A_2B_2-type ZnPcs in 19-25% yields. The deprotection of the Boc groups under acidic conditions (using TFA/DCM) at room temperature, gave ZnPcs **2.4** and **2.6** in quantitatiive yield. The yields of ZnPcs **2.4** and **2.6** were low when unprotected aminophenoxyphthalonitriles were used in the tetramerization reactions.

The free amino groups were quaternized using excess iodomethane and DIPA in DMF at room temperature.[15] The subsequent trimethylaminophenoxy-substituted ZnPcs **2.5** and **2.7** were obtained in 50-70% yields. The A_3B- and A_2B_2-type ZnPcs **2.5** and **2.7** were obtained mixtures of regioisomers as has been reported in literature before.[31-35] The di-cationic ZnPcs **2.7** and **2.14** are particularly complex mixtures of up to 15 regioisomers of both trans-ABAB and cis-AABB types. Due to their exceedingly similar retention times on reversed-phase HPLC, isomers of these Pcs were not isolated. There are chances that the distribution of isomers may slightly be different for the α- and β-substituted Pcs, due to the higher steric hindrance resulting from the neighboring α-substituents during the macrocyclization step as reported previously in literature.[36] The chromatograms for the cationic ZnPcs **2.7** and **2.14** obtained during reversed-phase HPLC using water/methanol (50:50 → 0:100) were consistent with the expected mixtures of regioisomers.

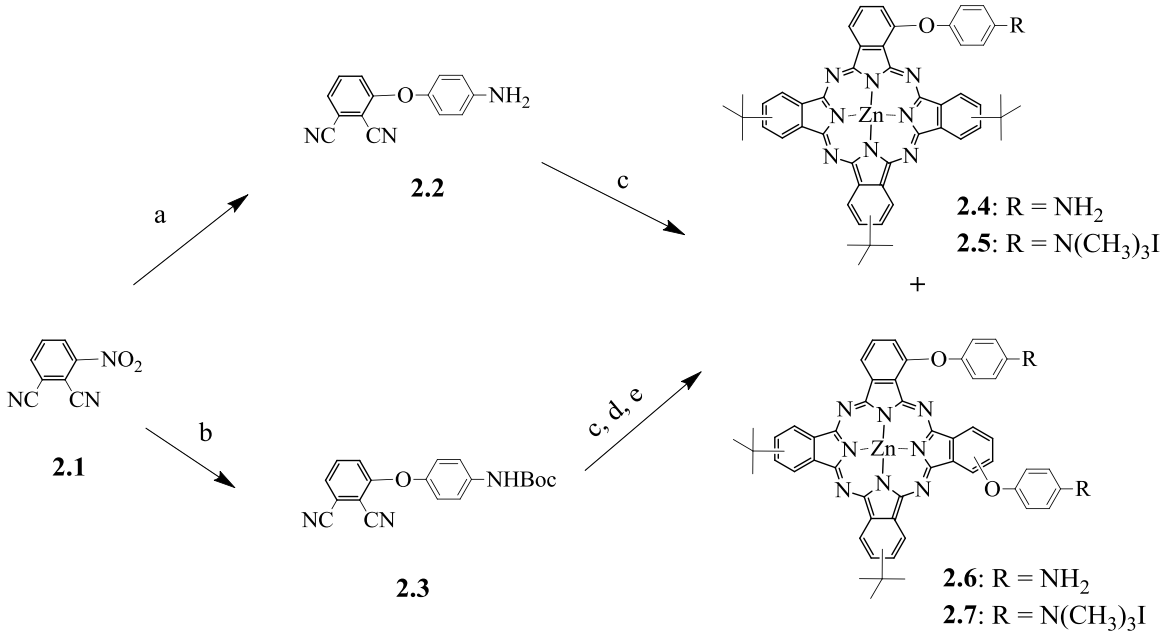

Scheme 2.1. Synthesis of mono- and di-cationic α-trimethylphenoxy-substituted ZnPcs **2.5** and **2.7**. Reagents and conditions: (a) K_2CO_3, DMF, 65 °C, 24 h (70%); (b) K_2CO_3, DMF, 80 °C, 3 h (80%); (c) 4-*tert*-butylphthalonitrile, $Zn(OAc)_2$, DMAE, 140 °C, 5 h (15-20%); (d) DCM/TFA, 0 °C, 4 h (quantitative); (e) CH_3I, DIPA, DMF, 3 days, r.t. (50-70%).

The macrocyclization of 4-(*p*-N-Boc-aminophenoxy)phthalonitrile **2.10** under similar conditions as described above, followed by acidic deprotection of N-Boc group using TFA, gave tetra-amino ZnPc **2.15** as a mixture of regioisomers, in 20 % yield (Scheme 2.2). The quaternization of amino groups using excess iodomethane gave ZnPc **2.16** in 82% yield.

Using a similar strategy, the di-amino ZnPc **2.19** was synthesized from 4,5-di(N-Boc-phenoxyl)phthalonitrile **2.18** and 4-*tert*-butylphthalonitrile (Scheme 2.3). The A_3B-type ZnPc **2.19** was isolated in 9% yield after TFA deprotection of N-Boc groups. The octa-amino ZnPc **2.21** was achieved in 50% yield from self condensation of phthalonitrile **2.18**. The quaternization of the amino groups on ZnPcs **2.19** and **2.21** using a large excess of iodomethane gave the subsequent cationic ZnPcs **2.20** and **2.22** in 50-90% yields.

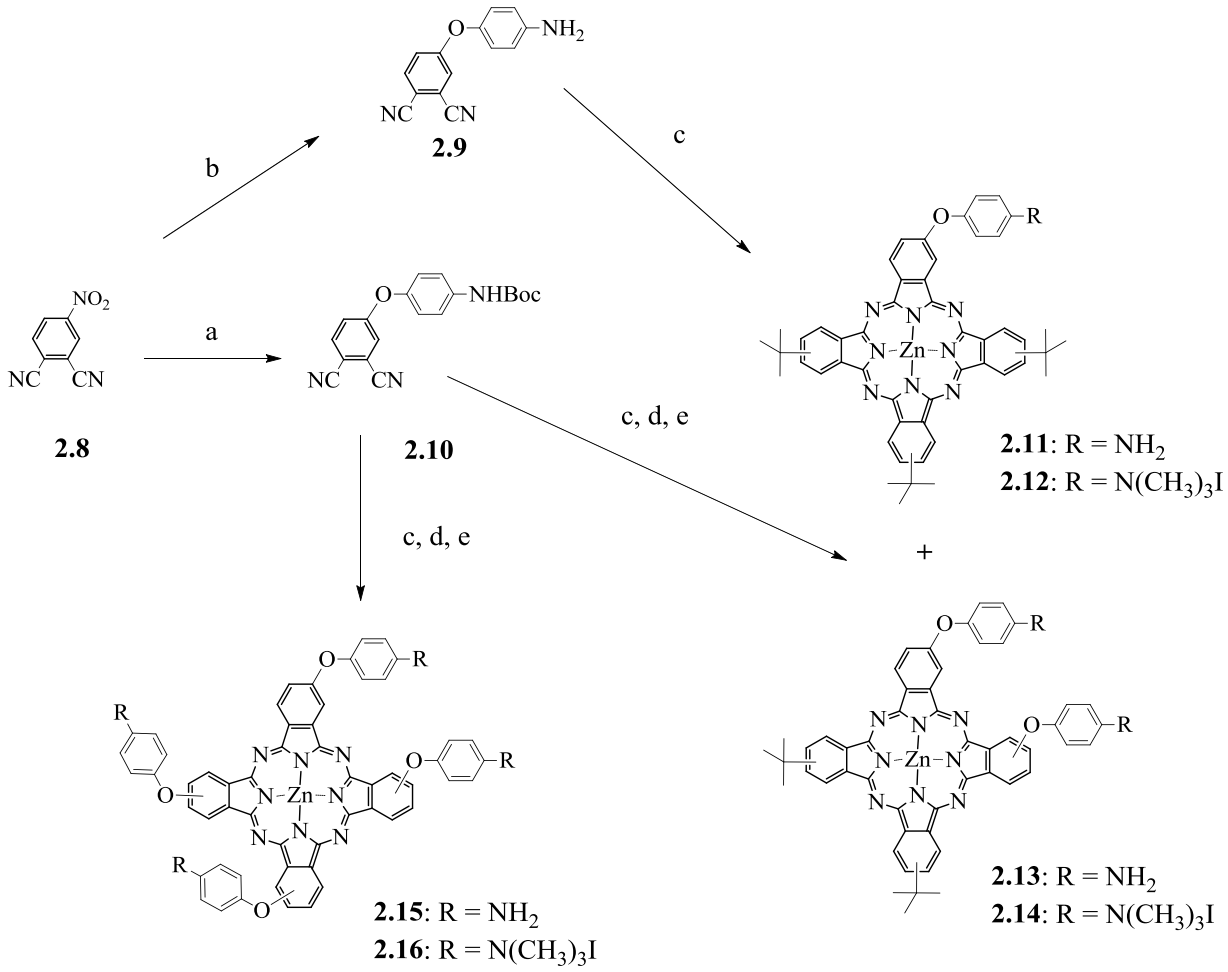

Scheme 2.2. Synthesis of mono-, di- and tetra-cationic β-trimethylphenoxy-substituted ZnPcs **2.12**, **2.14**, and **2.16**. Reagents and conditions: (a) K_2CO_3, DMF, 65 °C, 24 h (87%); (b) K_2CO_3, DMF, 63 °C, 4 h (73%); (c) 4-*tert*-butylphthalonitrile, $Zn(OAc)_2$, DMAE, 140 °C, 5 h (9-50%); (d) DCM/TFA, 0 °C, 4 h (quantitative); (e) CH_3I, DIPA, DMF, 3 days, r.t. (50-90%).

All the Pcs synthesized in this Chapter are a mixture of isomers, as discussed in Chapter 1, except Pc **2.21**. In order to decrease the number of isomers, adjacent-substituted di-aminophenoxy-Pcs **2.24** and **2.26** were synthesized (Schemes 2.4 and 2.5). The diphthalonitrile **2.23**, linked *via* the *ortho* positions of biphenyl, was synthesized according to a literature procedure.[29] The bis-phthalonitrile prevented the formation of the trans-ABAB Pc species and reduced the number of probable regioisomers in the

cyclotetramerization reaction from fifteen to only three. The trimethylation of the amino groups on ZnPcs **2.24** and **2.26** using excess of iodomethane gave the subsequent cationic ZnPcs **2.25** and **2.27** in 80-90% yields.

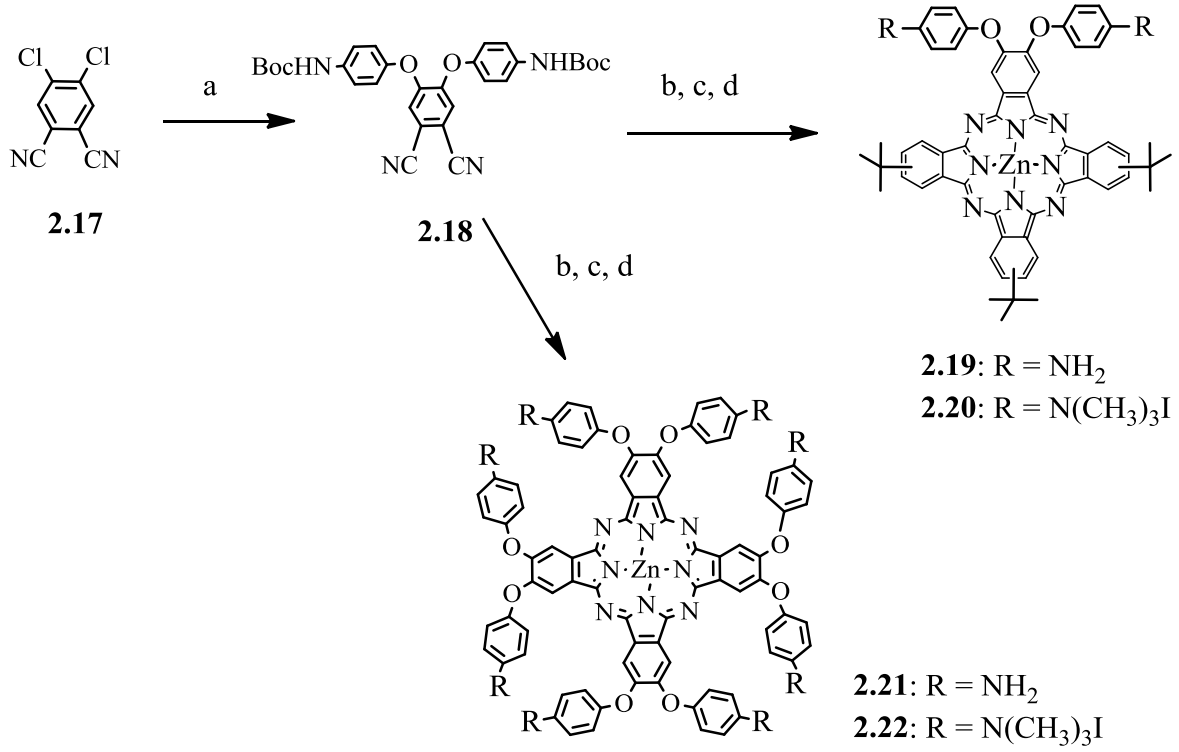

Scheme 2.3. Synthesis of β-substituted di- and octa-cationic ZnPcs **2.20** and **2.22**. Reagents and conditions: (a) K_2CO_3, DMF, 63 °C, 24 h (83%); (b) 4-*tert*-butylphthalonitrile, $Zn(OAc)_2$, DMAE, 140 °C, 5 h (15-50%); (c) DCM/TFA, 0 °C, 4 h (quantitative); (d) CH_3I, DIPA, DMF, 3 days, r.t. (50-70%).

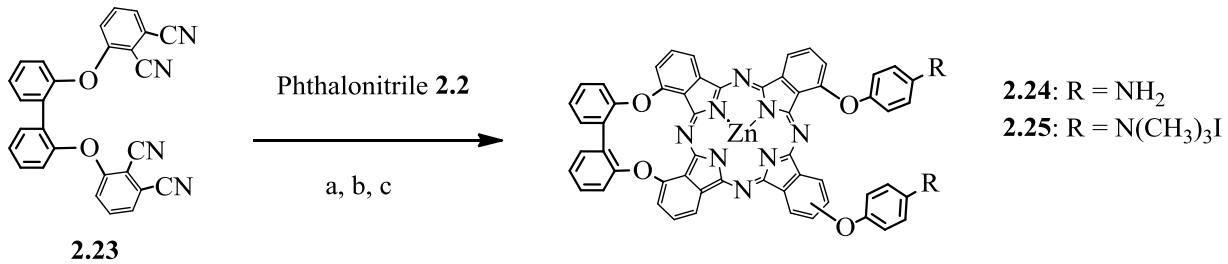

Scheme 2.4. Synthesis of cis-A_2B_2 α-substituted di-cationic ZnPc **2.25**. Reagents and conditions: (a) 3-(4-N-Boc-aminophenoxy)phthalonitrile, $Zn(OAc)_2$, DMAE, 140 °C, 5 h (13.9%); (b) DCM/TFA, 0 °C, 4 h (quantitative); (c) CH_3I, DIPA, DMF, 3 days, r.t. (53.3%).

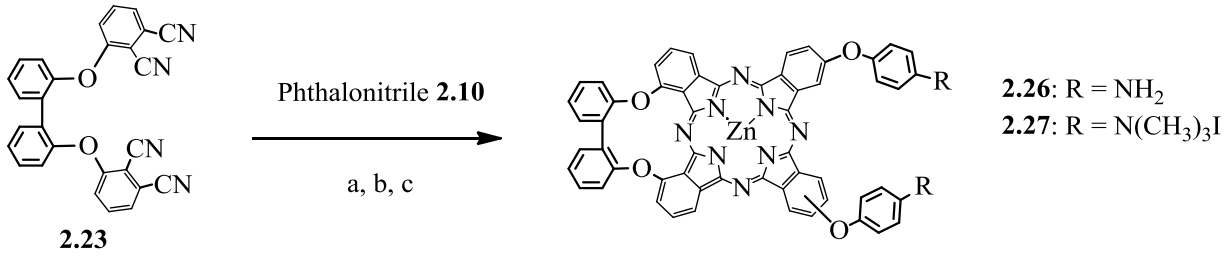

Scheme 2.5. Synthesis of cis-A_2B_2 β-substituted di-cationic ZnPc **2.27**. Reagents and conditions: (b) 4-(4-N-Boc-aminophenoxy)phthalonitrile, $Zn(OAc)_2$, DMAE, 140 °C, 5 h (11.4%); (b) DCM/TFA, 0 °C, 4 h (quantitative); (c) CH_3I, DIPA, DMF, 3 days, r.t. (58.3%).

2.3. Spectroscopic and Photophysical Characterization

The solubility in polar organic solvents such as DMSO, DMF, THF, and methanol of all cationic ZnPcs **2.5**, **2.7**, **2.12**, **2.14**, **2.16**, **2.20**, **2.22**, **2.25** and **2.27** was investigated. They were all soluble in these solvents. Captivatingly, the solubility of these ZnPcs in organic solvents was observed to reduce with increase in cationic charge, whereas their solubilityin water increased with cationic charge (**2.5 ~ 2.12 ~ 2.7 ~ 2.20 ~ 2.25 ~ 2.27 < 2.14 < 2.16 < 2.22**). The tetra- and octa-cationic ZnPcs **2.16** and **2.22** precipitated after quaternization reaction in DMF and DIPA and therefore, were easily isolated upon exhaustive methylation. After removal of reaction solvent, the solids were washed with acetone to remove the base and excess iodomethane. Only Pcs **2.14**, **2.16** and **2.22** were water-soluble: Pc **2.22** at 2.69×10^{-3} M, Pc **2.16** at 4.75×10^{-3} and Pc **2.14** at 4.03×10^{-3} M in distilled water. In addition, Pc **2.22** was highly hygroscopic. The other Pcs remained aggregated in water, even after sonicating them. Nevertheless, all the Pcs remained soluble when diluted from concentrated stocks in DMF or DMSO into PBS (final DMF or DMSO concentration of 1%) at 10 μM concentrations.

The N-Methylated Pcs are known to be sensitive to heat and therefore, require special handling.[37] After the trimethylation reactions, the solvent and the base were

removed at temperatures < 50 °C to avoid loss of N-methyls and immediately followed by their NMR and MS characterization. MS analyses revealed that the ZnPcs can be readily N-demethylated; for example, the mass spectrum of ZnPc **2.22** displayed a large number of fragments, dominated by a peak at *m*/*z* 1671.679 $[M\text{-}8I\text{-}7CH_3]^+$. N-Demethylation of these cationic ZnPcs was also observed upon prolonged storage at room temperature.[38]

The ZnPcs were characterized by NMR, using mainly deuterated DMF solvent since it dissolved most Pcs. The complexity of the ^{1}H- and ^{13}C-NMR spectra of ZnPcs **2.5**, **2.7**, **2.12**, **2.14** and **2.16** (Appendix A.2 – A.6), suggested the presence of various regioisomers (up to fifteen for the di-cationic ZnPcs), which was expected for the cyclotetramerization reaction of two mono-substituted phthalonitriles, and also in agreement with the observations from reversed-phase HPLC. The ^{1}H-NMR of the N-Boc-protected Pc precursors, gave two sets of signals were observed for the *tert*-butyl protons on the macrocycle (centered at ~ 1.9 ppm) and the N-Boc group(s) (centered at ~ 1.5 ppm). Notably, the α-substituted N-Boc Pc-precursors had two sets of signals for the N-Boc group (centered at 1.4 and 1.5 ppm), while the β-substituted N-Boc protected Pc precursors had only one set centered at 1.6 ppm. The N-Boc precursors of Pcs **2.24**, and **2.26** gave similar results. Equally, the mono- and di-cationic ZnPcs exhibited distinct variations in their chemical shifts of the $-N(CH_3)_3$ protons, possibly due to macrocycle distortion and/or hindered rotation. This is illustrated by the β-substituted ZnPc **2.12**, which had only one singlet for the $N(CH_3)_3$ protons at 3.98 ppm, while the α-substituted ZnPc **2.5** (Figure 2.2) exhibited two singlets at 3.62 and 3.72 ppm. In the same way, the di-cationic β-substituted ZnPc **2.20** (Figure 2.3) showed only one singlet for the $N(CH_3)_3$ protons at 3.96 ppm, while each of the di-cationic **2.7** and **2.14** had several signals.

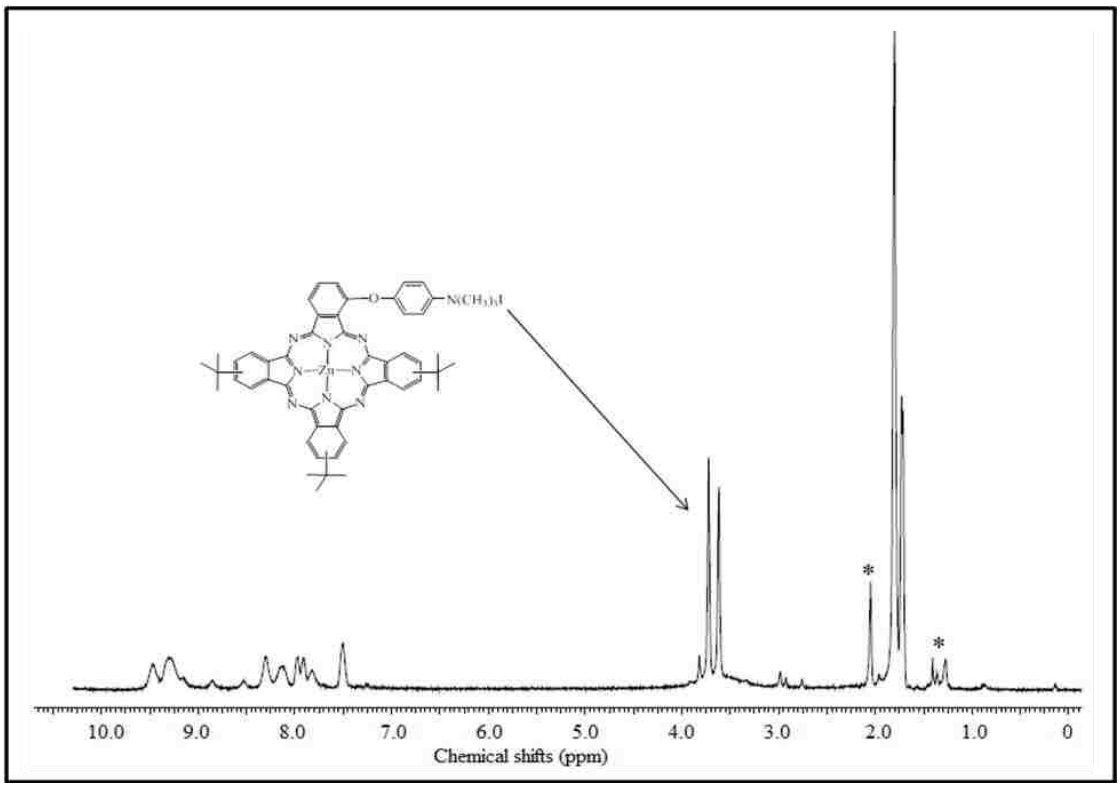

Figure 2.2. ^{1}H NMR spectrum of ZnPc **2.5** at 400 MHz (* denotes solvent).

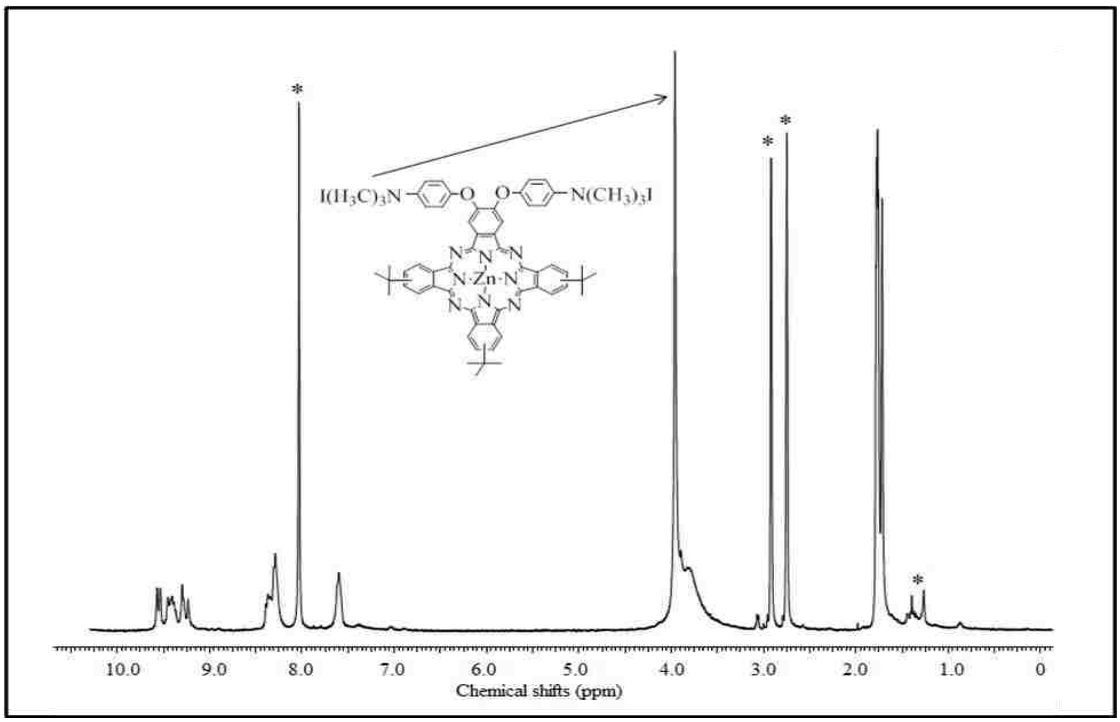

Figure 2.3. ^{1}H NMR spectrum of ZnPc **2.20** at 400 MHz (* denotes solvent).

The spectroscopic properties of cationic ZnPcs **2.5**, **2.7**, **2.12**, **2.14**, **2.16**, **2.20**, **2.22**, **2.25** and **2.27** in DMF and PBS at pH 7.4 were investigated and summarized in Tables 2.1 and 2.2 respectively. All the ZnPcs showed strong absorption Q-bands between 680-686 nm and emissions between 682-689 nm in DMF solvent. In PBS (pH 7.4), the bands were broader and less intense. The fluorescence was also quenched, indicating aggregation (Figure 2.4). The Stokes' shifts were in the range of 2-4 nm (Table 2.1 and 2.2) in both DMF and PBS. Only minor red shifts (1-5 nm) were observed in the absorption bands of the α- versus the β-substituted ZnPcs. The Pcs did not aggregate at concentrrations up to 8.8 µM in DMF. Within this range, all the ZnPcs showed a Soret absorption band between 330 – 370 nm, a strong Q-band centered at ~ 684 nm and two vibrational bands at around 620 and 650 nm. The bands strictly followed the Lambert-Beer law, which is characteristic of non-aggregated Pcs in DMF (Figure 2.5).[39]

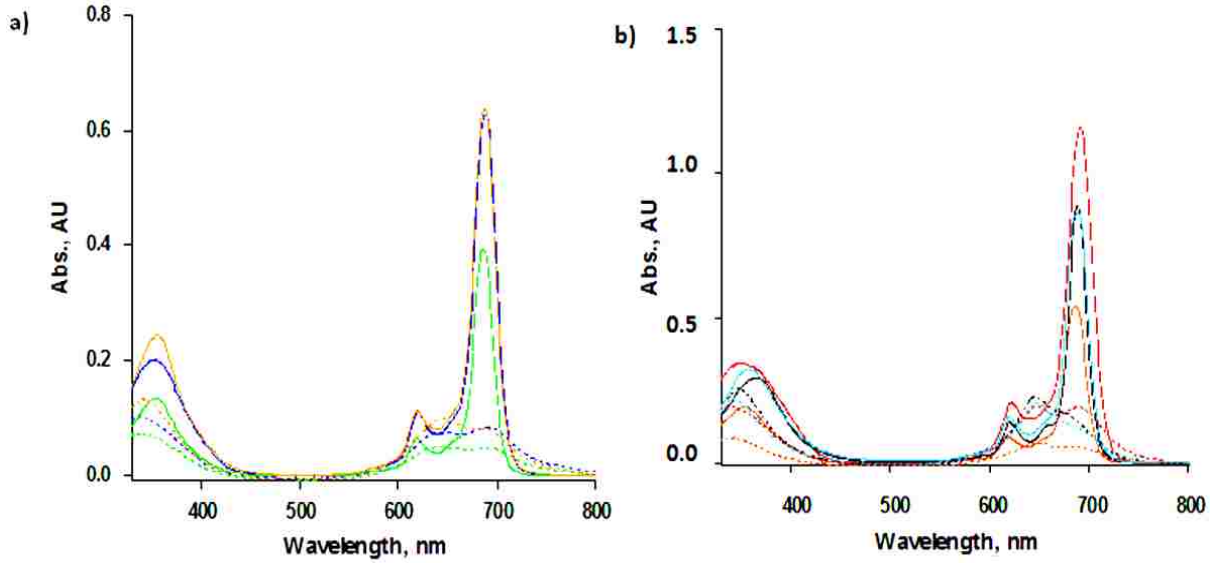

Figure 2.4. UV-Vis spectra for **a)** Pc **2.5** (blue), **2.12** (green), and **2.20** (orange) at 8.8 µM in DMF; **2.5** (dotted blue), **2.12** (dotted green), and **2.20** (dotted orange) at 8.8 µM in PBS, pH 7.4. **b)** Pc **2.7** (red), **2.14** (brown), **2.16** (violet) and **2.22** (black) at 8.8 µM in DMF; **2.7** (dotted red), **2.14** (dotted brown), **2.16** (dotted violet) and **2.22** (dotted black) at 8.8 µM in PBS, pH 7.4.

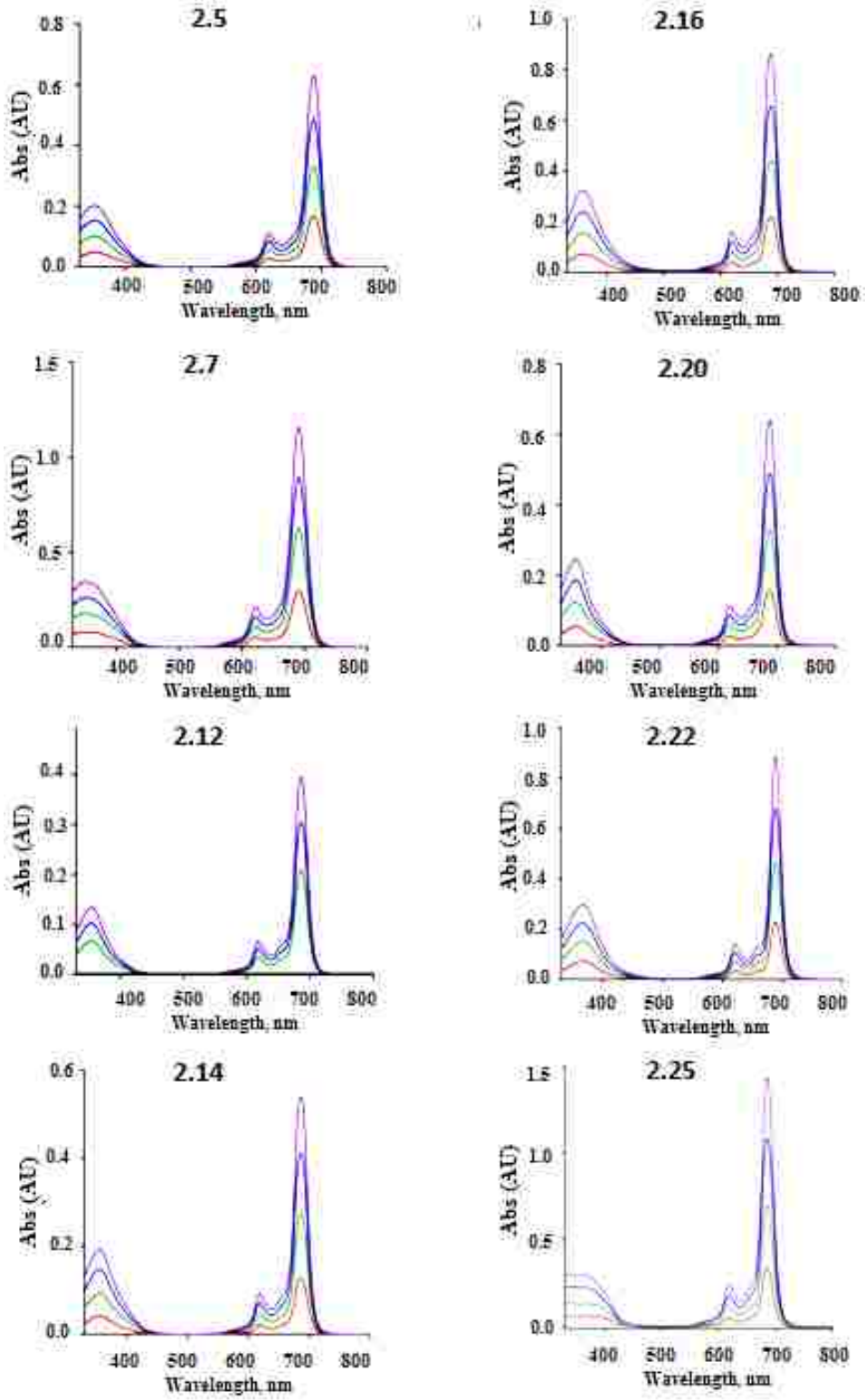

Figure 2.5. UV-Vis spectra for Pc **2.5**, **2.7**, **2.12**, **2.14**, **2.16**, **2.20**, **2.22**, and **2.25** in DMF: 2.0 µM (red), 4.0 µM (green), 6.0 µM (blue) and 8.0 µM (purple).

The ZnPcs at 1000 μM concentrations in DMF showed no evidence for colloidal solution formation, indicating that no large aggregates were formed.[40] The fluorescence quantum yields for the ZnPcs were determined in the same solvent and all compounds had fluorescence quantum yields in the range 0.11-0.21 (Table 2.1), characteristic of this type of compound.[40-42]

The determination of singlet oxygen quantum yields using ZnPc as the reference and 1,3-diphenylisobenzofuran (DPBF) as the scavenger of singlet oxygen was accomplished in DMF.[43] The absorption decay of DPBF measured at 417 nm was used to calculate the singlet oxygen quantum yields, within accuracy of ~ 10% (Table 2.1). The mono-cationic ZnPc **2.5** (0.47) gave the highest quantum, yield while that of ZnPc **2.20** (0.16) was the lowest. This suggests that synthesized series of ZnPcs consists of efficient producers of singlet oxygen and therefore, could find application as PDT photosensitizers. The di-cationic ZnPc **2.14** may find use in PDT due to its high $^1O_2$ quantum yields.

Table 2.1. Spectral properties of ZnPcs **2.5**, **2.7**, **2.12**, **2.14**, **2.16**, **2.20**, **2.22**, **2.25** and **2.27** in DMF at room temperature. a: excitation at 640 nm; b: calculated using ZnPc (Φ_f = 0.17) as the standard; c: calculated using ZnPc (Φ_Δ = 0.56) as the standard in DMF.

ZnPc	Absorption λ_{max} (nm)	Emission[a] λ_{max} (nm)	Stokes shift (nm)	Φ_f[b]	Φ_Δ[c]
2.5	684	686	2	0.16	0.47
2.7	686	689	3	0.21	0.31
2.12	683	687	4	0.13	0.33
2.14	683	686	3	0.18	0.44
2.16	684	687	3	0.13	0.35
2.20	684	687	3	0.19	0.16
2.22	686	688	2	0.13	0.28
2.25	685	687	2	0.11	0.33
2.27	680	682	2	0.14	0.22

Table 2.2. Spectral properties of ZnPcs **2.5**, **2.7**, **2.12**, **2.14**, **2.16**, **2.20**, **2.21**, **2.22**, **2.25** and **2.27** in PBS (pH = 7.4) at room temperature.

ZnPc	Absorption λ_{max} (nm)	Emission[a] λ_{Em} (nm)	Stokes shift (nm)
2.5	679	681	2
2.7	680	684	4
2.12	677	680	3
2.14	678	681	3
2.16	679	682	3
2.20	678	681	3
2.21	682	685	3
2.22	680	684	4
2.25	680	683	3
2.27	677	679	2

a: excitation at 630 nm.

2.4. Cellular Studies

The *in vitro* properties including the time-dependent cellular uptake, cytotoxicity and intracellular localization for this series of cationic ZnPcs, were investigated in human carcinoma HEp2 cells. The cytotoxicity of the ZnPcs was evaluated using the Promega's CellTiter Blue viability assay, as previously reported in litetrature,[15] at concentrations up to 400 μM for each positively charged ZnPc and for the octa-amino-Pc **2.21**. The results from these studies are summarized in Table 2.3. The IC_{50} values for the ZnPcs were calculated from dose-response curves. The cytotoxicity for ZnPcs is considerably varied and it depends not only on the number of charges but also on the Pc's substitution site, i.e. on α- vs. β-substitution. While it has been previously reported that a mono-cationic porphyrin bearing one $-N(CH_3)_3^+$ group[15] and a mono-cationic Pc with a $-NH_3^+$ group,[25] gave high phototoxicities, this series of Pcs has di-cationic as the most phototoxic photosensitizers, and in particular the α-substituted Pcs.

The compounds showed low dark cytotoxicity with calculated IC_{50} > 150 μM. The mono- and di-cationic ZnPcs were phototoxic toward HEp2 cells at 1.5 J/cm^2 light dose. The most phototoxic were the di-cationic ZnPcs **2.7** ~ **2.25** > **2.27** ~ **2.14** > **2.20** with determined IC_{50} of 2.7, 2.7, 12.1, 13.4 and 39.6 μM, respectively, followed by mono-cationic ZnPc **2.5** with IC_{50} of 46.3 μM. The other Pcs showed IC_{50} > 100 μM at 1.5 J/cm^2, including the mono-cationic **2.12** and the octa-amino-Pc **2.21**. There was no correlation between phototoxicity observed for the ZnPcs and the determined single oxygen quantum yields, because in addition to $^1O_2$ other ROS can be involved in the observed photo-induced cytotoxicity, and their site(s) of generation will also determine the mechanisms and efficacy of cell death. It is very interesting to note that the α-substituted Pcs (i.e. **2.5**, **2.7** and **2.25**) were considerably more phototoxic (ca. 5-fold enhancement) than their β-substituted analogs.

Additionally, there was no major variation in the phototoxicity of the di-cationic ZnPcs **2.7** and **2.25**, nor of ZnPcs **2.14** and **2.27**, even if ZnPcs **2.7** and **2.14** were mixtures of about 15 regioisomers, containing both the cis-A_2B_2 and trans-ABAB macrocycles, while **2.25** and **2.27** were mixtures of 3 regioisomers of only the cis-A_2B_2 type. These results suggest that the cis-A_2B_2 ZnPcs were the most phototoxic of this series. Moreover, ZnPc **2.7** bearing the di-cationic charges on both adjacent and opposite benzene rings was 15-fold more phototoxic than ZnPc **2.20** bearing di-cationic charges on the same benzene ring, further indicating the imortance of the α- vs. β-substitution on Pc phototoxicity. Amongst all the ZnPcs investigated, **2.7** and **2.25** were the most phototoxic and to had the highest dark cytotoxicity/phototoxicity ratio of > 120. This makes it the most promising candidate for PDT applications.

Table 2.3. Dark and phototoxicity (at 1.5 J/cm^2 light dose) of ZnPcs **2.5**, **2.7**, **2.12**, **2.14**, **2.16**, **2.20**, **2.22**, **2.25** and **2.27** toward HEp2 cells using the Cell Titer Blue assay.

ZnPc	Dark toxicity IC_{50} (μM)	Phototoxicity IC_{50} (μM)	Ratio
2.5	> 400	46.3	> 9
2.7	344	2.7	128
2.12	> 400	> 100	> 4
2.14	156	13.4	12
2.16	> 400	> 100	> 4
2.20	> 400	39.6	> 10
2.21	> 400	> 100	> 4
2.22	> 400	> 100	> 4
2.25	> 400	2.7	> 148
2.27	> 400	12.1	> 33

Considerable differences were also observed in the cellular uptake of this series of ZnPcs, as shown in Figure 2.6. All the ZnPcs exhibited similar uptake patterns with rapid accumulation within a short period followed by a plateau, which was reached 1-2 h after Pc exposure. The octa-amino-Pc **2.21** accumulated the highest cellular uptake, possibly due to its higher hydrophobicity compared with the other cationic ZnPcs. Of all the postively charged ZnPcs, the di-cationic ZnPc **2.20** had the highest uptake values at all time points investigated, while the tetra-cationic Pc **2.16** had the lowest uptake. From these results, it can be concluded that the amphiphilicity of the cationic Pcs plays a crucial role on the extent of their cellular uptake, which is in concurrence with previous literature reports;[15,25,44] in the porphyrin series, the di-cationic macrocycles were also found to accumulate the most within HEp2 cells. The two positive charges on the β-positions of a single isoindole unit in ZnPc **2.20** confers higher amphiphilicity to the Pc compared with the regioisomeric mixtures in **2.7**, **2.14**, **2.25** and **2.27**, which enhances hydrophobic/hydrophilic interactions that lead to amplified cellular uptake.

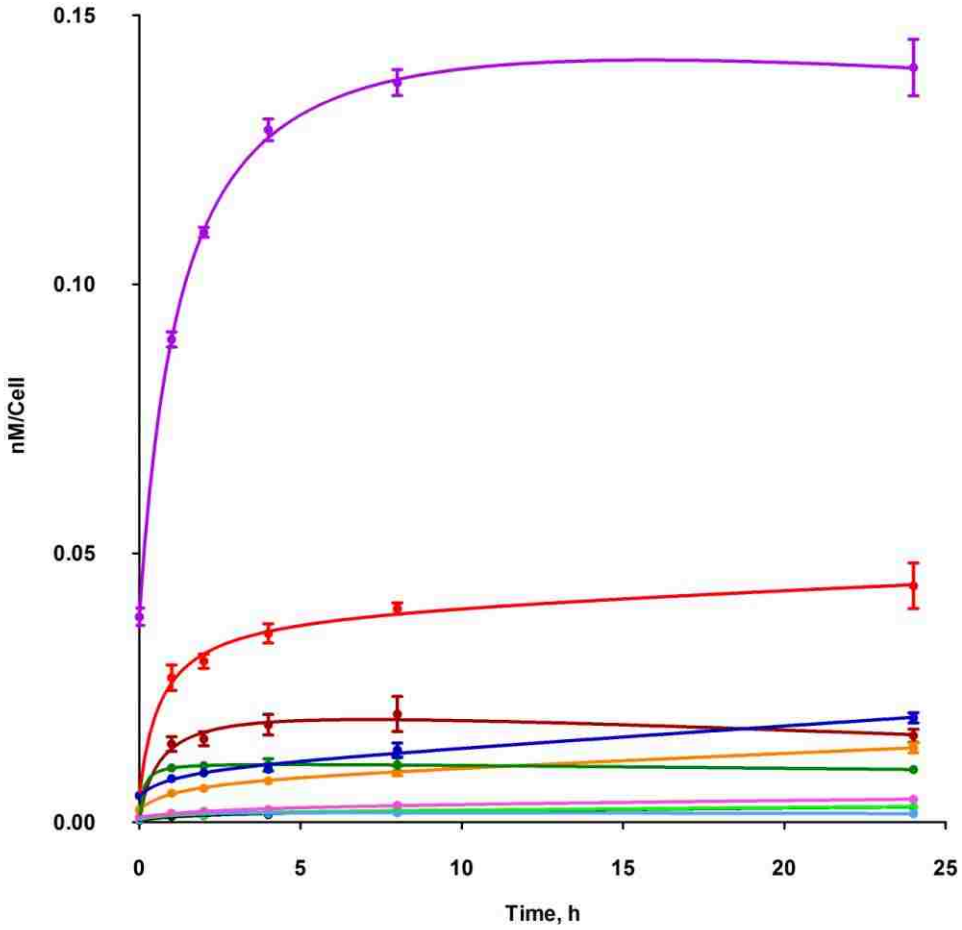

Figure 2.6. Time-dependent uptake of cationic Pcs at 10 μM by HEp2 cells: Pc **2.5** (black), **2.7** (orange), **2.12** (brown), **2.14** (green), **2.16** (light-blue), **2.20** (red), **2.21** (purple), **2.22** (dark-green), **2.25** (blue) and **2.27** (pink).

The main sites of localization of the cationic ZnPcs within the cells were also examined by fluorescence microscopy, upon exposure of HEp2 cells to 10 μM Pc for 6 h. Figures 2.7 – 2.11 show the fluorescent patterns observed for each cationic ZnPc. The co-localization investigations of the ZnPcs were accomplished using the organelle specific fluorescent probes: ER Tracker Blue/White (for endoplasmic reticulum, ER), MitoTracker Green (mitochondria), BODIPY Ceramide (golgi) and LysoSensor Green (lysosomes) to evaluate the main sites of localization within the cells. The di-cationic ZnPc **2.7** localized mainly in mitochondria, and to a lesser degree in the lysosomes and ER. The ZnPc **2.25**

localized mostly in the ER and lysosomes, but not in mitochondria. In contrast, the tetra- and octa-cationic Pcs **2.16** and **2.22** were largely located in mitochondria and to a lower degree in the Golgi; it was not found in the ER.

The di-cationic ZnPcs **2.14** and **2.20** were found mostly in the lysosomes and Golgi, respectively, and to a lesser degree in the ER. ZnPc **2.27** was also found mostly in the Golgi and ER. Nevertheless, the mono-cationic ZnPcs **2.5** and **2.12** were found largely in the lysosomes and Golgi, respectively, and were also localized in the ER. These results exhibit very diverse subcellular distributions for these cationic ZnPcs. This is possibly due their varied interactions with membranes in addition to other biological substrates, and probably their diverse cellular uptake mechanisms.

It had been previously observed that a octa-cationic-Pcs localized intracellularly mainly in the lysosomes,[19] and that cationic porphyrins bearing up to four charges were mainly found in mitochondria, ER and/or lysosomes.[13-15] The high phototoxicity observed for the ZnPcs **2.5**, **2.7**, **2.14**, **2.20**, **2.25** and **2.27** might possibly be, in part, due to their localization in the ER; some of these Pcs were also found in the mitochondria and/or the lysosomes. All these organelles are key targets for PDT-induced cell apoptosis.[45-47] It is interesting to note that the octa-amino Pc **2.21** was mainly found in mitochondria and Golgi, and to a lesser degree in lysosomes. No localization was observed for ZnPc **2.21** in the ER (Figure 2.12), in a similar case to the cationic ZnPcs **2.16** and **2.22**. These incredible results show that cationic ZnPcs are attaractive photosensitizers, which can be tuned to obtain amphiphilic drug agents. Di-cationic Pcs, particulaly α-substituted ones, have been shown to be promising PDT candidates. The subcellular localization of the cationic Pcs is shown in Figures 2.7 – 2.11.

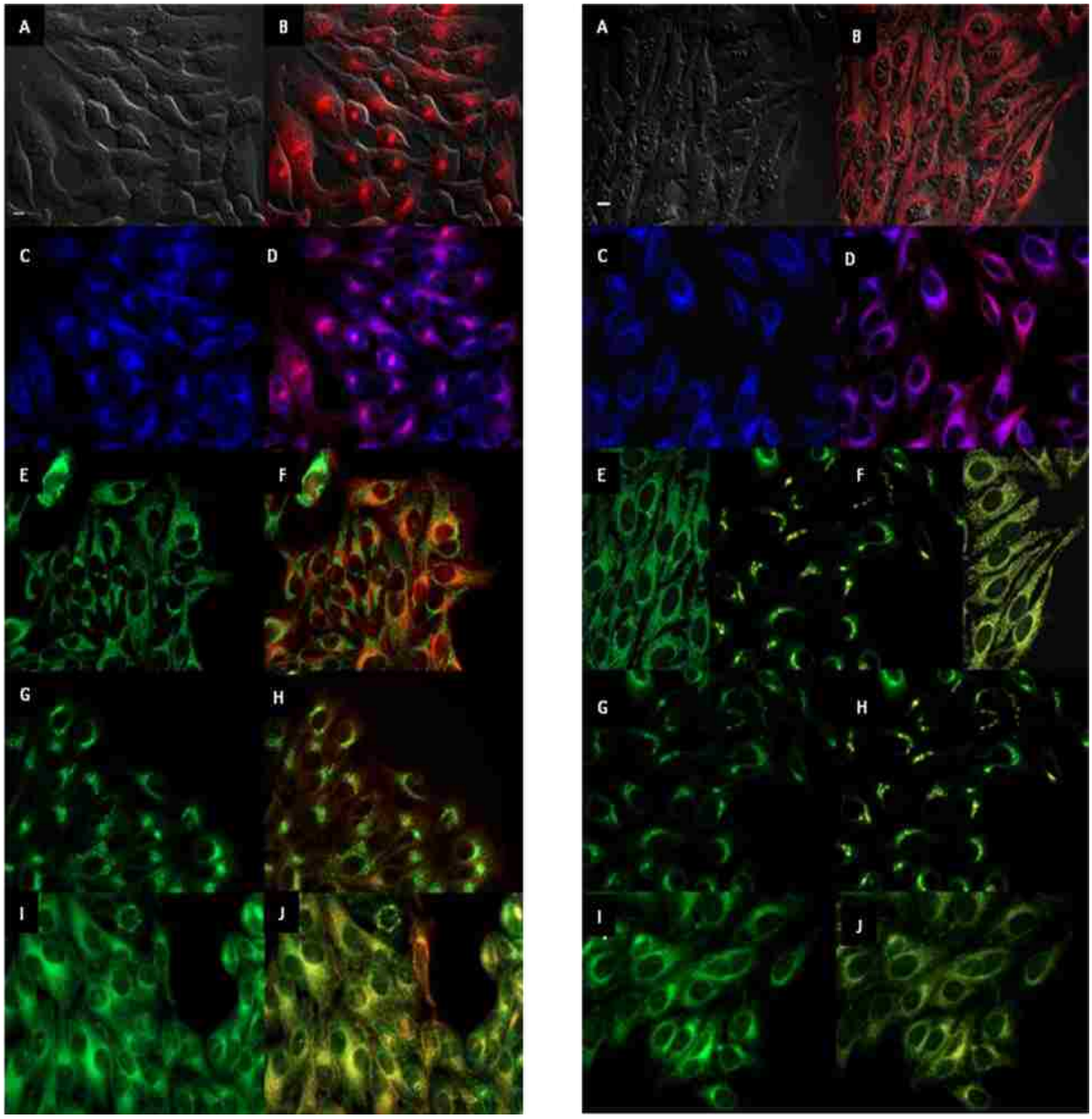

a) **b)**

Figure 2.7. Subcellular localization: **a)** Pc **2.5** in HEp2 cells at 10 μM for 6 h: (A) Phase contrast, (B) Overlay of **2.5** and phase contrast, (C) ER tracker Blue/White fluorescence, (E) MitoTracker Green fluorescence, (G) BoDIPY Ceramide, (I) LysoSensor Green fluorescence, and (D, F, H, J) overlays of organelle tracers with compound fluorescence. Scale bar: 10 μm. **b)** Pc **2.7** in HEp2 cells at 10 μM for 6 h: (A) Phase contrast, (B) Overlay of **2.7** and phase contrast, (C) ER tracker Blue/White fluorescence, (E) MitoTracker Green fluorescence, (G) BoDIPY Ceramide, (I) LysoSensor Green fluorescence, and (D, F, H, J) overlays of organelle tracers with compound fluorescence. Scale bar: 10 μm.

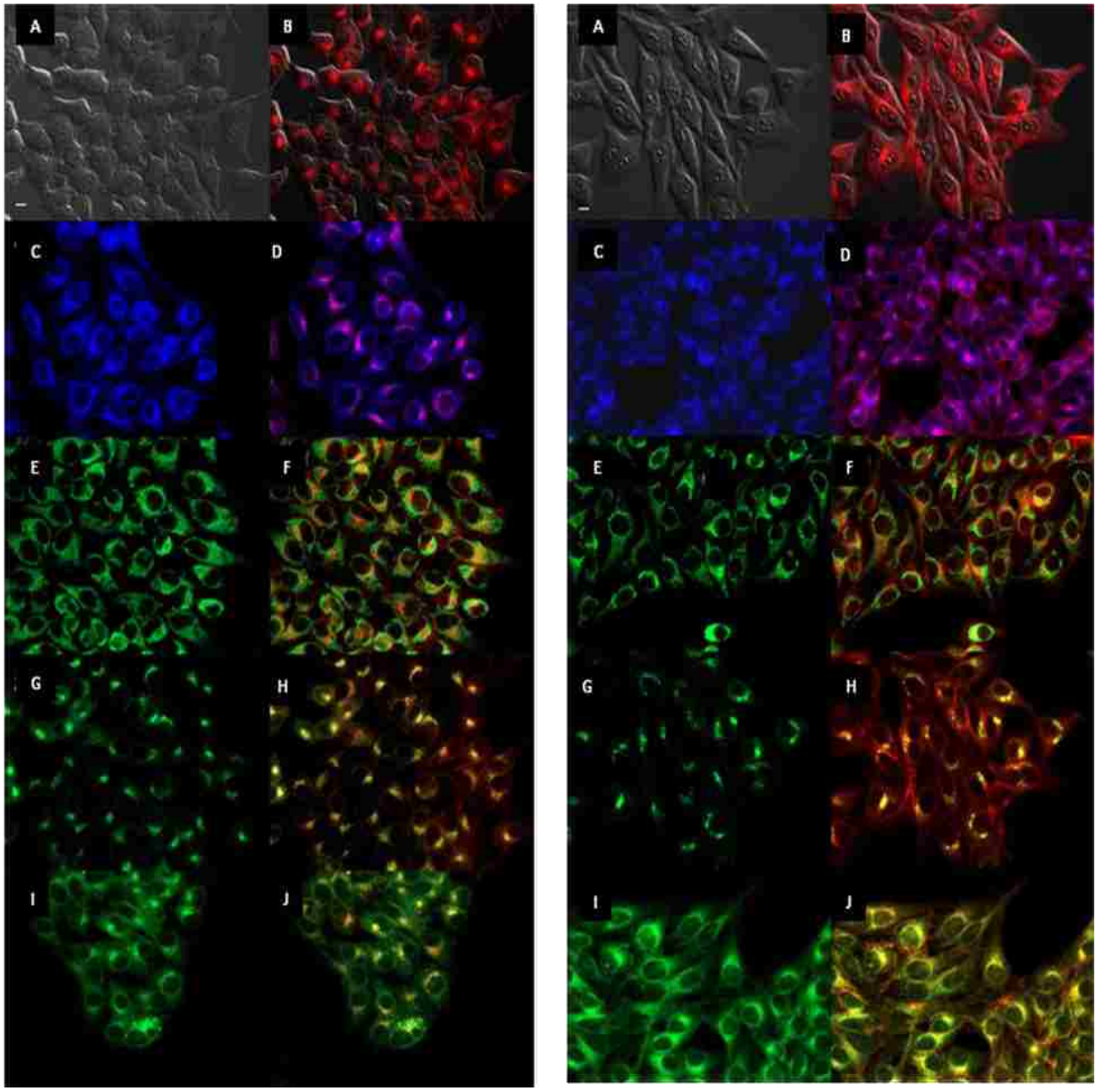

a) **b)**

Figure 2.8. Subcellular localization: **a)** Pc **2.12** in HEp2 cells at 10 µM for 6 h: (A) Phase contrast, (B) Overlay of **2.12** and phase contrast, (C) ER tracker Blue/White fluorescence, (E) MitoTracker Green fluorescence, (G) BoDIPY Ceramide, (I) LysoSensor Green fluorescence, and (D, F, H,J) overlays of organelle tracers with compound fluorescence. Scale bar: 10 µm. **b)** Pc **2.14** in HEp2 cells at 10 µM for 6 h: (A) Phase contrast, (B) Overlay of **2.14** and phase contrast, (C) ER tracker Blue/White fluorescence, (E) MitoTracker Green fluorescence, (G) BoDIPY Ceramide, (I) LysoSensor Green fluorescence, and (D, F, H,J) overlays of organelle tracers with compound fluorescence. Scale bar: 10 µm.

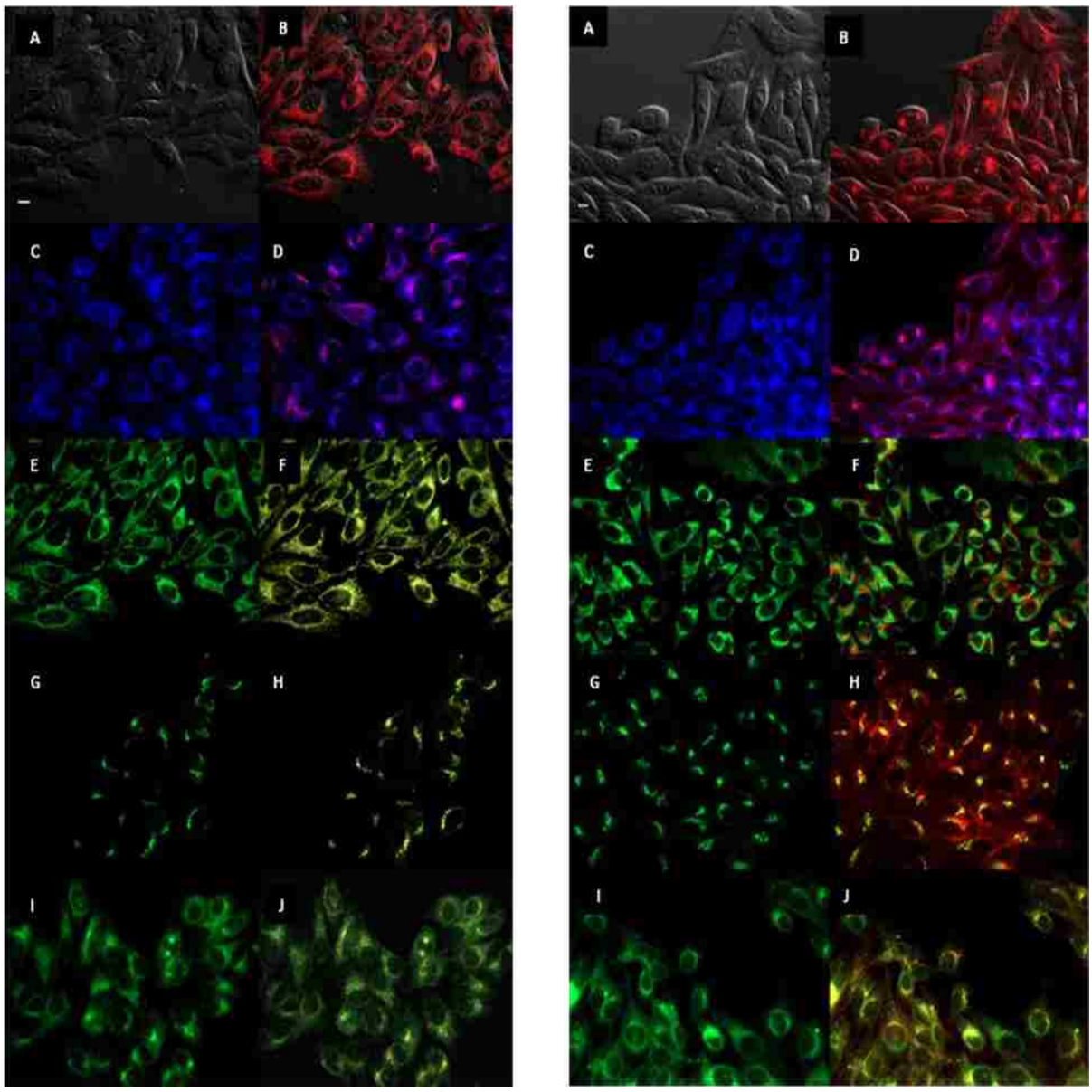

a) **b)**

Figure 2.9. Subcellular localization: **a)** Pc **2.16** in HEp2 cells at 10 µM for 6 h: (A) Phase contrast, (B) Overlay of **2.16** and phase contrast, (C) ER tracker Blue/White fluorescence, (E) MitoTracker Green fluorescence, (G) BoDIPY Ceramide, (I) LysoSensor Green fluorescence, and (D, F, H,J) overlays of organelle tracers with compound fluorescence. Scale bar: 10 µm. **b)** Pc **2.20** in HEp2 cells at 10 µM for 6 h: (A) Phase contrast, (B) Overlay of **2.20** and phase contrast, (C) ER tracker Blue/White fluorescence, (E) MitoTracker Green fluorescence, (G) BoDIPY Ceramide, (I) LysoSensor Green fluorescence, and (D, F, H,J) overlays of organelle tracers with compound fluorescence. Scale bar: 10 µm.

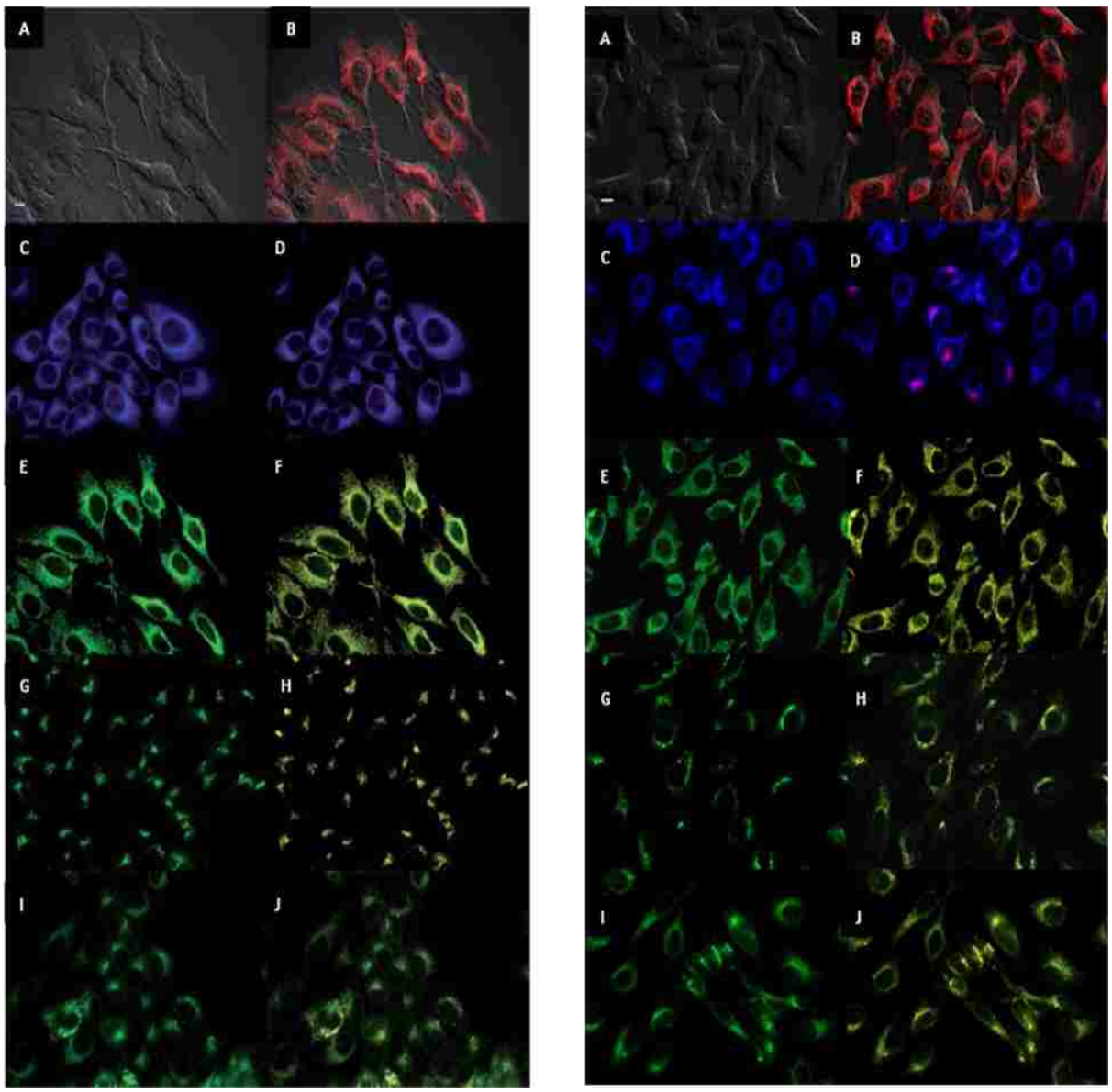

a) **b)**

Figure 2.10. Subcellular localization: **a)** Pc **2.21** in HEp2 cells at 10 µM for 6 h: (A) Phase contrast, (B) Overlay of **2.21** and phase contrast, (C) ER tracker Blue/White fluorescence, (E) MitoTracker Green fluorescence, (G) BoDIPY Ceramide, (I) LysoSensor Green fluorescence, and (D, F, H,J) overlays of organelle tracers with compound fluorescence. Scale bar: 10 µm. **b)** Pc **2.22** in HEp2 cells at 10 µM for 6 h: (A) Phase contrast, (B) Overlay of **2.22** and phase contrast, (C) ER tracker Blue/White fluorescence, (E) MitoTracker Green fluorescence, (G) BoDIPY Ceramide, (I) LysoSensor Green fluorescence, and (D, F, H,J) overlays of organelle tracers with compound fluorescence. Scale bar: 10 µm.

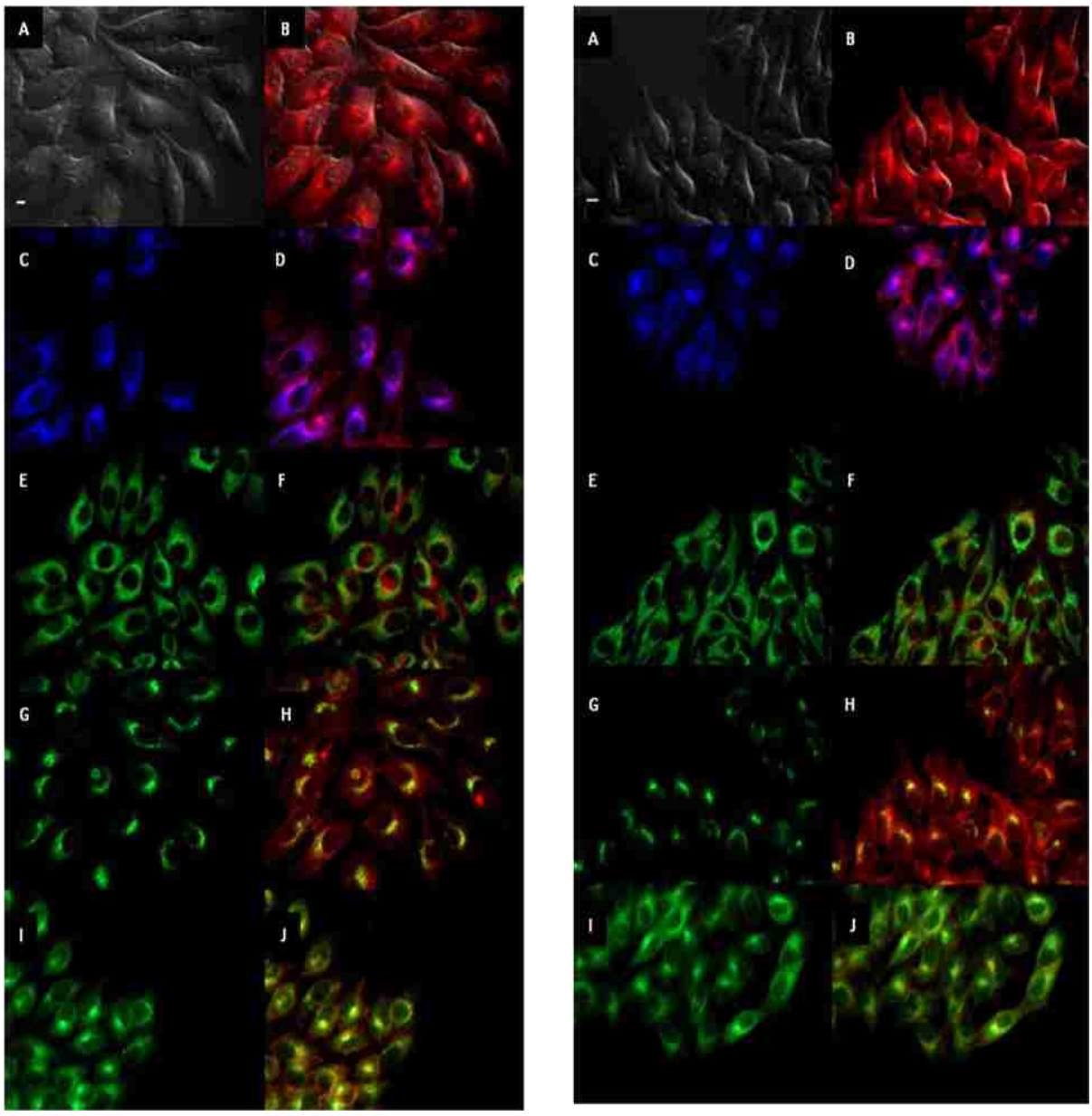

a) **b)**

Figure 2.11. Subcellular localization: **a)** Pc **2.25** in HEp2 cells at 10 µM for 6 h: (A) Phase contrast, (B) Overlay of **2.25** and phase contrast, (C) ER tracker Blue/White fluorescence, (E) MitoTracker Green fluorescence, (G) BoDIPY Ceramide, (I) LysoSensor Green fluorescence, and (D, F, H,J) overlays of organelle tracers with compound fluorescence. Scale bar: 10 µm. **b)** Pc **2.27** in HEp2 cells at 10 µM for 6 h: (A) Phase contrast, (B) Overlay of **2.27** and phase contrast, (C) ER tracker Blue/White fluorescence, (E) MitoTracker Green fluorescence, (G) BoDIPY Ceramide, (I) LysoSensor Green fluorescence, and (D, F, H,J) overlays of organelle tracers with compound fluorescence. Scale bar: 10 µm.

2.5. Conclusions

The syntheses and characterizations of a series of nine cationic ZnPcs are described. All ZnPcs were synthesized by a one-step cyclotetramerization of one or two phthalonitriles and consequently are mixtures of regioisomers, except for the octa-cationic and symmetrical ZnPc **2.22**. The positive charges conferred by the trimethylaminophenoxy substituents and the presence of bulky *tert*-butyl groups in Pcs **2.5**, **2.7**, **2.12**, **2.14** and **2.20** induced high solubility in polar organic solvents. In contrast, ZnPcs **2.25** and **2.27** were obtained using a biphenyl-linked diphthalonitrile and consequently consist of only the cis-A_2B_2 Pc regioisomers. The cytotoxicity of this series of compounds was dependent both on the number of charges, and on their site of substitution (α vs. β) on the Pc isoindole units.

The amphiphilicity of the molecules strongly affected their uptake bby the cells; the amphiphilic di-cationic ZnPc **2.20** accumulated the most within cells, it had reasonable phototoxicity (IC_{50} = 39.6 μM at 1.5 J/cm^2) and was preferentially locallized in the Golgi apparatus. Of all the ZnPcs synthesized, the di-cationic α-substituted ZnPcs **2.7** and **2.25** exhibited the highest phototoxicity (IC_{50} = 2.7 μM at 1.5 J/cm^2). The partial localization of the ZnPcs in the ER, and the highest ratio (> 120) for their dark cytotoxicity/phototoxicity, make them the most promising agents for PDT applications.

The tetra- and octa-cationic ZnPcs had very low cytotoxicities and were mainly found in the mitochondria, suggesting a possibility for application as mitochondria delivery vehicles for therapeutic agents. This Chapter presents a comprehensive study of cationic ZnPcs, with attractive features that may be exploited in imaging or PDT. Most of the Pcs synthesized here are soluble in polar organic solvents and aqueous media.

2.6. Experimental Section

2.6.1. Chemistry

All the reagents and solvents were obtained from commercial sources and used directly without further purification. Silica gel 60 (230×400 mesh) and alumina neutral (activity I, 50-200 μm) from Sorbent Technologies were used for column chromatography. Sephadex G-100 and LH-20 were obtained from Amersham Biosciences. Analytical thin-layer chromatography (TLC) was carried out using polyester backed TLC plates 254 (pre-coated, 200 μm) from Sorbent Technologies. NMR spectra were recorded on an AV-400 LIQUID Bruker spectrometer (400 MHz for ^{1}H, 100 MHz for ^{13}C). Chemical shifts are reported in δ (ppm) using the following deuterated solvents as internal references: Acetone-d_6 2.05 ppm (^{1}H), 29.92 ppm (^{13}C); DMF-d_7 8.03 ppm (^{1}H), 163.15 ppm (^{13}C); Pyridine-d_5 7.58 ppm (^{1}H), 135.91 ppm (^{13}C); D_2O 4.80 ppm (^{1}H); THF-d_8 3.58 ppm (^{1}H), 67.57 ppm (^{13}C); CD_2Cl_2 5.32 ppm (^{1}H), 54.00 ppm (^{13}C); $CDCl_3$ 7.27 ppm (^{1}H), 77.23 ppm (^{13}C). The HPLC analyses were performed on a Dionex system fitted with a P680 pump and UVD340U detector. Electronic absorption spectra were measured on a PerkinElmer, Lambda 35 UV-Vis spectrometer and emission spectra were measured on a Fluorolog® HORIBA JOBIN YVON (Model LFI-3751) spectrofluorimeter. Dithranol matrix was used for MALDI-TOF mass spectra measurement on a Bruker ProFlex III spectrometer; high-resolution ESI mass spectra (HRMS-ESI) were obtained using an Agilent Technologies 6210 Time-of-Flight LC/MS spectrometer. Melting points were obtained using MEL-TEMP electrothermal instrument.

2.6.2. Synthesis of Phthalocyanines and Their Precursors

Mono-N-Boc-amino-phthalonitrile 2.3. A 3-nitrophthalonitrile **2.1** (2 g, 11.6 mmol) and 4-N-Boc-aniline (3.6 g, 17.0 mmol) mixture was dissolved in DMF (30 mL). Potassium

carbonate (2.5 g, 18.0 mol) was added to the solution in five portions and the mixture heated to 80 °C for 3 h. The reaction mixture was cooled to room temperature, poured into ice-cold water and filtered to obtain a solid. The solid was purified using alumina column chromatography, eluted with DCM to afford a white solid (3.1 g, 80.0%), mp 165 – 166 °C. ^{1}H NMR (acetone-d_6): δ 8.58 (br, 1H, NH), 7.80 (t, J = 8.2 Hz, 1H, Ar-H), 7.70 -7.66 (m, 3H, Ar-H), 7.25 – 7.14 (m, 3H, Ar-H), 1.48 (s, 9H, $C(CH_3)_3$). ^{13}C NMR (acetone-d_6): δ 162.1, 153.7, 149.4, 138.6, 136.2, 128.1, 121.7, 121.5, 120.7, 117.4, 116.2, 113.8, 105.9 (Ar-C, CN), 80.2, 28.4 ($C(CH_3)_3$). HRMS-ESI: m/z 336.1340 $[M+H]^+$, calcd. for $[C_{19}H_{18}N_3O_3]^+$ 336.1342; 353.1604 $[M+H_2O]^+$, calcd. for $[C_{19}H_{19}N_3O_4]^+$ 353.1376; 358.1163 $[M+Na]^+$, calcd. for $[C_{19}H_{17}N_3O_3Na]^+$ 358.1168.

Mono-α-amino-ZnPc 2.4. A mixture of 4-*tert*-butylphthalonitrile (770.0 mg, 4.1 mmol), phthalonitrile **2.3** (462.0 mg, 1.4 mmol) and zinc(II) acetate (509.4 mg, 2.8 mmol) was dissolved in DMAE (6.0 mL). Catalytic amount of DBN was added and reaction refluxed for 5 h. The solvent was removed and the residue purified by silica column chromatography using hexane/ethyl acetate 4:1 for elution. The N-Boc protected ZnPc was isolated as a blue solid (272 mg, 20.4%), mp > 250 ^{o}C. ^{1}H NMR (acetone-d_6): δ 9.51-8.07 (m, 11H, Ar-H), 7.78-7.23 (m, 5H, Ar-H), 1.86-1.82 (m, 27H, $C(CH_3)_3$), 1.51-1.48, 1.41 (m, 9H, $C(CH_3)_3$). ^{13}C NMR (acetone-d_6): δ 171.0 (C=O), 155.7, 155.0, 154.0, 153.9, 152.8, 151.9, 141.2, 139.3, 136.9, 135.6, 134.9, 134.8, 130.3, 127.7, 127.6, 127.3, 123.0, 122.4, 120.7, 120.5, 119.2, 119.0, 117.5, 117.5, 117.4, 117.3, 79.8, 79.7 (N-Boc-$C(CH_3)_3$), 60.6 (N-Ar-C), 36.5, 32.7, 32.5 (Ar-C, $C(CH_3)_3$), 28.7, 28.6 (N-Boc-$C(CH_3)_3$). MS (MALDI-TOF) *m/z* 952.389 $[M+H]^+$, calcd for $C_{55}H_{54}N_9O_3Zn$, 952.3641. The N-Boc group was removed using DCM/TFA, 1:1 (8 mL), and ZnPc **2.4** was obtained as a blue solid (180 mg, 14.7% overall yield), mp > 250 ^{o}C.

UV–Vis (DMF): λ_{max} (log ε) 349 nm (5.09), 614 nm (4.82), 682 nm (5.58). ^{1}H NMR (DMF-d_7): δ 9.58-9.29 (m, 7H, Ar-H), 8.41-8.28 (m, 4H, Ar-H), 7.28-7.24 (m, 2H, Ar-H), 6.69-6.63 (m, 2H, Ar-H), 4.65-5.05 (br, 2H, NH_2), 1.80-1.65 (m, 27H, $C(CH_3)_3$). ^{13}C NMR (DMF-d_7): δ 156.6, 155.2, 155.0, 154.9, 154.8, 154.7, 154.6, 154.6, 154.1, 154.1, 153.9, 152.9, 150.1, 148.9, 145.7, 145.0, 142.1, 142.1, 139.8, 139.7, 139.4, 137.4, 137.3, 137.0, 131.5, 128.5, 128.4, 128.3, 127.5, 123.2, 123.0, 121.4, 119.7, 119.6, 119.4, 118.4, 117.6, 116.5, 116.4, 32.3 (Ar-C, $C(CH_3)_3$). MS (MALDI-TOF) *m/z* 852.341 $[M+H]^+$, calcd for $C_{50}H_{46}N_9OZn$ 852.312.

Mono-α-(trimethylamino)-ZnPc 2.5. Pc **2.4** (20 mg, 0.023 mmol), DIPA (0.2 mL, 1.44 mmol) and CH_3I (0.5 mL, 8.0 mmol) were dissolved in dry DMF (0.3 mL) and the mixture was stirred at 25 °C for 3 days and the excess solvents was removed. The solid was dissolved in DCM (15 mL), washed with water (20 mL × 2) and the organic layer was concentrated and purified on Sephadex G-100 column using DCM/methanol 5:1 for elution. The product was obtained as a blue solid (18.2 mg, 75.8%), mp 204-206 ^{o}C. UV–Vis (DMF): λ_{max} (log ε) 351 nm (4.11), 620 nm (4.13), 684 nm (4.97). ^{1}H NMR (acetone-d_6): δ 9.47-9.16 (m, 6H, Ar-H), 8.85-7.82 (m, 8H, Ar-H), 7.50 (br, 2H, Ar-H), 3.72 (s, 4H, N-CH_3), 3.62 (s, 5H, N-CH_3), 1.80-1.71 (m, 27H, $C(CH_3)_3$). ^{13}C NMR (acetone-d_6): δ 162.2, 156.0, 153.9, 150.4, 142.8, 140.3, 137.9, 130.9, 128.0, 123.2, 123.0, 122.8, 122.6, 119.9, 118.2, 117.7 (Ar-C), 71.3 (N-Ar-C), 58.0, 57.9 (N-CH_3), 36.5, 32.6 ($C(CH_3)_3$). MS (MALDI-TOF) *m/z* 894.434 $[M-I]^+$, calcd for $C_{53}H_{52}N_9OZn$ 894.359.

Di-α-amino-ZnPc 2.6. A procedure related to that described for Pc **2.4** was used and the purification via silica column chromatography using hexane/ethyl acetate 1:1 gave the N-Boc protected ZnPc as a blue solid (76 mg, 19.4% yield), mp > 250 ^{o}C. ^{1}H NMR (DMF-d_7): δ 9.58-8.92 (m, 8H, Ar-H), 8.41-8.12 (m, 4H, Ar-H), 7.92-7.66 (m, 5H, Ar-H), 7.60-7.47 (m,

4H, Ar-H), 1.81-1.77 (m, 18H, $C(CH_3)_3$), 1.57, 1.51, 1.50, 1.46, 1.46, 1.42 (s, 18H, CH_3). ^{13}C NMR (acetone-d_6): δ 169.5, 169.2, (C=O), 155.9, 155.7, 155.3, 155.0, 154.9, 154.7, 154.6, 154.4, 154.2, 154.0, 153.9, 153.8, 153.7, 153.5, 153.5, 153.3 153.0, 153.0, 152.9, 151.9, 151.6, 150.6, 142.0, 141.9, 141.4, 141.3, 141.0, 140.0, 139.9, 139.7, 139.5, 139.4, 139.2, 137.6, 137.3, 137.0, 136.7, 135.8, 135.6, 135.5, 135.0, 134.9, 130.4, 130.1, 129.7, 129.6, 129.2, 128.8, 128.6, 128.0, 127.6, 127.5, 127.3, 127.2, 123.7, 123.4, 123.3, 122.8, 122.7, 122.4, 122.1, 121.5, 121.3, 120.7, 120.1, 119.9, 119.4, 119.3, 119.1, 118.8, 118.4, 118.1, 117.6, 117.5, 117.4, 117.2 (Ar-C), 80.0, 79.8, 79.7 (N-Boc, $C(CH_3)_3$), 36.5, 36.4, 32.7, 32.5, 31.6, 31.4 (Ar-C, $C(CH_3)_3$), 28.9, 28.7, 28.6 (N-Boc, $C(CH_3)_3$). MS (MALDI-TOF) *m/z* 1102.455 $[M]^+$, calcd for $C_{62}H_{58}N_{10}O_6Zn$ 1102.383. The protected ZnPc was dissolved in DCM/TFA, 1:1 (8 mL) and the solution was stirred for 2 h to afford Pc **2.6** (163.1 mg, 93.1%), mp > 250 ^oC. UV–Vis (DMF): λ_{max} (log ε) 350 nm (4.55), 618 nm (4.31), 686 nm (5.07). ^1H NMR (DMF-d_7): δ 9.57-8.99 (m, 6H, Ar-H), 8.41-8.16 (m, 4H, Ar-H), 7.93-7.69 (m, 2H, Ar-H), 7.35 (br, 4H, Ar-H), 6.82 (br, 4H, Ar-H), 1.83-1.67 (m, 18H, $C(CH_3)_3$). ^{13}C NMR (DMF-d_7): δ 156.2, 156.1, 155.6, 155.3, 155.1, 155.0, 154.8, 154.6, 154.5, 154.4, 154.1, 153.9, 153.5, 153.3, 153.2, 152.4, 150.9, 143.3, 142.3, 141.6, 140.2, 140.0, 139.8, 137.8, 137.6, 137.4, 132.5, 131.8, 131.5, 129.9, 129.2, 128.7, 128.5, 128.1, 123.9, 123.4, 122.2, 121.3, 120.0, 119.6, 119.5, 118.5, 118.1, 118.1, 117.5 (Ar-C), 32.6 (Ar-C, $C(CH_3)_3$). MS (MALDI-TOF) *m/z* 903.352 $[M+H]^+$, calcd for $C_{52}H_{43}N_{10}O_2Zn$ 903.286.

Di-α-(trimethylamino)-ZnPc 2.7. ZnPc **2.6** (20 mg, 0.022 mmol), DIPA (0.15 mL, 1.07 mmol) and CH_3I (0.2 mL, 3.21 mmol) mixture was dissolved in dry DMF (0.5 mL) and stirred at room temperature for 3 days. Excess iodomethane was removed and the residue purified as described above for ZnPc **2.5**. The title compound **2.7** was isolated as a blue solid

(16.2mg, 58.9% yield), mp 195-197 ^{o}C. UV–Vis (DMF): λ_{max} (log ε) 350 nm (4.64), 622 nm (3.79), 686 nm (5.25). ^{1}H NMR (acetone-d_6): δ 9.55-9.36 (m, 4H, Ar-H), 9.04-8.93 (m, 1H, Ar-H), 8.72-8.59 (m, 1H, Ar-H), 8.33-8.04 (m, 7H, Ar-H), 7.91-7.75 (m, 2H, Ar-H), 7.66-7.54 (m, 4H, Ar-H), 3.85-3.65 (m, 18H, N-CH_3), 1.79-1.64 (m, 27H, C(CH_3)$_3$). ^{13}C NMR (acetone-d_6): δ 162.1, 161.7, 154.1, 153.7, 150.4, 143.0, 141.8, 140.5, 140.1, 138.1, 137.7, 132.1, 131.4, 130.3, 129.8, 128.2, 127.8, 123.8, 123.4, 123.0, 121.3, 119.8, 118.3, 117.7, (Ar-C), 66.3 (N-Ar-C), 57.9 (N-CH_3), 36.4, 32.7, 32.3 (C(CH_3)$_3$). MS (MALDI-TOF) *m/z* 973.373 [M-2I-CH_3]$^{+}$, calcd for $C_{57}H_{53}N_{10}O_2Zn$ 973.364.

Monoaminophenoxyphthalonitrile 2.9. A mixture of 4-nitrophthalonitrile (1 g, 5.8 mmol) and 4-aminophenol (0.7 g, 6.4 mmol) was dissolved in DMF (15 mL) and heated to 63°C. Then K_2CO_3 (2.63 g, 20 mmol) was added in six portions after every five minutes and the mixture stirred 4 h under argon. It was cooled to room temperature and poured into ice-cold water (500 mL). The filtered crude product (brown solid) was purified via silica column chromatography using DCM/methanol (98:2). Organic solvents were removed to obtain a yellow solid (1.0 g, 73.3%), mp 130 - 131°C. ^{1}H NMR (d-CD_2Cl_2, 400 MHz): δ 7.70 (d, J = 8.6 Hz, 1H, Ar-H), 7.23 (t, J = 8.8 Hz, 2H, Ar-H), 6.87 (d, J = 7.8 Hz, 2H, Ar-H), 6.73 (d, J = 7.8, 2H, H-Ar), 3.86 (br, 2H, NH_2). ^{13}C NMR (d-$CDCl_3$, 100 MHz): δ 162.89, 145.32, 144.96, 135.36, 121.71, 120.98, 120.82, 117.31, 116.16, 115.84, 115.40, 107.96 (Ar-C, CN). MS (MALDI-TOF) *m/z* 236.0813 [M+H]$^{+}$, calcd for, $C_{14}H_9N_3O$, 23.0818.

Mono-N-Boc-aminophenoxyphthalonitrile 2.10. A procedure related to that described for phthalonitrile **2.3** was used the product obtained in 87.8% yield, mp 169-171 °C. ^{1}H NMR (CD_2Cl_2): δ 7.73 (d, *J* = 8.7 Hz, 1H, Ar-H), 7.47 (d, *J* = 8.8 Hz, 2H, Ar-H), 7.27 (d, *J* = 2.3 Hz, 1H, Ar-H), 7.23 (dd, *J* = 8.6, 1H, Ar-H), 7.03 (d, *J* = 8.6, 2H, Ar-H), 6.72 (br, 1H,

N-H), 1.51 (s, 9H, $C(CH_3)_3$). ^{13}C NMR ($CDCl_3$): δ 162.2, 152.6, 148.5, 136.8, 135.4, 121.3, 121.2, 121.1, 117.5, 115.6, 115.2, 108.6 (Ar-C, CN), 80.7 (C=O), 28.0 ($C(CH_3)_3$). MS (HRMS-ESI) *m/z* 336.1351 $[M+H]^+$, calcd for $C_{19}H_{18}N_3O_3$ 336.1348; 358.1189 $[M+Na]^+$, calcd for $C_{19}H_{17}N_3O_3Na$ 358.1162.

Mono-β-amino-ZnPc 2.11. A mixture of 4-*tert*-butylphthalonitrile (385 mg, 2.09 mmol), phthalonitrile **2.10** (231 mg, 0.69 mmol) and zinc(II) acetate (254.7 mg, 1.4 mmol) was refluxed for 5 h, cooled and purified as described above for Pc **2.4** to afford a blue solid (121.6 mg, 18.5%), mp > 250 ^oC. ^1H NMR (acetone-d_6): δ 9.31-8.55 (m, 8H, Ar-H), 8.40-8.12 (m, 4H, Ar-H), 8.10-7.85 (m, 2H, Ar-H), 7.75-7.60 (m, 2H, Ar-H), 1.95-1.87 (m, 27H, $C(CH_3)_3$), 1.62 (d, *J* = 7.6, 9H, $C(CH_3)_3$). ^{13}C NMR (acetone-d_6): δ 159.9, 159.8, 159.3, 159.2, 154.1, 154.0, 153.7, 153.4, 153.0, 152.7, 152.4, 139.2, 138.9, 138.8, 138.7, 138.4, 138.2, 137.1, 137.0, 136.8, 136.7, 136.4, 136.2, 127.3, 125.9, 124.0, 123.8, 123.6, 122.9, 122.6, 122.4, 121.9, 121.5, 121.3, 121.0, 120.8, 120.7, 119.6, 119.2, 112.2, 111.4, 110.8 (Ar-C), 80.2 (N-Boc-$C(CH_3)_3$), 55.5 (N-Ar-C), 36.4, 32.6 (Ar-C, $C(CH_3)_3$), 28.9 (N-Boc-$C(CH_3)_3$). MS (MALDI-TOF) *m/z* 952.395 $[M+H]^+$, calcd for $C_{55}H_{54}N_9O_3Zn$ 952.364. The product was dissolved in DCM/TFA, 1:1 (8 mL) and stirred for 2 h to afford product **2.11** (94.7 mg, 93.7 %), mp > 250 ^oC. UV–Vis (DMF): λ_{max} (log ε) 349 nm (5.01), 610 nm (4.71), 677 nm (5.46). ^1H NMR (Pyridine-d_5): δ 10.02-9.70 (m, 6H, Ar-H), 9.63-9.41 (m, 1H, Ar-H), 8.44-7.96 (m, 4H, Ar-H), 7.47-7.39 (m, 2H, Ar-H), 7.18-7.10 (m, 2H, Ar-H), 5.09 (br, 2H, N-H), 1.72-1.65 (m, 27H, $C(CH_3)_3$). ^{13}C NMR (DMSO-d_6): δ 160.6, 160.6, 160.3, 160.3, 152.4, 152.2, 152.0, 151.9, 151.8, 151.7, 151.6, 151.4, 151.1, 147.2, 147.0, 146.5, 146.4, 146.2, 145.0, 143.9, 139.6, 139.5, 138.2, 138.0, 137.9, 137.7, 135.8, 135.7, 135.6, 135.5, 135.4, 131.9, 131.7, 131.2, 130.1, 126.9, 126.6, 125.1, 123.5, 122.8, 122.0, 121.8, 121.5, 121.4, 120.9, 120.7,

119.7, 118.7, 118.3, 115.9, 115.6, 115.0, 109.6, 109.4, 108.5, 108.3, (Ar-C), 59.8 (N-Ar-C), 35.6, 31.4 (Ar-C, $C(CH_3)_3$). MS (MALDI-TOF) *m/z* 852.348 $[M+H]^+$, calcd for $C_{50}H_{46}N_9OZn$ 852.312.

Mono-β-(trimethylamino)-ZnPc 2.12. ZnPc **2.11** (20 mg, 0.023 mmol), DIPA (0.2 mL, 1.44 mmol) and CH_3I (0.5 mL, 8.0 mmol) were dissolved in dry DMF (0.3 mL). The excess CH_3I was removed and the resultant residue purified as described above to give a blue solid (15.7 mg, 65.4%), mp 201-203 ^oC. UV–Vis (DMF): λ_{max} (log ε) 355 nm (4.22), 618 nm (3.90), 683 nm (4.80). ^1H NMR (DMF-d_7): δ 9.54-9.23 (m, 7H, Ar-H), 8.95 (br, 1H, Ar-H), 8.41-8.34 (m, 5H, Ar-H), 7.97-7.70 (m, 4H, Ar-H), 3.99 (s, 9H, N-3CH_3), 1.82-1.76 (m, 27H, $C(CH_3)_3$). ^{13}C NMR (DMF-d_7): δ 160.2, 159.4, 157.9, 155.32, 154.8, 154.2, 154.1, 153.9, 143.7, 141.3, 140.1, 139.9, 137.7, 137.5, 132.5, 128.3, 125.3, 124.0, 123.8, 123.3, 122.3, 120.7, 120.3, 119.9, 115.9, 113.8, 113.6 (Ar-C), 71.3 (N-Ar-C), 57.3 (N-CH_3), 32.6 ($C(CH_3)_3$). MS (MALDI-TOF) *m/z* 894.442 $[M-I]^+$, calcd for $C_{53}H_{52}N_9OZn$ 894.359.

Di-β-amino-ZnPc 2.13. A procedure related to that described for Pc **2.11** was used and purification via silica column chromatography using hexane/ethyl acetate 1:1 gave the title ZnPc as a blue solid (98.0 mg, 25% yield), mp 214-216 ^oC. ^1H NMR (DMF-d_7): δ 9.67-9.59 (m, 2H, Ar-H), 9.39-8.40 (m, 9H, Ar-H), 8.00-7.81 (m, 5H, Ar-H), 7.64-7.60 (m, 4H, Ar-H), 1.88-1.82 (m, 18H, $C(CH_3)_3$), 1.61-1.59 (m, 18H, N-Boc-$C(CH_3)_3$). ^{13}C NMR (DMF-d_7): δ 164.9, 161.1, 161.0, 160.7, 154.5, 154.3, 153.9, 153.8, 153.6, 153.4, 153.3, 153.0, 152.8, 150.5, 141.2, 139.8, 138.7, 138.0, 139.7, 137.4, 136.8, 134.1, 128.3, 127.6, 126.2, 124.8, 123.1, 122.2, 121.9, 121.8, 121.6, 121.5, 121.3, 121.1, 120.9, 119.8, 112.3, 111.4, 110.9, (Ar-C), 80.2 (C=O), 60.9 (N-Ar-C), 36.8, 32.7 (Ar-C, $C(CH_3)_3$), 29.0, 28.8 (N-Boc-$C(CH_3)_3$). MS (MALDI-TOF) *m/z* 1103.463 $[M+H]^+$, calcd for $C_{62}H_{59}N_{10}O_6Zn$ 1103.391. The N-Boc-

protected ZnPc was dissolved in DCM/TFA, 1:1 (8 mL) and stirred for 2 h to obtain ZnPc **2.13** (73.8, 92.0% yield), mp > 250 ^{o}C. UV–Vis (DMF): λ_{max} (log ε) 351 nm (4.90), 611 nm (4.59), 679 nm (5.32). ^{1}H NMR (DMSO-d_6): δ 9.40-8.82 (m, 9H, Ar-H), 8.56-8.18 (m, 5H, Ar-H), 7.87-7.60 (m, 4H, Ar-H), 7.28-6.77 (m, 7H, Ar-H), 5.20-5.00 (br, 3H, N-H), 1.82-1.77 (m, 18H, C(CH_3)$_3$). ^{13}C NMR (DMSO-d_6): δ 160.7, 152.4, 152.2, 146.0, 139.6, 138.0, 135.4, 132.0, 131.8, 127.1, 123.8, 123.6, 121.5, 120.9, 118.8, 115.4, 114.9, 109.6, 108.3 (Ar-C), 35.6, 31.9, 31.5, 31.0, 30.7 (Ar-C, C(CH_3)$_3$). MS (MALDI-TOF) *m/z* 903.587 $[M+H]^+$, calcd for $C_{52}H_{43}N_{10}O_2Zn$ 903.286.

Di-β-(trimethylamino)-ZnPc 2.14. ZnPc **2.13** (20 mg, 0.022 mmol), DIPA (0.15 mL, 1.07 mmol) and CH_3I (0.2 mL, 3.21 mmol) were used to synthesize the title compound following the same procedure described above for Pc **2.7**. Product **2.14** was obtained as a blue solid (14.6 mg, 53.1% yield), mp > 218-220 ^{o}C. UV–Vis (DMF): λ_{max} (log ε) 355 nm (4.41), 618 nm (4.08), 683 nm (4.96). ^{1}H NMR (DMF-d_7): δ 9.60-9.9.06 (m, 9H, Ar-H), 8.36-8.24 (m, 6H, Ar-H), 7.66-7.57 (m, 4H, Ar-H), 7.40-7.37 (m, 1H, Ar-H), 7.05-7.02(m, 1H, Ar-H), 3.98-3.93 (m, 18H, N-6CH_3), 1.78-1.71 (m, 18H, C(CH_3)$_3$). ^{13}C NMR (DMF-d_7): δ 160.1, 158.1, 155.4, 154.0, 149.4, 143.7, 141.9, 140.4, 137.9, 136.4, 128.2, 125.3, 124.0, 123.1, 122.3, 122.1, 120.3, 119.9, 119.8, 115.1, 113.6, (Ar-C), 71.3 (N-Ar-C), 58.0 (N-CH_3), 41.5, 32.5 (C(CH_3)$_3$). MS (MALDI-TOF) *m/z* 973.654 $[M-2I-CH_3]^+$, calcd for $C_{57}H_{53}N_{10}O_2Zn$ 973.364.

Tetra-β-amino-ZnPc 2.15. A mixture of phthalonitrile **2.10** (0.5 g, 1.49 mmol) and zinc(II) acetate (0.095 g, 0.5 mmol) was dissolved in DMAE (5.0 mL) and refluxed under argon. Two drops of DBN were added and the solution refluxed for another 6 h. The solvent was removed and the crude purified via alumina column chromatography using

DCM/methanol 95:5 for elution. The product was further purified via a second alumina column using DCM/methanol 9:1 for elution to isolate a dark green solid (105.6 mg, 20.2%), mp > 250 ^{o}C. ^{1}H NMR (THF-d_8): δ 9.12-8.66 (m, 12H, Ar-H), 7.93-7.68 (m, 8H, Ar-H), 7.46-7.31 (br, 8H, Ar-H), 7.16 (br, 8H, Ar-H), 1.55 (s, 36H, C(CH_3)$_3$). ^{13}C NMR (THF-d_8): δ 160.9, 154.6, 154.1, 153.2, 152.8, 141.5, 137.6, 137.1, 134.4, 124.9, 121.2, 120.6, 112.1, 111.5 (Ar-C), 79.9 (N-Boc-C(CH_3)$_3$), 62.9, 59.1, 45.9 (N-Ar-C), 28.87 (N-Boc, C(CH_3)$_3$). MS (MALDI-TOF) *m/z* 1405.819 $[M+H]^+$, calcd for $C_{76}H_{69}N_{12}O_{12}Zn$ 1405.445. The solid was dissolved in DCM/TFA, 1:1 and stirred at 0 °C for 3 h. The solvent was removed and the resulting residue was treated with 2 N NaOH (1 mL). The product was re-dissolved in 20 mL DCM/methanol and washed with water (2 x 50 mL). The organic phase was concentrated to obtain a green solid (72.4 mg, 96.1%), mp > 250 ^{o}C. UV-Vis (DMF): λ_{max} (log ε) 352 nm (4.63), 613 nm (4.31), 682 nm (5.01). ^{1}H NMR (DMF-d_7): δ 9.89 (br, 1H, Ar-H), 9.34-9.28 (m, 3H, Ar-H), 8.88-8.70 (m, 3H, Ar-H), 7.46-7.31 (m, 8H, Ar-H), 7.83 (br, 7H, Ar-H), 7.47 (br, 4H, Ar-H), 7.21 (br, 4H, Ar-H), 6.93 (br, 4H, Ar-H). ^{13}C NMR (DMF-d_7): δ 160.0, 159.5, 155.2, 154.0, 147.5, 142.0, 137.3, 135.4, 134.9, 134.3, 131.6, 124.8, 122.5, 121.2, 120.0, 116.5, 111.4, 110.1 (Ar-C), 63.4, 59.2, 154.5, 46.3 (N-Ar-C), 28.9 (N-Boc, C(CH_3)$_3$). MS (MALDI-TOF) *m/z* 1004.313 $[M+H]^+$, calcd for $C_{56}H_{36}N_{12}O_4Zn$ 1004.227.

Tetra-β-trimethylamino-ZnPc 2.16. Zn Pc **2.15** (24.4 mg, 0.023 mmol) was dissolved in DMF (0.4 mL). Methyl iodide (3 mL, 48.2 mmol) and DIPA (0.2 mL, 1.42 mmol) were added and the mixture was stirred at 25 °C for 3 days. Excess iodomethane was removed, acetone added to triturate the product and then solution centrifuged to isolate title compound as a blue-green solid (31.9 mg, 82.4%), mp 194-196 ^{o}C. UV–vis (DMF): λ_{max} (log ε) 358 nm (4.62), 620 nm (4.31), 684 nm (5.08). ^{1}H NMR (DMF-d_7): 9.49-9.32 (m, 2H, Ar-

H), 9.00-8.89 (m, 2H, Ar-H), 8.34 (br, 5H, Ar-H), 7.85-7.75 (m, 7H, Ar-H), 7.71-7.64 (m, 7H, Ar-H), 7.53-7.47 (m, 6H, Ar-H), 4.07-4.01 (m, 36H, N-CH_3). ^{13}C NMR (DMSO-d_6): δ 158.2, 156.9, 153.1, 152.2, 151.8, 142.5, 142.3, 140.1, 139.9, 135.4, 134.9, 134.5, 133.5, 124.45, 124.3, 124.2, 123.0, 122.9, 122.7, 121.3, 121.1, 120.4, 120.1, 119.9, 119.5, 119.2, 119.1, 114.2, 112.8, 112.1 (Ar-C), 64.2 (N-Ar-C), 58.1, 56.8, 53.2 (N-CH_3). MS (MALDI-TOF) *m/z* 1131.406 $[M-4I-3CH_3]^+$, calcd for $C_{65}H_{55}N_{12}O_4Zn$ 1131.3761.

4,5-Di-*N*-Boc-amino-phthalonitrile 2.18. The compound was obtained by reacting 4,5-dichlorophthalonitrile and N-Boc-4-aniline in DMF and isolated in 82.6% yield, following the procedure described above for phthalonitrile **2.3**; mp 203-205 °C. ^{1}H NMR ($CDCl_3$): δ 7.47 (d, *J* = 8.8 Hz, 4H, Ar-H), 7.15 (s, 2H, Ar-H), 7.05 (d, *J* = 8.8 Hz, 4H, Ar-H), 6.66 (br, 2H, N-H), 1.51 (s, 18H, 2×$C(CH_3)_3$). ^{13}C NMR ($CDCl_3$): δ 152.8, 152.2, 148.9, 136.9, 136.5, 121.0, 120.9, 120.5, 115.6, 115.01, 110.0, 101.5 (Ar-C, CN), 81.0 (C=O), 28.3 ($C(CH_3)_3$). MS (ESI) *m/z* 565.2036 $[M+Na]^+$, calcd for $C_{30}H_{30}N_4O_6Na$ 565.2058.

Di-β-amino-ZnPc 2.19. A mixture of 4-*tert*-butylphthalonitrile (385 mg, 2.09 mmol), phthalonitrile **2.18** (374 mg, 0.69 mmol) and zinc(II) acetate (254.7 mg, 1.4 mmol) was used and a procedure related to that described for Pc **2.4** was followed to obtain a blue solid (81 mg, 10.1%), mp > 250 ^{o}C ^{1}H NMR (DMF-d_7): δ 9.56 - 9.24 (m, 7H, Ar-H), 9.12 - 9.02 (m, 1H, Ar-H), 8.91 – 8.83 (m, 2H, Ar-H), 8.42 – 8.31 (m, 3H, Ar-H), 7.89 – 7.79 (m, 4H, Ar-H), 7.52 – 7.40 (m, 4H, Ar-H), 1.85 -1.79 (m, 27H, $C(CH_3)_3$), 1.58 – 1.53 (m, 18H, Boc-$C(CH_3)_3$). ^{13}C NMR (DMF-d_7): δ 154.5, 154.2, 154.0, 153.3, 152.7, 152.2, 151.6, 151.4, 151.1, 150.6, 150.4, 139.6, 137.5, 137.3, 137.0, 135.6, 135.2, 128.5, 123.2, 121.0, 120.6, 120.4, 120.3, 119.7, 119.5, 119.4, 119.2, 115.5, 113.7, 80.2 (C=O), 80.0 (C=O), 32.6 (Ar-C, $C(CH_3)_3$), 29.9 ($C(CH_3)_3$), 28.9 ($C(CH_3)_3$). MS (MALDI-TOF) *m/z* 1158.465 $[M]^+$, calcd for

$C_{66}H_{66}N_{10}O_6Zn$ 1158.446. The product was dissolved in DCM/TFA, 1:1 and for 2 h to obtain the product as a blue solid (61 mg, 9.2% overall yield), mp > 250 ^oC. UV–vis (DMF): λ_{max} (log ε) 353 nm (4.98), 611 nm (4.65), 677 nm (5.43). ^1H NMR (DMSO-d_6): δ 9.34-9.13 (m, 6H, Ar-H), 9.07-8.97 (m, 1H, Ar-H), 8.74-8.71 (m, 1H, Ar-H), 8.31-8.26 (m, 1H, Ar-H), 8.16-8.11 (m, 2H, Ar-H) 7.17-7.11 (m, 3H, Ar-H), 6.94-6.88 (m, 3H, Ar-H), 6.70-6.58 (br, 2H, Ar-H), 4.93 (br, 4H, N-H), 1.79-1.71 (m, 27H, $C(CH_3)_3$). ^{13}C NMR (DMSO-d_6): δ 152.9, 151.5, 147.1, 138.6, 136.2, 136.1, 133.8, 133.3, 127.6, 122.4, 121.1, 121.0, 120.1, 119.9, 118.8, 116.1, 115.8, 110.7, 32.3 (Ar-C, $C(CH_3)_3$). MS (MALDI-TOF) *m/z* 959.34 $[M+H]^+$, calcd for $C_{56}H_{51}N_{10}O_2Zn$ 959.35.

Di-β-trimethylamino-ZnPc 2.20. A mixture of ZnPc **2.19** (20 mg, 0.023 mmol), DIPA (0.2 mL, 1.44 mmol) and CH_3I (1.0 mL, 16.0 mmol) was dissolved in dry DMF (0.4 mL) and stirred at 25 °C for 3 days. Excess iodomethane was removed and the residue purified as described above for Pc **2.5**. The product was isolated as a blue solid (19.5 mg, 72.0%), mp 190 ^oC (decomp). UV–vis (DMF): λ_{max} (log ε) 357 nm (4.50), 619 nm (4.16), 684 nm (5.01). ^1H NMR (DMF-d_7): δ 9.56-9.23 (m, 9H, Ar-H), 8.45-8.28 (m, 7H, Ar-H), 7.60 (br, 3H, Ar-H), 3.96 (s, 18H, N-6CH_3), 1.78-1.71 (m, 27H, $C(CH_3)_3$). ^{13}C NMR (DMF-d_7): δ 159.8, 156.2, 155.5, 154.8, 154.1, 152.3, 149.0, 143.7, 140.3, 137.9, 137.1, 128.2, 123.9, 123.0, 119.8, 119.4, 119.1, 117.2, 116.3 (Ar-C), 71.3 (N-Ar-C), 58.0 (CH_3), 32.6 ($C(CH_3)_3$). MS (MALDI-TOF) *m/z* 1029.416 $[M-2I-CH_3]^+$, calcd for $C_{61}H_{61}N_{10}O_2Zn$ 1029.427.

Octa-β-amino-ZnPc 2.21. A mixture of phthalonitrile **2.18** (0.745 g, 1.37 mmol) and zinc(II) acetate (0.420 g, 2.29 mmol) was dissolved in DMAE (6.0 mL) under argon. Catalytic amount of DBN was added and the solution was refluxed for 6 h. The solvent was removed and the residue was purified on a Sephadex LH-20 column using methanol for elution. The

product was isolated as a green solid (462.0 mg, 59.0%), mp > 250 ^{o}C ^{1}H NMR (DMSO-d_6): δ 8.97 (s, 4H, Ar-H), 8.55 (s, 4H, Ar-H), 7.55 (s, 16H, Ar-H), 7.16 (s, 16H, Ar-H), 1.52 (s, 72H, $C(CH_3)_3$). ^{13}C NMR (DMSO-d_6): δ 154.6, 154.0, 151.7, 136.9, 135.9, 120.4, 120.0, 119.5, 115.3, (Ar-C), 79.8 (C=O), 63.1, 62.9, 59.4, 59.3 (N-Ar-C), 46.1, 28.9 (N-Boc, $C(CH_3)_3$). MS (MALDI-TOF) *m/z* 2277.901 $[M]^+$, $C_{123}H_{129}N_{16}O_{24}Zn$ 2277.866. The compound was dissolved in DCM/TFA, 1:1 and the solution was stirred for 2 h. The title product was isolated as a green solid (246.4 mg, 84.8%), mp > 250 ^{o}C. UV–vis (DMF): λ_{max} (log ε) 361 nm (4.62), 615 nm (4.22), 689 nm (5.06). ^{1}H NMR (DMSO-d_6): δ 7.52 (br, 8H, Ar-H), 7.16-6.60 (m, 32H, Ar-H). ^{13}C NMR (DMSO-d_6): δ 153.6, 152.3, 145.7, 134.5, 120.0, 119.8, 115.2, (Ar-C), 61.7, 57.7, 53.1, 45.3 (N-Ar-C). MS (MALDI-TOF) *m/z* 1432.383 $[M]^+$, calcd for $C_{80}H_{56}N_{16}O_8Zn$ 1432.376.

Octa-β-trimethylamino-ZnPc 2.22. ZnPc **2.21** (18.0 mg, 0.0126 mmol) was dissolved in DMF (8 mL). Methyl iodide (3 mL, 48.2 mmol) and DIPA (0.2 mL, 1.42 mmol) were added and the mixture stirred at 25 °C for 3 days. Excess solvents were removed, acetone (5 mL) added to triturate the product and the solution centrifuged to obtain the product as a green solid (31.9 mg, 90.9%), mp 188-190 ^{o}C. UV–vis (DMF): λ_{max} (log ε) 365 nm (4.57), 620 nm (4.24), 686 nm (5.17). ^{1}H NMR (D_2O): δ 7.96-7.47 (m, 40H, Ar-H), 3.80-3.30 (m, 72H, N-CH_3). ^{13}C NMR (D_2O): δ 158.1, 152.1, 142.0, 136.01, 134.8, 122.7, 120.1, 118.2, 117.6, 116.3, 114.4, (Ar-C), 64.1 (N-Ar-C), 62.6, 58.0, 56.7, 53.1, 42.2, 16.2 (N-CH_3). MS (MALDI-TOF) *m/z* 1671.679 $[M\text{-}8I\text{-}7CH_3]^+$, calcd for $C_{97}H_{91}N_{16}O_8Zn$ 1671.650.

Di-α-amino-ZnPc 2.24. A mixture of 2,2'-bis(2,3-dicyanophenoxy)biphenyl **2.23**[29] (302.3 mg, 0.69 mmol), phthalonitrile **2.3** (480.0 mg, 1.43 mmol) and zinc acetate (254.7 mg, 1.4 mmol) was dissolved in DMAE (5.0 mL). Catalytic amount of DBN was added and the

mixture refluxed at for 5 h. The solvent was removed and the residue purified via silica gel column chromatography using ethyl acetate solvent for elution. Further purification via a second silica column using hexane/ethyl acetate 1:1 for elution, gave a blue solid (112.2 mg, 13.9 %), mp > 250 ^{o}C. ^{1}H NMR (DMF-d_7): δ 9.53-9.07 (m, 5H, Ar-H), 8.41-8.06 (m, 4H, Ar-H), 7.80-7.15 (m, 19H, Ar-H), 1.56 - 1.49 (m, 18H, C(CH_3)$_3$). ^{13}C NMR (DMF-d_7): δ 161169.6, 168.0 (C=O), 159.0, 156.3, 156.2, 156.1, 154.9, 154.7, 154.6, 154.5, 154.4, 154.3, 154.2, 154.1, 154.0, 153.8, 153.6, 153.4, 153.0, 152.5, 152.4, 151.0, 150.8, 138.7, 137.4, 137.1, 136.6, 136.3, 135.5, 133.2, 132.0, 131.6, 131.3, 131.0, 130.8, 130.6, 130.3. 129.9, 129.3, 129.0, 128.9, 128.2, 126.5, 126.3, 125.7, 124.7, 124.2, 122.3, 122.2, 122.1, 121,6, 121.5, 121.3,121.2, 121.0, 120.9, 120.8, 119.7, 119.6, 119.2, 118.2, 118.1, 117.5, 117.0, 116.4, 112.9 (Ar-C), 80.3, 80.1, 80.0 (O-C(CH_3)$_3$), 28.94, 28.86 (C(CH_3)$_3$). MS (MALDI-TOF) *m/z* 1173.440 $[M+H]^+$, calcd for $C_{66}H_{49}N_{10}O_8Zn$ 1173.303. The N-Boc-protected ZnPc (85.06 mg, 0.073 mmol) was dissolved in a 1:1, mixture of DCM/TFA (6 mL) and the solution was stirred at 0 °C for 3 h. The work-up as described above, gave a blue-greenish solid (65.4 mg, 92.1 %). UV-Vis (DMF): λ_{max} (log ε) 336 nm (4.37), 624 nm (4.13), 691 (4.89) nm. ^{1}H NMR (DMF-d_7): δ 9.41-6.27 (m, 28H, Ar-H), 4.12 (br, 4H, NH_2). ^{13}C NMR (DMF-d_7): δ 159.0, 155.2, 155.0, 154.1, 153.0, 152.3, 150.9, 148.5, 146.5, 146.2, 142.8, 140.4, 133.1, 131.0, 129.9, 129.6, 129.3, 127.9, 126.3, 122.2, 122.0, 121.8, 121.1, 117.9, 117.3, 116.6, 116.3, 112.9 (Ar-C). MS (MALDI-TOF) *m/z* 973.210 $[M+H]^+$, calcd for $C_{56}H_{33}N_{10}O_4Zn$, 973.1978.

Di-α-(trimethylamino)-ZnPc 2.25. ZnPc **2.24** (20 mg, 0.021 mmol), DIPA (0.15 mL, 1.07 mmol) and CH_3I (0.2 mL, 3.21 mmol) were added to dry THF (0.5 mL) and the mixture stirred at 25 °C for 3 days. The reaction was treated as described above for ZnPc **2.22** to give

Pc **2.25** as a pale-green solid (14.7 mg, 53.3%), mp > 250 ^{o}C. UV–Vis (DMF): λ_{max} (log ε) 337 nm (4.61), 613 nm (4.51), 685 nm (5.26). ^{1}H NMR (DMF-d_7): δ 9.52-9.36 (m, 3H, Ar-H), 8.79-8.63 (m, 1H, Ar-H), 8.44-8.36 (m, 2H, Ar-H), 8.30-8.18 (m, 6H, Ar-H), 8.10-7.95 (m, 2H, Ar-H), 7.78-7.72 (m, 5H, Ar-H), 7.58-7.55 (m, 2H, Ar-H), 7.33-7.06 (m, 7H, Ar-H), 3.95 (s, 8H, N-CH_3), 3.85-3.81 (m, 10H, N-CH_3). ^{13}C NMR (DMF-d_7): δ 161.5, 160.0, 159.0, 154.5, 154.3, 153.8, 153.5, 153.2, 152.7, 151.0, 150.7 143.9, 143.2, 143.1, 142.7, 133.2, 132.4, 131.8, 131.2, 129.9, 129.3, 126.7, 126.5, 126.2, 124.2, 124.0, 123.6, 123.4, 122.1, 121.9 121.4, 121.0, 119.7, 118.5, 118.3, 112.9 (Ar-C), 66.29 (N-Ar-C), 58.1, 58.0 (N-CH_3). MS (MALDI-TOF) *m/z* 1045.304 $[M\text{-}2I\text{-}CH_3+2H]^+$, calcd for $C_{61}H_{45}N_{10}O_4Zn^+$ 1045.2917.

Di-β-amino-ZnPc 2.26. A mixture of 2,2'-bis(2,3-dicyanophenoxy)biphenyl **2.23**[29] (302.3 mg, 0.69 mmol), phthalonitrile **2.10** (480.0 mg, 1.43 mmol) and zinc acetate (254.7 mg, 1.4 mmol) was dissolved in DMAE (100.0 mL). Catalytic amount of DBN was added and the reaction refluxed for 15 h. The product was purified as described above for **2.24** to give N-Boc-protected title compound as a blue solid (94.6 mg, 11.4%), mp > 250 ^{o}C. ^{1}H NMR (DMF-d_7): δ 9.59-9.54 (m, 2H, Ar-H), 9.26-9.06 (m, 2H, Ar-H), 8.67-8.26 (m, 3H, Ar-H), 810-8.05 (m, 1H, Ar-H), 7.98-7.14 (m, 19H, Ar-H), 1.59 - 1.51 (m, 18H, $C(CH_3)_3$). ^{13}C NMR (DMF-d_7): δ 169.6, 168.0 (C=O), 161.3, 161.2, 161.14, 161.06, 159.11, 159.07, 154.9, 154.5, 154.3, 154.0, 153.6, 153.1, 152.9, 152.8, 152.5, 151.6, 150.8, 15.7, 142.7, 142.4, 141.2, 137.9, 137.8, 137.4, 136.4, 133.6, 133.2, 131.3, 131.2, 130.8, 130.7, 130.3, 129.9, 129.4, 126.3, 126.2, 125.7, 125.0, 124.9, 124.8, 122.1, 121.7, 121.5, 121.3, 121.1, 120.9, 118.2, 112.9, 111.9 (Ar-C), 80.2 (O-$C(CH_3)_3$), 28.9, 28.8 ($C(CH_3)_3$). MS (MALDI-TOF) *m/z* 1173.419 $[M+H]^+$, calcd for $C_{66}H_{48}N_{10}O_8Zn$ 1173.303. The N-Boc-protected ZnPc (51.6 mg, 0.044 mmol) was dissolved in 6 mL of DCM/TFA (1:1) and stirred at 0 °C for 3 h. The product was

isolated as a blue-greenish solid (38.2 mg, 89.2 %). UV-Vis (DMF): λ_{max} (log ε) 350 nm (4.29), 616 nm (3.99), 684 (4.72) nm. ^{1}H NMR (DMF-d_7): δ 9.84-6.34 (m, 28H, Ar-H), 4.30 (br, 4H, NH_2). ^{13}C NMR (DMF-d_7): δ 159.1, 156.2, 155.0, 154.3, 153.0, 150.9, 150.6, 148.8, 143.0, 142.2, 140.4, 134.2, 133.2, 131.2, 131.0, 130.9, 129.9, 129.6, 129.3, 126.2, 125.7, 125.4, 122.2, 122.0, 121.2, 116.9, 112.8, 109.8h (Ar-C). MS (MALDI-TOF) *m/z* 973.228 $[M+H]^+$, calcd for $C_{56}H_{33}N_{10}O_4Zn$, 973.1978.

Di-β-(trimethylamino)-ZnPc 2.27. A mixture of ZnPc **2.26** (20 mg, 0.021 mmol), DIPA (0.15 mL, 1.07 mmol) and iodomethane (0.2 mL, 3.21 mmol) was added to dry THF (0.5 mL) and stirred at 25 °C for 3 days. The ZnPc **2.27** was isolated as a blue-green solid (16.1 mg, 58.3%), mp > 250 ^{o}C. UV–Vis (DMF): λ_{max} (log ε) 350 nm (4.72), 613 nm (4.48), 680 nm (5.23). ^{1}H NMR (DMF-d_7): δ 9.27-8.66 (m, 3H, Ar-H), 8.37-8.30 (m, 5H, Ar-H), 8.15-8.06 (m, 1H, Ar-H), 7.91-7.55 (m, 9H, Ar-H), 7.41-7.25 (m, 7H, Ar-H), 4.02-3.97 (m, 18H, N-CH_3). ^{13}C NMR (DMF-d_7): δ 159.9, 158.9, 158.4, 158.2, 154.4, 154.0, 153.6, 150.8, 143.9, 143.8, 141.8, 141.4, 136.2, 135.9, 135.6, 133.3, 131.6, 131.3, 131.0, 130.0, 129.3, 126.2, 125.3, 124.1, 122.5, 122.1, 121.1, 120.6, 120.2, 114.2, 113.8, 113.0 (Ar-C), 66.29 (N-Ar-C), 58.1 (N-CH_3). MS (MALDI-TOF) *m/z* 1312.435 $[M]^+$, 1029.296 $[M-2I-2CH_3+H]^+$, calcd for $C_{62}H_{46}N_{10}I_2O_4Zn^+$ 1312.1084, $C_{60}H_{41}N_{10}O_4Zn^+$ 1029.2604.

2.6.3. Phthalonitrile Molecular Structures

X-ray structure analyses of phthalonitriles **2.3**, **2.9**, **2.10**, **2.18** and **2.23** were based on data collected at T=90K on either a Nonius KappaCCD diffractometer equipped with Mo*K*α radiation (compound **2.3**) or a Bruker Kappa Apex-II CCD diffractometer with Cu*K*α radiation (compounds **2.10**, **2.18** and **2.23**). The crystals were grown by slow evaporation of mixed solvents DCM/hexanes 5:1. The X-ray structures of these phthalonitriles confirm their

successful syntheses. Crystal data: **2.3**, $C_{19}H_{17}N_3O_3$, M_r = 335.36, monoclinic space group $P2_1/c$, a = 16.266(4), b = 11.114(3), c = 9.8401(16) Å, β = 101.629(13)°, V = 1742.4(7) Å^3, Z = 4, D_x = 1.278 Mg m^{-3} , θ_{max} = 30.0°, R = 0.047 for 5047 data and 232 refined parameters, CCDC 810389; **2.10**, $C_{19}H_{17}N_3O_3$, M_r = 335.36, orthorhombic space group $Pca2_1$, a = 10.139(2), b = 8.597(2), c = 20.157(5) Å, V = 1757.0(7) Å^3, Z = 4, D_x = 1.268 Mg m^{-3} , θ_{max} = 68.1°, R = 0.032 for 2507 data and 233 refined parameters, CCDC 810390; **2.18**, $C_{30}H_{30}N_4O_6$, M_r = 542.58, triclinic space group P-1, a = 10.0348(5), b = 12.0728(6), c = 13.3158(10) Å, α = 110.460(5), β = 102.622(4), γ = 101.132(4)°, V = 1409.38(15) Å^3, Z = 2, D_x = 1.279 Mg m^{-3}, θ_{max} = 68.6°, R = 0.037 for 4972 data and 373 refined parameters, CCDC 810391. **2.23**, $C_{28}H_{14}N_4O_2$, 2.4(CH_2Cl_2), M_r = 642.25, triclinic space group P-1, a = 8.9371(4), b = 10.3208(5), c = 16.1899(7) Å, α = 77.863(2), β = 81.983(2), γ = 78.622(2)°, V = 1423.75(11) Å^3, Z = 2, D_x = 1.498 Mg m^{-3} , θ_{max} = 69.4°, R = 0.066 for 5068 data and 334 refined parameters, CCDC 835347.

2.6.4. Spectroscopic Studies

The absorption spectra for the ZnPcs were measured on a PerkinElmer, Lambda 35 UV-Vis spectrometer. The solvents used in these measurements were HPLC grade. The stock solutions of 0.1-1 mM of each ZnPc in DMF were prepared and successive dilutions were obtained by spiking 20 – 250 µL of the corresponding stock solution into 10 or 18 mL of DMF solvent. The emission spectra were recorded on a Fluorolog®-HORIBA JOBIN YVON (Model LFI-3751) spectrofluorimeter. The optical densities for the solutions used in emission measurements ranged between 0.05 – 0.10 at excitation wavelengths. All the measurements were performed within 2 h of solution preparation at 25 °C, using a 10 mm path length spectrophotometric cell. The fluorescent quantum yields (Φ_f) were measured in DMF solvent

using a secondary standard method,[33] and ZnPc (Φ_f = 0.17) used as reference.[40,41,48] The singlet oxygen quantum yields (Φ_Δ) were measured in DMF using a relative method,[43] where ZnPc (Φ_f = 0.56) served as reference and DPBF as a scavenger. The samples, both the stock and dilutions, were prepared in the dark. The concentration of DPBF was kept at ~ 3.0×10^{-5} mol/l to avoid multiple reactions. The monitoring of DPBF absorption decay at 417 nm was used to calculate the singlet oxygen quantum yields for the ZnPcs within ~ 10% accuracy

2.6.5. Cell Studies

The human carcinoma HEp2 cells used in this study were maintained in a 50:50 mixture of DMEM:AMEM (Invitrogen) supplemented with 5% FBS (Invitrogen), Primocin antibiotic (Invitrogen) and 5% CO_2 at 37 ^oC. By subculturing the cells twice weekly, subconfluency of stocks was maintained. The 4^{th} to 15^{th} passage cells were used for all the measurements.

Time-Dependent Cellular Uptake: The HEp2 cells for cellular uptake experiments were plated at 7500 cells per well in a Costar 96-well plate. They were then allowed to grow for 48 h. The ZnPc stock solutions were prepared at 32 mM in DMSO. Subsequent dilution gave 20 µM in medium (a 2X stock). Further dilution into the cells of the 96-well plate gave a final concentration of 10 µM, with a maximum DMSO concentration of 1%. The uptake of the ZnPcs was allowed to continue for 0, 1, 2, 4, 8, 12 and 24 h. The termination of the uptake was achieved by removing the loading medium and washing the wells with PBS. The concentration of the ZnPcs was calculated from standard curves using intrinsic fluorescence as measured with a BMG FLUOstar plate reader fitted with a 355 nm excitation and a 650 nm emission filter, as it has been previously described.[15] The cells were measured using a

CyQuant cell proliferation assay (Invitrogen) as per manufactures instruction, and the uptake was expressed in terms of nM compound per cell.

Dark Cytotoxicity: The plating of the HEp2 cells was performed as described above for the uptake measurements. The ZnPcs were diluted into medium to a 400 µM concentration. Then 2-fold serial dilutions were prepared to 50 µM, and the cells incubated overnight. The cell toxicity was obtained using Promega's Cell Titer-Blue Viability assay according to manufacturer's instructions. The untreated cells were considered 100% viable while those treated with 0.2% saponin were considered 0% viable. The IC_{50} values were calculated from dose-response curves, which were obtained using GraphPad Prism software.

Phototoxicity: The plating of the HEp2 cells was achieved as described above with compounds concentration range from 6.25-100 µM. After overnight loading, the medium was replaced with the medium containing 50 mM HEPES at pH 7.2. The cells were then exposed to a NewPort light system with 175 W halogen lamp for 20 min and filtered through a water film to provide approximately 1.5 J/cm^2 light dose. The cells were cooled by placing the culture on a 5 ^{o}C Echotherm chilling/heating plate (Torrey Pines Scientific, Inc.) and the plate was incubated overnight. The cell viability was then calculated as described above for the dark cytotoxicity.

Microscopy: The cells for microscopy were incubated in a glass bottom 6-well plate (MatTek) and allowed to grow for 48 h. They were then exposed to 10 µM of each ZnPc overnight. Organelle tracers from Invitrogen were used at the following concentrations: LysoSensor Green 50 nM, MitoTracker Green 250 nM, ER Tracker Blue/white 100 nM, and BODIPY FL C5 ceramide 1 µM. The organelle tracers diluted in medium and the cells were incubated concurrently with ZnPcs and tracers for 30 minutes before washing 3 times with

PBS and microscopy. The microscopy images were obtained using a Leica DMRXA microscope with 40× NA 0.8dip objective lens and DAPI, GFP and Texas Red filter cubes (Chroma Technologies).

2.7. References

1. Han, G-F.; Wang, J-J.; Shim, Y. K. *J. Photosci.* **2001**, *8* (2), 71-73.
2. Richter, A. M.; Cerruti-Sola, S.; Sternberg, E. D.; Dolphin, D.; Levy, J. G. *J. Photochem. Photobiol. B: Biology* **1990,** *5* (2), 231-244.
3. Stolik, S.; Delgado, J. A.; Pérez, A.; Anasagasti, L. *J. Photochem. Photobiol. B, Biology* **2000,** *57* (2-3), 90-93.
4. Martins, J.; Almeida, L.; Laranjinha, J. *Photochem. Photobiol.* **2004,** *80* (2), 267-273.
5. Ali, H.; van Lier, J. E. *Chem. Rev.* **1999**, *99*, 2379-2450.
6. Allen, C. M.; Sharman, W. M.; van Lier, J. E. *J. Porphyrins Phthalocyanines* **2001**, *5*, 161-169.
7. Ben-Hur, E.; Chan, W.-S. In *The Porphyrin Handbook*, K. M. Kadish, K. M. Smith, R. Guilard, R. (Eds.), *Academic Press: Boston* **2003**, *19*, 1-35.
8. Wohrle, D.; Iskander, N.; Graschew, G.; Sinn, H.; Friedrich, E. A.; Maierborst, W.; Stern, J.; Schlag, P. *Photochem. Photobiol.* **1990**, *51*, 351-356.
9. Reddi, E.; Ceccon, M.; Valduga, G.; Jori, G.; Bommer, J. C.; Elisei, F.; Latterini, L.; Mazzucato, U. *Photochem. Photobiol.* **2002**, *75*, 462-470.
10. Sol, V.; Branland, P.; Chaleix, V.; Granet, R.; Guilloton, M.; Lamarche, F.; Verneuil, B.; Krausz, P. *Bioorg. Med. Chem. Lett.* **2004**, *14*, 4207-4211.
11. Minnock, A.; Vernon, D. I. Schofield, J.; Griffiths, J.; Parish, J. H.; Brown, S. B. *J. Photochem. Photobiol. B: Biol.* **1996**, *32*, 159-164.
12. Dummin, H.; Cernay, T.; Zimmermann, H. W. *J. Photochem. Photobiol. B:Biol.* **1997**, *37*, 219-229.
13. Kessel, D.; Luguya, R.; Vicente, M. G. H. *Photochem. Photobiol.* **2003**, *78*, 431-435.
14. Sibrian-Vazquez, M.; Nesterova, I. V.; Jensen, T. J.; Vicente, M. G. H. *Bioconjugate Chem.* **2008**, *19*, 705-713.
15. Jensen, T. J.; Vicente, M. G. H.; Luguya, R.; Norton, J.; Fronczek, F. R.; Smith, K. M. *J. Photochem. Photobiol. B: Biol.* **2010**, *100*, 100-111.

16. Duan, W. B.; Lo, P. C.; Duan, L.; Fong, W. P.; Ng, D. K. P. *Bioorg. Med. Chem.* **2010**, *18*, 2672-2677.

17. Ongarora, B. G.; Hu, X.; Li, H.; Fronczek, F. R.; Vicente, M. G. H. *MedChemComm* **2012,** *3* (2), 179-194.

18. Ricchelli, F.; Franchi, L.; Miotto, G.; Borsetto, L.; Gobbo, S.; Nikolov, P.; Bommer, J. C.; Reddi, E. *Int. J. Biochem. Cell Biol.* **2005**, *37*, 306-319.

19. Li, H.; Fronczek, F. R.; Vicente, M. G. H. *J. Med. Chem.* **2008**, *51*, 502-511.

20. Villanueva, A. *J. Photochem. Photobiol. B: Biol.* **1993**, *18*, 295-298.

21. McMillin, D. R.; Shelton, A. H.; Bejune, S. A.; Fanwick, P. E.; Wall, R. K. *Coord. Chem. Rev*. **2005**, *249*, 1451-1459.

22. Caminos, D. A.; Durantini, E. N. *J. Photochem. Photobiol. A: Chem.* **2008**, *198*, 274-281.

23. Fu, B. Q.; Zhang, D.; Weng, X. C.; Zhang, M.; Ma, H.; Ma, Y. Z.; Zhou, X. *Chem. Eur. J.* **2008**, *14*, 9431-9441.

24. B. Chen, B.; Wu, S.; Li, A. X.; Liang, F.; Zhou, X.; Cao, X. P.; He, Z. K. *Tetrahedron* **2006**, *62*, 5487-5497.

25. Sibrian-Vazquez, M.; Ortiz, J.; Nesterova, I. V.; Fernández-Lázaro, F.; Sastre-Santos, A.; Soper, S. A.; Vicente, M. G. H. *Bioconjugate Chem.* **2007**, *18*, 410-420.

26. Lowery, M. K.; Starshak, A. J.; Esposito, J. N.; Paul C. Krueger, P. C.; Kenney, M. E. *Inorg. Chem.* **1965** *4* (1), 128-128.

27. Wohrle, D.; Eskes, M.; Shigehara, K.; Yamada, A. *Synthesis-Stuttgart* **1993**, 194-196.

28. Sharman, W. M.; van Lier, J. E. In *The Porphyrin Handbook*, K. M. Kadish, K. M. Smith, R. Guilard, (Eds), *Academic Press: Boston* **2003**, *15*, 1-60.

29. Kobayashi, N.; Miwa, H.; Isago, H.; Tomura, T. *Inorg. Chem.* **1999**, *38*, 479-485.

30. Jiang, X.-J.; Yeung, S.-L.; Lo, P.-C.; Fong, W.-P.; Ng, D. K. P. *J. Med. Chem.* **2010,** *54* (1), 320-330.

31. Rodriguez-Morgade, M. S.; de la Torre, G.; Torres, T. In *The Porphyrin Handbook*, K. M. Kadish, K. M. Smith, R. Guilard, (Eds), *Academic Press: Boston* **2003**, *15*, 125-160.

32. Giuntini, F.; Nistri, D.; Chiti, G.; Fantetti, L.; Jori, G.; Roncucci, G. *Tetrahedron Lett.* **2003**, *44*, 515-517.

33. Brykina, G. D.; Uvarova, M. I.; Koval, Y. N.; Shpigun, O. A. *J. Anal. Chem.* **2001**, *56*, 940-944.

34. Uvarova, M. I.; Brykina, G. D.; Shpigun, O. A. *J. Anal. Chem.* **2000**, *55*, 910-925.

35. Wang, J.; Liu, H.; Xue, J. P.; Jiang, Z.; Chen, N. S.; Huang, J. L. *Chinese Sci. Bull.* **2008**, *53*, 1657-1664.

36. Rager, C.; Schmid, G.; Hanack, M. *Chem. Eur. J.* **1999**, *5*, 280-288.

37. Filippis, M. P.; Dei, D.; Fantetti, L.; Roncucci, G. *Tetrahedron Lett.* **2000**, *41*, 9143-9147.

38. Easson, M. W.; Fronczek, F. R.; Jensen, T. J.; Vicente, M. G. H. *Bioorg. Med. Chem.* **2008**, *16*, 3191-3208.

39. Hofman, J.-W.; van Zeeland, F.; Turker, S.; Talsma, H.; Lambrechts, S. A. G.; Sakharov, D. V.; Hennink, W. E.; van Nostrum, C. F. *J. Med. Chem*. **2007**, *50*, 1485-1494.

40. Zorlu, Y.; Dumoulin, M. Durmus, H.; Ahsen, V. *Tetrahedron* **2010**, *66*, 3248-3258.

41. Saka, E. T.; Durmus, M.; Kantekin, H. *J. Organomet. Chem.* **2011**, *696*, 913-924.

42. Masilela, N.; Nyokong, T. *J. Luminescence* **2010**, *130*, 1787-1793.

43. Maree, D. M.; Kuznetsova, M.; Nyokong, T. *Photochem. Photobiol. A: Chem.* **2001**, *140*, 117-125.

44. Engelmann, F. M.; Mayer, I.; Gabrielli, D. S.; Toma, H. E.; Kowaltowski, A. J.; Araki, K.; Baptista, M. S. *J. Bioenerg. Biomembranes* **2007**, *39*, 175-185.

45. Luo, Y.; Chang, C. K.; Kessel, D. *Photochem. Photobiol.* **1996**, *63*, 528-534.

46. Rao, R. V.; Hermel, E.; Castro-Obregon, S.; del Rio, G. Ellerby, L. M.; Ellerby, H. M.; Bredesen, D. E. *J. Biol. Chem.* **2001**, *276*, 33869-33874.

47. Kessel, D. *J. Porphyrins Phthalocyanines* **2004**, *8*, 1009-1014.

48. Fery-Forgues, S.; Lavabre, D. *J. Chem. Ed.* **1999**, *76*, 1260-1264.

CHAPTER 3

SYNTHESES, CHARACTERIZATION AND BIOLOGICAL EVALUATION OF PHTHALOCYANINE-PEPTIDE CONJUGATES FOR EPIDERMAL GROWTH FACTOR RECEPTOR TARGETING IN COLON CANCER*

3.1. Background

Colorectal cancer (CRC) is currently the second leading cause of cancer-related deaths among both men and women in the US.[1] It typically develops over several years from adenomatous polyps to carcinoma. Routine colon screening, detection and removal of polyp adenomas and early stage cancer reduces the incidence of CRC. However, most cancers are detected at a stage where they may become terminal because they lack outward signs or symptoms.[2] The current methods of detection for CRC such as flexible sigmoidoscopy, standard colonoscopy, radiography, and computer tomography (CT) colonoscopy frequently miss small adenomas (< 5 mm) and flat lesions, the two early stages of CRC.[2] Early detection of small adenomas and flat lesions could prevent the development of the malignant tumors.

The new detection methods currently being employed to accomplish this goal include chromoendoscopy, narrow band imaging, and blue light auto-fluorescence.[3] Chromoendoscopy utilizes an absorptive or contrast dye, such as methylene blue, to stain the mucosa for standard white light colonoscopy, enhancing tissue characterization, differentiation, and diagnosis of small adenomas.[2,3] Narrow band imaging uses a blue and green filter to narrow the white colonoscopic light to illuminate the mucosa, and blue light auto-fluorescence involves a UV light source to generate mucosal auto-fluorescence. In addition, confocal laser endomicroscopy (CLE) has been employed to image the mucosa, with fluorescein, acriflavine, or cresyl violet as the

---

* This chapter originally appeared in Ongarora, B. G.; Fontenot, K. R.; Hu, X.; Sehgal, I.; Satyanarayana-Jois, S. D.; Vicente, d. G. H., Phthalocyanine–Peptide Conjugates for Epidermal Growth Factor Receptor Targeting. *Journal of Medicinal Chemistry* **2012,** *55* (8), 3725-3738.[4]

fluorescent dyes. The drawbacks of these dyes are their poor selectivity for CRC, residual toxicity, and emission wavelengths in the visible region of the optical spectrum.[5]

On the other hand, phthalocyanines (Pcs) are tetrapyrrolic macrocycles with extended π-conjugated systems that typically emit at long wavelengths (> 670 nm) with high fluorescence quantum yields.[6,7] Near-IR fluorescence for bioimaging applications has several advantages: low Raman scattering cross-sections associated with the use of low energy excitation photons, larger Raman-free observation windows and reduced absorption and fluorescence from other compounds.[8] Pcs have been extensively investigated in the last decades for a variety of applications, including as colorant dyes, catalysts, sensors, and as photosensitizers for photodynamic therapy (PDT) of cancers.[9-11]

As pointed out in Chapter 1, PDT involves the administration of a photosensitizer followed by activation with red light to produce cytotoxic oxygen species that destroy malignant cells.[12,13] Due to their low dark toxicity, high photostability and ability to preferentially accumulation within tumor tissue, Pcs are promising cancer diagnostic and treatment agents. Furthermore, conjugation of Pcs with peptide ligands directed at specific receptors over-expressed in cancer cells, such as the human epidermal growth factor receptor (EGFR), is an attractive strategy for increasing their biological efficacy.[14-18] EGFR is over-expressed in CRC, including small cancers (< 5 mm) and the flat, dysplastic, aberrant crypt foci that are believed to precede cancer development.[19-21]

Among the EGFR-targeting biomolecules recently reported for selective delivery of cytotoxic drugs to the tumor sites,[22-26] two small peptides with sequences LARLLT (designated EGFR-L1)[27] and YHWYGYTPQNVI (designated EGFR-L2)[28] are particularly attractive due to their availability, low immunogenicity, ease of conjugation to various molecules, and reported

superior EGFR-targeting ability. EGFR-L1 was selected from computational screening of an EGFR peptide ligand virtual library, and shown to target EGFR both *in vitro* (in EGFR over-expressing H1299 cells) and *in vivo* (in H1299 tumor-bearing mice following intravenous (iv) administration).[27] On the other hand, EGFR-L2 was identified from screening of a phage display peptide library and also shown to bind to EGFR both *in vitro* (SMMC-7721 cells) and *in vivo* (SMMC-7721 tumor bearing mice following iv injection).[28]

In the continuing pursuit for tumor-selective fluorescent imaging and PDT agents, a Pc conjugated to a bifunctional nuclear localizing sequence and cell-penetrating peptide containing 32 amino acid residues, via either a short (5-atom) or a PEG (20-atom) linker, has been shown to display higher fluorescence quantum yield and increased cellular uptake compared with non-conjugated Pc.[29] In this Chapter, the synthesis, photophysical, and biological evaluation of Pc conjugates to either EGFR-L1 or EGFR-L2 peptide ligands is described.

3.2. Results and Discussion

3.2.1. Synthesis and Characterization

The Pc-peptide conjugates described in this Chapter were designed to specifically target EGFR. The synthetic routes to conjugates **3.5**, **3.6**, **3.9** and **3.11** are shown in Schemes 1 and 2. Pcs **3.1** and **3.7** were prepared by statistical condensation of 3- or 4-(*p*-*N*-Boc-aminophenoxy)-phthalonitrile and 4-*tert*-butylphthalonitrile (in 1:3 ratio) in DMAE at 140 ºC for 5 h, and in the presence of Zn(II) acetate and DBN, followed by TFA deprotection of the Boc groups, as described in Chapter 1 and also in literature.[30] Reaction of Pc **3.1** with diglycolic anhydride in DMF gave the corresponding α-substituted carboxy-terminated Pc **3.2**, in 86.6% yield, following reported literature procedure.[29,31] The coupling of Pc **3.2** with commercially available *tert*-butyl protected PEG using HOBt, EDCI and DIEA, following by deprotection of the *tert*-butyl group

afforded the Pc **3.4** in 68.3% overall yield;[31] lower yields were obtained when TBTU was used in place of EDCI, due to a more difficult purification of the target Pc-PEG compounds. Solid-phase conjugation of Pc **3.4** to the two peptide sequences LARLLT[27] (EGFR-L1) and GYHWYGYTPQNVI[28] (EGFR-L2) using DIEA, HOBt and TBTU or HATU in DMF and at room temperature, gave the targeted Pc-peptide conjugates **3.5** and **3.6** in 40-80% yields, after cleavage from the solid support and reversed-phase chromatographic purification. A glycine residue at the N-terminus of the EGFR-L2 peptide was meant to enhance the conjugation reaction yields.[31,32] Coupling reactions with Pc **3.3** gave traces of the product (MALDI-TOF).

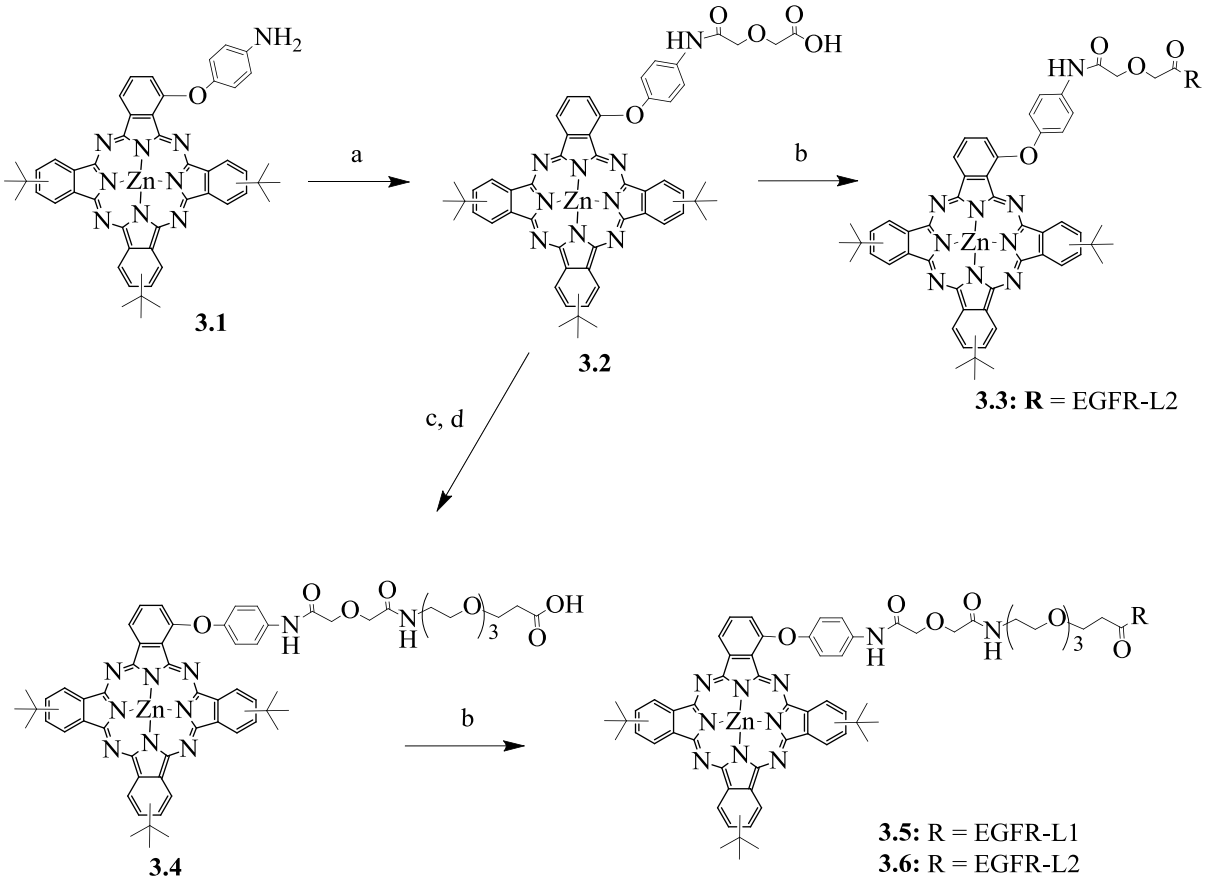

Scheme 3.1: Synthesis of *mono*-peptide α-substituted ZnPc. Conditions: (a) 1,4-dioxane-2,6-dione, DMF, r.t., (86.6%). (b) DIEA, HOBt, TBTU, EGFR-L1/L2, DMF, 24 h, r.t., 40-79% (c) *tert*-butyl-12-amino-4,7,10-trioxadodecanoate, DIEA, HOBt, EDCI, DMF, 48 h, r.t., (76.5%). (d) TFA, dichloromethane, 4 h, (89.3%).

Reaction of Pc **3.7** with diglycolic anhydride in DMF gave the corresponding β-substituted carboxy-terminated Pcs **3.8**, in 92.2% yield, following the procedure for Pc **3.2** above. The coupling of Pc **3.8** with commercially available *tert*-butyl protected PEG using HOBt, EDCI and DIEA, following by deprotection of the *tert*-butyl group afforded Pc **3.10** in 72.7% overall yield. Lower yields were also obtained when TBTU was used in place of EDCI, just as in Pc **3.2** above. Solid-phase conjugation of Pcs **3.8** and **3.10** to the two peptides EGFR-L1 and EGFR-L2 using DIEA, HOBt and TBTU or HATU in DMF and at room temperature, gave the targeted Pc-peptide conjugates **3.9** and **3.11** in 35-84% yields, after cleavage and purification. Reacting EGFR-L2 with Pc **3.10** gave traces Pc **3.12** (MALDI-TOF).

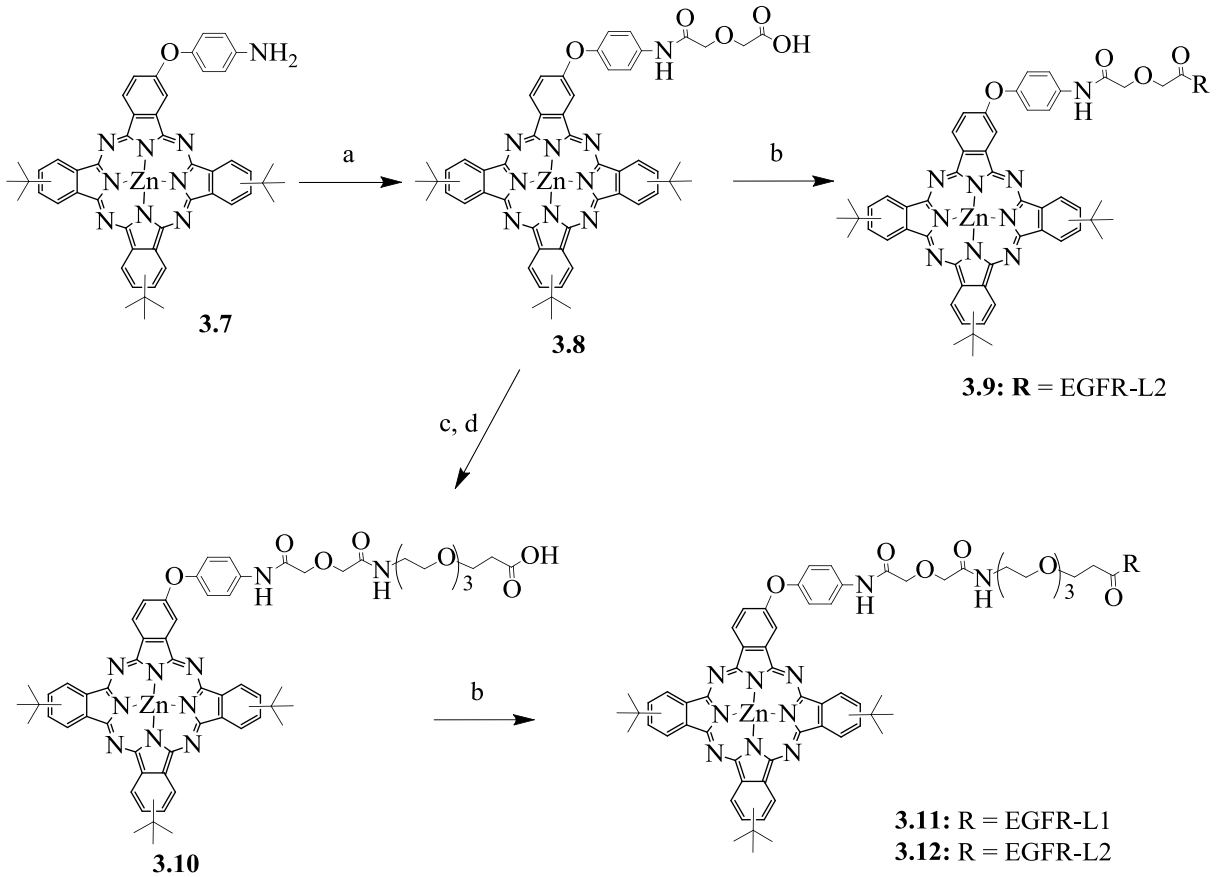

Scheme 3.2: Synthesis of *mono*-peptide β-substituted ZnPc. Conditions: (a) 1,4-dioxane-2,6-dione, DMF, r.t., (92.2%). (b) DIEA, HOBt, TBTU, EGFR-L1/L2, DMF, 24 h, r.t., 35-84% (c) *tert*-butyl-12-amino-4,7,10-trioxadodecanoate, DIEA, HOBt, EDCI, DMF, 48 h, r.t., (82.3%). (d) TFA, dichloromethane, 4 h, (88.3%).

The synthesize of di-peptidic conjugates was attempted using Pc **3.13**, which was prepared as described in Chapter 1 (Scheme 3). The reaction of Pc **3.13** with diglycolic anhydride in DMF gave the corresponding β-substituted di-carboxy-terminated Pc **3.14**, in 87.6% yield. The coupling of Pc **3.14** with commercially available *tert*-butyl protected PEG using HOBt, EDCI and DIEA afforded Pc **3.15** in trace amounts and therefore, conjugation to peptides was not possible. Solid-phase conjugation of Pc **3.14** to EGFR-L1 and EGFR-L2 using DIEA, HOBt and TBTU or HATU in DMF and at room temperature, was not successful either.

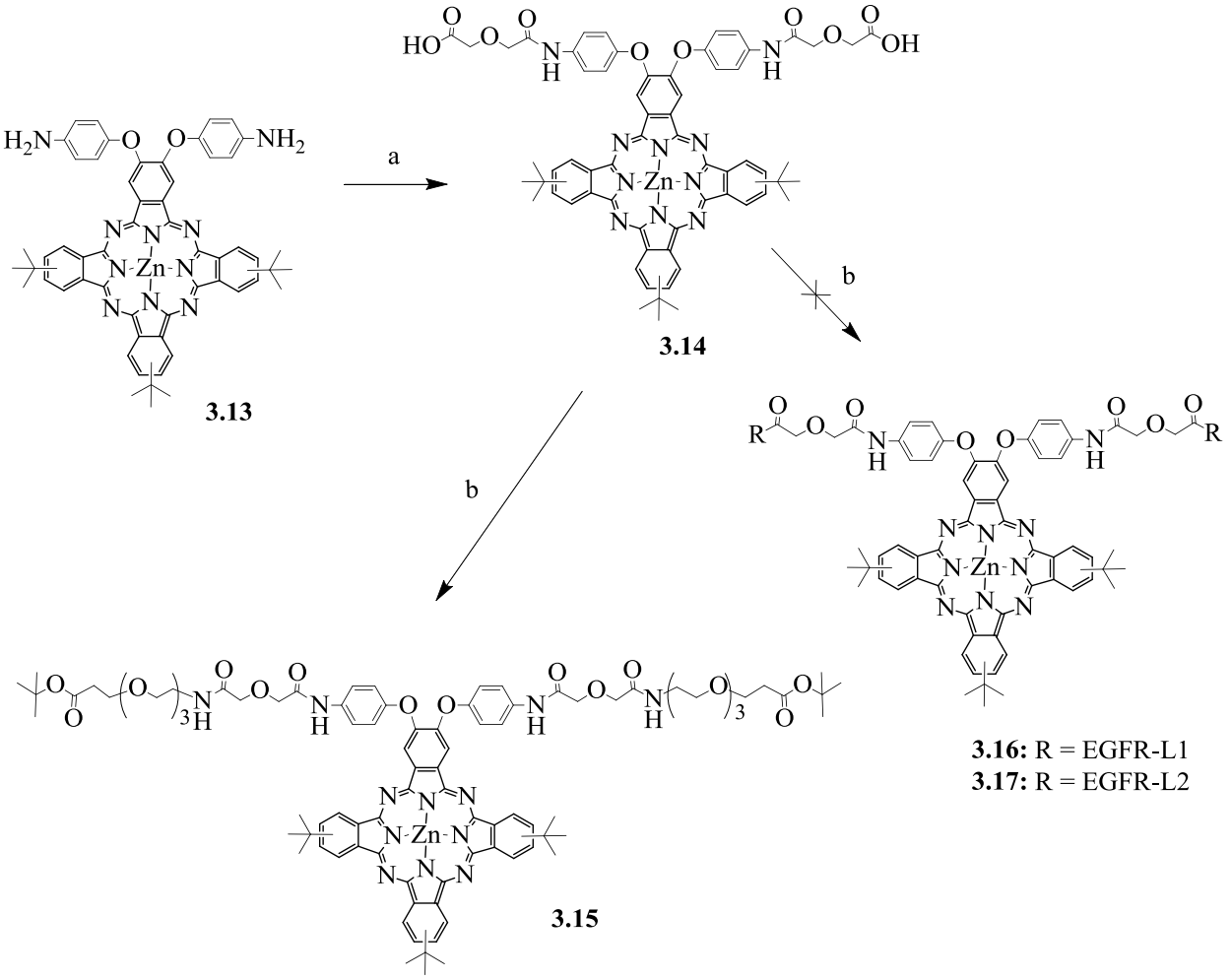

Scheme 3.3: Synthesis of *di*-peptide-conjugated ZnPc. Conditions: (a) 1,4-dioxane-2,6-dione, DMF, r.t., (87.6%). (b) DIEA, HOBt, TBTU, EGFR-L1/L2, DMF, 24 h, r.t. (c) *tert*-butyl-12-amino-4,7,10-trioxadodecanoate, DIEA, HOBt, EDCI, DMF, 48 h, r.t., (Trace amount).

A Pc macrocycle has previously been conjugated to a lysine-rich bifunctional peptide sequence containing 32 amino acid residues, via a similar short (5-atom) and a long (20-atom) PEG linker, and observed that the PEG linker increased cellular uptake into human HEp2 cells, and decreased cytotoxicity of the Pc conjugate.[29] On the other hand, the short linker Pc conjugate showed higher fluorescence quantum yield, probably as a result of its lower conformational flexibility compared with the PEG group. In the current work, a short (5-atom) and a low molecular weight PEG (13-atom) linker between the Pc and the peptide ligand were investigated; the smaller PEG group has the advantages of being commercially available and potentially less flexible than the penta(ethylene glycol) previously used. In addition, the PEG linker is believed to favor an extended conformation for conjugates **3.5** and **3.6** and **3.11**,[31] which might favor EGFR target binding, and to increase their aqueous solubility compared with conjugate **3.9** (*vide infra*).

EGFR over-expression has been found in a variety of human cancers, including breast, ovarian, prostate, pancreatic, and colorectal;[33] for this reason EGFR has been an important target for cancer treatment.[14-18] Monoclonal antibodies (mAbs), such as cetuximab and trastuzumab, and tyrosine kinase inhibitors (TKIs), such as erlotinib and gefitinib, are HER1/EGFR-targeted agents currently in clinical development, or already approved, for use in several countries. Peptides EGFR-L1 and EGFR-L2 were designed to act as a substitute for the natural ligand EGF, which has reported mitogenic and neoangiogenic activity, and has been shown to specifically target EGFR over-expressing tumor cells both *in vitro* and *in vivo*.[27,28] Advantages of using small peptide ligands as target units include their easy synthesis and coupling to fluorophores, their low immunogenicity and high binding affinity for the biological target. The EGFR-L1 conjugates have the potential of being used as dyes, as shown in the biological section.

All Pcs in this series were characterized by MS, NMR, UV-Vis and fluorescence spectroscopy; MALDI-TOF was used to confirm the amino acid sequence in the Pc-peptide conjugates. The spectroscopic properties for Pcs **3.4**, **3.5**, **3.6**, **3.9**, **3.10** and **3.11** are summarized in Table 3.1 and Figure 3.1). All Pcs showed strong Q absorption bands between 677 - 680 nm in DMF, and emissions between 680 - 683 nm in the same solvent, with fluorescence quantum yields in the range 0.10-0.13 and Stokes' shifts of 2 – 4 nm, characteristic of this type of compound.[29,30] All Pc-peptide conjugates were soluble in polar organic solvents, such as DMSO and DMF, up to 1.0 mM concentrations, though, precipitation was observed upon dilution into aqueous solutions. Cremophor EL, a non-ionic solubilizer and emulsifier was, therefore, added to all Pc stock solutions used in the biological experiments. The cell studies were conducted in PBS/DMSO/Cremophor (94:1:5) and the mice studies in PBS/DMSO/Cremophor (85:10:5).

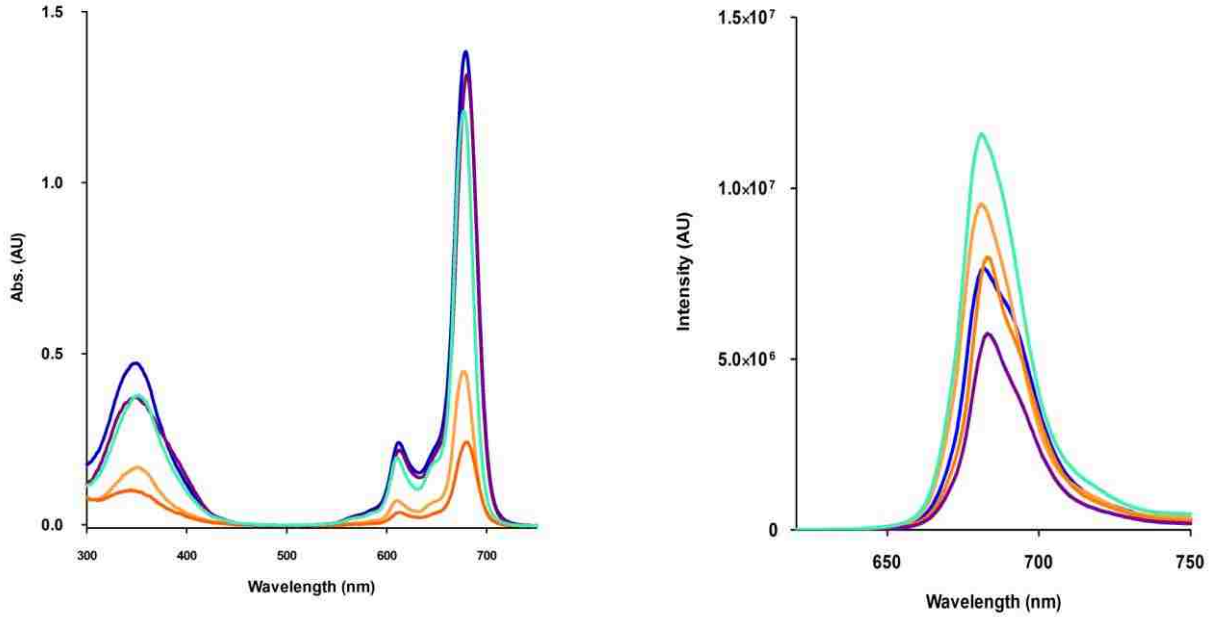

a) **b)**

Figure 3.1. (a) Absorption spectra for Pc conjugates at 8.0 μM and, (b) Emission spectra for Pc conjugates. Pc-conjugates **3.4** (blue), **3.5** (purple), **3.6** (red), **3.9** (tangerine), and **3.11** (turquoise) in DMF solvent.

The solubility of the Pcs decreased in the order Pc-PEG (**3.4** and **3.10**) > Pc-EGFR-L1 (**3.5** and **3.11**) > Pc-EGFR-L2 (**3.6**) > Pc-EGFR-L2 (**3.9**), due to the high hydrophobicity of the longer EGFR-L2 sequence (containing 11 hydrophobic amino acids and only two polar), compared with EGFR-L1 (containing 4 hydrophobic amino acids, one polar and one cationic). Indeed, the uncharged Pc conjugates **3.9** and **3.6** exhibited low solubility in polar protic solvents such as methanol, compared with the positively charged Pc conjugates **3.5** and **3.11**. The least soluble was the Pc-EGFR-L2 conjugate **3.9** bearing a short 5-atom linker.

Table 3.1. Spectroscopic Properties of Pcs in DMF.

Pc	Absorption (nm)	Emission[a] (nm)	Stokes' Shift	ε ($M^{-1}cm^{-1}$)[1]	ϕ_F[b]
3.4	678	682	4	5.35	0.10
3.5	680	683	3	5.33	0.12
3.6	680	683	3	4.60	0.13
3.8	677	680	3	5.19	0.13
3.9	677	681	4	4.85	0.10
3.11	680	682	2	5.27	0.11

[a] Excitation at 670 nm. [b] Calculated using ZnPc (Φ_f = 0.17) as the standard.

3.2.2. Docking

To model the interaction of peptides EGFR-L1 and EGFR-L2, docking studies were carried out using Autodock.[34,35] EGFR-L1 is known to bind to a pocket away from the EGF binding pocket in EGFR,[27] while EGFR-L2 binds to the EGF binding pocket.[28] Hence, for EGFR-L1 grid box for docking calculations were around Glu71, Asn134, Gly177. The low energy docked structure (docking energy of -6.06 kcal/mol) of EGFR-L1 is shown in Figure 3.2a. The Leu4 backbone carbonyl and Thr6 side chain hydroxyl groups form hydrogen-bonding interaction with EGFR. The RLLT sequence of the peptide acquired a β-turn conformation when bound to the receptor EGFR.

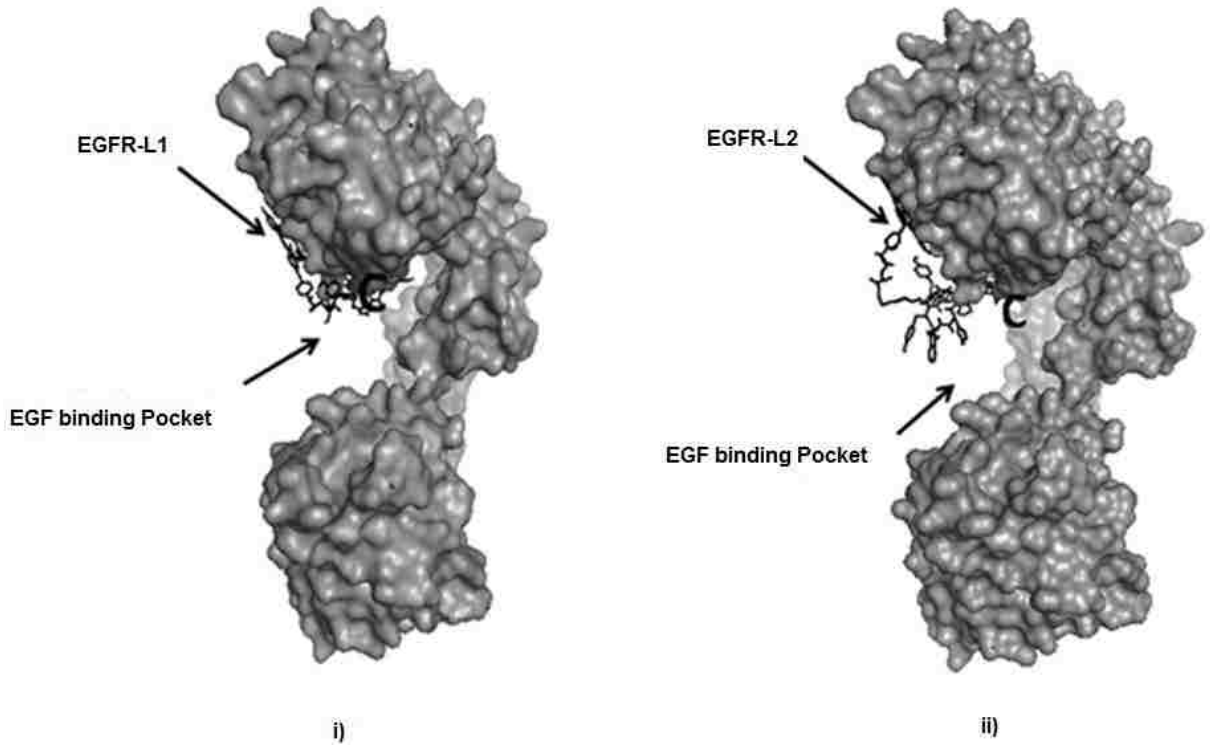

Figure 3.2. Low energy docked structure of (i) EGFR-L1 and (ii) EGFR-L2 peptides with EGF receptor. EGFR is shown in surface and the peptide is shown as dark sticks. The EGF binding pocket is also shown.

The low energy docked structure of EGFR-L2 peptide is shown in Figure 3.2b. EGFR-L2 peptide binds to EGF binding pocket with docking energy of -5.96 kcal/mol. Tyr1 and Ile12 residues from the peptide formed hydrogen-bonding interactions with the EGFR stabilizing the peptide-receptor interaction. Overall, the peptide did not have any particular secondary structure as shown in the Figure 3.2b. Peptide was bound in the cavity of EGF binding pocket of EGFR. These results indicate that both peptides EGFR-L1 and EGFR-L2 can bind to EGFR.

3.2.3. Cell Culture

Four cell lines with different EGFR expressions were used to investigate the cytotoxicity, uptake and subcellular distribution of Pc-peptide conjugates **3.5**, **3.6**, **3.9** and **3.11**: human squamous cell carcinoma HEp2,[29-32] human epidermoid carcinoma A431,[36-38] cercopithecus aethiops kidney Vero (as negative control),[39] and human colorectal adenocarcinoma HT-29

cells.[40-42] The model human HEp2 cells are often used in the investigation of peptide-fluorophore conjugates, while the human A431 cells are a positive control for high EGFR expression (~1-3 million EGFR per cell), and the African green monkey Vero cells are a negative control (lowest expression of EGFR). The human colorectal adenocarcinoma HT-29 cells over-express EGFR, although to a lower degree (~9000 EGFR per cell) than the A431 cells.[39-41]

Cytotoxicity. The dark- and photo-cytotoxicity for Pc-PEG **3.4** and Pc-peptide conjugates **3.5**, **3.6**, **3.9** and **3.11** were evaluated in all cell lines at concentrations up to 125 μM, using the Cell Titer Blue Assay, and the results are summarized in Table 3.2, and shown in Figures 3.3 and 3.4. None of the Pcs was found to be toxic in the dark, with determined IC_{50} values for all Pcs above 125 μM, the highest concentration investigated. Upon exposure to a low light dose (1 J/cm^2), only Pc **3.5** bearing the EGFR-L1 peptide was found toxic to A431, HEp2 and Vero cells (IC_{50} = 16, 17 and 47 μM, respectively).

In human carcinoma HEp2 cells, Pc conjugate **3.5** was significantly more phototoxic than **3.11** (IC_{50} ~ 100 μM), and was in agreement with our observations in Chapter 1, showing that α-substituted Pcs tend to be more phototoxic than the corresponding β-substituted Pcs.[30] On the other hand, none of the Pcs were phototoxic to human HT-29 cells, suggesting that this type of conjugate could potentially be used for imaging of colorectal tumors.

Low toxicity is an important feature of potential new imaging agents to be employed in conjunction with CLE. The Pc-EGFR-L1 conjugate **3.5** was significantly more phototoxic than the corresponding Pc-EGFR-L2 conjugate **3.6**, which might be a result of its higher uptake into cells due to its cationic charge (*vide infra*). The presence of the PEG linker did not have any significant impact on the observed cytotoxicity of the conjugates, although it increased their aqueous solubility.

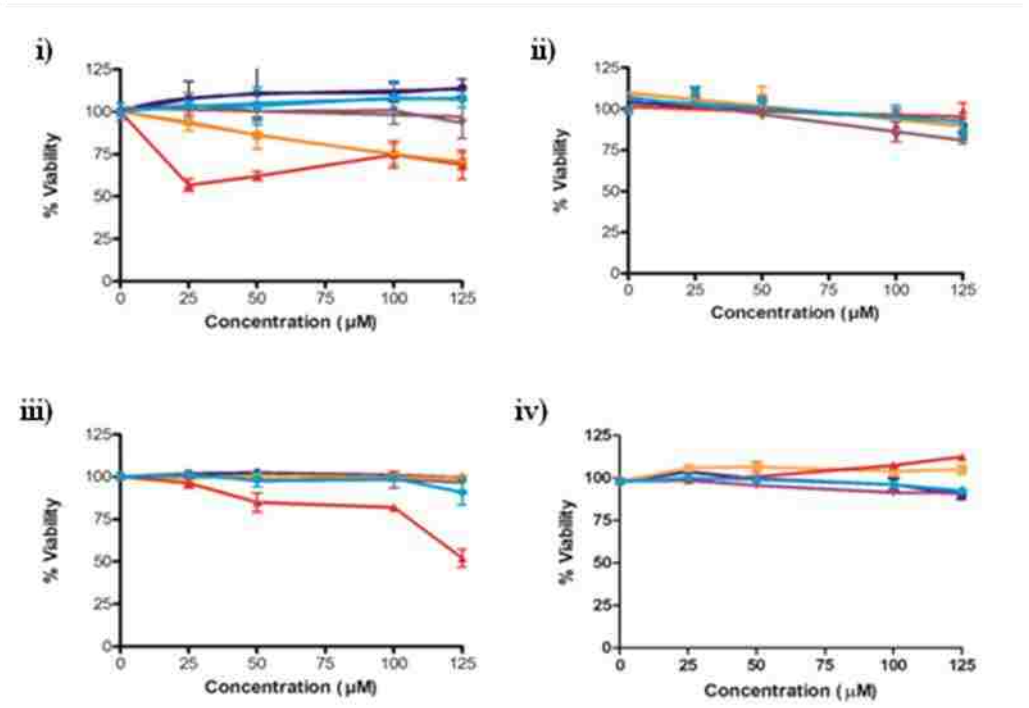

Figure 3.3. Dark toxicity of conjugates Pc **3.4** (blue), **3.5** (purple), **3.6** (red), **3.9** (tangerine), and **3.11** (turquoise) at 10 μM toward (i) A431, (ii) Vero, (iii) HEp2 and (iv) HT-29 cells, using the Cell Titer Blue assay.

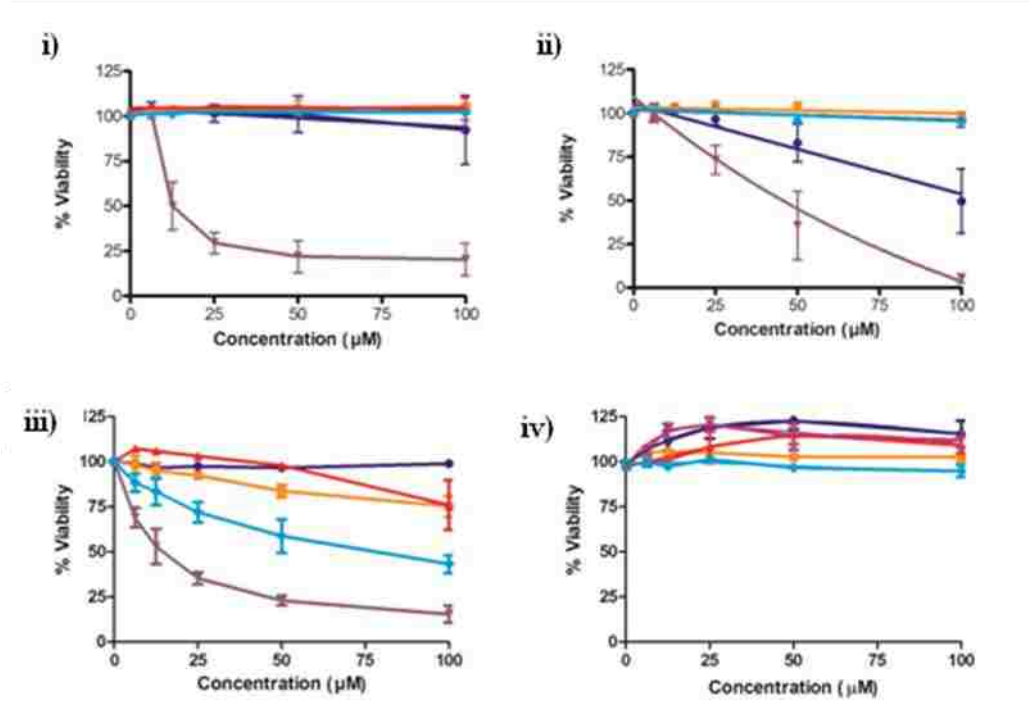

Figure 3.4. Phototoxicity of conjugates Pc **3.4** (blue), **3.5** (purple), **3.6** (red), **3.9** (tangerine), and **3.11** (turquoise) at 10 μM toward (i) A431, (ii) Vero, (iii) HEp2 and (iv) HT-29 cells, using the Cell Titer Blue assay.

Table 3.2. Dark and photo cytotoxicity for Pc conjugates using the Cell Titer Blue assay.

Compound	**A431 cells** IC_{50} (μM) Light/dark	**Vero cells** IC_{50} (μM) Light/dark	**HEp2 cells** IC_{50} (μM) Light/dark	**HT-29 cells** IC_{50} (μM) Light/dark
3.4	>100/>125	>100/>125	>100/>125	>100/>125
3.5	15.8/>125	47.0/>125	17.0/>125	>100/>125
3.6	>100/>125	>100/>125	>100/>125	>100/>125
3.9	>100/>125	>100/>125	>100/>125	>100/>125
3.11	>100/>125	>100/>125	>100/>125	>100/>125

Time-Dependent Uptake. The time-dependent cellular uptake for all Pcs was performed at the non-toxic concentration of 10 μM in all cell lines, and the results are shown in Figure 3.5. There were marked differences in the cellular uptake of the Pc-EGFR-L1 conjugates compared with the Pc-EGFR-L2 conjugates, which might be due to their different overall charge, solubility and tendency for aggregation. While the highly hydrophobic and uncharged Pc-EGFR-L2 conjugates **3.6** and **3.9** were poorly taken up by all cell lines, in particular by A431 and HT-29 cells which over-express EGFR, the positively charged Pc-EGFR-L1 conjugates **3.5** and **3.11** accumulated within cells to a much higher extent. Cells with higher EGFR expression showed higher uptake of the Pc conjugates, about 4-fold increase in A431 vs Vero cells, and a 3- or 2-fold increase in HT-29 colorectal and HEp2 cancer cells, respectively. This result shows that Pc conjugates **3.5** and **3.11** can indeed target cancer cells over-expressing EGFR, in particular CRC cells. Very different Pc uptake into Vero cells, with low expression of EGFR was observed; Pc conjugate **3.11** accumulated the fastest, followed by **3.5** and precursor Pc-PEG **3.4**.

The Pc-EGFR-L2 conjugates **3.9** and **3.6** were taken up by Vero cells to a much lower extent than the Pc-EGFR-L1 conjugates **3.5**, **3.6** and **3.11** bearing a PEG linker accumulated ~ 2-fold higher than **3.9**. These results show that the Pc macrocycle has a natural tendency to accumulate within cells, with or without over-expression of EGFR, and that the PEG-containing

compounds tend to be taken up to a higher extent. The conjugation of the Pc to a small cationic peptide sequence (EGFR-L1) changes the uptake kinetics, as seen in Figure 3.5b, and as previously observed.[32] In EGFR over-expressing cells, Pc conjugates **3.5** and **3.11** clearly were taken up the most of all Pcs investigated. For example, in A431 cells, conjugates **3.5** and **3.11** accumulated ~15-fold more than Pc-PEG **3.4** and than the Pc-EGFR-L2 conjugates **3.6** and **3.9** (Figure 3.5a). Similarly in HT-29 and HEp2 cells, **3.5** and **3.11** were taken up to a higher extent than Pcs **3.4, 3.6** and **3.9**.

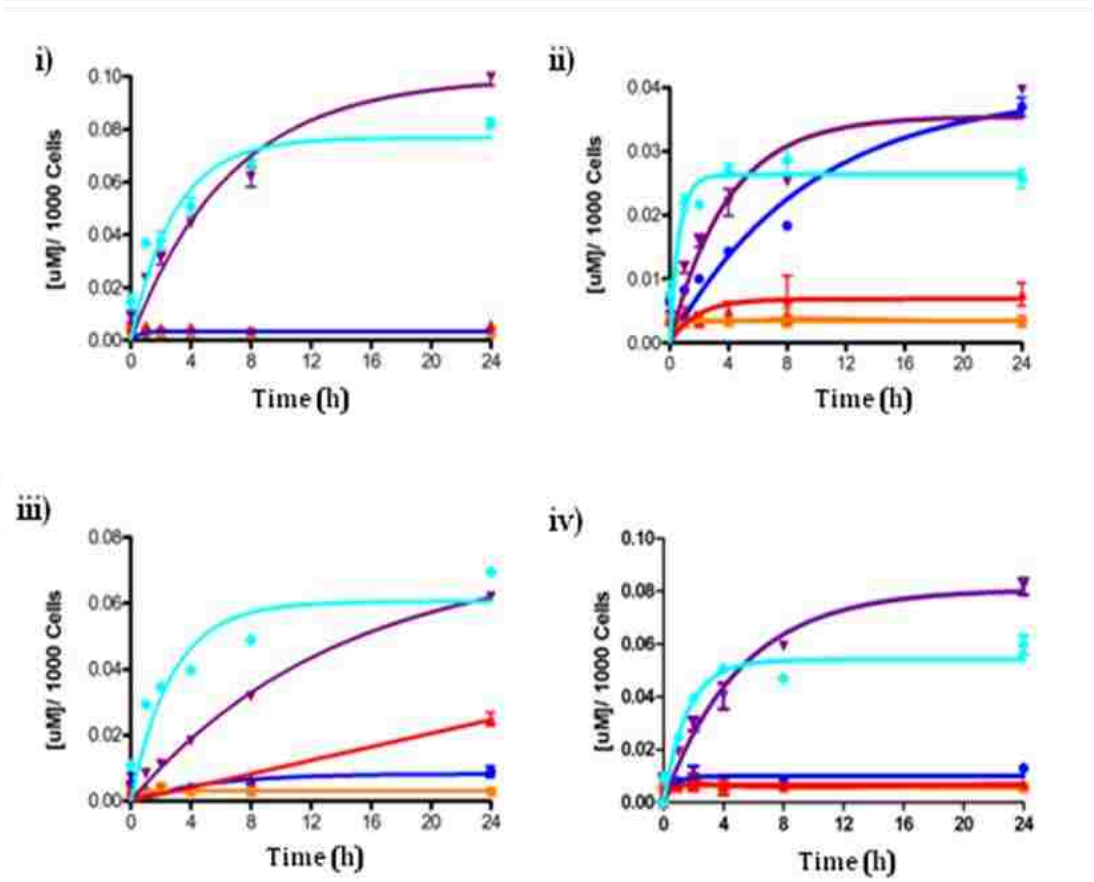

Figure 3.5. Time-dependent uptake of Pcs **3.4** (blue), **3.5** (purple), **3.6** (red) **3.9** (orange) and **3.11** (turquoise) at 10 μM by (i) A431, (ii) Vero, (iii) HEp2 and (iv) HT-29 cells.

These results indicate that the peptide sequence has a marked effect on the cell targeting and uptake ability of this type of Pc conjugates. Autodock investigations showed that both

peptides EGFR-L1 and –L2 can bind to EGFR, EGFR-L2 to the EGF binding site and EGFR-L1 to an outside pocket, as previously reported.[27,28] Although Pc-EGFR-L2 conjugates could potentially bind to EGFR with high specificity and be retained at the cell surface rather than internalized, their low uptake into Vero cells with low expression of EGFR suggests that their low solubility and high tendency for aggregation are responsible for their observed low cellular uptake. Indeed, the least soluble Pc **3.9** accumulated the least within cells compared with all Pcs investigated. On the other hand, the Pc-EGFR-L1 conjugates bearing an arginine residue and overall +1 charge were readily taken up by all cells, as previously observed for porphyrin-peptide conjugates bearing 1 to 4 positively charged residues.[43] Positively charged molecules have been observed to have enhanced ability for crossing negatively charged plasma membranes, in particular those containing arginine due to the unique ability of the protonated guanidinium group to form bidentate hydrogen bonds.[43-47]

Table 3.3. Main subcellular sites of localization for Pc conjugates in human cells.

ZnPc	A431 cells	HEp2 cells	HT-29 cells
3.4	Lyso, Golgi, Mito	Lyso, Golgi	Lyso
3.5	Lyso, Golgi, Mito, ER	Lyso, Golgi, Mito, ER	Lyso, Mito
3.6	Lyso, Golgi, Mito	Lyso, Golgi, Mito	Lyso, ER
3.9	Lyso, Golgi, Mito	Lyso, Golgi, Mito	Lyso, Golgi, Mito
3.11	Lyso, Golgi, Mito	Lyso, Golgi, Mito	Lyso, Golgi, Mito

Of all Pc-peptide conjugates investigated, **3.11** accumulated the fastest within all cell lines, followed by **3.5**, which was found in the highest amount within A431 and HT-29 cells, at times > 8 h after Pc exposure. Due to its rapid and efficient uptake into cells and low cytotoxicity, Pc-peptide **3.11** was chosen for further investigation in animal studies (*vide infra*).

Subcellular Localization. The preferential sites of intracellular localization of Pc-peptide conjugates **3.5**, **3.6**, **3.9** and **3.11** and Pc-PEG **3.4** were evaluated using fluorescence microscopy, in the three human cell lines over-expressing EGFR, i.e. A431, HT-29 and HEp2 cells. The results are summarized in Table 3.3 and shown in Figures 3.6 – 3.11 for conjugates **3.5**, **3.6**, **3.9** and **3.11**. Co-localization experiments were performed using the organelle-specific probes LysoTracker Green (lysosomes), ER Tracker Blue/White (ER), MitoTracker Green (mitochondria) and BODIPY Ceramide (Golgi).

All conjugates localized in multiple sites within the cells. The Pc-EGFR-L1 conjugate **3.11** was found in the lysosomes, mitochondria and Golgi of all cell lines; in addition its regioisomer **3.5** was also observed in the ER, which might in part explain its higher phototoxicity compared with **3.11**.[48,49] Pc-EGFR-L2 conjugates **3.6** and **3.9** were also found in lysosomes, Golgi and mitochondria. Lysosomal localization might result from an endocytic pathway of this type of molecules, as previously observed.[29,43]

The potential fluorescence from the Pc conjugates on the plasma membrane was also investigated, in order to detect any non-internalized EGFR-bound conjugate. However, no fluorescence was detected by microscopy, indicating that the Pc conjugates do not localize on the plasma membrane. No co-localization was observed with fluorescent probe 1-(4-trimethylammoniumphenyl)-6-phenyl-1,3,5-hexatriene *p*-toluenesulfonate (TMA-DPH) that specifically labels the plasma membrane. This result indicates that the Pc-EGFR-L2 conjugates have poor EGFR targeting ability, probably because of their low solubility and high tendency for aggregation. On the other hand, the Pc-EGFR-L1 conjugates **3.5** and **3.11** efficiently targeted EGFR over-expressing cells and were internalized, to a level that is dependent on the degree of EGFR expression.

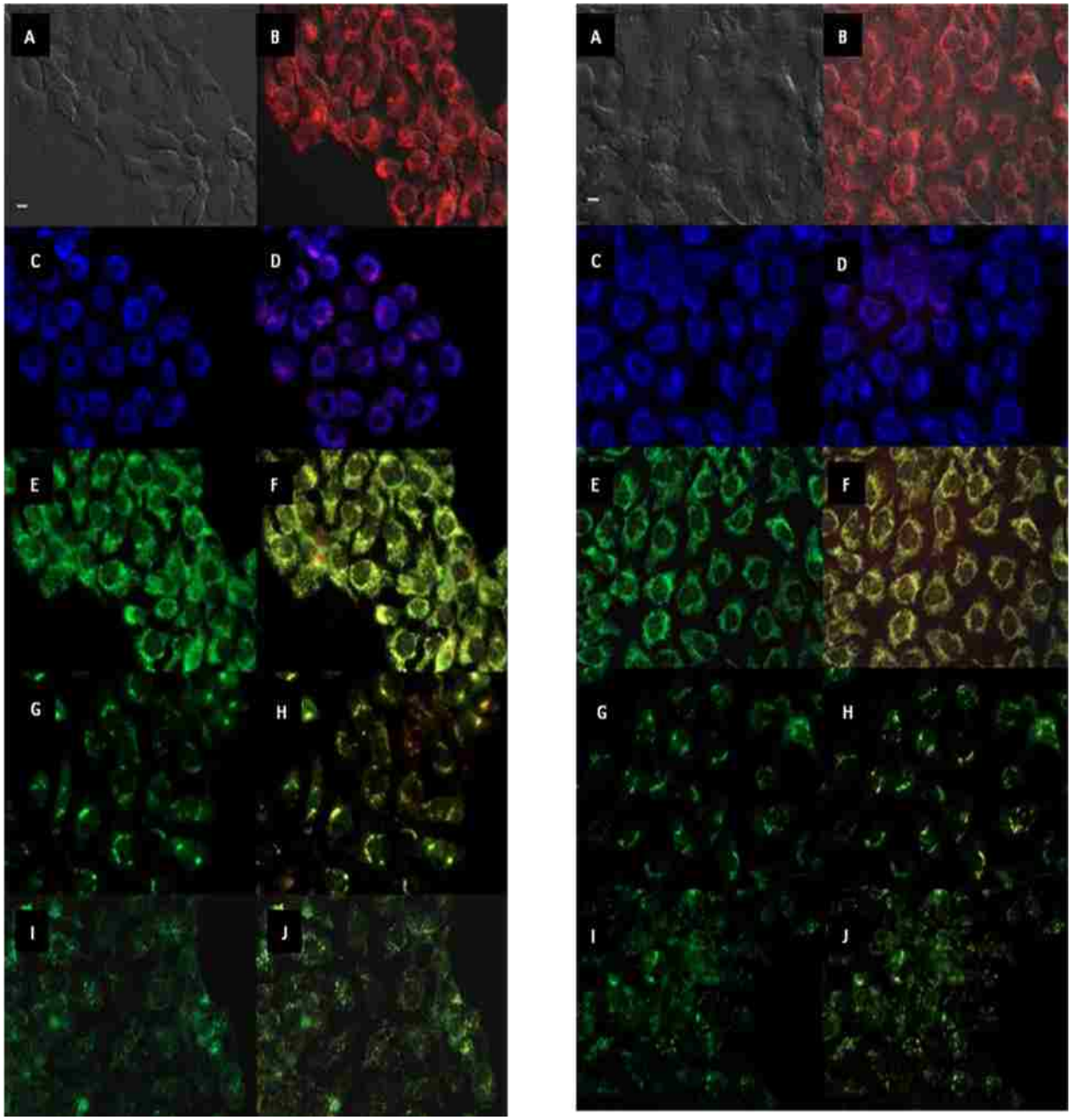

a) b)

Figure 3.6. Subcellular localization of (a) Pc **3.5** in A431 cells at 10 μM for 6 h. (A) Phase contrast, (B) Overlay of **3.5** fluorescence and phase contrast, (C) ER Tracker Blue/White fluorescence, (E) MitoTrack green fluorescence, (G) BoDIPY Ceramide, (I) LysoSensor green fluorescence, and (D, F, H, J) overlays of organelle tracers with **3.5** fluorescence. Scale bar: 10 μm. (b) Pc **3.6** in A431 cells at 10 μM for 6 h. (A) Phase contrast, (B) Overlay of **3.6** fluorescence and phase contrast, (C) ER Tracker Blue/White fluorescence, (E) MitoTrack green fluorescence, (G) BoDIPY Ceramide, (I) LysoSensor green fluorescence, and (D, F, H, J) overlays of organelle tracers with **3.6** fluorescence. Scale bar: 10 μm.

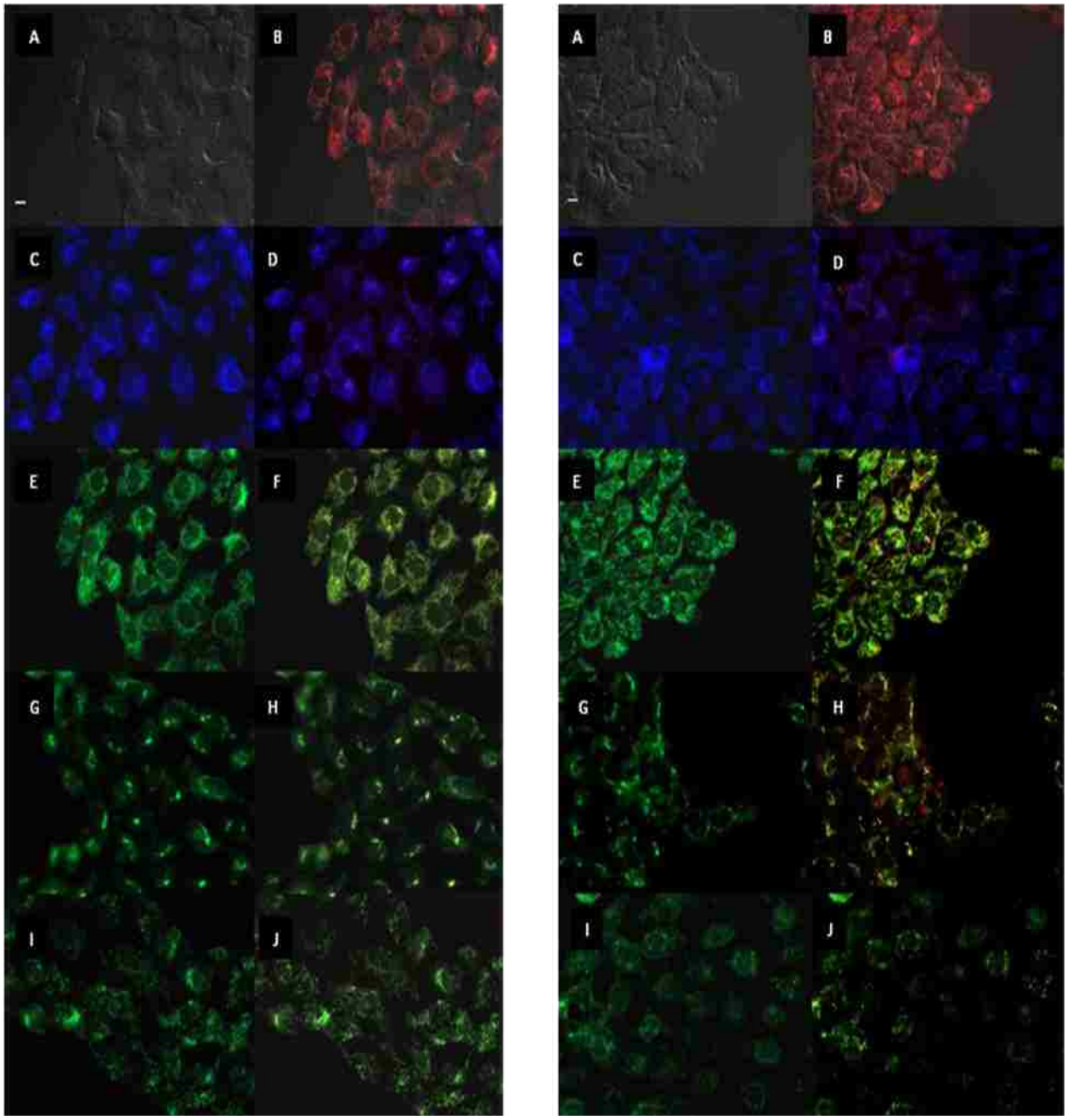

a) b)

Figure 3.7. Subcellular localization of (a) Pc **3.9** in A431 cells at 10 µM for 6 h. (A) Phase contrast, (B) Overlay of **3.9** fluorescence and phase contrast, (C) ER Tracker Blue/White fluorescence, (E) MitoTrack green fluorescence, (G) BoDIPY Ceramide, (I) LysoSensor green fluorescence, and (D, F, H, J) overlays of organelle tracers with **3.9** fluorescence. Scale bar: 10 µm. (b) Pc **3.11** in A431 cells at 10 µM for 6 h. (A) Phase contrast, (B) Overlay of **3.11** fluorescence and phase contrast, (C) ER Tracker Blue/White fluorescence, (E) MitoTracker green fluorescence, (G) BODIPY Ceramide, (I) LysoSensor green fluorescence, and (D, F, H, J) overlays of organelle tracers with **3.11** fluorescence. Scale bar: 10 µm.

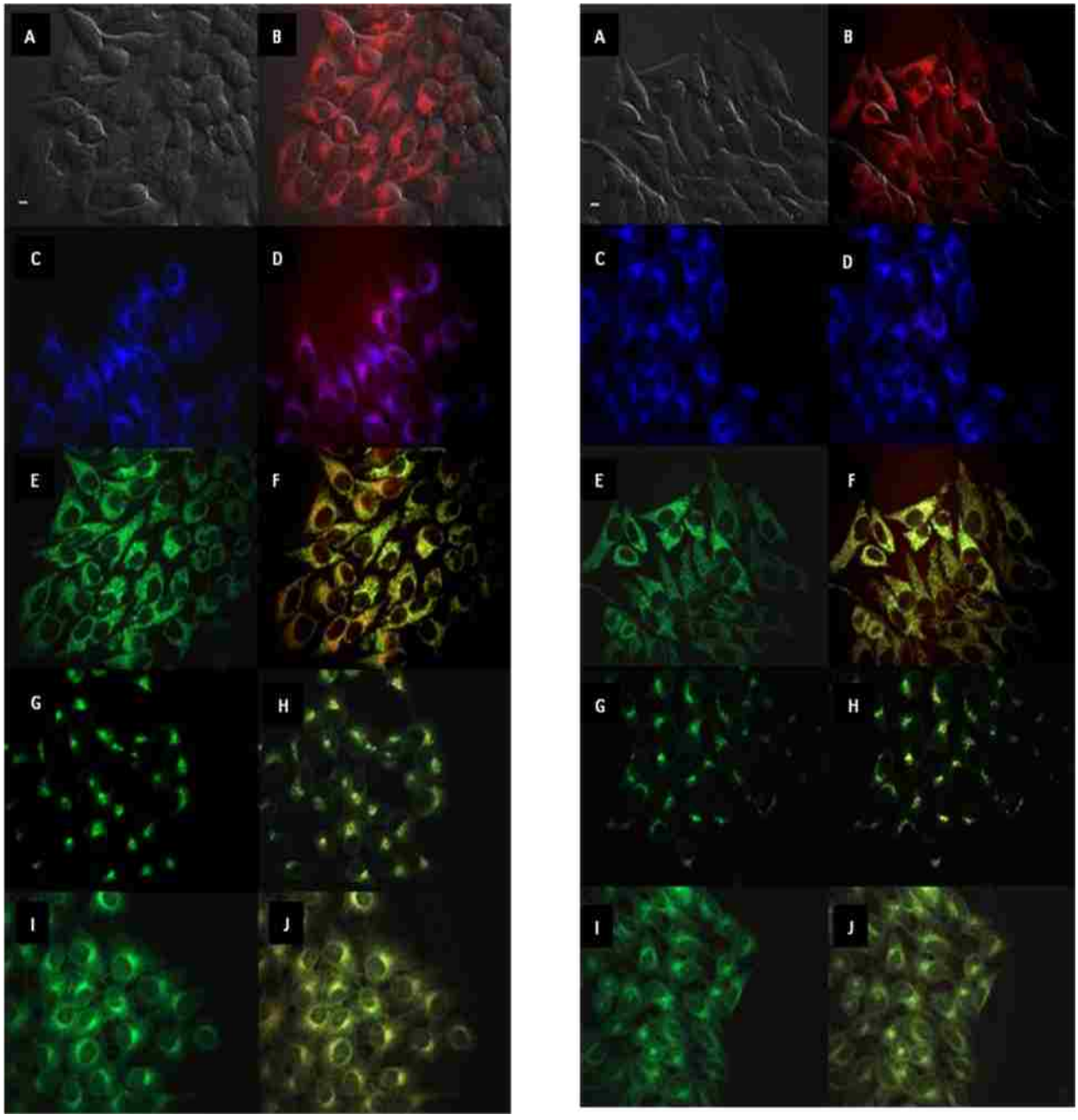

a) b)

Figure 3.8. Subcellular localization of (a) Pc **3.5** in HEp2 cells at 10 μM for 6 h. (A) Phase contrast, (B) Overlay of **3.5** fluorescence and phase contrast, (C) ER Tracker Blue/White fluorescence, (E) MitoTrack green fluorescence, (G) BoDIPY Ceramide, (I) LysoSensor green fluorescence, and (D, F, H, J) overlays of organelle tracers with **3.5** fluorescence. Scale bar: 10 μm. (b) Pc **3.6** in HEp2 cells at 10 μM for 6 h. (A) Phase contrast, (B) Overlay of **3.6** fluorescence and phase contrast, (C) ER Tracker Blue/White fluorescence, (E) MitoTrack green fluorescence, (G) BoDIPY Ceramide, (I) LysoSensor green fluorescence, and (D, F, H, J) overlays of organelle tracers with **3.6** fluorescence. Scale bar: 10 μm.

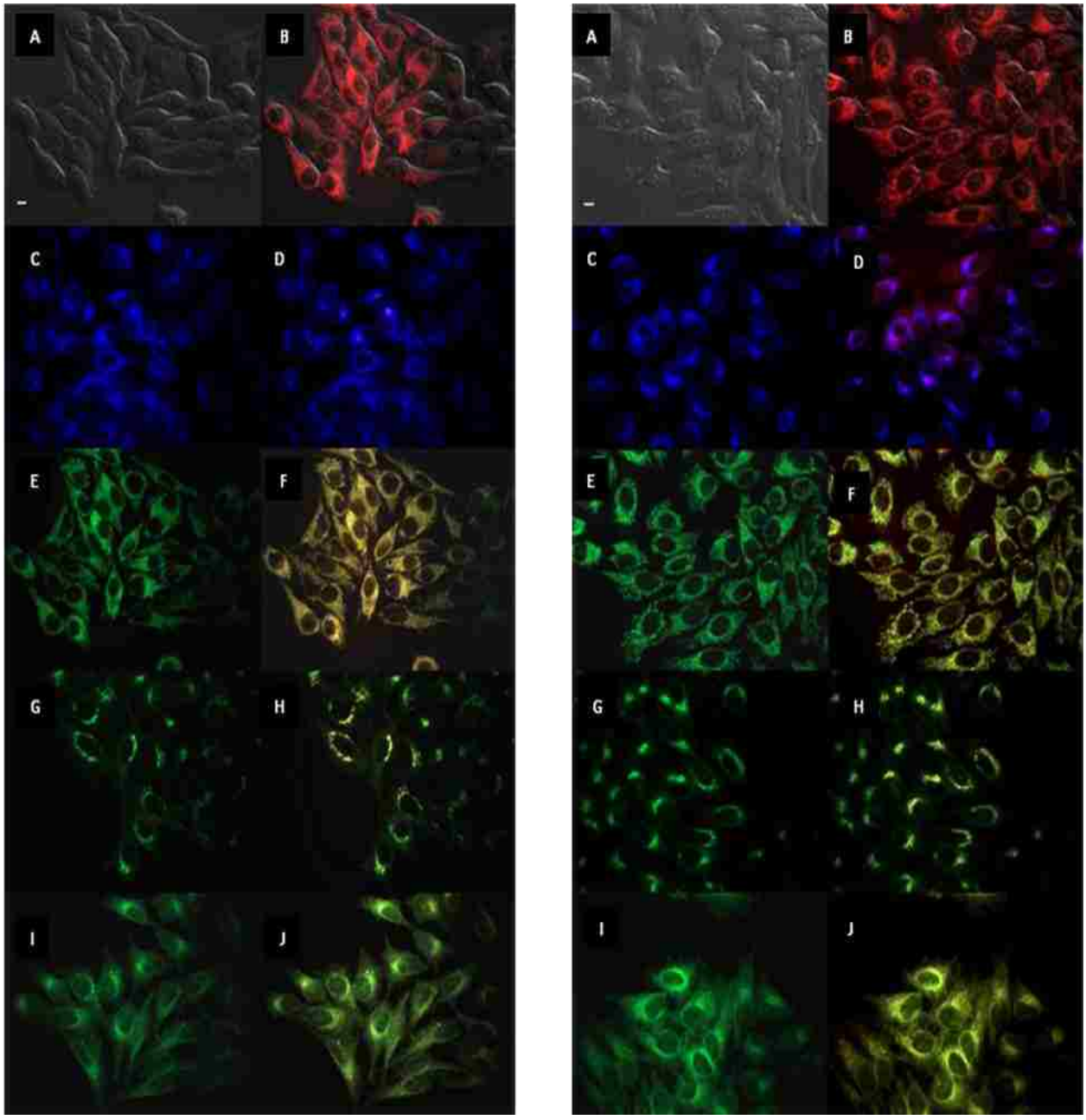

a) b)

Figure 3.9. Subcellular localization of (a) Pc **3.9** in HEp2 cells at 10 μM for 6 h. (A) Phase contrast, (B) Overlay of **3.9** fluorescence and phase contrast, (C) ER Tracker Blue/White fluorescence, (E) MitoTrack green fluorescence, (G) BoDIPY Ceramide, (I) LysoSensor green fluorescence, and (D, F, H, J) overlays of organelle tracers with **3.9** fluorescence. Scale bar: 10 μm. (b) Pc **3.11** in HEp2 cells at 10 μM for 6 h. (A) Phase contrast, (B) Overlay of **3.11** fluorescence and phase contrast, (C) ER Tracker Blue/White fluorescence, (E) MitoTrack green fluorescence, (G) BoDIPY Ceramide, (I) LysoSensor green fluorescence, and (D, F, H, J) overlays of organelle tracers with **3.11** fluorescence. Scale bar: 10 μm.

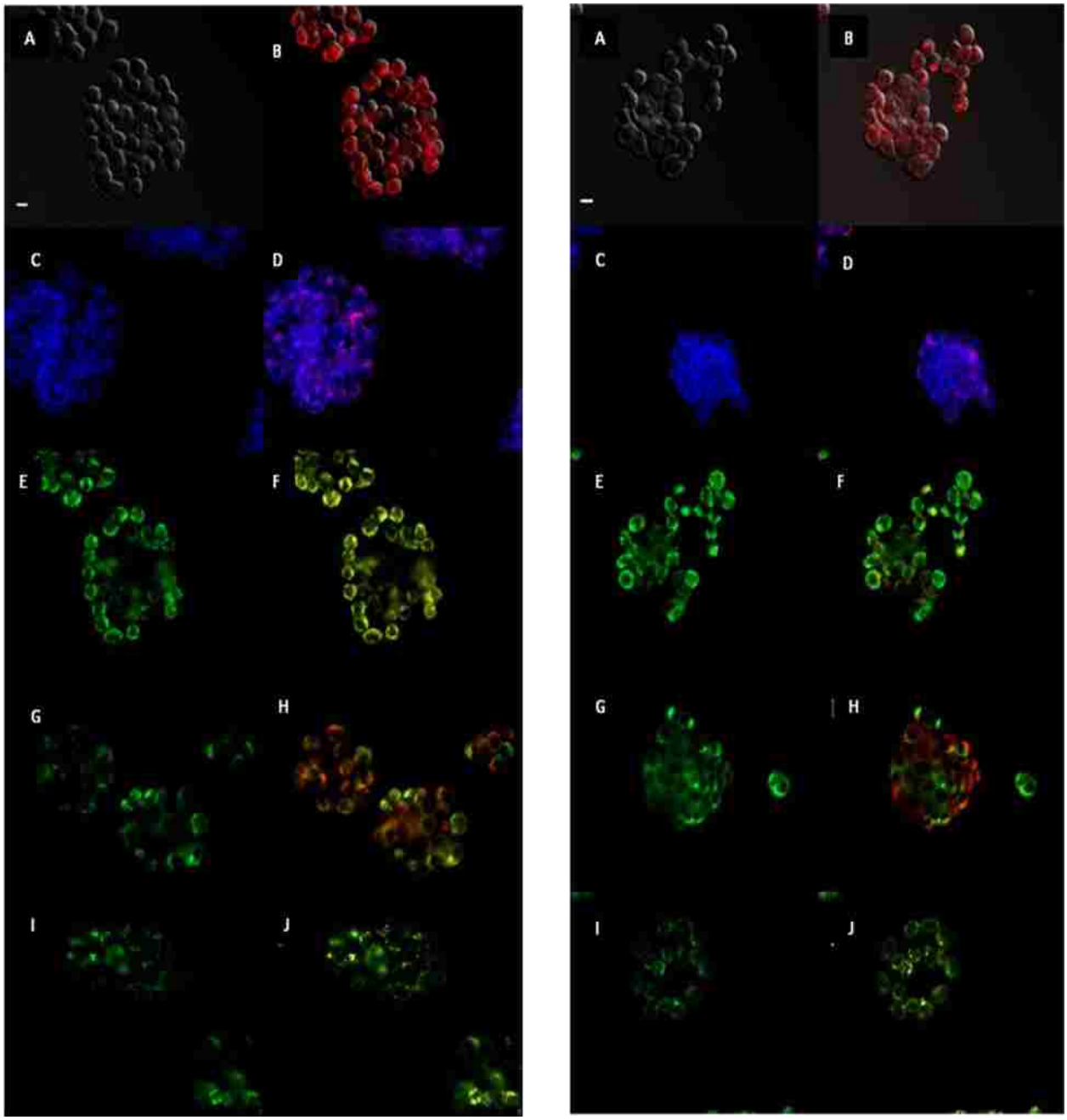

a) b)

Figure 3.10. Subcellular localization of (a) Pc **3.5** in HT-29 cells at 10 μM for 6 h. (A) Phase contrast, (B) Overlay of **3.5** fluorescence and phase contrast, (C) ER Tracker Blue/White fluorescence, (E) MitoTrack green fluorescence, (G) BoDIPY Ceramide, (I) LysoSensor green fluorescence, and (D, F, H, J) overlays of organelle tracers with **3.5** fluorescence. Scale bar: 10 μm. (b) Pc **3.6** in HT-29 cells at 10 μM for 6 h. (A) Phase contrast, (B) Overlay of **3.6** fluorescence and phase contrast, (C) ER Tracker Blue/White fluorescence, (E) MitoTrack green fluorescence, (G) BoDIPY Ceramide, (I) LysoSensor green fluorescence, and (D, F, H, J) overlays of organelle tracers with **3.6** fluorescence. Scale bar: 10 μm.

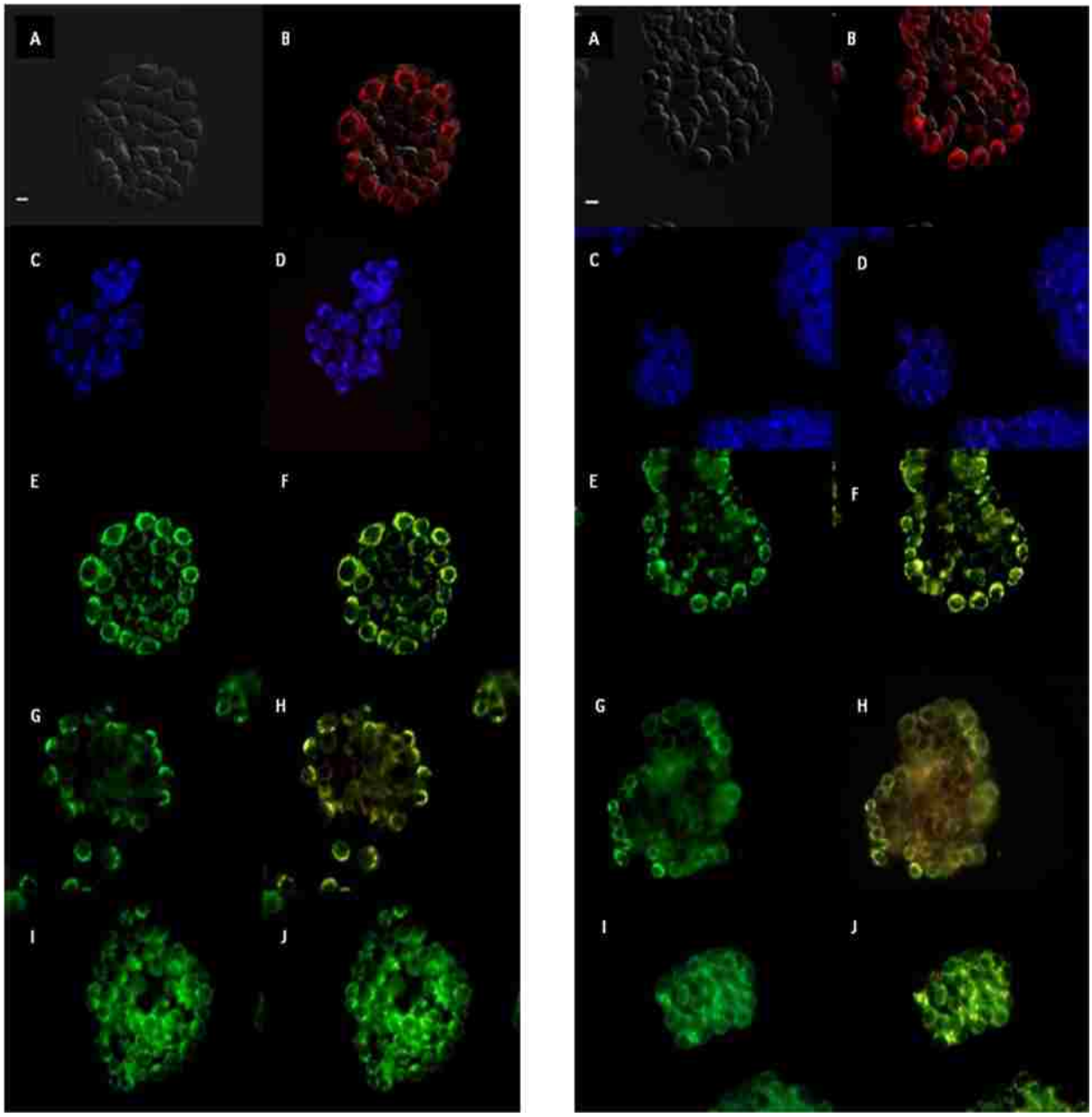

a) b)

Figure 3.11. Subcellular localization of (a) Pc **3.9** in HT-29 cells at 10 µM for 6 h. (A) Phase contrast, (B) Overlay of **3.9** fluorescence and phase contrast, (C) ER Tracker Blue/White fluorescence, (E) MitoTrack green fluorescence, (G) BoDIPY Ceramide, (I) LysoSensor green fluorescence, and (D, F, H, J) overlays of organelle tracers with **3.9** fluorescence. Scale bar: 10 µm. (b) Pc **3.11** in HT-29 cells at 10 µM for 6 h. (A) Phase contrast, (B) Overlay of **3.11** fluorescence and phase contrast, (C) ER Tracker Blue/White fluorescence, (E) MitoTrack green fluorescence, (G) BoDIPY Ceramide, (I) LysoSensor green fluorescence, and (D, F, H, J) overlays of organelle tracers with **3.11** fluorescence. Scale bar: 10 µm.

3.2.4. Mouse Studies

Pc-peptide conjugate **3.11** was chosen for further evaluation in mouse studies, due to its low cytotoxicity and rapid accumulation within cells *in vitro*. Following iv administration of 10 mg/kg of Pc **3.11**, nude mice showed the emergence of tumor-selective fluorescence indicating that the conjugate was taken up into both A431 and HT-29 s.c. tumors. Fluorescence signal which exceeded the background of adjacent skin regions became apparent at 24 h in both tumor types (representative mice shown in Figure 3.12). Microscopically, the deposition of **3.11** in the tumor tissue was not homogeneous, but rather seemed to occur in a multifocal pattern perhaps reflecting regions of greater vascularity (Figure 3.13); however, sufficient Pc **3.11** accumulated within the entire tumor to result in a near-IR fluorescence signal distinguishing tumor above adjacent normal tissue.

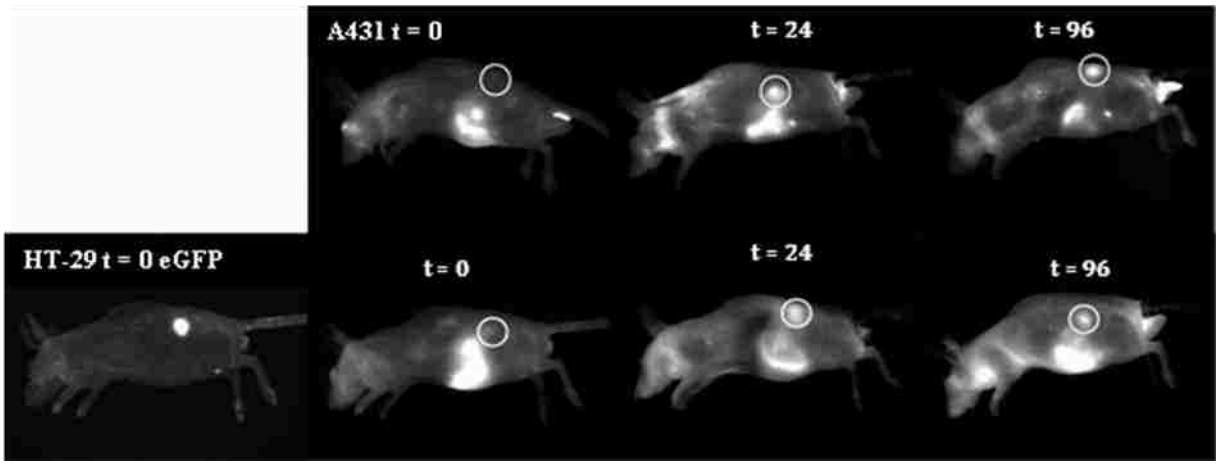

Figure 3.12. Fluorescent images (exc 630 nm/em 700 nm) of nude mice bearing subcutaneous tumor implants of A431 (top) or HT-29 (bottom) cancer cells at various times following iv administration of Pc **3.11**. The tumor positions are circled and the left panel of HT-29 mouse shows the eGFP tumor fluorescence (exc 490 nm/em 535 nm).

Quantitatively, the signal in the HT-29 tumors declined from 24 to 96 h and could not be readily differentiated from adjacent regions without tumor at 96 h. Preliminary studies with the Kodak In Vivo FX imager, demonstrated that in order to visualize a fluorescence signal, that

signal needed to be at least 1.2-fold greater than adjacent regions of the mouse. The fluorescence signal emission in the A431 tumor continued to increase to 96 h (Figure 3.14) suggesting continued uptake of the Pc conjugate over a longer time period in cells over-expressing EGFR. For purposes of comparison, the two tumor groups were not significantly different in tumor size (A431= 133.3 ± 28.7 cm^3 and HT-29 = 141.9± 21.4 cm^3 at 96 h). Neither tumor demonstrated auto-fluorescence at the 630/700 nm spectra window at time 0 when compared with adjacent skin surfaces.

Figure 3.13. Deposition of Pc **3.11** in the HT-29 tumor xenograph, 24 h following iv injection. Images show (A) eGFP indicating HT-29 tumor regions, (B) Pc **3.11** fluorescence, and (C) overlap of tumor and Pc deposition.

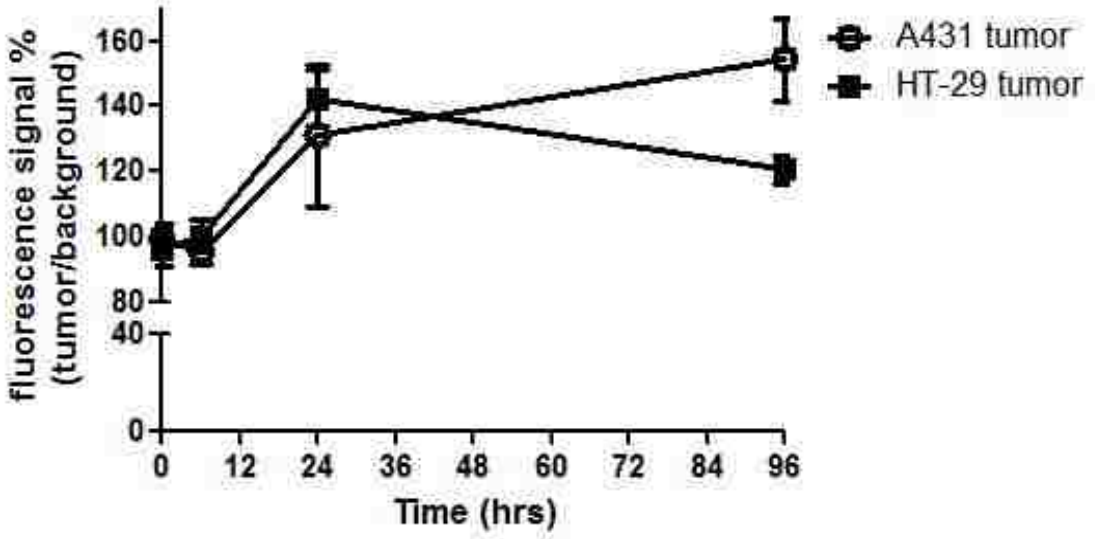

Figure 3.14. Emission signal of **Pc 3.11** at 700 nm in the s.c. human tumor xenographs, over the adjacent (background) skin regions, expressed as a percent. To visually distinguish tumors by fluorescence, the tumor needs to be at least 120% of adjacent regions.

In vivo, tumor-associated fluorescence excitable at 630 and emitted at 700 nm was detectable at 24 h. Correspondence of these wavelengths to the Pc conjugate spectra indicates uptake of the conjugate by the two subcutaneous human tumor xenografts. While both HT-29 and A431 cells over-express EGFR, there is a vast difference in the degree of receptor expression, with A431 ~ 200 times higher EGFR expression than HT-29.[40-42] If the Pc conjugate homed to the tumor tissue based solely on the presence of the EGFR ligand, then the comparable levels of fluorescence observed from both tumors at 24 h would not have been expected. Therefore, in addition to tumor attraction based on EGFR-peptide binding, our results suggest significant tumor homing by the Pc macrocycle itself, in agreement with the *in vitro* results (Figure 3.5b) and previous observations.[9] The extended fluorescence-time within the A431 tumor over the HT-29 tumor suggests that with greater quantities of EGFR, comes longer retention and/or greater capacity for selective uptake or re-uptake. At times prior to 24 h, there was either weak or no signal, suggesting a prolonged time period of plasma circulation with gradual tumor accumulation. A similar pattern of tumor uptake was recently described in a xenograph breast cancer model imaged following administration of a chiral porphyrazine,[50] which showed increasing signal over background up to 48 h post administration. On the other hand, chlorin e6-HSA nanoparticles were recently used for PDT of HT-29 tumor xenograph,[51] and shown to have higher tumor-targeting ability and accumulation than free chlorin e6 as a result of their prolonged blood circulation. Two other chlorin derivatives, HPPH-3Gd(II)ADTPA[52] and TCPCSO3H[53] were recently shown to accumulate within tumor-bearing mice, reaching maximum accumulation levels at 24 h post-administration.

There was no signal detected in adjacent non-tumor regions indicating a high degree of tumor selectivity; however, it was noted that normal gastrointestinal contents in the mice also

fluoresced at the near-IR spectral window required for this Pc-conjugate. This background fluorescence is difficult to remove in mice since prolonged fasting is not feasible. For imaging of colon or urogenital malignancies, it would likely be necessary to remove fecal material prior to tumor detection.

In order to evaluate the *in vivo* stability of conjugate **3.11**, the HT-29 tumors were harvested at 24 and 96 h following iv injection and extracted using acetone/methanol mixture. The UV-vis spectra of both the 24 and 96 h tumor extracts in methanol showed the characteristic Q band absorption of the Pc (Figure 3.15), indicating that the Pc macrocycle has high stability *in vivo*, allowing for prolonged and selective accumulation within tumor tissue. MALDI-TOF MS indicated that at 24 h, intact conjugate **3.11** was still present in the tumor extract, while at 96 h the major Pc species detected was Pc-PEG-LARL (Figures 3.16).

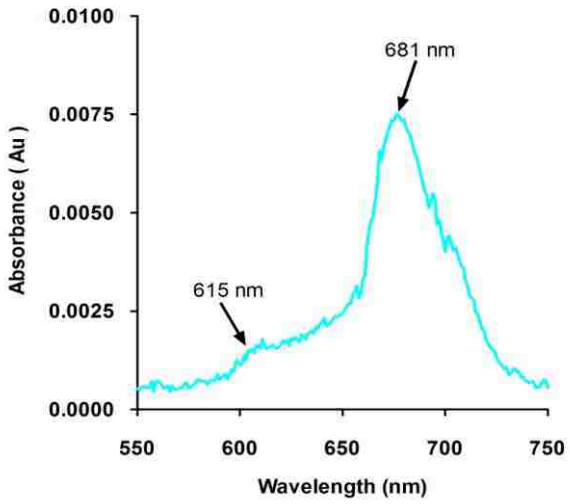

Figure 3.15. Absorption spectrum for Pc-conjugate **3.11** in methanol, extracted from HT-29 mice-tumor.

This result suggests that the EGFR-L1 peptide in Pc **3.11** is slowly degraded within tumor tissue by proteolytic enzymes, mainly losing the two terminal amino acids 96 h after iv injection. This result is in agreement with previous observations that this type of peptide conjugate can undergo metabolic degradation within tumor cells, with half-life ~ 24 h.[54]

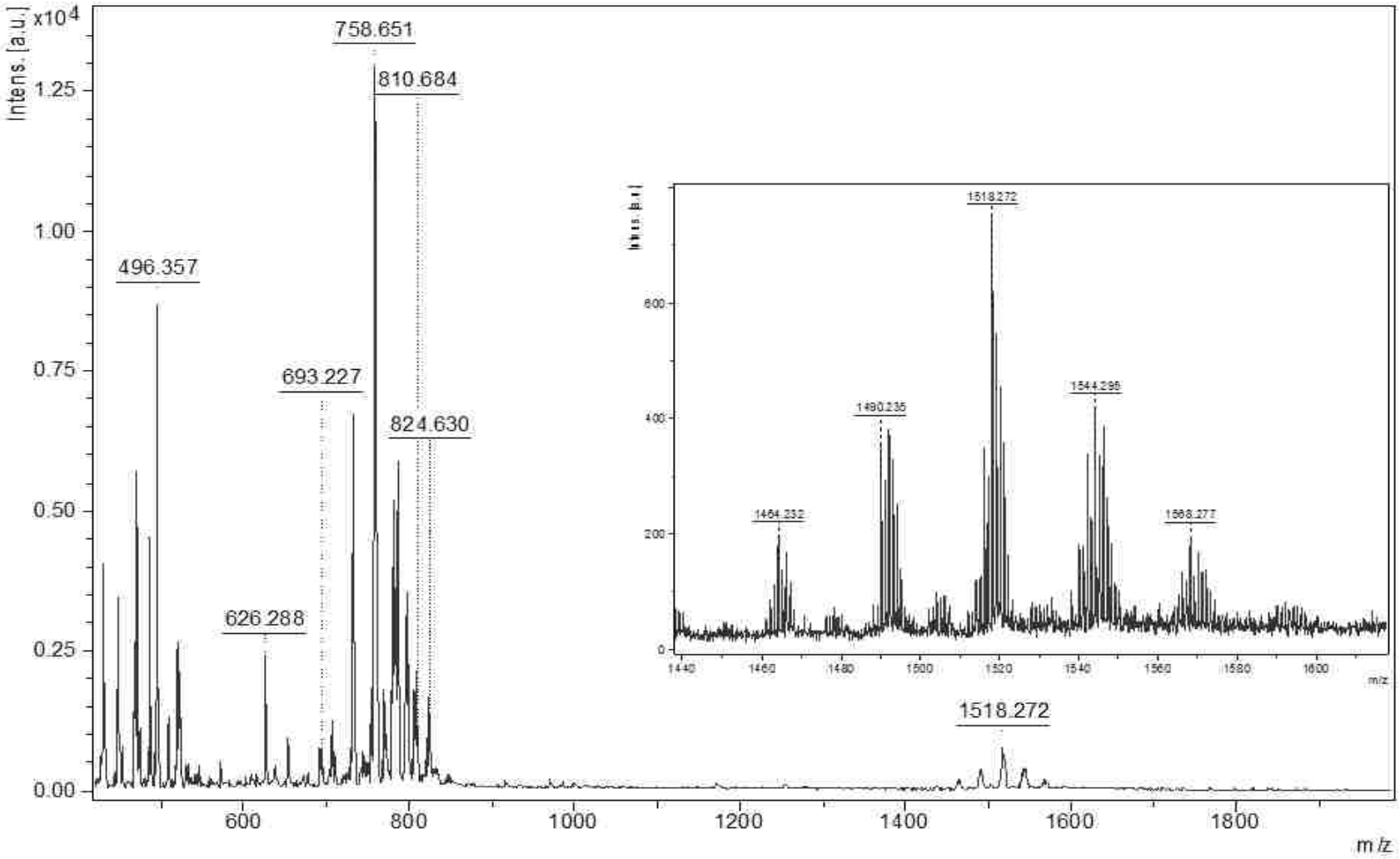

Figure 3.16. MALDI-TOF (MS) spectrum for Pc-conjugate **3.11** extract from HT-29 mouse-tumor after four days.

3.3. Conclusion

Four Pc-peptide conjugates (**3.5**, **3.6**, **3.9** and **3.11**) were designed and synthesized to target EGFR, and investigated as potential florescence imaging agents for cancers over-expressing EGFR, such as CRC. Two peptide ligands for EGFR containing 6 (LARLLT) and 13 (GYHWYGYTPQNVI) amino acid residues, were conjugated to the Pc via a short 5-atom, or a 13-atom PEG linker. The PEG group enhances the solubility of the Pc-peptide conjugates and tends to increase their cellular uptake. Using Autodock both peptide ligands were found to bind to EGFR, giving low energy (ca. - 6 kcal/mol) docking structures. The short EGFR-L1 peptide conjugates **3.5** and **3.11** are positively charged and were efficiently internalized by all cell lines (A431, HT-29, HEp2 and Vero cells), localizing preferentially in lysosomes, Golgi and mitochondria. However, the 13-residue EGFR-L2 peptide produced highly hydrophobic Pc conjugates **3.6** and **3.9** that poorly targeted EGFR and were poorly internalized. The amount of Pc-EGFR-L1 conjugates, **3.5** and **3.11**, taken up by cells was dependent on their degree of EGFR expression. While **3.5** and **3.11**, as well as Pc-PEG **3.4** also accumulated within the low EGFR expressing Vero cells, increased uptake was observed with increasing EGFR expression in the human cell lines (A431 > Ht-29 > HEp2). The observed uptake into low EGFR expressing cells indicates that the Pc-PEG has a natural tendency to target and accumulate within cancer cells.

All conjugates were found to be non-toxic (IC_{50} > 100 μM) to both low- and over-expressing EGFR cells, with exception of conjugate **3.5** that showed moderate phototoxicity toward A431, HEp2 and Vero cells (IC_{50} = 16, 17 and 47 μM, respectively). None of the conjugates were toxic towards human colorectal HT-29 cells (IC_{50} > 100 μM). This result, in addition to the observed near-IR fluorescence emissions of all Pc conjugates at ca. 682 nm with quantum yields in the range 0.10-0.13, and enhanced (~ 3-fold) uptake of **3.5** and **3.11** by cancer

cells, makes these Pc-EGFR-L1 conjugates highly promising fluorescent contrast agents for CRC, and potentially other EGFR over-expressing cancers, in particular the least phototoxic (IC_{50} > 100 μM at 1 J/cm^2) β-substituted Pc-peptide conjugate **3.11**.

Conjugate **3.11** was further investigated in nude mice bearing A431 and HT-29 human tumor xenografts. Twenty four hours after iv administration of **3.11**, a clearly near-IR fluorescence signal (exc 630 nm/ em 700 nm) was seen over background adjacent tissues, in both tumor types. While the fluorescence signal decreased in HT-29 tumors after 24 h, it continued to increase in the A431 tumors up to 96 h, the longest time investigated. The MS analysis of tumor extracts 96 h after iv injection of Pc-peptide **3.11** indicated partial degradation of the conjugate, by proteolytic enzymes, mainly leading to the cleavage of the last two amino acids of EGFR-L1.

Our studies show that Pc-peptide conjugates can be used for near-IR fluorescence imaging of cancers over-expressing EGFR, such as CRC. Due to the hydrophobic nature of the Pc macrocycle, a low molecular PEG linker and a polar or charged peptide ligand are required for adequate aqueous solubility and receptor targeting ability. In addition, a β-substituted Pc macrocycle appears to be the most suitable for imaging applications due to its lower phototoxicity compared with the corresponding α-substituted macrocycle.

3.4. Experimental Section

3.4.1. General Chemistry

All reagents and solvents were purchased from commercial sources and used directly without further purification. Silica gel 60 (230×400 mesh) and C18 (200×400), both from Sorbent Technologies, were used for column chromatography. Analytical thin-layer chromatography (TLC) was carried out using polyester backed TLC plates 254 (precoated, 200 μm) from Sorbent Technologies. NMR spectra were recorded on AV-400 LIQUID Bruker

spectrometer (400 MHz for ^{1}H, 100 MHz for ^{13}C). The chemical shifts are reported in δ ppm using the following deuterated solvents as internal references: Acetone-d_6 2.05 ppm (^{1}H), 29.92 ppm (^{13}C); DMF-d_7 8.03 ppm (^{1}H), 163.15 ppm (^{13}C); Pyridine-d_5 7.58 ppm (^{1}H), 135.91 ppm (^{13}C). HPLC analyses were carried on a Dionex system equipped with a P680 pump and UVD340U detector. Photophysical (absorption) spectra were measured on a UV-VIS NIR Scanning Spectrometer, using UV-3101PC SHIMADZU (Cell positioned)–CPS-260 lamp and emission spectra were obtained on a Fluorolog® - HORIBA JOBINVYON (Model LFI-3751) spectrofluorimeter. MALDI-TOF mass spectra were recorded on a Bruker ProFlex III mass spectrometer using dithranol as the matrix or Bruker UltrafleXtreme (MALDI-TOF/TOF) using 4-chloro-α-cyanocinnamic acid as the matrix; high resolution ESI mass spectra were obtained on an Agilent Technologies 6210 Time-of-Flight LC/MS. The melting points (mp) were determined using MEL-TEMP electrothermal instrument. HPLC separation was carried out on a Waters system including a 2545 quaternary gradient module pump, 2489 UV/Visible detector, and a fraction collector III. Analytical HPLC was carried out using a XBridge C_{18} 300Å, 5μm, 4.6 x 250 mm (Waters, USA) column using a stepwise gradient. Semipreparative HPLC was carried out using a XBridge C_{18} 300Å, 5 μm, 10 x 250 mm (Waters, USA) column using a stepwise gradient. The solvent system for peptides consisted of millipure water and HPLC grade acetonitrile, while it consisted of millipure water and HPLC grade methanol for the EGFR-L1 conjugates. Pcs **3.1**, and **3.7** were synthesized as previously described.[30]

3.4.2. Peptide Synthesis and Conjugations

Applied Biosystems Pioneer, Peptide Synthesis System was used to synthesize peptide sequences. Each peptide was synthesized using Fmoc-PAL-PEG-PS on 0.2 mmol scale using Fmoc strategy of solid-phase peptide synthesis. A 4-fold excess of the L-Fmoc protected amino

acids were coupled using HOBt and TBTU as the coupling agents. The peptide sequences, prepared using this methodology, were as follows: LARLLT and GYHWYGYTPQNVI. Removal of the Fmoc group from the last amino acid was the final step for each synthesis. This was followed by washing the peptide several times with DMF/DCM and dried under high vacuum for 24 h. The Pc-peptide conjugates were synthesized as previously described.[29]

In summary, resin containing either GYHWYGYTPQNVI or LARLLT was dissolved in DMF and soaked for 2 h. The Pcs were dissolved in DMF, the base and coupling reagents (HOBt and TBTU) added to the Pc solutions. The activated mixture was transferred into the reaction vessel containing the resin and left to shake for 4 days. The resin was washed under vacuum several times using DMF, then methanol and finally DCM. A cleavage cocktail – TFA/phenol/TIS/H_2O (88:5:2:5) – was added with constant shaking for 4 h. The solution was washed with TFA (2 × 2 mL) into a flask and concentrated under vacuum. Cold diethyl ether was added to the residue and the mixture centrifuged. The Pc-EGFR-L1 conjugates were purified using reverse-phase HPLC using a Waters system including a 2545 quaternary gradient module pump, 2489 UV/Visible detector, and a fraction collector III. Analytical HPLC was carried out using a XBridge C_{18} 300Å, 5μm, 4.6 x 250 mm (Waters, USA) column using a stepwise gradient. Semi-preparative HPLC was carried out a XBridge C_{18} 300Å, 5 μm, 10 x 250 mm (Waters, USA) column using a stepwise gradient. The solvent system consisted of millipure water and HPLC grade methanol (30:70 → 0:100). The purity of the conjugates was > 95% as obtained from HPLC.

ZnPc 3.2: A mixture of Pc **3.1**[30] (80.0 mg, 0.096 mmol) and 1,4-dioxane-2,6-dione (18.0 mg, 0.16 mmol) was dissolved in DMF (1.0 mL) and the solution stirred overnight at room temperature. Water (5.0 mL) was added to the solution to precipitate the product. The solid was

filtered under vacuum and washed with water and hexane. The solid was dried under vacuum for 2 days to afford the pure blue solid (80.4 mg, 86.6%), mp 235 – 236 °C. ^{1}H NMR (Pyridine-d_5): δ 10.78-10.71 (s, 1H, -COOH), 10.17 - 9.41 (m, 7H, Ar-H), 8.44 - 8.23 (m, 6H, Ar-H), 8.01 - 7.71 (m, 3H, Ar-H), 6.04 (br, 1H, N-H), 4.55 (d, J = 12.4 Hz, 2H, CH_2O), 4.47 (d, J = 10.5 Hz, 2H, CH_2O), 1.73 – 1.59 (m, 27H, $C(CH_3)_3$). ^{13}C NMR (Pyridine-d_5): δ 168.3, 168.2, 156.6, 155.9, 155.8, 154.7, 154.3, 154.0, 152.9, 150.6, 150.4, 150.1, 149.8, 142.4, 140.1, 140.0, 137.8, 137.7, 136.2, 136.0, 135.8, 135.5, 134.3, 134.8, 131.54, 128.46, 128.3, 124.8, 124.2, 124.0, 123.7, 123.4, 122.8, 122.5, 121.4, 120.6, 120.5, 120.4, 120.2, 119.4, 118.1, (Ar-C) 73.1, 70.5 (OCH_2), 35.8, 32.4 (Ar-C, $C(CH_3)_3$). MS (MALDI-TOF) *m/z* 968.319 $[M+H]^+$, calcd for $C_{54}H_{50}N_9O_5Zn$ 967.323. UV-vis (DMF): λ_{max} (log ε) 346 nm (5.04), 614 nm (4.80), 680 nm (5.50).

ZnPc 3.4: Pc **3.2** (30.0 mg, 0.032 mmol) was dissolved in DMF (400 µL). Et_3N (4.0 mg, 0.041 mmol), HOBt (4.6 mg, 0.034 mmol) and tert-butyl-12-amino-4,7,10-trioxadodecanoate (10.8 mg, 0.039 mmol) were added to the reaction mixture. EDCI (5.3 mg, 0.034 mmol) was then added in one portion. The reaction solution was stirred for 3 days at room temperature, diluted using ethyl acetate (10 mL) and washed subsequently with water (20 mL × 2). The organic layer was dried over anhydrous sodium sulfate. The solvent was evaporated and the crude product purified on silica column eluted with mixed solvents of DCM/methanol (98:2→ 96:4) to afford a blue solid (30.0 mg, 76.5%). ^{1}H NMR (DMF-d_7): δ 9.60 - 9.01 (m, 7H, Ar-H), 8.45 - 8.15 (m, 5H, Ar-H), 8.00 – 7.77 (m, 3H, Ar-H), 7.63 – 7.49 (m, 2H, Ar-H), 4.27 – 4.15 (m, 4H, CH_2O), 3.62 – 3.57 (m, 3H, CH_2O), 3.54 – 3.47 (m, 9H, CH_2O), 3.42 – 3.37 (m, 2H, CH_2O), 2.44 – 2.39 (m, 2H, CH_2CO), 1.82 – 1.78 (m, 27H, $C(CH_3)_3$), 1.40 (s, 9H, $C(CH_3)_3$). ^{13}C NMR (DMF-d_7): δ 171.7, 170.5, 168.8, 168.7, 156.8, 156.2, 155.6, 155.5, 155.2, 155.1, 155.0,

154.7, 154.6, 154.4, 154.3, 154.20, 154.16, 154.0, 153.4, 153.3, 153.2, 152.4, 152.1, 152.04, 151.96, 142.3, 140.03, 139.98, 139.9, 139.6, 137.64, 137.57, 137.5, 137.2, 135.10, 135.06, 143.5, 131.7, 131.6, 130.1, 129.4, 128.7, 128.6, 128.4, 123.6, 123.5, 123.3, 122.6, 122.4, 122.3, 122.0, 120.3, 120.1, 120.0, 119.8, 119.6, 119.0, 118.9, 117.5 (Ar-C), 80.8 (O-$C(CH_3)_3$), 72.4, 72.1, 71.20, 71.18, 71.15, 71.1, 71.0, 70.5, 70.32, 70.30, 67.2 (OCH_2), 39.64, 39.61, ($COCH_2$), 32.7, 32.6 (Ar-C, $C(CH_3)_3$), 28.5 (N-Boc $C(CH_3)_3$). MS (MALDI-TOF) *m/z* 1170.497 $[M-^tBu+H]^+$, calcd for $C_{63}H_{66}N_{10}O_9Zn$ 1170.431. The protected Pc **3.4** conjugate was dissolved in a mixture of DCM/TFA (4 mL/4 mL) and stirred at 0° C for 3 h. The solvent was evaporated, the residue treated with 2N NaOH (2 mL) and then extracted by ethyl acetate (15 mL). The product was dried under vacuum to afford blue product (24.0 mg, 89.3%), mp 191 – 192 °C. ^1H NMR (DMF-d_7): δ 10.15-10.13 (s, 1H, -COOH), 9.59 - 9.08 (m, 7H, Ar-H), 8.42 - 8.10 (m, 5H, Ar-H), 7.95 - 7.82 (m, 3H, Ar-H), 7.61 – 7.52 (m, 2H, Ar-H), 4.25 – 4.11 (m, 4H, CH_2O), 3.79–3.57 (m, 12H, CH_2O), 3.41–3.37 (m, 2H, CH_2O), 2.51–2.48 (m, 2H, CH_2CO), 1.79 (s, 27H, $C(CH_3)_3$). ^{13}C NMR (Pyridine-d_5): δ 173.7, 170.5, 168.7, 156.9, 156.2, 155.4, 154.5, 153.7, 152.6, 145.6, 142.6, 140.2, 139.8, 137.6, 135.2, 134.6, 131.7, 128.7, 123.5, 122.7, 122.4, 120.0, 119.1, 117.7 (Ar-C), 72.5, 72.2, 71.3, 70.4, 67.8 (OCH_2), 35.5 ($COCH_2$), 32.6 (Ar-C, $C(CH_3)_3$). MS (MALDI-TOF) *m/z* 1170.485 $[M]^+$, calcd for $C_{63}H_{66}N_{10}O_9Zn$ 1170.431. UV-vis (DMF): λ_{max} (log ε) 349 nm (4.90), 612 nm (4.61), 678 nm (5.35).

ZnPc conjugate 3.5: Resin (25.7 mg, 0.0052 mmol) containing LARLLT, was transferred into a reaction vial. DMF was added (5:1, DMF/resin) and left to soak for 4 h, after which it was washed four times with DMF. Pc **3.4** (10.0 mg, 0.010315 mmol) was weighed into a 2.0 mL vial and DMF (200 μL) added. DIEA (6.4 μL, 0.036745 mmol) was added to the solution and stirred for 1 h. Then HOBt (1.8 mg, 0.013321 mmol), HATU (4.0 mg, 0.010521

mmol) were added to the Pc solution. The mixture was added to the resin and left to shake for 4 days. The resin was washed under vacuum using DMF, followed by methanol and finally DCM. A cleavage cocktail – TFA/phenol/TIS/H_2O (88:5:2:5) – was added and shaken constantly for 4 h and the solution washed with TFA (2 × 2 mL) into a 50 mL flask under vacuum. Cold diethylether was added to the residue and the mixture centrifuged. The precipitate was purified using reverse-phase HPLC eluted by water/methanol (30:70 → 0:100) to afford a blue solid (7.6 mg, 79.2%), mp 151-152 °C. ^{1}H NMR (DMF-d_7): δ 10.18, 10.13 (s, 1H, N-H), 9.67-9.20 (m, 5H, Ar-H), 8.55-8.45 (m, 3H, Ar-H), 8.25-8.15 (m, 2H, Ar-H), 8.13-8.05 (m, 1H, Ar-H), 7.97-7.86 (m, 5H, Ar-H), 7.85-7.79 (m, 2H, Ar-H), 7.61-7.47 (m, 5H, Ar-H), 7.20 (s, 1H, Ar-H), 7.13 (s, 1H, Ar-H), 4.39-4.01 (m, 26H, CH_2O/CH_2NH), 3.77-3.70 (m, 3H, CH_2O), 3.56-3.50 (m, 12H, CH_2O), 3.43-3.31 (m, 3H, CH_2O), 2.55-2.41 (m, 2H, CH_2CO), 2.01-1.92 (m, 3H, CH_2), 1.85-1.71 (m, 27H, $C(CH_3)_3$/7H, CH_2), 1.69-1.62 (m, 3H, CH_2), 1.43-1.35 (m, 4H, CH_2), 1.21-1.15 (m, 4H, CH_2), 0.94-0.87 (m, 20H, CH_3). ^{13}C NMR (DMF-d_7): δ 175.5, 175.3, 174.10, 174.07, 173.7, 173.4, 170.5, 168.8, 168.7, 160.3, 159.9, 158.7, 156.8, 156.2, 155.6, 155.3, 155.1, 154.4, 152.4, 152.1, 140.0, 137.9, 137.6, 135.1, 134.5, 131.7, 128.6, 123.4, 122.6, 122.4, 120.0, 119.0, 117.5, 116.1 (Ar-C), 72.3, 72.0, 71.3, 71.2, 71.0, 70.9, 70.3, 68.2, 68.0, 66.3 (OCH_2), 60.1, 55.2, 54.6, 54.0, 53.5. 51.8, 41.9, 41.3, 41.2, 39.5, 37.2 (CH_2) 32.6 (Ar-C, $C(CH_3)_3$), 29.4, 26.5, 25.6, 25.5, 24.0, 23.8, 23.5, 22.3, 22.0, 21.8, 20.7, 17.5 (CH_3). MS (MALDI-TOF) *m/z* 1837.907 $[M+H]^+$, calcd for $C_{94}H_{125}N_{20}O_{15}Zn$ 1837.892. MS-MS (MALDI-TOF-TOF) *m/z* 1839.90 $[PcPEG\text{-}LARLLT+H]^+$, 1822.88 $[PcPEG\text{-}LARLLT\text{-}NH_2+H]^+$, 1794.88 $[PcPEG\text{-}LARLLT\text{-}CONH_2+H]^+$, 1723.042 $[PcPEG\text{-}LARLL\text{-}NH_2+H]^+$, 1580.75 $[PcPEG\text{-}LARL\text{-}CO+H]^+$, 1339.56 $[PcPEG\text{-}LA\text{-}NH_2+H]^+$, 1268.52 $[PcPEG\text{-}L\text{-}NH_2+H]^+$, 1240.53 $[PcPEG\text{-}L\text{-}CO+H]^+$, 1155.44 $[PcPEG\text{-}NH_2+H]^+$, calcd for $C_{94}H_{125}N_{20}O_{15}Zn$ 1837.892, $C_{94}H_{124}N_{19}O_{15}Zn$ 1822.882,

$C_{93}H_{124}N_{19}O_{14}Zn$ 1794.887, $C_{90}H_{117}N_{18}O_{13}Zn$ 1721.834, $C_{83}H_{106}N_{17}O_{11}Zn$ 1580.755, $C_{72}H_{83}N_{12}O_{10}Zn$ 1339.565, $C_{69}H_{78}N_{11}O_9Zn$ 1268.528, $C_{68}H_{78}N_{11}O_8Zn$ 1240.533, $C_{63}H_{67}N_{10}O_8Zn$ 1155.444. UV-vis (DMF): λ_{max} (log ε) 348 nm (4.79), 612 nm (4.56), 680 nm (5.33).

ZnPc conjugate 3.6: Resin (60.0 mg, 0.0052 mmol) containing GYHWYGYTPQNVI was transferred into a reaction vial. DMF was added (5:1, DMF/resin) and left to soak for one hour, after which it was washed four times with DMF. Pc **3.4** (12.1 mg, 0.010315 mmol) was weighed into a 2.0 mL vial and DMF (200 μL) added. Then HOBt (1.4 mg, 0.010315 mmol), HATU (3.9 mg, 0.010315 mmol) and DIEA (5.39 μL, 0.030946 mmol) were added to the Pc solution. The mixture was stirred for five minutes, transferred into the reaction chamber containing the resin and left to shake for 3 days. The resin was washed under vacuum using DMF (till DMF was clear), followed by methanol and finally DCM. A cleavage cocktail – TFA/phenol/TIS/H_2O (88:5:2:5) – was added and shaken constantly for 4 h. The solution was then washed with TFA (2 × 2 mL) into a 50 mL flask under vacuum. Cold diethylether was added to the residue and the mixture centrifuged. The precipitate was then sonicated in water and centrifuged several times to give the title compound (11.5 mg, 40.5%, mp 208 – 209 °C). ^{1}H NMR (DMF-d_7): δ 10.40, 10.35 (s, 1H, COOH), 9.51-9.20 (m, 6H, Ar-H), 8.45-8.10 (m, 10H, Ar-H), 7.80-7.75 (m, 2H, Ar-H), 7.70-7.50 (m, 2H, Ar-H), 7.45-7.20 (m, 30H, Ar-H), 7.15-6.95 (m, 14H, Ar-H), 6.90-6.78 (m, 4H, Ar-H), 6.74-6.65 (m, 9H, Ar-H), 4.75-4.10 (m, 16H, CH_2O/CH_2NH), 4.04-3.65 (m, 7H, CH_2O/CH_2NH), 2.25-2.04 (m, 6H, CH_2CO), 2.01-1.75 (m, 21H, $C(CH_3)_3$/CH_2), 1.43 (s, 4H, , CH_2), 1.31 (s, 3H, CH_2), 1.21-1.15 (m, 4H, CH_2), 1.05-1.00 (m, 8H, CH_2), 0.94-0.85 (m, 19H, CH_3). MS (MALDI-TOF) *m/z* 2748.17 $[M]^+$, calcd for $C_{140}H_{165}N_{29}O_{27}Zn$ 2748.1723. MS-MS (MALDI-TOF-TOF) *m/z* 2751.19 [PcPEG-

GYHWYGYTPQNVI]$^+$, 2733.25 [PcPEG-GYHWYGYTPQNVI-NH_2]$^+$, 2702.25 [Pc-PEG-GYHWYGYTPQNVI-$CONH_2$]$^+$, 2165.86 [PcPEG-YHWYGYT-NH_2-OH]$^+$, 1670.78 [PcPEG-GYHW-$CONH_2$]$^+$, 1490.70. [PcPEG-GYH-$CONH_2$]$^+$, 1346.53 [Pc-PEG-GY-$CONH_2$]$^+$, 1226.34 [PcPEG-G]$^+$, 1155.44 [PcPEG-NH_2+H]$^+$, calcd for $C_{140}H_{165}N_{29}O_{27}Zn$ 2748.17, $C_{140}H_{164}N_{28}O_{27}Zn$ 2733.16, $C_{139}H_{164}N_{28}O_{26}Zn$ 2705.17, $C_{115}H_{123}N_{21}O_{19}Zn$ 2165.86, $C_{90}H_{95}N_{17}O_{12}Zn$ 1669.66, $C_{79}H_{85}N_{15}O_{11}Zn$ 1483.58, $C_{73}H_{78}N_{12}O_{10}Zn$ 1346.53, $C_{65}H_{70}N_{12}O_9Zn$ 1226.47, $C_{63}H_{67}N_{10}O_8Zn$ 1155.44. UV-vis (DMF): λ_{max} (log ε) 345 nm (3.84), 612 nm (4.25), 680 nm (4.60).

ZnPc 3.8: A mixture of Pc **3.7**[30] (50.0 mg, 0.06 mmol) and 1,4-dioxane-2,6-dione (11.3 mg, 0.1 mmol) was dissolved in DMF (0.5 mL) and the solution stirred overnight at room temperature. The mixture was purified as **3.2** above to afford the pure blue solid (53.5 mg, 92.2%), mp 249 – 250 °C. ^{1}H NMR (Pyridine-d_5): δ 10.84-10.77 (s, 1H, -COOH), 10.01 - 9.35 (m, 8H, Ar-H), 8.50 - 8.21 (m, 5H, Ar-H), 8.10 - 7.90 (m, 1H, Ar-H), 7.54 – 7.41 (m, 2H, Ar-H), 6.74 (br, 1H, N-H), 4.69 (d, J = 5.4 Hz, 2H, CH_2O), 4.60 (d, J = 5.6 Hz, 2H, CH_2O), 1.75 – 1.64 (m, 27H, $C(CH_3)_3$). ^{13}C NMR (Pyridine-d_5): δ 173.9, 168.43, 168.38, 160.0, 159.7, 154.8, 154.7, 154.6, 154.5, 154.3, 153.9, 153.8, 153.5, 153.4, 153.0, 150.6, 150.4, 150.1, 140.8, 139.4, 139.2, 137.0, 136.8, 134.2, 134.0, 131.0, 127.7, 124.7, 122.0, 120.8, 120.7, 120.3, 119.8, 112.5, 111.6 (Ar-C) 72.5, 69.9 (OCH_2), 35.8, 31.7 (Ar-C, $C(CH_3)_3$). MS (MALDI-TOF) *m/z* 968.314 [M+H]$^+$, calcd for $C_{54}H_{50}N_9O_5Zn$ 968.323. UV-vis (DMF): λ_{max} (log ε) 351 nm (4.86), 611 nm (4.58), 679 nm (5.33).

ZnPc conjugate 3.9: Resin (60.0 mg) containing 0.0052 mmol GYHWYGYTPQNVI was transferred into a reaction vial. DMF was added (5:1, DMF/resin) and soaked for 2 h. The resin was washed four times with DMF. Pc **3.8** (10.0 mg, 0.010315 mmol) was weighed into a

vial and DMF (200 μL) added. Then HOBt (1.4 mg, 0.010315 mmol), TBTU (3.3 mg, 0.010315 mmol) and DIEA (5.39 μL, 0.030946 mmol) were added to the Pc solution. The mixture was stirred for 30 min, transferred into the vial containing the resin and left to shake for 3 days. The resin was washed under vacuum using DMF (till DMF was clear), followed by methanol and finally DCM. A cleavage cocktail – TFA/phenol/TIS/H_2O (88:5:2:5) – was added and shaken constantly for 4 h. The solution was then washed with TFA (2 × 2 mL) into a 50 mL flask under vacuum. Cold diethylether was added to the residue and the mixture centrifuged. The precipitate was then sonicated in water and centrifuged several times to give the title compound (9.2 mg, 35.0%), mp 211 – 212 °C. ^{1}H NMR (DMF-d_7): δ 9.51-9.20 (m, 5H, Ar-H), 8.45-8.10 (m, 9H, Ar-H), 7.80-7.75 (m, 2H, Ar-H), 7.70-7.50 (m, 2H, Ar-H), 7.35-7.20 (m, 24H, Ar-H), 7.07-6.91 (m, 14H, Ar-H), 6.80-6.70 (m, 4H, Ar-H), 6.65-6.53 (m, 9H, Ar-H), 4.68-4.30 (m, 12H, CH_2NH), 4.24-3.65 (m, 4H, CH_2O/CH_2NH), 3.45-3.30 (m, 4H, CH_2O/CH_2NH), 2.25-2.04 (m, 2H, CH_2CO), 2.01-1.75 (m, 21H, $C(CH_3)_3$/CH_2), 1.33 (s, 5H, , CH_3), 1.26 (s, 2H, CH_2), 1.18-1.10 (m, 4H, CH_2), 1.00-0.94 (m, 8H, CH_2), 0.85-0.75 (m, 18H, CH_3). MS (MALDI-TOF) *m/z* 2545.04 $[M]^+$, calcd for $C_{131}H_{148}N_{28}O_{23}Zn$ 2545.0563. UV-vis (DMF): λ_{max} (log ε) 351 nm (4.44), 610 nm (4.07), 677 nm (4.87).

ZnPc 3.10: Pc **3.8** (30.0 mg, 0.032 mmol) was dissolved in DMF (400 μL). Et_3N (4.0 mg, 0.041 mmol), HOBt (4.6 mg, 0.034 mmol) and *tert*-butyl-12-amino-4,7,10-trioxadodecanoate (10.8 mg, 0.039 mmol) were added to the reaction solution and the solution was stirred for 20 min. EDCI (5.3 mg, 0.034 mmol) was added to the reaction solution in one portion. The reaction was then treated as **3.4** above to afford a blue solid (32.2 mg, 82.3%). ^{1}H NMR (Acetone-d_6): δ 9.87 - 9.77 (m, 1H, Ar-H), 9.07 – 7.40 (m, 16H, Ar-H), 3.99 (s, 2H, CH_2O), 3.87 (s, 2H, CH_2O), 3.58 – 3.54 (m, 2H, CH_2O), 3.45 (s, 8H, CH_2O), 3.38 (s, 2H,

CH_2O), 3.22 (s, 2H, CH_2O), 2.36 – 2.33 (m, 2H, CH_2CO), 1.88 – 1.78 (m, 27H, $C(CH_3)_3$), 1.37 (s, 9H, $C(CH_3)_3$). ^{13}C NMR (DMF-d_7): δ 171.8, 170.7, 169.3, 169.2, 162.4, 160.8, 160.4, 155.0, 154.8, 154.3, 154.2, 141.4, 140.0, 139.8, 137.6, 136.7, 136.4, 134.5, 128.6, 125.2, 123.4, 123.0, 121.4, 121.3, 120.9, 120.0, 112.8, 111.7 (Ar-C), 81.0 (O-$C(CH_3)_3$), 72.6, 72.4, 71.5, 71.43, 71.36, 71.3, 70.6, 67.8 (OCH_2), 32.8 (Ar-C, $C(CH_3)_3$), 28.7 (N-Boc $C(CH_3)_3$). MS (MALDI-TOF) *m/z* 1227.682 $[M+H]^+$, 1170.495 $[M-^tBu+H]^+$, calcd for $C_{67}H_{75}N_{10}O_9Zn$ 1227.501, $C_{63}H_{66}N_{10}O_9Zn$ 1170.431. The protected Pc conjugate was then deprotected as **3.4** above to afford a blue solid (25.3 mg, 88.3%), mp 161 – 163 °C. ^1H NMR (DMF-d_7): δ 10.42-10.33 (s, 1H, COOH), 9.57 - 9.32 (m, 6H, Ar-H), 9.09 - 8.75 (m, 1H, Ar-H), 8.55 - 8.20 (m, 4H, Ar-H), 8.15 - 8.00 (m, 2H, Ar-H), 7.99 – 7.81 (m, 1H, Ar-H), 7.65 – 7.50 (m, 2H, Ar-H), 4.36 (d, J = 7.2 Hz, 2H, CH_2O), 4.28 (d, J = 5.1 Hz, 2H, CH_2O), 3.65 – 3.57 (m, 12H, CH_2O), 3.41 – 3.37 (m, 2H, CH_2O), 2.55 – 2.48 (m, 2H, CH_2O), 1.85 – 1.74 (m, 27H, $C(CH_3)_3$). ^{13}C NMR (DMF-d_7): δ 173.7, 170.6, 169.2, 169.1, 160.64, 160.58, 160.25, 160.18, 155.3, 155.22, 155.16, 155.1, 155.0, 154.9, 154.8, 154.7, 154.3, 154.2, 1154.15, 154.11, 153.0, 153.9, 153.4, 153.3, 153.2, 153.1, 141.5, 141.4, 140.1, 140.0, 139.8, 137.7, 137.64, 137.55, 137.5, 136.5, 136.2, 134.8, 134.7, 134.6, 128.3, 128.2, 126.2, 125.0, 123.3, 123.2, 122.8, 122.0, 121.2, 121.11, 121.06, 120.8, 120.7, 119.9, 119.8, 112.7, 111.6, (Ar-C), 72.4, 72.1, 71.28, 71.25, 71.14, 71.10, 70.4, 68.3, 67.7 (OCH_2), 39.7, 36.8 ($COCH_2$), 32.6 (Ar-C, $C(CH_3)_3$). MS (MALDI-TOF) *m/z* 1170.508 $[M]^+$, calcd for $C_{63}H_{66}N_{10}O_9Zn$ 1170.431. UV-vis (DMF): λ_{max} (log ε) 350 nm (4.65), 610 nm (4.41), 676 nm (5.19).

ZnPc conjugate 3.11: Resin (25.7 mg, 0.0052 mmol) containing LARLLT, was transferred into a reaction vial. DMF was added (5:1, DMF/resin) and left to soak for 4 h, after which it was washed four times with DMF. Pc **3.10** (10.0 mg, 0.010315 mmol) was weighed into

a 2.0 mL vial and DMF (200 μL) added. DIEA (6.4 μL, 0.036745 mmol) was added to the solution and stirred for 1 h. Then HOBt (1.8 mg, 0.013321 mmol), HATU (4.0 mg, 0.010521 mmol) were added to the Pc solution. The mixture was added to the resin and left to shake for 4 days. It was then cleaved and purified as described above for Pc **3.5** to afford a blue solid (8.1 mg, 84.4%, mp 167 – 168 °C). ^{1}H NMR (DMF-d_7): δ 10.40, 10.35 (s, 1H, N-H), 9.67-9.20 (m, 5H, Ar-H), 8.57-8.45 (m, 3H, Ar-H), 8.30-8.25 (m, 2H, Ar-H), 8.13-8.05 (m, 2H, Ar-H), 7.97-7.86 (m, 3H, Ar-H), 7.85-7.79 (m, 2H, Ar-H), 7.61-7.47 (m, 5H, Ar-H), 7.18 (s, 1H, Ar-H), 7.12 (s, 1H, Ar-H), 4.37 (d, J = 7.6, 4H, CH_2O), 4.29-4.21 (m, 9H, CH_2NH), 3.77-3.70 (m, 16H, CH_2NH), 3.65-3.57 (m, 12H, CH_2O), 3.54-3.43 (m, 2H, CH_2NH), 3.37-3.29 (m, 3H, CH_2NH), 2.61-2.56 (m, 2H, CH_2CO), 2.01-1.92 (m, 2H, CH_2), 1.91-1.71 (m, 27H, $C(CH_3)_3$/7H, CH_2), 1.69-1.58 (m, 5H, CH_2), 1.39-1.36 (m, 4H, CH_2), 1.17-1.15 (m, 4H, CH_2), 0.95-0.86 (m, 20H, CH_3). ^{13}C NMR (DMF-d_7): δ 175.5, 175.3, 174.1, 174.0, 173.7, 173.6, 173.4, 170.6, 169.2, 169.1, 160.2, 159.9, 158.8, 154.6, 154.2, 153.7, 140.2, 139.8, 136.7, 136.3, 128.6, 128.4, 122.8, 122.2, 121.4, 120.9, 119.3, 116.3 (Ar-C), 72.4, 72.2, 71.3, 71.1, 71.0, 70.4, 68.2, 68.1, 66.3 (OCH_2), 60.1, 55.2, 54.6, 54.0, 53.5. 51.8, 41.9, 41.34, 41.29, 39.7, 37.2 (CH_2) 32.6 (Ar-C, $C(CH_3)_3$), 29.4, 26.5, 25.7, 25.6, 25.5, 24.0, 23.8, 23.5, 22.4, 22.0, 21.8, 20.7, 17.6 (CH_3). MS (MALDI-TOF) *m/z* 1837.925 $[M+H]^+$, calcd for $C_{94}H_{125}N_{20}O_{15}Zn$ 1837.892. MS-MS (MALDI-TOF-TOF) *m/z* 1839.90 [PcPEG-LARLLT+H]$^+$, 1822.88 [PcPEG-LARLLT-NH_2+H]$^+$, 1794.88 [PcPEG-LARLLT-$CONH_2$+H]$^+$, 1721.83 [PcPEG-LARLL-NH_2+H]$^+$, 1580.75 [PcPEG-LARL-CO+H]$^+$, 1339.56 [PcPEG-LA-NH_2+H]$^+$, 1268.52 [PcPEG-L-NH_2+H]$^+$, 1240.53 [PcPEG-L-CO+H]$^+$, 1155.44 [PcPEG-NH_2+H]$^+$, calcd for $C_{94}H_{125}N_{20}O_{15}Zn$ 1837.892, $C_{94}H_{124}N_{19}O_{15}Zn$ 1822.882, $C_{93}H_{124}N_{19}O_{14}Zn$ 1794.887, $C_{90}H_{117}N_{18}O_{13}Zn$ 1721.834, $C_{83}H_{106}N_{17}O_{11}Zn$ 1580.755, $C_{72}H_{83}N_{12}O_{10}Zn$ 1339.565, $C_{69}H_{78}N_{11}O_9Zn$ 1268.528, $C_{68}H_{78}N_{11}O_8Zn$ 1240.533,

$C_{63}H_{67}N_{10}O_8Zn$ 1155.444. UV-vis (DMF): λ_{max} (log ε) 352 nm (4.79), 610 nm (4.52), 677 nm (5.29).

ZnPc 3.14. A mixture of Pc **3.13**[30] (50 mg, 0.05 mmol) and 1, 4-dioxane-2, 6-dione (17.4 mg, 0.15 mmol) was dissolved in DMF (0.5 mL) and the solution stirred overnight at room temperature. The reaction solution was evaporated to dry. The residue was dissolved in THF (1 mL) and water (20 mL) added to precipitate the product. The solid was filtered under vacuum, and washed with water and hexane. The solid was dried under vacuum for 2 days to afford a blue solid (52.1 mg, 87.6%). ^{1}H NMR (d-Pyridine, 400 MHz): δ 10.74 (s, 2H, -COOH), 10.07 - 9.50 (m, 7H, Ar-H), 8.39 - 8.10 (m, 8H, Ar-H), 7.50 – 7.40 (m, 4H, Ar-H), 6.56 (br, 2H, N-H), 4.63 (d, J = 3.5 Hz, 4H, CH_2O), 4.56 (d, J = 4.5 Hz, 4H, CH_2O), 1.71 – 1.58 (m, 27H, $C(CH_3)_3$). MS (MALDI-TOF) *m/z* 1191.360 $[M+H]^+$, calcd for $C_{64}H_{59}N_{10}O_{10}Zn$ 1191.371.

ZnPc 3.15. Pc **3.14** (20 mg, 0.017 mmol) was dissolved in DMF (500 μL). DIEA (26 mg, 0.2 mmol), HOBt (4.6 mg, 0.034 mmol) and TBTU (10.6 mg, 0.034 mmol) were added to the reaction solution and the solution was stirred for 2 min. Tert-butyl-12-amino-4,7,10-trioxadodecanoate (10.8 mg, 0.032 mmol) was added to the reaction solution in one portion. The reaction solution was stirred for 72 h at room temperature. The reaction solution was poured into 20 mL of ice-cold water and filtered under gravity. The residue was dissolved in ethyl acetate (10 mL). The organic solution washed subsequently with water (20 mL), saturated aqueous $NaHCO_3$ solution (20 mL) and water (20 mL). The organic layer was dried over anhydrous sodium sulfate. The solvent was evaporated and the crude product purified by silica column (1 cm in height) with the elution of mixed solvents of methanol/dichloromethane (1/9), eluting the first blue portion (mono-pegylated Pc). Methanol eluted the second portion (title compound) to

afford a blue solid in trace amounts. MS (MALDI-TOF) *m/z* 1711.720 $[M+H]^+$, calcd for $C_{90}H_{109}N_{12}O_{18}Zn$ 1711.729.

3.4.3. Spectroscopic Studies

All absorption spectra were measured on UV-VIS NIR Scanning Spectrometer UV-3101PC SHIMADZU (Cell positioned) equipped with a CPS-260 lamp. The DMF solvent used was HPLC grade and it was the solvent of choice since it dissolved all the Pcs relatively good. Stock solutions (1000 µM, 1.0 mL) of all Pcs were prepared and the dilutions were prepared by spiking 20 – 80 µL of the corresponding stock solution into 10.0 mL of solvent. Emission spectra were obtained on a Fluorolog®-HORIBA JOBINVYON (Model LFI-3751) spectrofluorimeter. The optical densities of the solutions used for emission studies ranged between 0.04 – 0.05 at excitation wavelengths. All experiments were carried out within 4 h of solution preparation at room temperature (23-25 °C) with 10 mm path length spectrophotometric cell. The fluorescent quantum yields (Φ_f) were determined using a secondary standard method.[55] By comparison with ZnPc (Φ_f = 0.17) as a reference, the values of fluorescence were obtained in DMF solvent.[56]

3.4.4. Computational Studies

Docking of EGFR-L1 and –L2 peptides to EGFR protein extracellular domain was performed using AUTODOCK 4 software.[34,35] EGFR crystal structure was obtained from a protein databank (PDB code: 1nql).[57] Solvent molecules were removed from the pdb file. Polar hydrogen atoms were added to the structure. For EGFR-L1 peptide docking a grid box was created with amino acid residue on EGFR Asn134 as center of the grid box, and for EGFR-L2 docking a grid box was created near EGF binding site on EGFR.[27,28] A grid box with dimensions of 128×128×128 $Å^3$ was used for calculations. Three dimensional structures of peptide EGFR-L1 and EGFR-L2 were generated using InsightII (Accelrys Inc., Sandiego, CA). Structures were

subjected to 300 K and molecular dynamics (MD) followed by simulated annealing MD.[58] The final structure from simulated MD was energy minimized and used for docking studies. In peptides EGFR-L1 and EGFR-L2 rotatable bonds were allowed to rotate during docking calculations. For docking 50 runs with 10 million energy evaluations were carried out using Lamarkian genetic algorithm. Docking calculations were performed on Linux cluster on high performance supercomputers at LSU Baton Rouge. Docked structures were listed in increasing order of energy, and low energy clusters were used as the most probable binding models. Structures from low energy docking were displayed and analyzed using PyMol software.

3.4.5. Cell Studies

All tissue culture medium and reagents were purchased from Invitrogen (Carlsbad, CA). Human carcinoma HEp2 cells, human epidermoid carcinoma A431, human colorectal adenocarcinoma HT-29, and cercopithecus aethiops kidney Vero cells, were purchased from ATCC. HT-29 cells were cultured and maintained in McCoy's 5A Medium Modified supplemented with 10% FBS and 1% antibiotic (Penicillin Streptomycin). HT-29 cells were infected with a lentivirus containing the enhanced green fluorescent protein (eGFP; virus purchased from Biogenova, Ellicott City, MD). Green fluorescent cells were sorted by flow cytometry and expanded to generate a line termed "HT-29 eGFP". Both A431 and Vero cells were cultured and maintained in ATCC formulated DMEM supplemented with 10% FBS and 1% antibiotic (Penicillin Streptomycin). HEp2 cells were cultured and maintained in 50:50 ATCC formulated DMEM/Advanced MEM containing 10% FBS and 1% antibiotic (Penicillin Streptomycin). The cells were split twice weekly to maintain a sub-confluent stock. All compound solutions were filter-sterilized using a 0.22 μm syringe filter. A 32 mM stock solution was prepared for each Pc by dissolving in DMSO containing 5% Cremophor EL (as a nonionic

emulsifier), to avoid compound precipitation upon dilution into media. From this solution, a 400 μM stock was also prepared in desired medium and filter-sterilized using a 0.22 μm syringe filter.

Time-Dependent Cellular Uptake: HEp2 cells and A431 cells were plated at 7,500 per well in a Costar 96 well plate and allowed to grow for 48 h. Vero cells were plated at 7,500 per well in a Costar 96 well plate and allowed to grow for 24 h. HT-29 cells were plated at 7,500 per well in a Costar 96 well plate and allowed to grow for 96 h. Pc stock solutions (32 mM) were diluted to 10 μM Pc solutions in media and added to the cells at different time periods of 0, 1, 2, 4, 8, and 24 h. Uptake of the compounds was stopped by removing loading medium and washing once with PBS. Cells were solubilized by adding 0.25% Triton X-100 in PBS. The Pc concentration was determined by reading its fluorescence emission at 650/700 nm (excitation/emission) using a BMG FLUOstar plate reader (Cary, NC). Cell number was quantified using CyQuant reagent.

Dark Cytotoxicity: The cells were plated and allowed to grow as described above. Pc stock solutions (32 mM) were diluted to concentrations of 25, 50, 100 and 125 μM in medium, and added to cells for 24 h. The loading medium was removed and medium containing Cell Titer Blue was added to determine the toxicity of the compounds (viable cells were measured fluorescently at 570/615 nm); untreated cells were considered 100% viable and cells treated with 0.2% saponin as 0% viable.

Phototoxicity: The cells were plated and allowed to grow as described above. The Pc stock solutions (32 mM) were diluted to concentrations of 6.25, 12.5, 25, 50 and 100 μM in medium and added to cells for 24 h. The loading medium was removed and fresh medium was added. The conjugates were exposed to light using a light system (Newport) at 1 J/cm^2 for 20

min. The plates were chilled at 5 °C using a cooling block. Water was used as a filter for IR radiation. The plates were then incubated for another 24 h followed by removing medium and adding medium containing Cell Titer Blue to determine the toxicity of the compounds.

Microscopy: The cells were inoculated in a glass-bottom 6-well plate (MatTek) and allowed to grow for 48 h. The cells were then exposed to 10 μM for each Pc for 6 h. Organelle tracers were obtained from Invitrogen and used at the following concentrations: LysoSensor Green 50 nM, MitoTracker Green 250 nM, ER Tracker Blue/white 100 nM, and BODIPY FL C5 ceramide 1 μM. Images were acquired using a Leica DMRXA microscope with 40× NA 0.8dip objective lens and DAPI, GFP and Texas Red filter cubes (Chroma Technologies).

3.4.6. In Vivo Uptake Studies

For the animal studies, Nu/nu mice were purchased from Charles Rivers Laboratories at 6 weeks of age. After approximately 2 weeks of quarantine, mice were implanted with tumor cells subcutaneously in the upper flank. For these injections, each cell line was cultured to approximately 75% confluence, then dissociated with trypsin, and concentrated by centrifugation. Since the two tumor lines were found to grow at different rates in nude mice, 1 x 10^6 A431 cells and 2 x 10^6 HT-29 eGFP cells were implanted in a volume of 100 μL. The injection material consisted of 4 parts DMEM and 1 part MatriGel basement membrane matrix (BD biosciences). Tumors were allowed to develop until palpable (approximately 6 days for A431 cells and 9 days for HT-29 eGFP cells), after which mice were imaged for time = 0, then injected through the tail vein with 20 μL of a 10 mM solution of Pc **3.11** in 10% DMSO and 5% Cremophor EL in PBS, for a dose of ~ 10 mg/kg. The mice were then observed for acute adverse responses to the injected Pc and returned to their box until imaged. Prior to imaging at selected time points after Pc administration, mice were anesthetized with isoflurane gas to effect then

imaged individually for 30 s at excitation 630 nm and emission 700 nm (x630/m700) in a Kodak In Vivo FX whole animal imager. All animal experiments were conducted by adherence to a protocol approved by the LSU IACUC committee.

To quantify relative fluorescence within the image of the tumor region, a region-of-interest (roi) was drawn around the tumor and the mean pixel intensity (mpi) of this roi was divided by the mpi's of 3 adjacent skin areas to obtain a percent of tumor fluorescence over adjacent regions. In order to visually distinguish one roi as more fluorescent than adjacent skin, it was found that the roi needed to be at least 120%.

At 24 and 96 h following iv injection of Pc **3.11**, the HT-29 tumor tissue was harvested from mice and flash frozen. The tissue was kept in 5 mL of acetone/methanol (5:1) at -20 °C overnight, then crushed repeatedly using a mortar, filtered and the organic solvents removed under reduced pressure. The residues were analyzed by MALDI-TOF and UV-Vis spectrophotometry. Frozen sections of tumor were cut to 10 µm thickness and mounted on glass slides. Tissues were immediately imaged for both eGFP indicating regions of HT-29 tumor and near-IR indicating Pc fluorescence using Chroma 41017 (450-490 nm excitation, 500-550 nm emission) and Omega Optical 140-2 (570-645 nm excitation, 668-723 nm emission) filter sets respectively.

3.5. References

1. Cancer, A. C. S. D. G. C. a. R. What are the key statistics for colorectal cancer?
2. Kiesslich, R.; Goetz, M.; Vieth, M.; Galle, P. R.; Neurath, M. F. *Nat. Clin. Pract. Oncol.* **2007**, *4*, 480-490.
3. Van den Broek, F. J.; Fockens, P.; Dekker, F. *Aliment. Pharmacol. Ther.* **2007**, *26*, 91-99.
4. Ongarora, B. G.; Fontenot, K. R.; Hu, X.; Sehgal, I.; Satyanarayana-Jois, S. D.; Vicente, d. G. H. *Journal of Medicinal Chemistry* **2012,** *55* (8), 3725-3738.

5. Kantsevoy, S. V.; Adler, D. G.; Conway, J. D.; Diehl, D. L.; Farraye, F. A.; Kaul, V.; Kethu, S. R.; Kwon, R. S.; Mamula, P.; Rodriguez, S. A.; Tierney, W. M.; Comm, A. T. *Gastrointestinal Endoscopy* **2009,** *70 (2),* 197-200.

6. Leznoff, C. C.; Lever, A. B. P., Eds. In *Phthalocyanines: Properties and Applications*. VCH: Weinheim, **1989-1996**; vols 1-4.

7. Sharman, W. M.; Van Lier, J. E. In *The Porphyrin Handbook*, Kadish, K. M.; Smith, K. M.; Guilard, R., Eds.; Academic Press: Boston, **2003**, 15, 1-60.

8. Liu, T. M.; Chu, S. W.; Sun, C. K.; Lin, B. L.; Cheng, P. C.; Johnson, I. *Scanning.* **2001**, *23*, 249-254.

9. Ben-Hur, E.; Chan, W.-S. In *The Porphyrin Handbook*, Kadish, K. M.; Smith, K. M.; Guilard, R., Eds.; Academic Press: Boston, **2003**, *19*, 1-35.

10. Erk, P.; Hengelsberg, H. In *The Porphyrin Handbook*, Kadish, K. M.; Smith, K. M.; Guilard, R., Eds.; Academic Press: Boston, **2003**, *19*, 106-146.

11. Kimura, M.; Shirai, H. In *The Porphyrin Handbook*, Kadish, K. M.; Smith, K. M.; Guilard, R., Eds.; Academic Press: Boston, **2003**, *19*, 151-173.

12. Dougherty, T. J.; Gomer, C. J.; Henderson, B. W.; Jori, G.; Kessel, D.; Korbelik, M.; Moan, J.; Peng, Q. *J. Natl. Cancer Inst.* **1998**, *90*, 889-905.

13. Pandey, R. K. *J. Porphyrins Phthalocyanines* **2000**, *4*, 368-373.

14. Sharman, W. M.; van Lier, J. E.; Allen, C. M. *Adv. Drug Delivery Rev.* **2004**, *56*, 53-76

15. Savellano, M. D.; Hasan, T. *Clin. Cancer Res.* **2005**, *11*, 1658-1668

16. Hudson, R.; Boyle, R. W. *J. Porphyrins Phthalocyanines* **2004**, *8*, 954-975.

17. Pérez-Soler, R. *The Oncologist* **2004**, *9*, 58-67.

18. Meric-Bernstam, F.; Hung, M.-C. *Clin. Cancer Res.* **2006**, *12*, 6326-6330.

19. Spano, J.–P.; Lagorce, C.; Atlan, D.; Milano, G.; Domont, J.; Bnamouzig, R.; Attar, A.; Benichou, J.; Martin, A.; Morere, J. –F.; Raphael, M.; Penault-Llorca, F.; Breau, J.–L.; Fagard, R.; Khayat, D.; Wind, P. *Ann. of Oncol.* **2005**, *16*, 102-108.

20. Galizia, G.; Iieto, E.; Ferraraccio, F.; De Vita, F.; Castellano, P.; Orditura, M.; Imperatore, V.; La Mura, A.; La Manna, G.; Pinto, M.; Catalano, G.; Pignatelli, C.; Ciardiello, F. *Ann. of Surg. Oncol.* **2006**, *13*, 823-835.

21. Dougherty, U.; Sehdev, A.; Cerda, S.; Mustafi, R.; Little, N.; Yuan, W.; Jagadeeswaran, S.; Chumsangsri, A.; Delgado, J.; Tretiakova, M.; Joseph, L.; Hart, J.; Cohen, E. E.; Aluri, L.; Fichera, A.; Bissonnette, M. *Clin. Cancer Res.* **2008**, *14*, 2253-2262.

22. Loeffler-Ragg, J.; Schwentner, I.; Sprinzl, G. M.; Zwierzina, H. *Expert Opin. Investig. Drugs* **2008**, *17*, 1517-1531.

23. Molema, G. *Acta Biochim. Polonica* **2005**, *52*, 301-310.

24. Dane, K. Y.; Chan, L. A.; Rice, J. J.; Daugherty, P. S. *J. Immun. Meth.* **2006**, *309*, 120-129.

25. Frochot, C.; Stasio, B. D.; Vanderesse, R.; Belgy, M.-J.; Dodeller, M.; Guillemin, F.; Viriot, M.-L.; Barberi-Heyob, M. *Bioorganic Chem.* **2007**, *35*, 205-220.

26. Song, S. X.; Liu, D.; Peng, J. L.; Sun, Y.; Li, Z. H.; Gu, J. R.; Xu, Y. H. *Int. J. Pharmac.* **2008**, *363*, 155-161.

27. Song, S.; Liu, D.; Peng, J.; Deng, H.; Guo, Y.; Xu, L. X.; Miller, A. D.; Xu, Y. *FASEB J.* **2009**, *23*, 1396-1404.

28. Li, Z.; Zhao, R.; Wu, X.; Sun, Y.; Yao, M.; Li, J.; Xu, Y.; Gu, J. *FASEB J.* **2005**, *19*, 1978-1985.

29. Sibrian-Vazquez, M.; Ortiz, J.; Nesterova, I. V.; Fernández-Lázaro, F.; Sastre-Santos, A.; Soper, S. A.; Vicente, M. G. H. *Bioconjugate Chem.* **2007**, *18*, 410-420.

30. Ongarora, B. G.; Hu, X.; Li, H.; Fronczek, F. R.; Vicente, M. G. H. *MedChemComm* **2012,** *3* (2), 179-194.

31. Sibrian-Vazquez, M.; Jensen, T. J.; Hammer, R. P.; Vicente, M. G. H. *J. Med. Chem.* **2006**, *49*, 1364-1372.

32. Sibrian-Vazquez, M.; Jensen, T. J.; Vicente, M. G. H. *Org. Biomol. Chem.* **2010**, *8*, 1160-1172.

33. Rocha-Lima, C. M.; Soares, P. H.; Raez, L. E.; Singal, R. *Cancer Control* **2007**, *14* (*3)*, 295-304.

34. Morris, G. M.; Goodsell, D. S.; Halliday, R. S.; Huey, R.; Hart, W. E.; Belew, R. K.; Olson, A. J. *J. Comp. Chem.* **1998**, 19, 1639–1662.

35. Huey, R.; Morris, G. A.; Olson, A. J.; Goodsell, D. S. *J. Comp. Chem.* **2006**, 28, 1145–1152.

36. Gulli, L. F.; Palmer, K. C.; Chen, Y. Q.; Reddy, K. B. *Cell Growth Diff.* **1996**, *7 (2)*, 173-178.

37. Kawamoto, T.; Sato, J. D.; Le, A.; Polikoff, J.; Sato, G. H.; Mendelsohn, J. *Proc. Nat. Acad. Sc. USA* **1983**, *80 (5)*, 1337-1341.

38. Haigler, H.; Ash, J. F.; Singer, S. J.; Cohen, S. *Proc. Nat. Acad. Sci.* **1978**, *75 (7)*, 3317-3321.

39. Macfarla, D.; Sommervi, Rg. *Archiv. Ges. Virusforsch.* **1969**, *27 (2-4*), 379-385.

40. Pellegrini, R.; Centis, F.; Martignone, S.; Mastroianni, A.; Tagliabue, E.; Tosi, E.; Menard, S.; Colnaghi, M. I. *Cancer Immunol. Immunotherapy* **1991**, *34 (1)*, 37-42.

41. Magné, N.; Fischel, J. L.; Dubreuil, A.; Formento, P.; Poupon, M.-F.; Laurent-Puig, P.; Milano, G. *Br. J. Cancer* **2002**, *86*, 1518–1523.

42. Giannopoulou, E.; Antonacopoulou, A.; Matsouka, P.; Kalofonos, H. P. *Anticancer Res.* **2009**, *29 (12)*, 5077-5082.

43. Sibrian-Vazquez, M.; Jensen, T. J.; Fronczek, F. R.; Hammer, R. P.; Vicente, M. G. H. *Bioconjugate Chem.* **2005**, *16 (4)*, 852-863.

44. Futaki, S.; Suzuki, T.; Ohashi, W.; Yagami, T.; Tanaka, S.; Ueda, K.; Sugiura, Y. Arginine-rich peptides. *J. Biol. Chem.* **2001**, *276*, 5836-5840.

45. Zuhorn, I. S.; Hoekstra, D. *J. Memb. Biol.* **2002**, *189 (3)*, 167-179.

46. Rothbard, J. B.; Jessop, T. C.; Lewis, R. S.; Murray, B. A.; Wender, P. A. *J. Am. Chem. Soc.* **2004**, *126*, 9506-9507.

47. He, J.; Haney, R. M.; Vora, M.; Verkhusha, V. V.; Stahelin, R. V.; Kutateladze, T. G. *J. Lipid Res.* **2008**, *49 (8)*, 1807-1815.

48. Rao, R. V.; Hermel, E.; Castro-Obregon, S.; del Rio, G.; Ellerby, L. M.; Ellerby, H. M.; Bredesen, D. E. *J. Biol. Chem.* **2001**, *276*, 33869-33874.

49. Kessel, D. *J. Porphyrins Phthalocyanines* **2004**, *8*, 1009-1014.

50. Trivedi, E. R.; Harney, A. S.; Olive, M. B.; Podgorski, I.; Moin, K.; Sloane, B. F.; Barrett, A. G. M.; Meade, T. J.; Hoffman, B. M. *Proc. Nat. Acad. Sci.* **2010**, *107 (4)*, 1284–1288.

51. Jeong, H.; Huh, M.; Lee, S. J.; Koo, H.; Kwon, I. C.; Jeong, S. Y.; Kim, K. *Theranostics* **2011**, *1*, 230-239.

52. Spernyak, J. A.; White III, W. H.; Ethirajan, M.; Patel, N. J.; Goswami, L.; Chen, Y.; Turowski, S.; Missert, J. R.; Batt, C.; Mazurchuk, R.; Pandey, R. K. *Bioconjugate Chem.* **2010**, *21*, 828-835.

53. Dabrowski, J. M.; Krzykawska, M.; Arnaut, L. G.; Pereira, M. M.; Monteiro, C. J. P.; Simoes, S.; Urbanska, K.; Stochel, G. *Chem. Med. Chem.* **2011**, *6 (9)*, 1715-1726.

54. Sibrian-Vazquez, M.; Jensen, T. J.; Vicente, M. G. H. *J. Med. Chem.* **2008**, *51*, 2915-2923.

55. Brykina, G. D.; Uvarova, M. I.; Koval, Y. N.; Shpigun, O. A. *J. Anal. Chem.* **2001**, *56*, 940-944.

56. Zorlu, Y.; Dumoulin, F.; Durmus, M.; Ahsen, V. *Tetrahedron* **2010**, *66*, 3248-3258.

57. Ferguson, K. M.; Berger, M. B.; Mendrola, J. M.; Cho, H.; Leahy, D. J., Lemmon, M. A. *Mol. Cell.* **2003**, *11*, 507-517.

58. Sutcliffe, M. J. In *NMR of Macromolecules: A Practical Approach.* Roberts G. C. K., Ed.; Oxford University Press: New York, **1993**, 359–390.

CHAPTER 4

SYNTHESES, CHARACTERIZATION AND PHOTOPHYSICAL EVALUATION OF REGIOMERICALLY PURE PHTHALOCYANINES FOR CANCER IMAGING AND PHOTODYNAMIC THERAPY APPLICATIONS

4.1. Background

Pcs exhibit strong absorptions in the near-IR, a feature that has made them find multiple applications in biology, medicine and materials science. They have found use as colorant dyes, optical sensors, bioimaging agents, and as photosensitizers for the photodynamic therapy (PDT) of cancers and the inactivation of bacteria and viruses.[1-3] Photofrin, a derivative of hematoporphyrin IX, has been used for nearly three decades in the PDT treatment of various cancers, including lung, skin, cervical and bladder.[4,5] Nevertheless, its persistence in healthy tissues for long periods of time after systemic administration causes unwanted side-effects, such as patient photosensitivity for several weeks post-PDT. This is what has caused great interest in the search for new PDT drugs. In PDT, a photosensitizer is activated by light and produces singlet oxygen and other reactive oxygen species (ROS) *in situ*, as discussed in Chapter 1. The ROS produced destroy proximal cells via necrosis and/or apoptosis.[6,7] Pcs are promising photosensitizers because they are photochemically stable and produce ROS upon light activation. Sulfonated Al(III)Pc or Photosense, and a Si(IV)Pc (Pc4) are in clinical trials for PDT.[8-10]

Addition of peripheral water-solubilizing substituents and/or axial ligands minimizes aggregation and increases Pc solubility in aqueous media. Polyethylene glycol (PEG) may serve as a delivery vehicle[11-13] and, in some cases, can be covalently bound to Pcs[14-16] for improved delivery to target tissues. Pegylation of photosensitizers increases their water-solubility, serum life, tumor accumulation, and also reduces their uptake by the reticuloendothelial system.[17-20] As a continuation of the investigation of Pcs as potential photosensitizers with enhanced biological effectiveness, this Chapter describes the syntheses and characterization of a new series of

regiomerially pure Pcs, containing at least a PEG group. It is anticipated that pegylation of the ZnPc macrocycle will increase solubility and biological efficacy. The Pcs described in this Chapter can serve as biomarkers or photosensitizers for PDT. They are also single isomers as opposed to those reported in earlier Chapters.

4.2. Synthesis of A_2B_2- and A_3B-type Pcs

In Chapter 1, some of the protocols for the tetramerization of two or more phthalonitriles that have been reported in the past were described. Kobayashi and coworkers developed a method to synthesize A_3B-type Pcs via ring expansion of a subphthalocyanine template.[21] The polymeric-support synthesis of A_3B-type Pcs was developed by Leznoff and coworkers in 1982, where a mono-functionalized diiminoisoindoline precursor bound to solid polymer support reacts with another precursor to form A_3B-type Pcs.[22-24] Tomoda method – by optimization of reactant ratios and reaction conditions – gives differently substituted Pcs, not including constitutional isomers.[21] The use of one of the phthalonitriles in excess is one such modification that may favor the formation A_3B-type Pcs.[25] In some cases, half Pcs have been used in the preparation of A_2B_2-type Pcs.[26] Side-strapped Pcs have also been synthesized, with the aim of reducing the number of isomers obtained in case of A_2B_2-type Pcs. These bridged Pcs may be obtained via bis-phthalonitriles. Suitable bis(3-phthalonitriles) can be synthesized from 2,2-dialkyl propane-1,3-diols or chiral bis-naphthols, although it has been reported that many other bis(3-phthalonitriles) do not form side-strapped Pcs.[27] A chiral side-strapped Pc with D_{2h} symmetry has been synthesized from bis(4-phthalonitrile) containing flexible linker.[28] Another example is the synthesis of 1,2-bis(3,4-dicyanophenoxymethyl)benzene, using 1,2-bis(hydroxymethyl)benzene and 4-nitrophthalonitrile.[29] In our synthetic strategy, a carefully designed a protecting group (1,2-bis(bromomethyl)benzene) was reacted with mono-pegylated 2,3-dicyanohydroquinone to obtain

the target di-pegylated bis-phthalonitrile. The bis-phthalonitrile facilitated the formation of A_2B_2-type Pc. The other product formed during this reaction led to the formation of A_3B-type Pc, following acidic deprotection of the precursor Pc.

4.2.1. Synthesis of Phthalonitriles

The synthesis of the regiomerically pure Pcs started with a reaction of 3-nitrophthalonitrile and N-Boc-serinol. Mass spectrum and X-ray structure of the crude revealed that the reaction did not yield the desired product, *tert*-butyl-(1,3-bis(2,3-dicyanophenoxy)propan-2-yl)carbamate **4.2** (Scheme 4.1). Instead, it formed a bis-phthalonitrile ether **4.3** (Figure 4.1). It was probably formed via nucleophilic attack of the nitro group by hydroxyl group, and then a nucleophilic attack by the 3-hydroxyphthalonitrile on another 3-nitrophthalonitrile to form ether **4.3**.

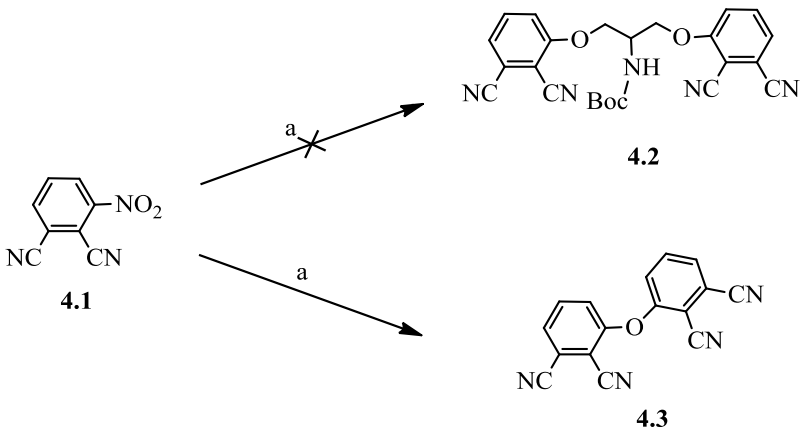

Scheme 4.1. Synthetic strategy to *tert*-butyl-(1,3-bis(2,3-dicyanophenoxy)propan-2-yl)carbamate **4.2**. Conditions and reagents, a: N-Boc-serinol, K_2CO_3, DMF, 65 °C, 24 h.

This led to new strategy where a mixture of 3-nitrophthalonitrile and 1,2-bis(hydroxymethyl)benzene gave 3,3'-((1,2-phenylenebis(methylene))bis(oxy))diphthalonitrile, **4.4**, which was characterized by NMR and MS (HRMS-ESI). Dimerization of the bis-phthalonitrile in the presence of Zn(II) acetate and a catalytic amount of DBN in DMAE resulted in trace amounts of Pc **4.5** (Scheme 4.2), which was characterized by MS (MALDI-TOF) *m/z*

peak at 844.177 $(M)^+$, calcd for **$C_{48}H_{28}N_8O_4Zn$ 844.153**. The formation of the macrocycle could not be achieved in reasonable amounts by varying reaction conditions, such as temperature, concentration and reaction time. This indicated that the formation of this type of side-strapped Pc was difficult. Construction of a model of Pc **4.5** revealed that there was a lot of strain in the molecule. This explained why the product was obtained in trace amounts.

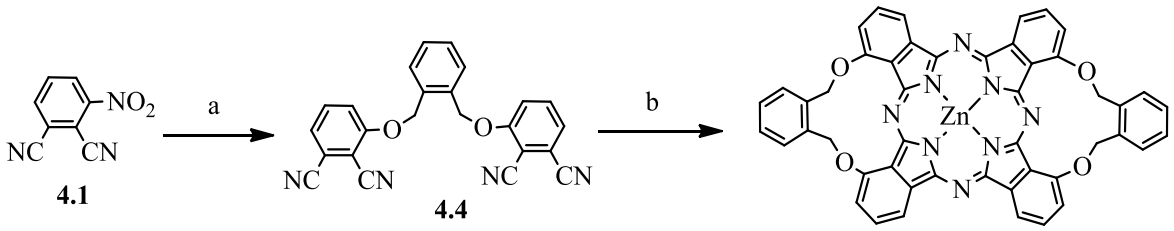

4.1 **4.4** **4.5**

Scheme 4.2. Synthetic strategy to 3,3'-[(1,2-phenylenebis(methylene))bis(oxy)]diphthalonitrile **4.4** and bis-phthalocyanine **4.5**. Conditions and reagents: (a) 1,2-benzenedimethanol, K_2CO_3, DMF, 65 °C, 24 h, 71.2% (b) $Zn(OAc)_2$, DMAE, 140 °C, 5 h.

4.3

4.7

Figure 4.1. X-ray structures of phthalonitriles **4.3** and **4.7** from crystal structure determinations (N atoms are blue, O atoms red and H atoms white).

The above strategy seemed promising but due to solubility issues and difficulties in the macrocyclization, a new approach was sought. To enhance solubility, a mixture of 3-nitrophthalonitrile and 3-cyclohexene-1,1-dimethanol was reacted and after tedious purification of the crude, yellow crystals of mono-substituted adduct **4.7** were obtained (Scheme 4.3). When the conversion of the mono-substituted adduct to di-substituted product **4.6** was attempted, the bis-phthalonitrile ether **4.3** was formed – obtained from an earlier reaction (Scheme 4.1).

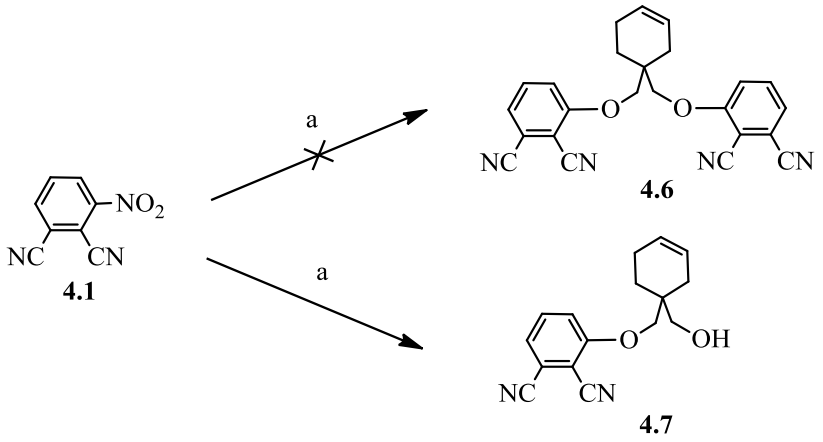

Scheme 4.3. Synthetic strategy to 3,3'-[(cyclohex-3-ene-1,1-diylbis(methylene))bis(oxy)]-diphthalonitrile **4.6**. Conditions and reagents: 3-cyclohexene-1,1-dimethanol, K_2CO_3, DMF, 65 °C, 24 h, 25%.

In Chapter 1, a review of the published syntheses of bridged-Pcs, or side-strapped Pcs obtained from single phthalonitriles precursors, was presented. The synthesis of these Pcs is usually carried out under dilute conditions for the cyclotetramerization of bis-phthalonitriles. Suitable bis(3-phthalonitriles) are prepared from 2,2-dialkyl propane-1,3-diols or chiral bis-naphthols, although not many bis(3-phthalonitriles) form side-strapped Pcs.[27] This suggests that the choice of precursor phthalonitriles is important in the syntheses of A_2B_2-type Pcs.

Therefore, in our synthesis of pegylated and regiomerically pure Pcs, a mixture of phthalonitrile **4.8**, synthesized according to a literature procedure,[15] and 1,2-bis(bromomethyl)benzene reacted to give the target di-pegylated bis-phthalonitrile **4.9** in 84.3% yield (Scheme 4.4). The yield for this bis-phthalonitrile was higher compared with those obtained in prior attempts. Its purification was relatively easy. In addition, it had a better solubility in organic solvents, a feature that made it a suitable candidate for the synthesis of regiomerically pure Pcs. The PEG groups on either side of the bis-phthalonitrile molecule resulted in enhanced solubility of the Pcs described in this Chapter. This made it possible to use column chromatography to purify the products.

The 1,2-bis(bromomethyl)benzene used in this synthesis was designed to introduce a 1,2-dimethylbenzene protecting group that was later removed under acidic conditions to give the desired product. The ^{1}H NMR spectrum of bis-phthalonitrile **4.9** is shown in Figure 4.2.

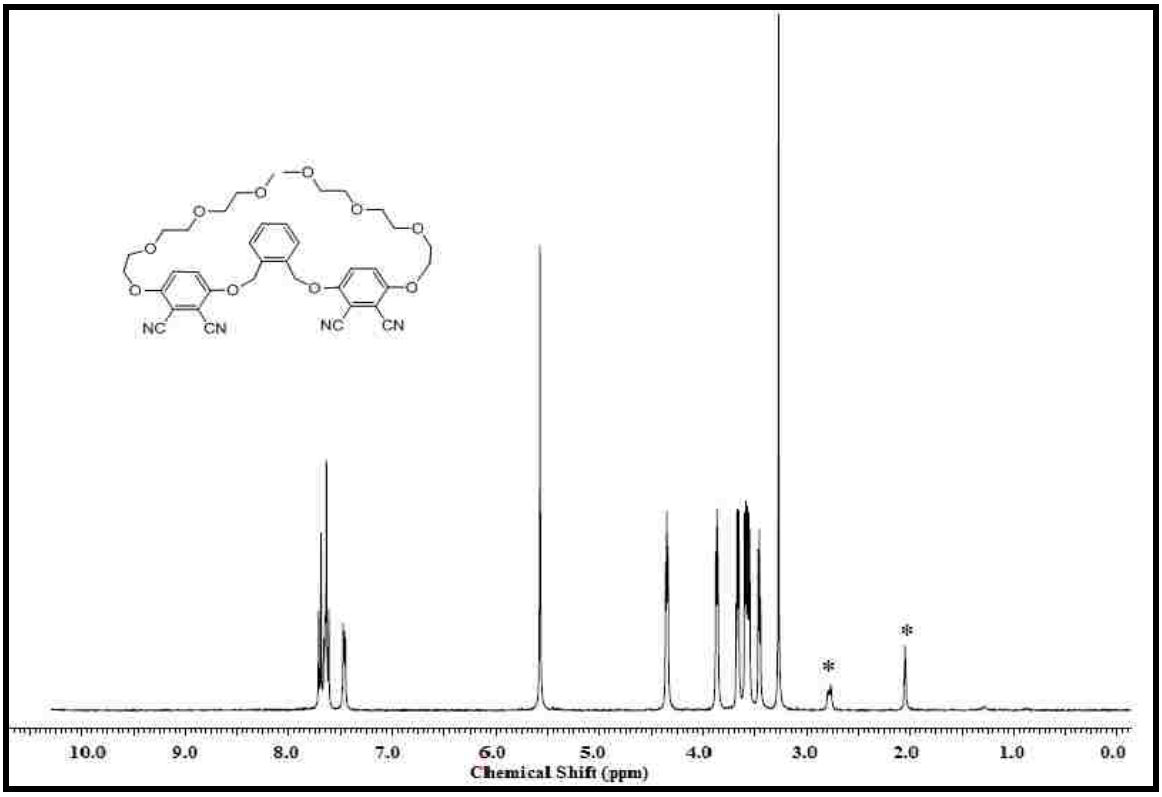

Figure 4.2. ^{1}H NMR spectrum of phthalonitrile **4.9** at 400 MHz (* denotes solvent).

4.2.2. Synthesis of Pcs

The methodology developed in this Chapter was specifically meant to afford A_3B- and A_2B_2-type regiomerically pure photosensitizers. Their synthetic route is shown in Scheme 4.4. The condensation of phthalonitrile **4.9** and unsubstituted phthalonitrile in refluxing DMAE, and in the presence of Zn(II) acetate and 1,5-diazabicyclo(4.3.0)non-5-ene (DBN) gave the protected Pcs **4.10** and **4.11** in 5 – 7% yields. Reaction of Pcs **4.10** and **4.11** with concentrated H_2SO_4 gave deprotected Pcs **4.12** and **4.13** respectively, in 95% and 40% yields.[29,30] Pc **4.13** reacted with 3,3'-dimethylaminopropyl chloride hydrochloride to give Pc **4.14** in 50.0% yield.

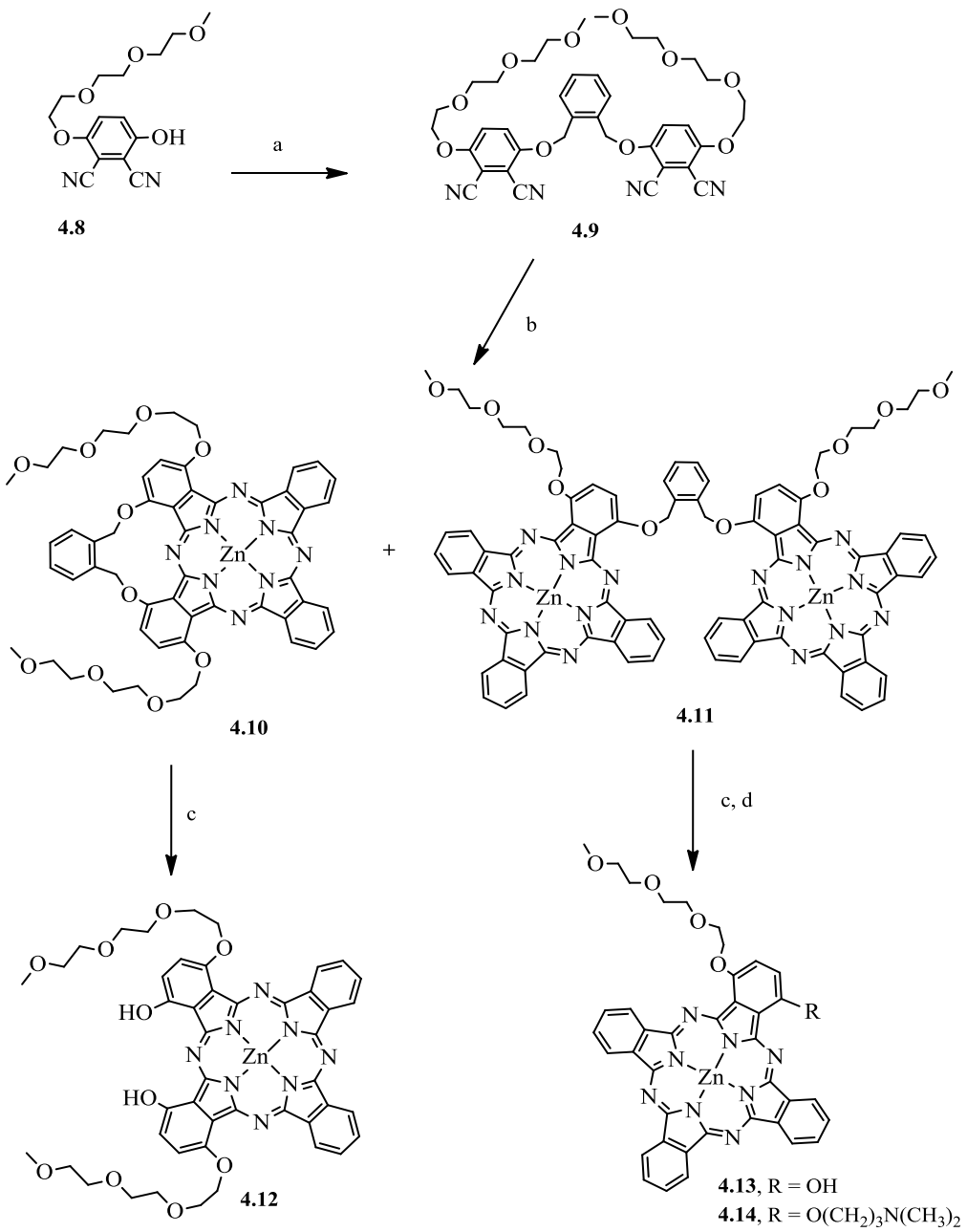

Scheme 4.4. Synthetic strategy to Pcs **4.12**, **4.13** and **4.14**. Conditions and reagents: (a) 1,2-bis(bromomethyl)benzene, K_2CO_3, DMF, 65 °C, 24 h, 84.3% (b) $Zn(OAc)_2$, DMAE, 140 °C, 5 h, 5-7% (c) H_2SO_4, 0 °C. 15-30 min, 40-95% (d) 3,3'-(dimethylamino)propyl chloride hydrochloride, K_2CO_3, DMF, 65 °C, 6 h, 50%.

Attempts to dimerize bis-phthalonitrile **4.9** into a Pc with four PEG groups failed. No evidence of the Pc was present in the MALDI-TOF spectra. This was in agreement with the macrocyclization experiment described earlier, involving bis-phthalonitrile **4.4**. This result

confirmed that the strain in this type of Pcs does not favor their formation. Although Pc **4.5** was formed in traces, bis-phthalonitrile **4.9** failed to form a similar type of macrocycle. Instead, this reaction gave A_2B_2-type Pc **4.10** and clamshell-type Pc **4.11** in 5.1 and 7.2% yields respectively.

Initial attempts to deprotect Pcs **4.10** and **4.11** at room temperature using BCl_3/pentamethylbenzene did not work.[31] Metal-catalyst mediated deprotection of Pcs using Palladium on carbon and hydrogen gas in THF did not work either. The anticipated hydrogenolysis of the 'benzylic ether' did not occur. Instead, the palladium catalyst resulted in decomposition of Pc **4.10**, while Pc **4.11** was all recovered. The use of hydrobromic acid (HBr) or acetic acid did not work either; it instead, removed Zn from the Pc core. Therefore, even the deprotection experiments using H_2SO_4 (strong acid), which gave us the desired products, had to be performed within a short duration to avoid the removal of the Zn metal.

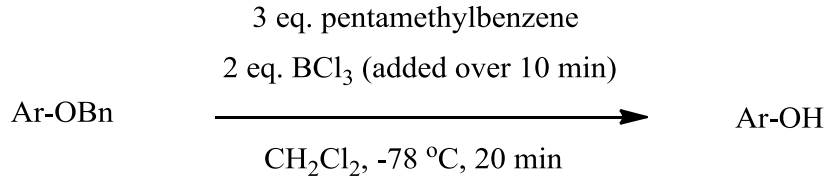

Scheme 4.5. Strategy for the deprotection of benzyl groups under mild conditions.

It has been previously observed that a PEG group increases cellular uptake into human HEp2 cells, and decreased cytotoxicity of the Pc macrocycles.[32] In this Chapter, a low molecular weight PEG (10-atom, triethylene glycol) on the Pc macrocycle as a solubilizing group was investigated; this PEG group has the advantage of being commercially available and is also relatively less flexible than the penta(ethylene glycol) previously reported. These Pcs have a mono- or di-hydroxyl group(s), which may be used in further functionalization of the macrocycles as illustrated in Scheme 4.4. Such functionalization of the Pcs is essential, especially when coupling the photosensitizers to various biomolecules.

4.3. Spectroscopic and Photophysical Characterization

N-Methylated Pcs are sensitive to heat and therefore, the solvents used during the synthesis and column chromatography of ZnPc **4.14** were removed at temperatures < 70 °C, to avoid loss of N-methyls. The Pc was then immediately characterized by NMR and MS. Although N-Demethylation in ZnPc **4.14** was not observed, MS analysis of previously synthesized N-Methylated Pcs had shown N-Demethylation of ZnPcs upon prolonged storage at room temperature.[33] This observation may not be used to draw a conclusive observation, but may suggest that N-demethylation is limited to benzylic N-methyls.

The Pcs were characterized by MS, NMR, UV-Vis and fluorescence spectroscopy; MALDI-TOF was used to confirm the NMR data in deuterated DMF or acetone solvents. The relative simplicity of the aromatic region of ^{1}H-NMR spectra of ZnPcs **4.10**, **4.11**, and **4.14** suggested the regiomeric purity of the Pcs, compared with the ZnPcs synthesized in Chapters 2 and 3 (see Appendix C.1 and C.2 for ^{13}C NMR). Various regioisomers (up to fifteen for the di-cationic ZnPcs) were expected from the cyclotetramerization reaction of two mono-substituted phthalonitriles.[33] The ^{1}H NMR spectra of Pcs **4.10** and **4.11** are shown in Figures 4.3 and 4.4, respectively. The 1,2-dimethylenebenzene protecting group had a peak at 6.42 (s, 4H, OCH_2), and other multiplets within the aromatic region for the benzene ring. Removal of the protecting group under acidic conditions was confirmed by disappearence of these peaks from the ^{1}H NMR spectrum of ZnPc **4.11**. MS spectrum of the deprotected ZnPc also agreed with the NMR observations. In the ^{1}H-NMR data of ZnPc **4.14** (Figure 4.5), the aromatic region remained relatively simple in spite of the two different substituents added to the macrocycle. The two N-methyls in ZnPc **4.14**, have a peak at 2.53 ppm while the O-methyl peak is at 3.25 ppm. All the chemical shifts of the PEG groups appeared between 3.5 – 5.2 ppm.

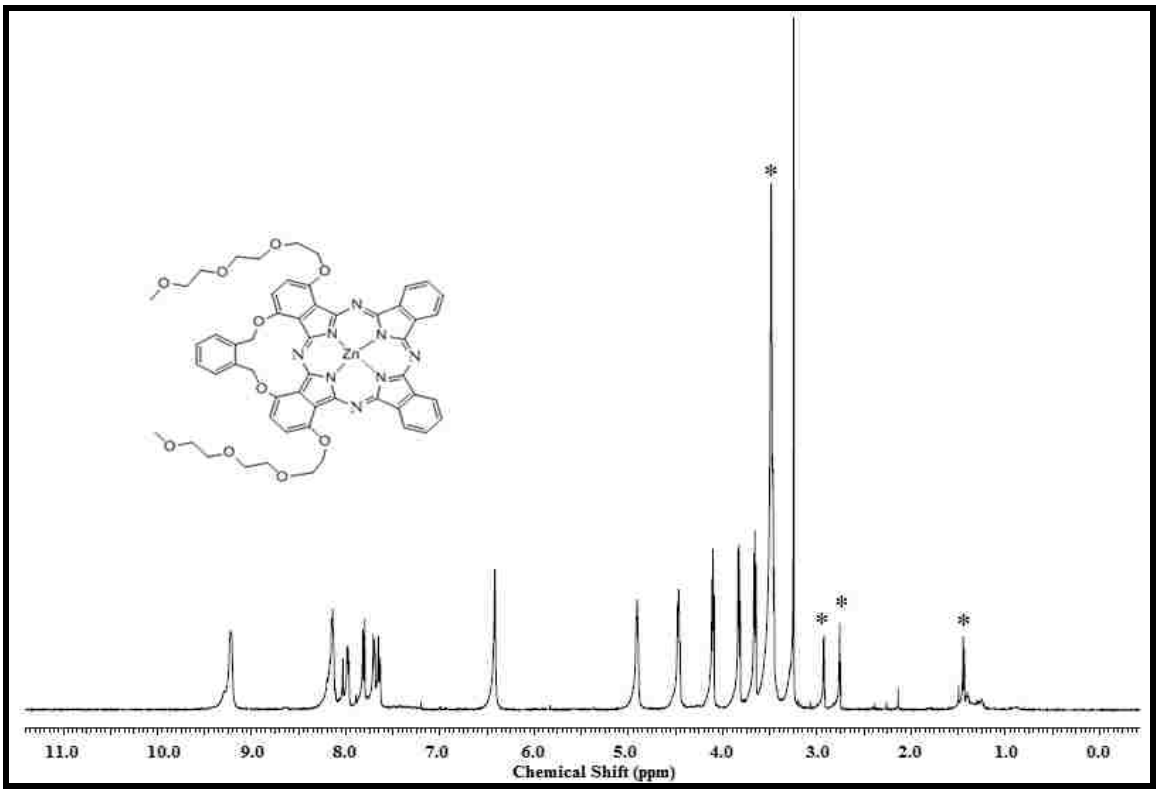

Figure 4.3 ^{1}H NMR spectrum of ZnPc **4.10** at 400 MHz (* denotes solvent).

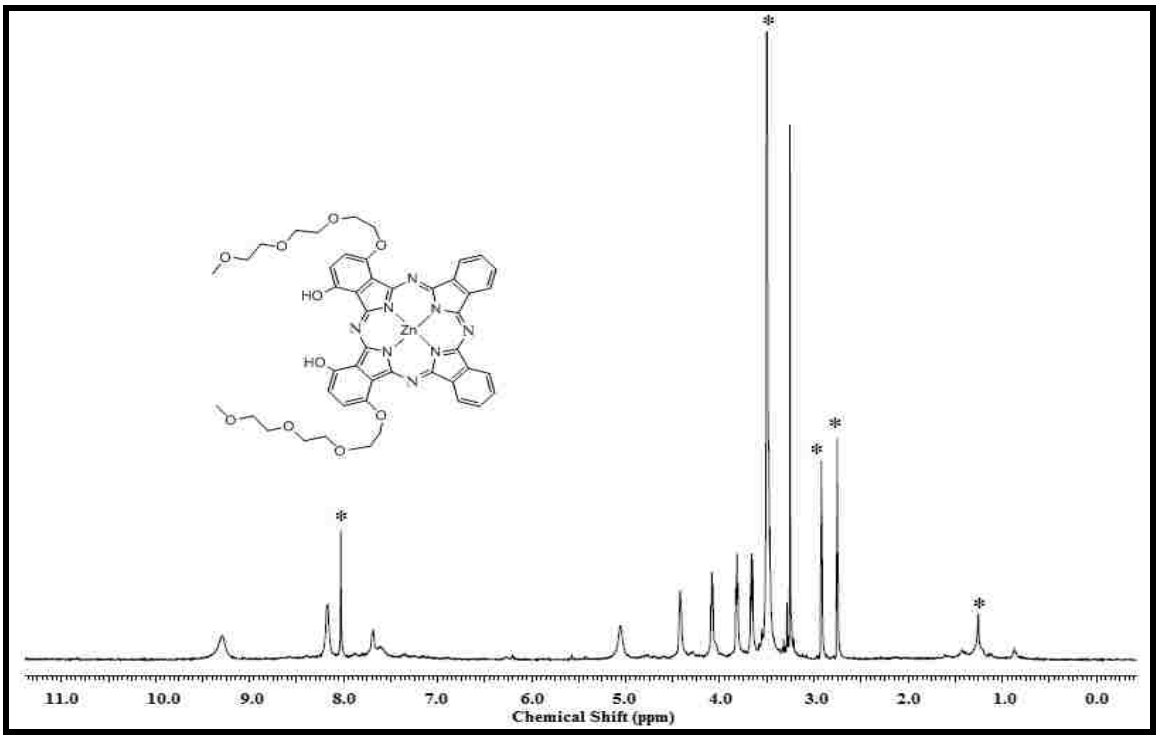

Figure 4.4 ^{1}H NMR spectrum of ZnPc **4.11** at 400 MHz (* denotes solvent).

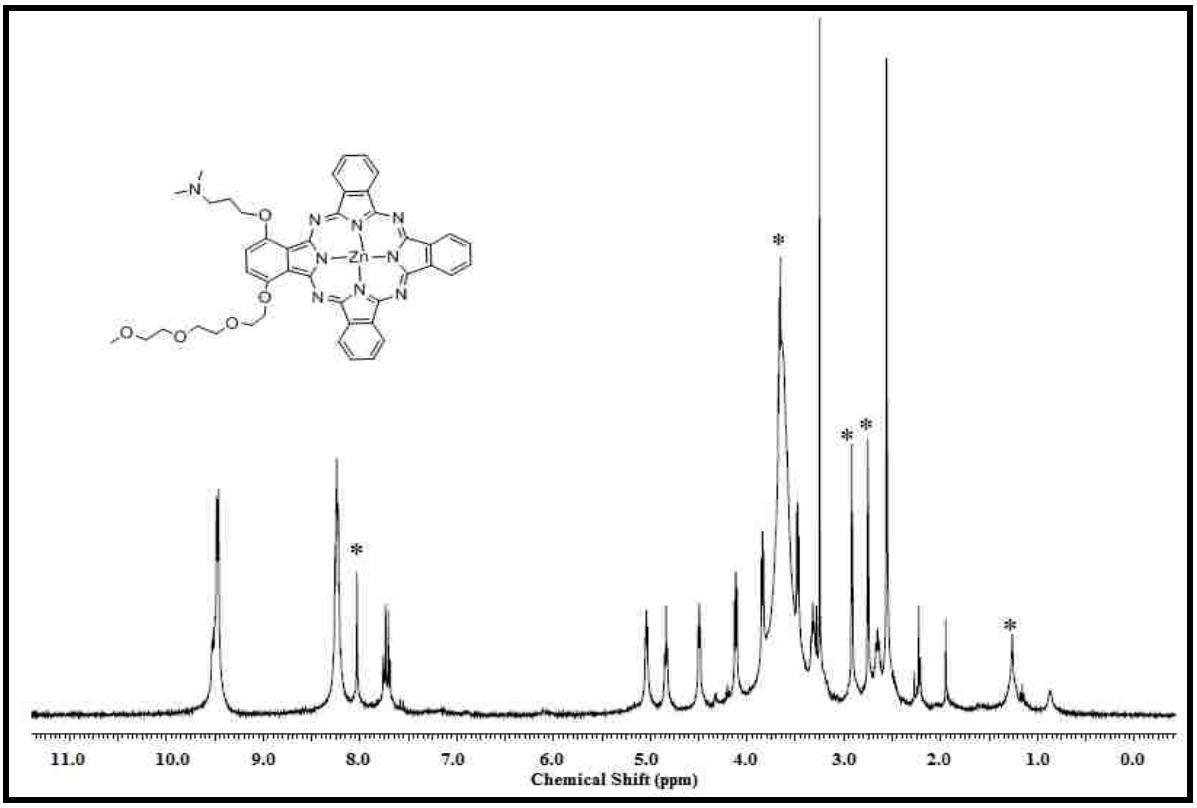

Figure 4.5 ^{1}H NMR spectrum of ZnPc **4.14** at 400 MHz (* denotes solvent).

The spectroscopic properties for Pcs **4.10**, **4.11**, **4.12**, **4.13** and **4.14** are summarized in Table 4.1. All Pcs showed strong Q-band absorption bands between 687 – 697 nm in DMF, except for ZnPc **4.12**, which absorbed at 718 nm. In Chapter 1, a reviewed of the UV-vis spectroscopic properties of ZnPcs with four substituents at the α-position revealed a bathochromic shift in their Q-bands of approximately 15 nm, and 20 nm in their Soret-bands compared with the mono-substituted Pcs was observed.[34] This may explain the 10 nm difference in the Q-bands of ZnPc **4.10** and **4.11**, since **4.10** has two more α-substituents compared with **4.11**. Removal of the protecting group from ZnPc **4.10** gives two hydroxyl (-OH) groups, which are strong donors and therefore, results in further red-shift of the Q-band of ZnPc **4.11** by about 20 nm. The effect of –OH group is also seen in ZnPc **4.13**, where the Q-band of the Pc is red-shifted by 4 nm, compared to ZnPc **4.14**.

Table 4.1. Spectral properties of ZnPcs **4.10**, **4.11**, **4.12**, **4.13** and **4.14** at room temperature. a: excitation at 640 nm; b: calculated using ZnPc (Φ_f = 0.17) as the standard in DMF.

Pc	Excitation[a] (nm)	Emission (nm)	Stokes' Shift	ϕ_F[b]
4.10	697	700	3	0.12
4.11	687	697	10	0.23
4.12	718	722	4	0.10
4.13	694	696	2	0.14
4.14	690	693	3	0.21

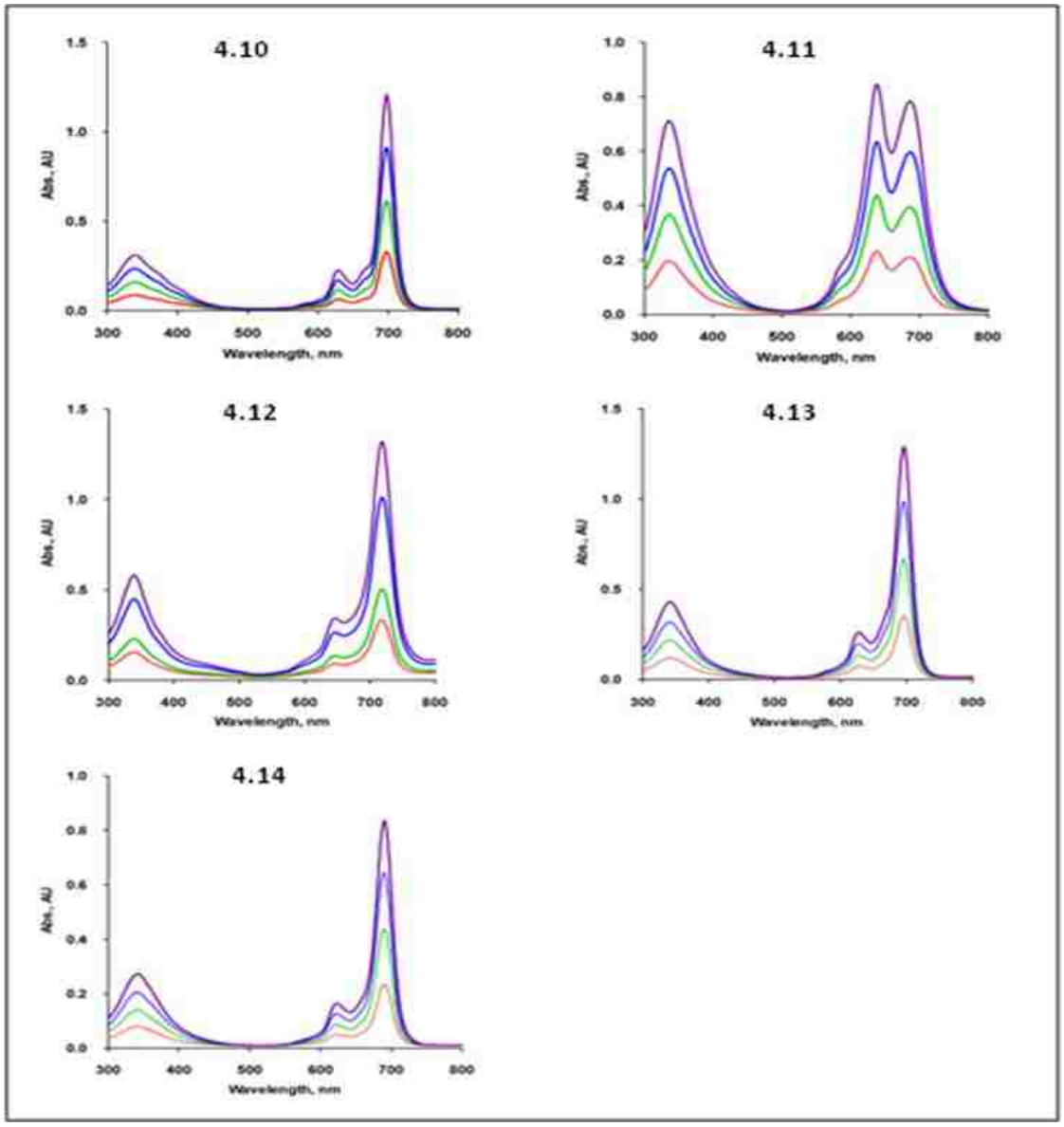

Figure 4.6 UV-Vis spectra for Pc **4.10**, **4.11**, **4.12**, **4.13** and **4.14** in DMF: 2.0 µM (red), 4.0 µM (green), 6.0 µM (blue) and 8.0 µM (purple).

All the Pcs exhibit UV-vis absorption spectra that are typical of monomeric species (Figure 4.6). The bis-phthalocyanine **4.11** shows substantial broadening of the Q-band centering at 687 nm and the Soret-band at 340 nm, which are characteristic of aggregation phenomena. The observation of both a blue shifted Q-band peak at 635 nm in addition to a red shifted 680–750 nm shoulder points to mixed dimer-types Pcs.[35] Since the shapes of the absorption spectra of ZnPc **4.11** remained unchanged by the concentration of the Pc, this is a sign of intramolecular assembly of the Pc molecules – probably an open clamshell type assembly of the molecules.

The emissions observed ranged between 693 – 722 nm in DMF solvent. The Stoke's Shifts were characteristics of ZnPcs, except for Pc **4.11**, which had a 10 nm shift. A similar shift was reported for bis-phthalocyanine by Yoshiyama *et al*. in chloroform solvent.[35] The fluorescence quantum yields observed for our ZnPcs were in the range 0.10 – 0.23, also characteristic of ZnPcs.[33,35,36]

The solubility of the ZnPcs **4.10**, **4.11**, **4.12**, **4.13** and **4.14** in polar organic solvents such as DMSO, DMF and THF was investigated and all were found to be soluble in these solvents. The Pcs were also fairly soluble in common organic solvents, such as DCM and ethyl acetate. None of the Pcs could dissolve in water, even upon sonication, except Pc **4.11**. However, all Pcs remained in aqueous solution when diluted from concentrated stocks in DMSO/cremophor EL into PBS (final DMSO concentration of 1%, cremophor 5%) at 10 µM concentrations. No aggregation of the Pcs was observed at up to 8.0 µM concentrations in DMF. At this concentration, all the ZnPcs show a Soret absorption band between 330 – 370 nm, a strong Q band centered at ~ 684 nm and two vibrational bands at around 620 and 650 nm that strictly follow the Lambert-Beer law. This is characteristic of non-aggregated Pcs in DMF (Figure 4.6).[37]

4.4. Summary

Photosensitizing drugs associated with different types of delivery vehicles have received interest within the field of PDT of tumors.[38] Pcs containing a PEG group on the macrocycle have been shown to increase the Pc tumor-cell targeting ability[32] They also express increased water solubility and cell permeability. A series of Pcs with either a short spacer or a low molecular weight PEG-linker have also been reported recently.[15] A low molecular PEG-linker was added to some of the Pcs to increase water solubility (by reducing the hydrophobicity originating from *tert*-butyl groups) and/or increase cellular uptake.[39]

In our synthesis, the starting material – phthalonitrile **4.8** – was synthesized according to the literature procedure.[15] The summary of the synthetic strategy is shown in Scheme 4.4. The di-pegylated, bis-phthalonitrile **4.9** was used in macrocyclization reaction, with a 30 molar equiv. excess of phthalonitrile to give di-PEG-Pc **4.10** and bis-phthalocyanine **4.11**, respectively. The PEG group(s) on the Pcs significantly increased their solubility in organic solvents, which made their purification and characterization relatively easy. The target mono- and di-pegylated macrocycles were mono-hydroxylated Pc **4.12** and di-hydroxylated **4.13** respectively, and were obtained via acidic cleavage of the protecting group, using concentrated sulfuric acid.[29,30] The ^{1}H NMR spectra of our Pcs were relatively simple in the aromatic region compared to those synthesized in Chapters 2 and 3, an indication of regiomerically pure macrocycles.

Synthesis of A_3B-type and A_2B_2-type Pcs often gave us statistical mixtures of isomers in our syntheses in Chapters 2, 3 and 5. By eliminating the *tert*-butyl groups from the macrocycle, pure regiomeric isomers of the Pcs were synthesized. Such pure regiomeric Pcs, may result in reproducible photosensitizers as opposed to Photofrin, an oligomer of up to eight porphyrin units, which is not easily reproducible.

4.5. Conclusions

Five regiomerically pure Pcs **4.10**, **4.11**, **4.12**, **4.13** and **4.14** were synthesized in this study. They might find application as potential florescence imaging agents for cancers, or for PDT applications. Due to the hydrophobic nature of the Pc macrocycle, pegylation of the macrocycles significantly improved the solubility of the Pcs, making their purification possible. The spectroscopic data for the bis-phthalocyanine was significantly different from the other Pcs. It had a Stoke's Shift of 10 nm, and it also had two strong Q-bands in the 600 – 700 nm region (characteristic of clamshell-type Pcs).

4.6. Experimental Section

General. All reagents and solvents were purchased from commercial suppliers and used directly without further purification. Analytical thin-layer chromatography (TLC) was carried out using plastic backed TLC plates 254 (precoated, 200 μm) from Sorbent Technologies. Silica gel 60 (230×400 mesh, Sorbent Technologies) was used for column chromatography. NMR spectra were recorded on Liquid AV-400 Bruker spectrometer (400 MHz for ^{1}H, 100 MHz for ^{13}C). The chemical shifts are reported in δ ppm using the following deuterated solvents as internal references: CD_3COCD_3 2.04 ppm (^{1}H), 29.92 ppm (^{13}C); DMF-d_7 8.03 ppm (^{1}H), 163.15 ppm (^{13}C). MALDI-TOF mass spectra were recorded on a Bruker UltrafleXtreme (MALDI-TOF/TOF) using 4-chloro-α-cyanocinnamic acid (CCA) as the matrix while high resolution ESI mass spectra were obtained on an Agilent Technologies 6210 Time-of-Flight LC/MS. Absorption spectra were measured on a UV-Vis NIR scanning spectrophotometer using 10 mm path length quartz cuvettes. Stock solutions (1.0 mM, 1.0 mL each) of each Pc in DMF solvent (HPLC grade) were prepared and dilutions achieved by spiking 20 – 80 μL of each stock solution into DMF to give a 10 mL final volume. Emission spectra were obtained on a

Fluorolog® - HORIBA JOBINVYON, Model LFI-3751 spectrofluorimeter. The optical densities of the solutions used for emission studies ranged between 0.04 – 0.05 at excitation wavelengths. All measurements were taken within 4 h of solution preparation and carried out at (25 °C).

4.6.1. Synthesis of Phthalonitriles

3,3'-((1,2-phenylenebis(methylene))bis(oxy))diphthalonitrile 4.4. A mixture of 3-nitrophthalonitrile (0.9 g, 5.2 mmol) and **1,2-benzenedimethanol** (360.6 mg, 2.61 mmol) was dissolved in DMF (10 mL) and heated to 65 °C. Potassium carbonate, K_2CO_3 (2.07 g, 0.015 mol) were added into solution in four portions after every five minutes. The reaction mixture was stirred for 24 h under argon at the same temperature. It was left to cool to room temperature and poured into ice-cold water (200 mL). This was then filtered, washed with water, dried to obtain (0.722 g, 71.2%. The product was used without purification due to solubility issues. ^{1}H NMR (DMF-d_7, 400 MHz): δ 7.96-7.88 (m, 4H, Ar-H), 7.75-7.72 (m, 4H, Ar-H), 7.54-7.52 (m, 2H, Ar-H), 5.71 (s, 4H, CH_2).

3,3'-((cyclohex-3-ene-1,1-diylbis(methylene))bis(oxy))-diphthalonitrile 4.6. A mixture of 3-nitrophthalonitrile (0.935 g, 5.4 mmol) and 3-cyclohexene-1,1-dimethanol (371.2 mg, 2.61 mmol) was dissolved in DMF (7.0 mL) and heated to 65 °C. Potassium carbonate, K_2CO_3 (2.07 g, 0.015 mol) were added into solution in four portions after every five minutes. The reaction mixture was stirred for 24 h under argon at the same temperature. It was then left to cool to room temperature and poured into ice-cold water (200 mL). This was then filtered and washed with water. The crude was characterized by MS (MALDI-TOF) *m/z* 395.1494 $[M+H]^+$, calcd for, $C_{24}H_{18}N_4O_2$, 395.1508. The tedious purification of the crude product using a silica column eluted with DCM/methanol (99:1 → 98:2) gave the first fraction as white solid on concentration. Recrystallization from acetone and slow evaporation gives yellow crystals of mono-substituted

adduct **4.7**. Mp = 120 - 121°C. Trying to form di-substituted product gave the bis-phthalonitrile ether **4.3** formed earlier.

4.6.2. Synthesis of Pcs

Side-strapped Pc **4.5.** A mixture of phthalonitrile **4.4** (42.5 mg, 0.1 mmol) and zinc acetate (11.0 mg, 0.06 mmol) were mixed together in DMAE (5.0 mL). The solution was refluxed under the flow of argon, and two drops of DBN were added into the reaction solution. The reaction solution was further refluxed at 130 °C for 5 hours. After the reaction, the solvent was removed under vacuum. The residue was purified by tedious column chromatography with the elution of DCM/methanol (98:2) to give a green solid 0.93 mg, 2.2 %. The product was characterized by MS (MALDI-TOF) *m/z* peak at 844.177 $(M)^+$, calcd for $C_{48}H_{28}N_8O_4Zn$ 844.153.

Di-pegylated bis-phthalonitrile 4.9. A mixture of phthalonitrile **4.8**[15] (1.592 g, 5.2 mmol) and 1,2-bis(bromomethyl)benzene (688.9 mg, 2.61 mmol) was dissolved in DMF (10 mL) and heated to 67 °C. Potassium carbonate, K_2CO_3 (2.07 g, 0.015 mol) were added into solution in four portions after every five minutes. The reaction mixture was stirred for 4 h under argon at the same temperature. It was then left to cool to room temperature, poured into ice-cold water (100 mL) and filtered. The crude product was purified using alumina column eluted with DCM/methanol (95:5) to give a light-yellow solid on concentration (1.572 g, 84.3%). ^{1}H NMR (Acetone-d_6, 400 MHz): δ 7.71-7.61 (m, 6H, Ar-H), 7.48-7.45 (m, 2H, Ar-H), 5.57 (s, 4H, OCH_2), 4.35 (t, J = 4.52, 4H, OCH_2), 3.87 (t, J = 4.64, 4H, OCH_2), 3.70-3.66 (m, 4H, OCH_2), 3.60-3.55 (m, 10H, OCH_2), 3.45 (t, 4H, OCH_2), 3.27 (s, 6H, OCH_3). ^{13}C NMR (Acetone-d_6, 100 MHz): δ 156.6, 155.7, 135.1, 130.1, 129.9, 121.3, 121.0, 114.3, 114.1, 105.34, 105.28 (Ar-H), 72.7, 71.7, 71.3, 71.1, 71.0, 70.7, 70.2 (OCH_2), 58.9 (OCH_3). MS (MALDI-TOF) *m/z* 715.2981

$[M+H]^+$, 737.2794 $[M+Na]^+$, 753.2525 $[M+K]^+$, calcd for, $C_{38}H_{43}N_4O_{10}$, 715.2974, $C_{38}H_{43}N_4KO_{10}$, 737.2533.

Di-pegylated ZnPc 4.10. A mixture of phthalonitrile **4.9** (172.0 mg, 0.24 mmol), phthalonitrile (845.6 mg, 6.60 mmol), and zinc acetate (220.0 mg, 1.20 mmol) were mixed together in DMAE (13.0 mL). The solution was heated at 140 °C under the flow of argon, and one drop of DBN was added to the reaction solution. The reaction solution was further refluxed at 140 °C for 5 hours. After the reaction, the solvent was removed under vacuum. The residue was dissolved in acetone and filtered under gravity to give a green viscous residue on concentration. A silica column eluted by DCM/methanol (95:5) gave the Pcs as a green fraction. A second silica column eluted by DCM/methanol (95:5) gave fraction green fraction. A third silica column eluted by DCM/THF (3:1) gave **Pc 4.10** as a green solid 12.7 mg, 5.1%. ^{1}H NMR (DMF-d_7, 400 MHz): δ 9.28-9.17 (m, 4H, Ar-H), 8.19-8.11 (m, 4H, Ar-H), 8.02-7.95 (m, 2H, Ar-H), 7.82-7.80 (m, 2H, Ar-H), 7.71-7.63 (m, 4H, Ar-H), 6.42 (s, 4H, OCH_2), 4.95-4.48 (m, 4H, OCH_2), 4.46 (t, J = 3.92, 4H, OCH_2), 4.10 (t, J = 4.64, 4H, OCH_2), 3.83 (t, J = 3.88, 4H, OCH_2), 3.65 (m, J = 4.64, 4H, OCH_2), 3.54-3.42 (m, 4H, OCH_2), 3.24 (s, 6H, OCH_3). ^{13}C NMR (DMF-d_7, 100 MHz): δ 155.1, 154.6, 154.3, 154.1, 153.8, 152.6, 150.9, 140.0, 139.5, 135.4, 134.7, 133.6, 133.0, 132.9, 130.4, 130.3, 130.0, 129.8, 129.1, 128.2, 126.2, 124.1, 124.0, 123.8, 123.5, 123.4, 122.7, 121.5, 116.7 (Ar-C), 76.6, 72.8, 72.0 71.63, 71.57, 71.3, 71.2, 70.7, 70.4, 70.2 (OCH_2), 59.0 (OCH_3). MS (MALDI-TOF) *m/z* 1034.302 $[M]^+$ calcd for, $C_{54}H_{50}N_8O_{10}Zn$, 1034.294. UV-vis (DMF): λ_{max} (log ε) 340 (4.57), 629 (4.43), 697 (5.16) nm.

Deptrotected **di-pegylated ZnPc 4.12.** A mixture of **Pc 4.10** (22.5 mg, 21.7 mmol) was dissolved in H_2SO_4 (5.0 mL) at 0°C. The reaction mixture was stirred for 15 minutes at 0°C and then poured into ice (50.0 mg), in a separatory funnel containing DCM/methanol (9:1, 50.0 mL).

To the mixture, 2N $NaHCO_3$ (90.0 mL) was added and the product extracted from the organic layer using DCM/methanol (9:1, 50.0 mL × 3) and washed with water (5 mL × 2). Organics were removed under reduced pressure and the residue purified by column chromatography using mixed solvents, DCM/methanol (98:2→ 95:5 → 9:1) to give deprotected di-pegylated bis-phthalocyanine **4.12** as a green solid (19.2 mg, 95.0 %). ^{1}H NMR (DMF-d_7, 400 MHz): δ 9.29 (s, 4H, Ar-H), 8.17 (m, 4H, Ar-H), 7.75-7.51 (m, 4H, Ar-H), 5.06 (br, 4H, OCH_2), 4.53-36 (br, 4H, OCH_2), 4.09 (t, J = 4.72, 4H, OCH_2), 3.66 (t, J = 4.52, 4H, OCH_2), 3.51-3.43 (m, 4H, OCH_2), 3.26 (s, 6H, OCH_3). ^{13}C NMR (DMF-d_7, 100 MHz): δ 155.0, 154.2, 153.7, 151.5, 150.6, 149.8, 139.7, 139.4, 136.3, 130.0, 129.9, 124.0, 123.6, 123.2, 122.8, 119.8, 118.2 (Ar-C), 72.9, 72.8, 72.0 71.6, 71.33, 71.29, 70.7, (OCH_2), 59.1, 59.0 (OCH_3). MS (MALDI-TOF) *m/z* peak at 932.294 $(M)^+$, calcd for $C_{46}H_{44}N_8O_{10}Zn$ 932.247. UV-vis (DMF): λ_{max} (log ε) 341 (4.86), 648 (4.63), 718 (5.23) nm.

Di-pegylated bis-phthalocyanine 4.11. This Pc was isolated during the first column using DCM/methanol (95:5) as a greenish solid (28.2 mg, 7.2%). ^{1}H NMR (DMF-d_7): δ 9.11-9.02 (m, 7H, Ar-H), 8.53-8.41 (m, 7H, Ar-H), 8.30-8.23 (m, 4H, Ar-H), 8.17-8.08 (m, 4H, Ar-H), 7.93-7.90 (m, 2H, Ar-H), 7.82-7.77 (m, 4H, Ar-H), 7.46-7.44 (m, 2H, Ar-H), 7.01 (s, 4H, OCH_2), 6.87-6.84 (m, 2H, Ar-H), 4.65-4.55 (m, 8H, OCH_2), 4.13-4.11 (m, 4H, OCH_2), 3.89-3.86 (m, 4H, OCH_2), 3.73-3.70 (m, 4H, OCH_2), 3.55-3.52 (m, 4H, OCH_2), 3.30 (s, 6H, OCH_3). ^{13}C NMR (DMF-d_7, 100 MHz): δ 154.1, 153.5, 152.9, 152.4, 152.3, 151.8, 151.1, 150.6, 150.4, 140.4, 139.6, 139.4, 139.2, 139.0, 137.8, 130.2, 130.0, 129.2, 129.1, 129.4, 129.0, 128.2, 126.7, 126.3, 123.6, 123.34, 123.26, 123.0, 122.7, 119.2, 118.7, 117.4, 114.4 (Ar-C), 73.5, 72.9, 72.1, 72.0, 71.7, 71.6, 71.5, 71.4, 69.5 (OCH_2), 59.1 (OCH_3). MS (MALDI-TOF) *m/z* peak at

1614.396 $(M)^+$, calcd for $C_{86}H_{66}N_{16}O_{10}Zn_2$ 1614.3717. UV-vis (DMF): λ_{max} (log ε) 336 (4.93), 638 (5.01), 687 (4.98) nm.

A mixture of ZcPc **4.11** (22.5 mg, 13.9 mmol) was dissolved in H_2SO_4 (5.0 mL) at 0°C. The reaction mixture was stirred for 30 minutes at 0°C and then poured into ice (50.0 mg), in a separating funnel containing DCM/methanol (9:1, 50.0 mL). To the mixture, ~ 2N $NaHCO_3$ (90.0 mL) added to attain a neutral pH. The product was extracted from the organic layer using DCM/methanol (9:1, 50.0 mL × 3) and washed with water (5 mL × 2). Organics were removed under reduced pressure and the residue purified using silica column chromatography with eluting solvent system of DCM/ethyl acetate (1:2) to give a greenish solid (10.1 mg, 41.0 %). ^{1}H NMR (DMF-d_7): δ 9.32 - 9.02 (m, 6H, Ar-H), 8.29-8.12 (m, 6H, Ar-H), 7.82-7.42 (m, 2H, Ar-H), 6.99 (br, 1H, OH), 5.11-4.97 (m, 2H, OCH_2), 4.45-4.42 (m, 2H, OCH_2), 4.12 (t, J = 4.76, 2H, OCH_2), 3.68 (t, J = 3.52, 2H, OCH_2), 3.48 (t, J = 4.68, 2H, OCH_2), 3.30-3.27 (s, 3H, OCH_3). ^{13}C NMR (DMF-d_7, 100 MHz): δ 154.4, 153.9, 152.9, 150.7, 139.3, 138.0, 130.3, 130.2, 129.4, 126.7, 123.8, 123.5, 123.4, 123.2, 123.0, 119.7, 117.7 (Ar-C), 72.9, 72.1, 71.7, 71.4 (OCH_2), 59.1 (OCH_3). MS (MALDI-TOF) *m/z* peak at **755.225** $(M+H)^+$, calcd for **$C_{39}H_{31}N_8O_5Zn$ 755.1709**. UV-vis (DMF): λ_{max} (log ε) 342 (4.71), 628 (4.49), 694 (5.19) nm.

3-(Dimethylamino)propyl substituted ZnPc 4.14. A procedure reported in literature was used, with little modification, to furnish the desired product.[40,41] A mixture of Pc **4.13** (18.1 mg, 0.024 mmol) and 3-(Dimethylamino)propyl chloride hydrochloride (4.7 mg, 0.030 mmol) were mixed together in DMF (5.0 mL), the solution heated at 65 °C under argon, and K_2CO_3 (50.0 mg, 3.6 mmol) added to the reaction solution. The reaction solution was heated at the same temperature for 6h. The solvent was removed under reduced pressure and the residue dissolved in DCM/methanol (9:1, 5.0 mL). The mixture was diluted using ethyl acetate, washed with water

(20 mL) and dried to obtain a blue solid. The solid was purified by silica column chromatography using DCM/methanol (9:1) to give a blue-green solid (10.0 mg, 49.8 %). ^{1}H NMR (DMF-d_7): δ 9.52-9.45 (m, 6H, Ar-H), 8.27-8.19 (m, 6H, Ar-H), 7.71 (dd, J = 8.54, 2H, OCH_2), 5.03 (t, J = 5.16, 2H, OCH_2), 4.82 (t, J = 5.80, 2H, OCH_2), 4.49 (t, J = 4.68, 2H, OCH_2), 4.11 (t, J = 4.76, 2H, OCH_2), 3.84 (t, J = 5.08, 2H, OCH_2), 3.67-3.65 (m, 2H, OCH_2), 3.47 (t, J = 4.96, 2H, OCH_2), 3.34-3.28 (m, 2H, OCH_2), 3.25 (s, 3H, OCH_3), 2.66-2.60 (m, 2H, OCH_2), 2.53 (s, 6H, $N(CH_3)_2$). ^{13}C NMR (DMF-d_7): δ 154.9, 154.8, 154.7, 154.5, 154.2, 152.3, 151.6, 140.3, 140.0, 130.1, 130.0, 129.3, 128.7, 123.8, 123.4, 123.4, 123.3, 117.9, 116.2 (Ar-C), 72.8, 72.0, 71.6, 71.3, 68.9 (OCH_2), 59.0 (OCH_3), 57.8 (N-CH_2), 45.9 ($N(CH_3)_2$), 28.9 (CH_2). MS (MALDI-TOF) *m/z* peak at **840.341** $(M+H)^+$, calcd for **$C_{44}H_{42}N_9O_5Zn$ 840.2600**. UV-vis (DMF): λ_{max} (log ε) 341 (4.51), 624 (4.28), 690 (5.00) nm.

2.6.3. Phthalonitrile Molecular Structures

Crystal structure analyses of phthalonitriles **4.3** and **4.7** were based on data collected at T=90K on a Bruker Kappa Apex-II CCD diffractometer with a Cu*K*α radiation (compound **4.3**) and a Bruker Kappa Apex-II DUO diffractometer with a Mo*K*α radiation (compounds **4.7**). The crystals were obtained by slow evaporation of mixed solvents DCM/acetone 5:1. The crystal structure analyses of these phthalonitriles confirm the formation of the side product or intermediate. Crystal data: **4.3**, $C_{16}H_6N_4O$, M_r = 270.25, triclinic space group P-1, a = 7.9348 (10) Å, b = 12.0783 (14) Å, c = 13.8674 (17) Å, α = 74.402 (7)°, β = 88.148 (8)°, γ = 78.258 (8)°, V = 1252.9 (3) Å^3, Z = 4, D_x = 1.433 Mg m^{-3} , θ_{max} = 67.9°, R = 0.081 for 4363 data and 380 refined parameters; **4.7**, $C_{16}H_{16}N_2O_2$, M_r = 268.31, triclinic space group P-1, a = 6.7586 (4) Å, b = 8.0397 (4) Å, c = 12.7269 (7) Å, V = 684.71 (6) Å^3, Z = 2, D_x = 1.301 Mg m^{-3} , θ_{max} = 30.6°, R = 0.044 for 4161 data and 184 refined parameters.

4.7. Spectroscopic Studies

All absorption spectra were measured on UV-VIS NIR Scanning Spectrometer UV-3101PC SHIMADZU (Cell positioned) equipped with a CPS-260 lamp. Stock solutions (1000 µM, 1.0 mL) of all Pcs were prepared in DMF (HPLC grade) and the dilutions achieved by spiking 20 – 80 µL of the corresponding stock solution into DMF to a 10.0 mL final volume. Emission spectra were recorded on a Fluorolog®-HORIBA JOBINVYON (Model LFI-3751) spectrofluorimeter. The optical densities of the solutions used for emission studies were kept between 0.04 – 0.05 (AU) at the excitation wavelengths for all the ZnPcs. All the measurements were recorded within 3 h of preparation at 25 °C, using a 10 mm path length spectrophotometric cell. The fluorescence quantum yields (Φ_f) were determined using a secondary standard method.[42] Unsubstituted ZnPc (Φ_f = 0.17) was used as a reference and the values of fluorescence determined in DMF solvent.[43]

4.8. References

1. Ben-Hur, E.; Chan, W-S. In *The Porphyrin Handbook*, Kadish, K. M.; Smith, K. M.; Guilard, R. (Eds.), *Academic Press: Boston* **2003**, *19*, 1-35.
2. Leznoff, C. C.; Lever, A. B. P. Eds. In Phthalocyanines: Properties and Applications. *VCH: Weinheim*. **1989-1996**; 1-4.
3. Jori, G.; Coppellotti, O. *Anti-Infective Agents in Medicinal Chemistry* **2007**, *6*, *2*, 119-131.
4. Huang, Z. *Tech. Cancer Res. Treatment* **2005**, 4, 283-293.
5. Brown, S. B.; Brown, E. A.; Walker, I. *Lancet. Oncol*. **2004**, *5*, 497-508.
6. Pandey, R. K. *J. Porph. Phthal*. **2000**, *4*, 368-373.
7. Dougherty, T. J.; Gomer, C. J.; Henderson, B. W.; Jori, G.; Kessel, D.; Korbelik, M.; Moan, J.; Peng, Q. *J. Natl. Cancer Inst.* **1998**, *90*, 889-905.
8. Kinsella, T. J.; Baron, E. D.; Colussi, V. C.; Cooper K. D.; Hoppel, C. L.; Ingalls, S. T.; Kenney, M. E.; Li, X.; Oleinick, N. L. Stevens, S. R.; Remick, S. C. *Front. Oncol.* **2011**, *1*, *14*, 1-6.
9. Sokolov, V. V.; Chissov, V. I.; Yakubovskya, R. I.; Aristarkhova, E. I.; Filonenko, E, V.; Belous, T. A.; Vorozhtsov, G. N.; Zharkova, N. N.; Smirnov, V. V.; Zhitkova, M. B.

Proceedings of SPIE (Photochemistry: Photodynamic Therapy and Other Modalities) **1996**, *2625*, 281-287.

10. Baron, E. D.; Malbasa, C. L.; Santo-Domingo, D.; Fu, P.; Miller, J. D.; Hanneman, K. K.; Hsia, A, H.; Oleinick, N. L.; Colussi, V. C.; Cooper, K. D. *Lasers Surg. Med.* **2010**, 42, *10*, 728–735.

11. Arnida; Nishiyama, N.; Kanayama, N.; Jang, W-D.; Yamasaki, Y.; Kataoka, K. *J. Controlled Release* **2006**, *115*, *2*, 208-215.

12. Gijsens, A.; Derycke, A.; Missiaen, L.; de Vos, D.; Huwyler, J.; Eberle, A.; de Witte, P. *Int. J. Cancer* **2002**, *101*, 78-85.

13. Suzuki, T.; Oishi, M.; Nagasaki, Y. *J. Photopoyml. Sci. and Technol.* **2009**, *22* (4), 547-550.

14. Bai, M.; Lo, P-C.; Ye, J.; Wu, C.; Fong, W-P.; Ng Dennis, K. P. *Org. & Biomol. Chem.* 2011, *9* (20), 7028-7032.

15. Li, H.; Fronczek, F. R.; Vicente, M. G. H. *Tetra. Lett.* **2011**, *52*, 6675-6678.

16. Durmus, M.; Ayhan, M. M.; Gürek, A. G.; Ahsen, V. *Dyes and Pigments* **2008**, *77*, 570-577.

17. Fang, J.; Sawa, T.; Akaike, T.; Greish, K.; Maeda, H. *Int. J. Cancer.* **2004**, *109*, 1-8.

18. Ichikawa, K.; Hikita, T.; Maeda, N.; Takeuchi, Y.; Namba, Y.; Oku, N. *Biol. Pharm. Bull.* **2004**, *27*, 443-444.

19. Krueger, T.; Altermatt, H. J.; Mettler, D.; Scholl, B.; Magnusson, L.; Ris, H. B. *Lasers Surg. Med*. **2003**, *32*, 61-68.

20. Rovers, J. P.; Saarnak, A. E.; de Jode, M.; Sterenborg, H. J.; Terpstra, O. T.; Grahn, M. F. *Photochem. Photobiol.* **2000**, *71*, 211-217.

21. Sharmam, W. M.; Van Lier, J. E. *The Porphyrin Handbook (Kadish, K. M.; Smith, K. M.; Guilard, R., Eds.), Academic Press: Boston*, **2003**, *15*, 1-60.

22. Leznoff, C. C. *Can. J. Chem.* **2000**, *78*, 167-183.

23. Hall, T. W.; Greenberg, S.; McArthur, C. R.; Khouw, B.; Leznoff, C. C. *J. Chem.* **1982**, *6*, 653-658.

24. Leznoff, C. C.; Hall, T. W. *Tetra. Lett.* **1982**, *23*, 3023-3026.

25. Li, H.; Fronczek, F. R.; Vicente, M. G. H. *J. Organomet. Chem.* **2009**, *694* (11), 1607-1611.

26. Oliver, S. W.; Smith, T. D. *J.Chem. Soc., Perkin Trans. II* **1987**, (11), 1579-1582.

27. Leznoff, C. C.; Drew, D. M. *Can J. Chem.* **1996**, *74*, 307-318.

28. Kobayashi, N.; Kobayashi, Y; Osa, T. *J. Am. Chem. Soc.* **1993**, *115*, 10994-10995.

29. Tolbin, A. Y.; Ivanov, A. V.; Tomilova, L. G.; Sefirov, N. S. *Mendeleev Commun.* **2002**, *3*, 96-97.

30. Tolbin, A. Y.; Pushkarev, V. E.; Nikitin, G. F.; Tomilova, L. G. *Tetra. Lett.* **2009**, 50, 4848-4850.

31. Okano, K.; Okuyama, K.-I.; Fukuyama, T.; Tokuyama, H. *Synlett*. **2008**, 1977-1980.

32. Sibrian-Vazquez, M.; Ortiz, J.; Nesterova, I. V.; Fernández-Lázaro, F.; Sastre-Santos, A.; Soper, S. A.; Vicente, M. G. H. *Bioconj. Chem.* **2007**; *18*: 410-420.

33. Ongarora BG, Hu X, Li H, Fronczek FR, Vicente MGH. *Med. Chem. Commun.* **2012**, *3*, 179-194.

34. Li, Y.; Pritchett, T. M.; Huang, J.; Ke, M.; Shao, P.; Sun, W. *J. Phys. Chem. A.* **2008**, *112* (31), 7200-7207.

35. Yoshiyama, H.; Shibata, N.; Sato, T.; Nakamura, S.; Toru, T. *Organic & Biomolecular Chemistry* **2008**, *6* (24), 4498-4501.

36. Ongarora, B. G.; Fontenot, K. R.; Hu, X.; Sehgal, I.; Satyanarayana-Jois, S. D.; Vicente, M. G. H. *J. Med. Chem.* **2012**, *55*, 3725-3738.

37. Hofman, J.-W.; van Zeeland, F.; Turker, S.; Talsma, H.; Lambrechts, S. A. G.; Sakharov, D. V.; Hennink, W. E.; van Nostrum, C. F. *J. Med. Chem*. **2007**, *50*, 1485-1494.

38. Reddi, E. *J. Photochem. and Photobiol. B: Bio.* **1997**, *37*, *3*, 189-195.

39. Ongarora, B. G.; Hu, X.; Verberne-Sutton, D.; Garno, J. C.; Vicente, M. G. *J. Theranostics* **2012**, *2* (9), 850-870.

40. Chandrika, P. M.; Yakaiah, T. Gayatri, G.; Kumar, K. P.; Narsaiah, B.; Murthy, U. S. N.; Rao, A. R. R. *Eur. J.Med. Chem.* **2010**, *45*, 78–84.

41. Merkas, S.; Litvic, M.; Cepanec, I.; Vinkovic, V. *Molecules* **2005**, *10*, 1429-1437

42. Brykina, G. D.; Uvarova, M. I.; Koval, Y. N.; Shpigun, O. A. *J. Anal. Chem.* **2001**, *56*, 940-944.

43. Zorlu, Y.; Dumoulin, F.; Durmus, M.; Ahsen, V. *Tetra.* **2010**, *66*, 3248-3258.

CHAPTER 5

SYNTHESES AND BIOLOGICAL EVALUATION OF PEGYLATED AND CATIONIC ZINC(II)-PHTHALOCYANINES AND MONOCLONAL ANTI-CARCINOEMBRYONIC ANTIGEN CONJUGATES FOR IMAGING AND TREATMENT OF CANCER*

5.1. Background

Pcs are promising second-generation photosensitizers with intense absorptions at wavelengths (λ_{max}) > 670 nm. They also have capacity to penetrate cellular membranes and can produce ROS upon light activation. Some Pcs, such as Photosense, and a Si(IV)Pc, Pc4, have been evaluated in clinical trials for PDT.[1-3] These Pcs and other potential Pc-based photosensitizers have tangential water-solubilizing substituents and/or axial ligands that can minimize their aggregation or increase solubility the Pcs in aqueous media. The enhancing of these features results in improved photodynamic activity of the photosensitizers. Polyethylene glycol (PEG) groups have been investigated either as delivery vehicles,[4-6] or as covalently attached substituents[7-9] for enhanced delivery to target tissues. Their covalent attachment to photosensitizers is known to enhance water-solubility, serum life and tumor accumulation of photosensitizers, but reduces their uptake by the reticuloendothelial system.[10-15]

Cationic photosensitizers are attractive for PDT applications[16-23] and the photoinactivation of virus and bacteria,[24-26] due to their stronger interaction with the negatively charged cell membranes. They also target biomolecules (e.g. DNA and RNA) within the cell nucleus, which may result in effective photodamage and overall enhanced photodynamic efficacy. In Chapter 2, di-cationic α-substituted ZnPcs were synthesized and found to be the most phototoxic within a series of Pcs containing positively-charged trimethylaminophenoxy groups,

---

* Part of this chapter was published in *Journal of Theranostics*: Ongarora, B. G.; Hu, X.; Verberne-Sutton, D.; Garno, J. C.; Vicente, M. G. *J. Theranostics* **2012**, *2* (9), 850-870.[27] Reprinted with permission from IVY Spring.

in addition to being the most promising photosensitizers for PDT. In this Chapter, the syntheses of a new series of di-cationic Pcs containing a PEG group or a diglycolic spacer between the ZnPc and the positively charged quaternary ammonium groups is described. The synthesis of pegylated ZnPcs, which were conjugated with monoclonal antiCEA for application in the diagnosis of cancer is also described.

5.2. Results and Discussion

5.2.1. Syntheses of Cationic ZnPcs

The synthetic strategy to di-cationic ZnPcs **5.4**, **5.6**, **5.9**, **5.11**, **5.15**, **5.17**, **5.20**, **5.22**, **5.27** and **5.32** is shown in Schemes 5.1 – 5.4, starting from 3- or 4-nitrophthalonitrile (**5.23** and **5.28**). The ZnPcs **5.1**, **5.2**, **5.12** and **5.13** were prepared according to procedures prescribed in Chapters 2 and 3. The nitrophthalonitriles reacted with *p*-*N*-Boc-aminophenol in DMF at 80 ºC under basic conditions to give the corresponding *p*-(*N*-Boc-aminophenoxy)phthalonitriles. The phthalonitrile was then heated at 140 ºC in DMAE and in the presence of zinc(II) acetate, 3 equiv. 4-*tert*-butylphthalonitrile and a catalytic amount of DBN, giving the Boc-protected α- or β-substituted A_3B-type ZnPcs in 15-20% yields. Deprotection of the Boc groups was achieved using TFA. Reaction with diglycolic anhydride gave the α- and β- substituted ZnPcs **5.1** and **5.12** respectively, which were conjugated with commercially available *tert*-butyl-12-amino-4,7,10-trioxadodecanoate, using HOBt, EDCI and TEA in DMF to produce pegylated ZnPcs **5.2** and **5.13** upon deprotection usning TFA.[28] Reaction of ZnPcs **5.1** and **5.2** with 1,4-bis(*N*-Boc)-triazaheptane using similar coupling reagents, followed by acidic Boc-deprotection gave ZnPcs **5.5** and **5.3**, respectively, in 69-73% yields. Trimethylation of the amino groups was achieved using excess methyl iodide and DIPA in DMF as described in Chapter 2, giving the respective di-cationic ZnPcs **5.6** and **5.4** in 53-68% yields. Reaction of **5.1** with di-*tert*-butyl ester protected

L-aspartic acid in DMF gave ZnPc **5.7**, followed by deprotection with TFA.[29] In this reaction, TEA was used as a base, while HATU and HOBt served as coupling reagents.

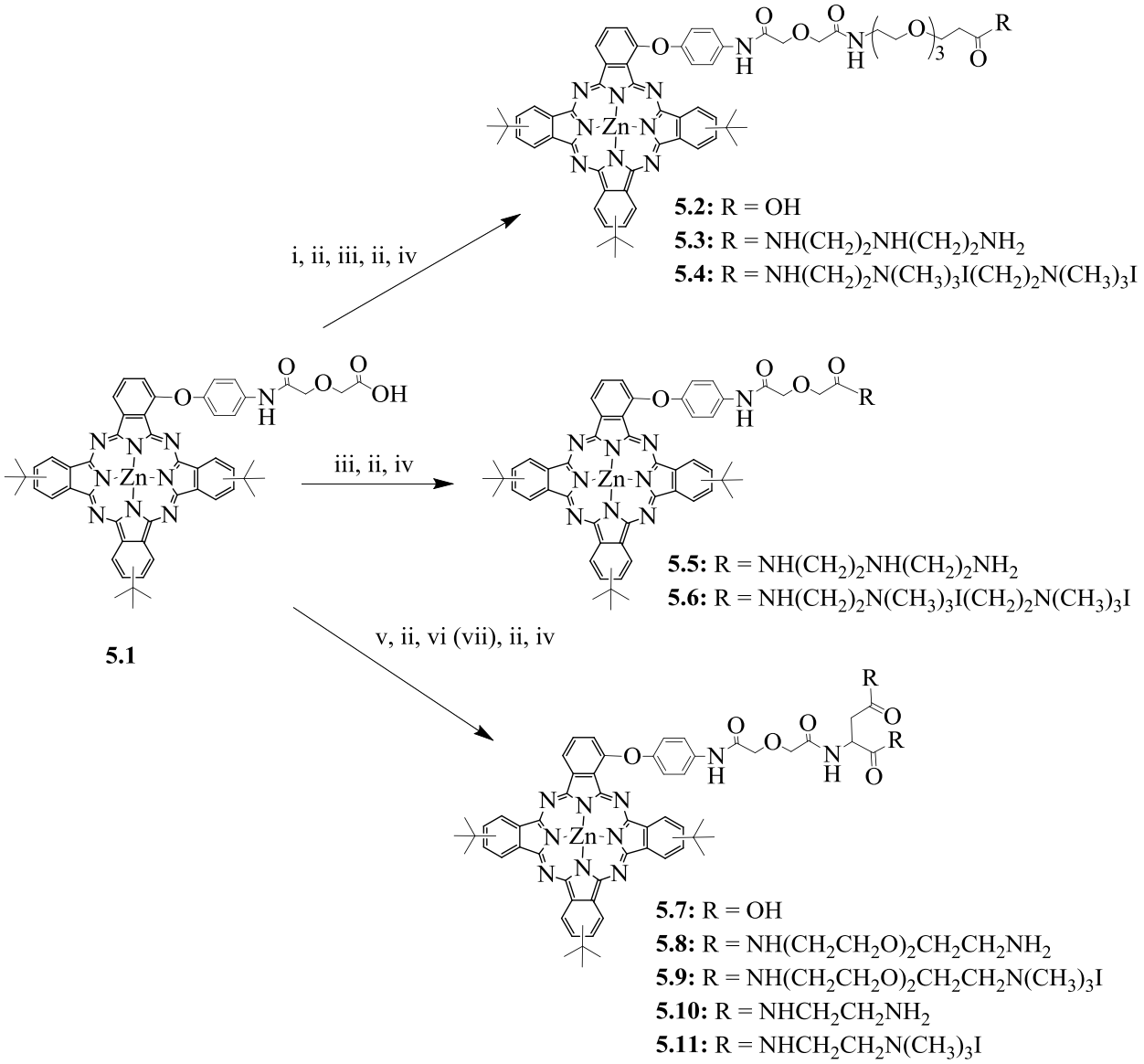

Scheme 5.1. Synthesis of dicationic α-substituted ZnPcs **5.4**, **5.6**, **5.9** and **5.11**. Reaction conditions: (i) *tert*-butyl-12-amino-4,7,10-trioxadodecanoate, TEA, HOBt, EDCI, DMF (82%); (ii) TFA, DCM. 0 ^{o}C, 3 h (89%); (iii) 1,4-bis(*N*-Boc)-triazaheptane, TEA, HOBt, EDCI, DMF (77%); (iv) CH_3I, DIPA, DMF (59-68%); (v) L-aspartic acid di(*tert*-butyl) ester, TEA, HATU, DMF (89%); (vi) *N*-Boc-2,2′-(ethylenedioxy)diethylamine, TEA, HOBt, EDCI, DMF (52%); (vii) *N*-Boc-ethylenediamine, TEA, HOBt, EDCI, DMF (58%).

The dicarboxylate terminated ZnPc **5.7** was coupled to *N*-Boc-2,2′-(ethylenedioxy)diethylamine or *N*-Boc-ethylenediamine using TEA, HOBt and EDCI following

a similar protocol as that described for ZnPc **5.3** above, giving ZnPcs **5.8** and **5.10** respectively after deprotection. The ZnPcs **5.8** and **5.10** were quaternized following the procedure described above, to afford di-cationic ZnPcs **5.9** and **5.11** in 68 and 59% yields, respectively (Scheme 5.1).

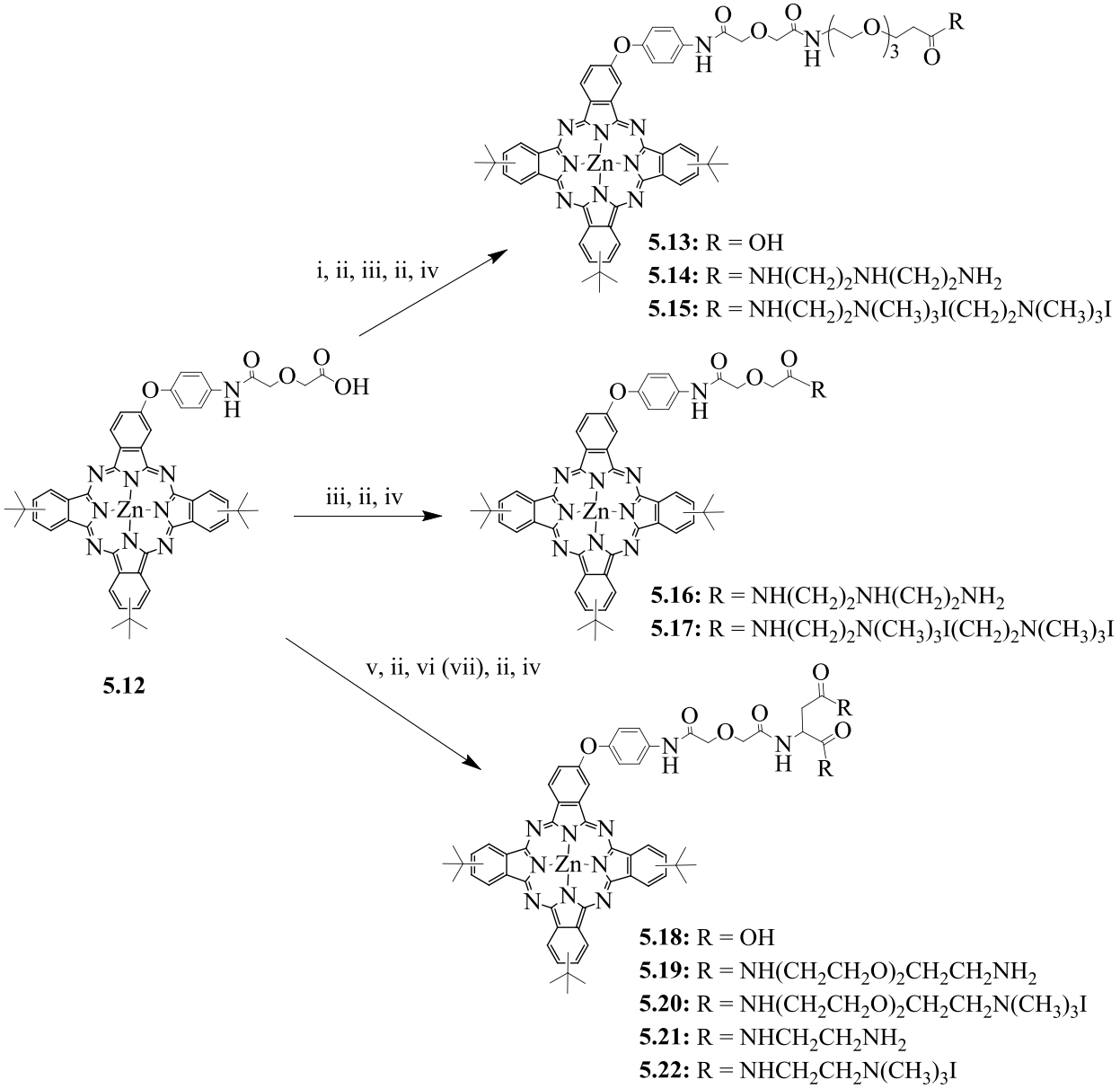

Scheme 5.2. Synthesis of dicationic β-substituted ZnPcs **5.15**, **5.17**, **5.20** and **5.22**. Reaction conditions: (i) *tert*-butyl-12-amino-4,7,10-trioxadodecanoate, TEA, HOBt, EDCI, DMF (77%); (ii) TFA, DCM. 0 ^{o}C, 3 h (83-91%); (iii) 1,4-bis(*N*-Boc)-triazaheptane, TEA, HOBt, EDCI, DMF (80-89%); (iv) CH_3I, DIPA, DMF (58-67%); (v) L-aspartic acid di(*tert*-butyl) ester, TEA, HATU, DMF (89%); (vi) *N*-Boc-2,2′-(ethylenedioxy)diethylamine, TEA, HOBt, EDCI, DMF (51%); (vii) *N*-Boc-ethylenediamine, TEA, HOBt, EDCI, DMF (62%).

Reaction of ZnPcs **5.12** and **5.13** with 1,4-bis(*N*-Boc)-triazaheptane following a similar protocol as that described for ZnPc **5.7** above, gave ZnPcs **5.16** and **5.14** in 72 and 79% yields respectively, after N-Boc-deprotection by TFA. Quaternization of the amino groups using excess methyl iodide and diisopropylamine (DIPA) in DMF gave the corresponding di-cationic ZnPcs **5.17** and **5.15** in 58 and 64% yields, respectively. The pronged ZnPcs **5.18** was synthesized via reaction of **5.12** with di-*tert*-butyl ester protected L-aspartic acid in DMF, using TEA, HATU and HOBt, followed by N-Boc-deprotection using TFA. Coupling ZnPc **5.18** to *N*-Boc-2,2′-(ethylenedioxy)diethylamine or *N*-Boc-ethylenediamine as described above, gave ZnPcs **5.19** and **5.21** in 47 and 56% yields, respectively. Reacting the Pcs with methyl iodide, gave the di-cationic ZnPcs **5.20** and **5.22** in 64 and 67% yields respectively (Scheme 5.2).

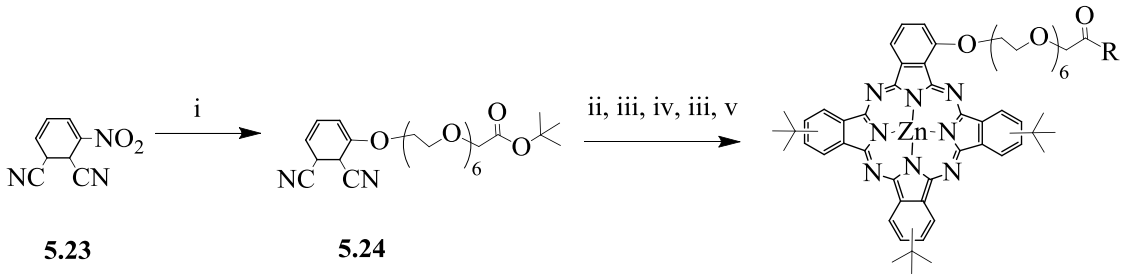

5.23 **5.24**

5.25: R = OH
5.26: R = $NH(CH_2)_2NH(CH_2)_2NH_2$
5.27: R = $NH(CH_2)_2N(CH_3)_3I(CH_2)_2N(CH_3)_3I$

Scheme 5.3. Synthesis of pegylated α-substituted ZnPc **5.27**. Reaction conditions: (i) *tert*-butyl-20-hydroxy-3,6,9,12,15,18-hexaoxaicosan-1-oate, K_2CO_3, THF, 65 ^oC, 6 h (78%); (ii) 4-*tert*-butylphthalonitrile, $Zn(OAc)_2$, DMAE, 145 ^oC, 5 h (17%); (iii) TFA, DCM, 0 ^oC, 3 h (91-94 %); (iv) 1,4-bis(*N*-Boc)-triazaheptane, TEA, HOBt, EDCI, DMF (64%); (v) CH_3I, DIPA, DMF, r.t., 2 days (67%).

Pegylated phthalonitrile **5.24** was obtained by reacting *tert*-butyl 20-hydroxy-3,6,9,12,15,18-hexaoxaicosan-1-oate,[30] with 3-nitrophthalonitrile in THF at 65 ºC, in the presence of K_2CO_3 (Scheme 5.3). Phthalonitrile **5.24** was then tetramerized with excess 4-*tert*-butylphthalonitrile in the presence of zinc(II) acetate and 2-3 drops of DBN in DMAE, followed by N-Boc-deprotection to give the corresponding A_3B-type ZnPc **5.25** in about 16% yield.

Pegylated ZnPc **5.25** was conjugated with 1,4-bis(*N*-Boc)-triazaheptane using TEA, HOBt and EDCI, followed by N-Boc-deprotection to give ZnPc **5.26** in 58% yields. Reaction of ZnPc **5.26** with methyl iodide using the procedure described above gave the corresponding di-cationic ZnPc **5.27** in 67% yield.

Using a similar methodology, phthalonitrile **5.29** was obtained by reacting *tert*-butyl 20-hydroxy-3,6,9,12,15,18-hexaoxaicosan-1-oate with 4-nitrophthalonitrile in THF at 65 ºC, in the presence of K_2CO_3 (Scheme 5.4). Phthalonitrile **5.29** was tetramerized as described for ZnPc **5.25** above to give the corresponding A_3B-type ZnPc **5.30** in about 15% yield. Conjugation of the pegylated ZnPc **5.30** with 1,4-bis(*N*-Boc)-triazaheptane using TEA, HOBt and EDCI, followed by TFA cleavage of N-Boc gave ZnPc **5.31** in 61% yields. Reaction of ZnPc **5.31** with methyl iodide as described above gave di-cationic ZnPc **5.32** in 63% yield.

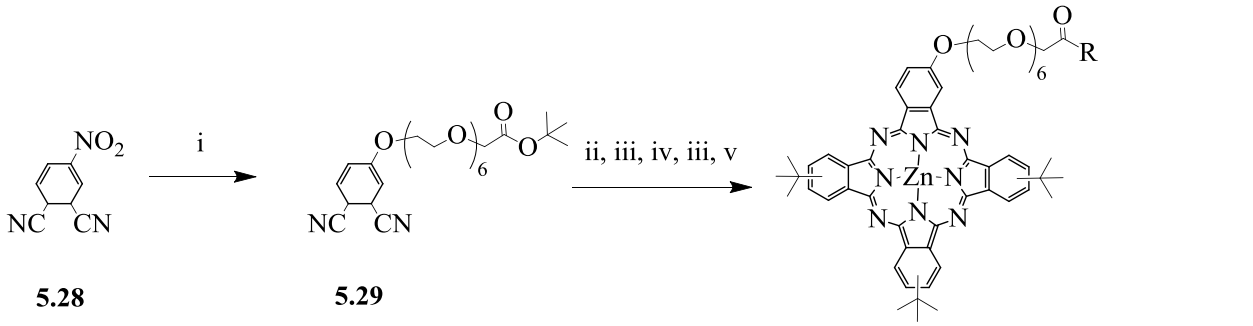

Scheme 5.4. Synthesis of pegylated β-substituted ZnPc **5.32**. Reaction conditions: (i) *tert*-butyl-20-hydroxy-3,6,9,12,15,18-hexaoxaicosan-1-oate, K_2CO_3, THF, 65 ^oC, 6 h (78%); (ii) 4-*tert*-butylphthalonitrile, $Zn(OAc)_2$, DMAE, 145 ^oC, 5 h (16%); (iii) TFA, DCM, 0 ^oC, 3 h (93-94 %); (iv) 1,4-bis(*N*-Boc)-triazaheptane, TEA, HOBt, EDCI, DMF (61%); (v) CH_3I, DIPA, DMF, r.t., 2 days (63%).

All the synthesized di-cationic ZnPcs **5.4**, **5.6**, **5.9**, **5.11**, **5.15**, **5.17**, **5.20**, **5.22**, **5.27** and **5.32** were soluble in polar organic solvents, such as DMF, THF and methanol. None of the cationic Pcs was water soluble; they remained aggregated in water, even after sonication.

Nevertheless, upon dilution from concentrated Pc stocks in DMF or DMSO into PBS (final DMF or DMSO concentration of 1%) at 10 µM concentrations, the Pcs remained in aqueous solution. Cationic ZnPcs may undergo *N*-demethylation upon prolonged storage at room temperature, as observed for this type of Pcs in Chapter 2. The spectroscopic properties of the ZnPcs in DMF are summarized in Table 5.1 and shown in Figure 5.1.

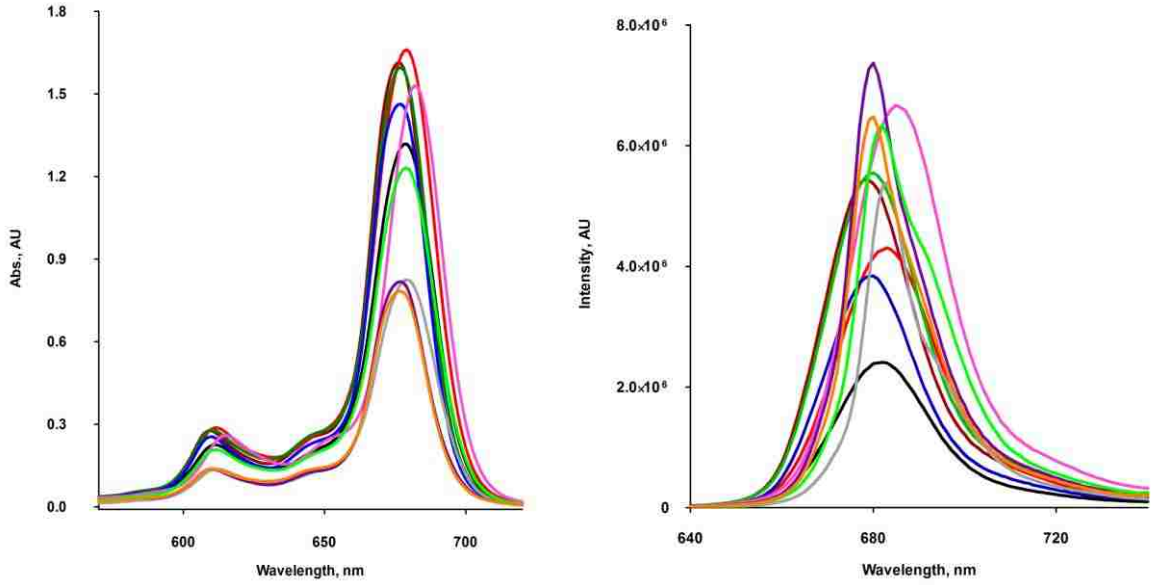

i) **ii)**

Figure 5.1. (i) Absorption and (ii) fluorescence spectra for Pc **5.4** (red), **5.6** (black), **5.9** (grey), **5.11** (light green), **5.15** (green), **5.17** (brown), **5.20** (purple), **5.22** (orange), **5.27** (pink), **5.32** (blue) at 8.0 and 0.5-0.8 µM concentrations, respectively, in DMF.

For concentrations < 10 µM, the ZnPcs did not aggregate in DMF. They all exhibited strong Q absorptions and emissions in the near-IR between 679 – 686 nm in the same solvent, with small Stokes' shifts between 2 – 4 nm, as has been observed for this type of macrocycle.[31-33] The all had a Soret absorption between 330 – 360 nm. A strong Q-band between 677 – 683 nm and a vibrational band at around 620 nm, that strictly followed the Lambert-Beer law was also observed in for each Pc. There was no colloidal solution formations observed for the ZnPcs at 1000 µM in DMF. This is indicative that large

aggregates were not formed at this concentration for this ZnPcs.[32] The expected fluorescence quantum yields ca. 0.09 – 0.23 for ZnPcs in DMF were observed.[31-33]

Table 5.1. Spectroscopic Properties of Pcs in DMF at 25 °C.

ZnPc	Absorption λ_{max} (nm)	Emission[a] λ_{max} (nm)	Stokes' Shift	log ε ($M^{-1}cm^{-1}$)	ϕ_F[b]
5.3	680	684	4	5.52	0.23
5.4	679	683	4	5.32	0.15
5.5	680	684	4	5.19	0.19
5.6	679	682	3	5.23	0.21
5.7	679	682	3	5.17	0.13
5.8	680	683	3	5.20	0.14
5.9	680	683	3	5.01	0.14
5.10	680	683	3	5.23	0.13
5.11	679	682	3	5.19	0.09
5.14	677	680	3	5.28	0.15
5.15	677	680	3	5.30	0.14
5.16	677	679	2	5.19	0.20
5.17	676	679	3	5.31	0.15
5.18	677	680	3	5.28	0.10
5.19	677	681	4	5.27	0.11
5.20	677	680	3	5.01	0.11
5.21	677	680	3	5.19	0.12
5.22	677	680	3	4.99	0.11
5.25	681	684	3	5.34	0.19
5.26	683	686	3	5.31	0.21
5.27	682	685	3	5.28	0.18
5.30	676	680	4	5.14	0.19
5.31	678	681	3	5.35	0.18
5.32	677	680	3	5.26	0.17

[a] Excitation at 640 nm. [b] Calculated using ZnPc (Φ_f = 0.17) as the standard in DMF.

5.2.2. Biological Evaluation of Cationic ZnPcs

The time-dependent cellular uptake, cytotoxicity and intracellular localization of the ZnPcs, were investigated in human carcinoma HEp2 cells. The Promega's Cell Titer Blue was

used in the evaluation of cytotoxicity viability assay, as reported previously in literature,[20,29,34] at concentrations up to 400 µM for all the cationic ZnPcs. Low toxicity in the dark (IC_{50} > 180 µM), especially for the branched dicationic Pcs **5.9**, **5.11**, **5.20** and **5.22** was observed, which exhibited remarkably low dark toxicity (IC_{50} > 400 µM). This could be due to their low uptake into cells as seen in Figure 5.2. Cationic ZnPcs **5.6**, **5.27** and **5.32** may not suitable candidates for imaging due to their relatively high dark toxicity at higher concentrations, although ZnPc **5.27** may be used for PDT; it has higher dark- to photoxicity IC_{50} ratio. Due to its low dark toxicity and higher phototoxicity, cationinc ZnPc **5.11** may find application as a PDT agent. These results also indicate that Pcs **5.20** and **5.22** may be useful as bioimaging dyes due to the low phototoxicity observed. Table 5.2 summarizes the IC_{50} results obtained for the cationic ZnPcs.

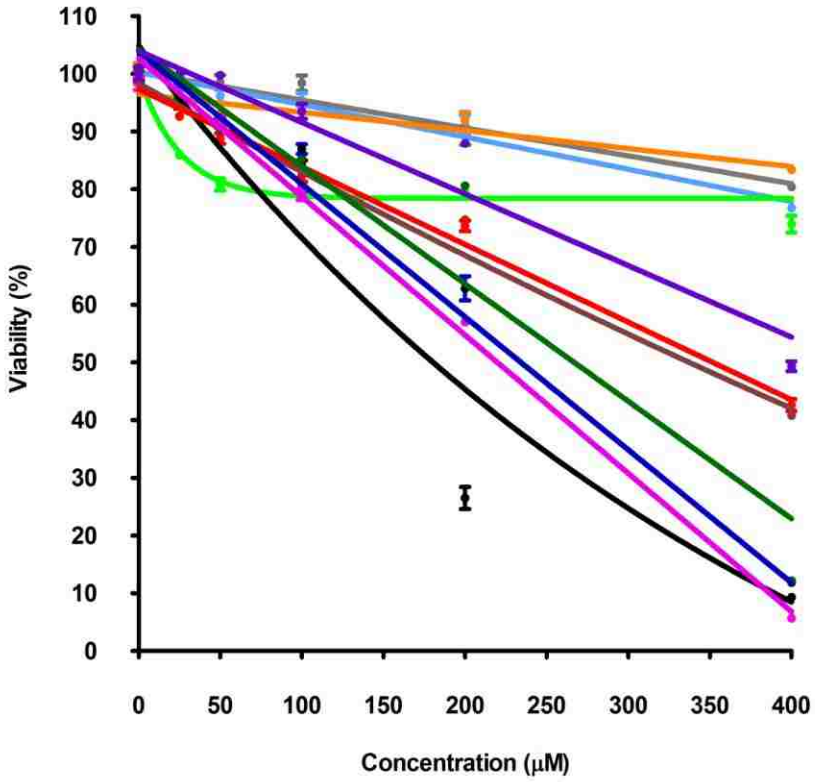

Figure 5.2. Dark toxicity of Pc **5.4** (red), **5.6** (black), **5.9** (grey), **5.11** (light green), **5.13** (purple), **5.15** (green), **5.17** (brown square), **5.20** (light-blue), **5.22** (orange), **5.27** (pink), **5.32** (blue) at 10 µM in HEp2 cells.

Table 5.2. Cytotoxicity and localization sites for ZnPcs in HEp2 cells.

ZnPc	Dark toxicity (IC_{50}, μM)	Phototoxicity (IC_{50}, μM)	Ratio	Major sites of localization
5.4	351.7	10.7	32.9	ER
5.6	179.9	14.8	12.2	Golgi
5.9	>400.0	28.8	>13.9	Lysosomes
5.11	>400.0	12.7	>31.5	Lysosomes
5.13	397.3	>100.0	>4.0	Mitochondria
5.15	280.0	>100.0	>2.8	Mitochondria, Golgi
5.17	346.3	>100	>3.5	Mitochondria, Lysosomes
5.20	>400.0	>100.0	>4.0	Lysosomes
5.22	>400.0	>100.0	>4.0	Mitochondria
5.27	220.1	8.7	25.3	Mitochondria, ER
5.32	249.7	47.0	5.3	ER

The uptake of each Pc into HEp2 cells with time was investigated at a concentration of 10 μM of over 24 h (Figure 5.3a). In Chapter 2, it was observed that the cytotoxicity of cationic Pcs depends on the position of the substituent on the macrocycle periphery. The α-substituted compounds were found be more toxic than their β-substituted counterparts. All β-substituted ZnPcs were not toxic even at 100 μM concentrations upon irradiation with low light dose (~1.5 J/cm^2); only ZnPc **5.22** was relatively phototoxic (IC_{50} = 47 μM). The α-substituted ZnPcs **5.4**, **5.6**, **5.9**, **5.11** and **5.27** were the most phototoxic, with calculated IC_{50} values of 10.7, 14.8, 28.8, 12.7 and 8.7 μM, respectively (see dose-response curves, Figure 5.3b). Of the cationic Pcs synthesized in this Chapter, **5.4**, **5.11** and **5.27** are the most promising for PDT applications due to their high ratio (>25) of dark toxicity and high phototoxicity. As noted in Chapter 1, a good PDT drug should have low dark toxicity to phototoxicity ratio. The results in Table 5.2 show that the dark toxicity IC_{50} value should be large enough compared to the phototoxicity IC_{50}, for a photosensitizer to find application in PDT.

a)

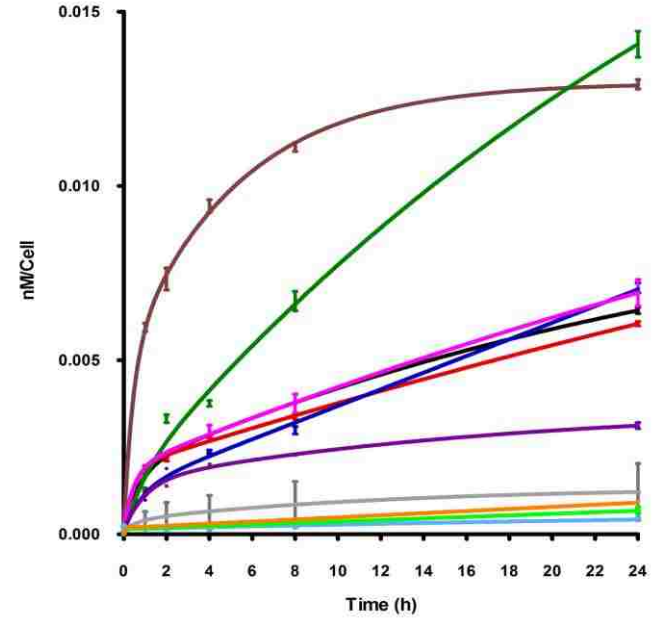

b)

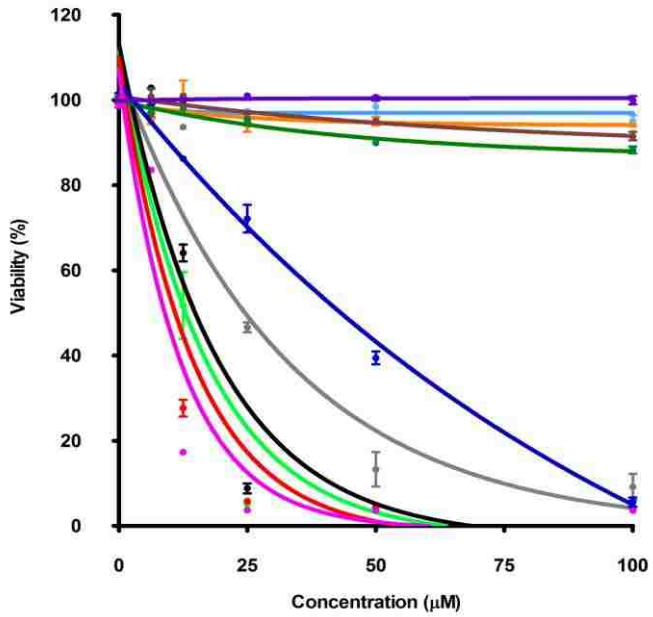

Figure 5.3. (a) Time-dependent uptake at 10 μM, and (b) Phototoxicity of ZnPcs **5.4** (red), **5.6** (black), **5.9** (grey), **5.11** (light green), **5.13** (purple), **5.15** (green), **5.17** (brown), **5.20** (light blue), **5.22** (orange), **5.27** (pink), **5.32** (blue) in HEp2 cells.

It was remarkable to note that both of the most phototoxic ZnPcs (**5.4** and **5.27**) had a PEG group. The two cationic charges were only separated by an ethylene group and the two ZnPcs localized in the cell ER. It is reported in literature that pegylation of Pc macrocycles

favors intracellular localization in the ER,[28] whereas the positive charges may favor their localization at the plasma membrane, or subcellularly within mitochondria and lysosomes.[34-37]

The β-substituted ZcPcs **5.15** and **5.17** accumulated within HEp2 cells to a great extent than the other Pcs. The fastest of all ZnPcs in terms of cellular uptake was Pc **5.17**, although the uptake slowed down to a plateau approximately 8 h post exposure. The PEG group in ZnPc **5.15** probably resulted in continued accumulation within cells up to 24 h post exposure. The di-cationic Pcs (**5.15** and **5.17**) containing the two cationic charges in close proximity on the same chain, exhibited increased uptake unlike the neutral Pc-PEG **5.13**, or the cationic Pcs **5.9**, **5.11**, **5.20** and **5.22**, which were branched.

With exception of **5.20**, which was found mainly in the lysosomes (Table 5.2), all the other cationic ZnPcs localized within multiple subcellular sites. Other ZnPcs (**5.4**, **5.6**, **5.11** and **5.32**) were localized at the plasma membrane. The most phototoxic compounds (**5.4**, **5.11** and **5.27**) were all localized within the ER. The ER is an important organelle that is responsible for the regulation of protein synthesis and stress responses, which in turn induces cell apoptosis in PDT.[38,39] The results in this Chapter show that the subcellular localization of the ZnPcs, and not the extent of cellular uptake, or their charge distribution about the macrocycle determines their photodynamic activity. This could be due to their different interactions with the subcellular units. The fluorescence microscopy experiments were carried out, 6 h post exposure of HEp2 cells (Figures 5.4 – 5.8). The following organelle specific fluorescent tracers for co-localization experiments were used: ER Tracker Blue/White (ER), MitoTracker Green (mitochondria), BODIPY Ceramide (Golgi) and LysoSensor Green (lysosomes). The results indicate that the α-substituted ZnPcs were more toxic than the corresponding β-substituted ZnPcs in the dark. Upon exposure of the ZnPcs to approximately 1.5 J/cm^2 light dose, similar observation was made.

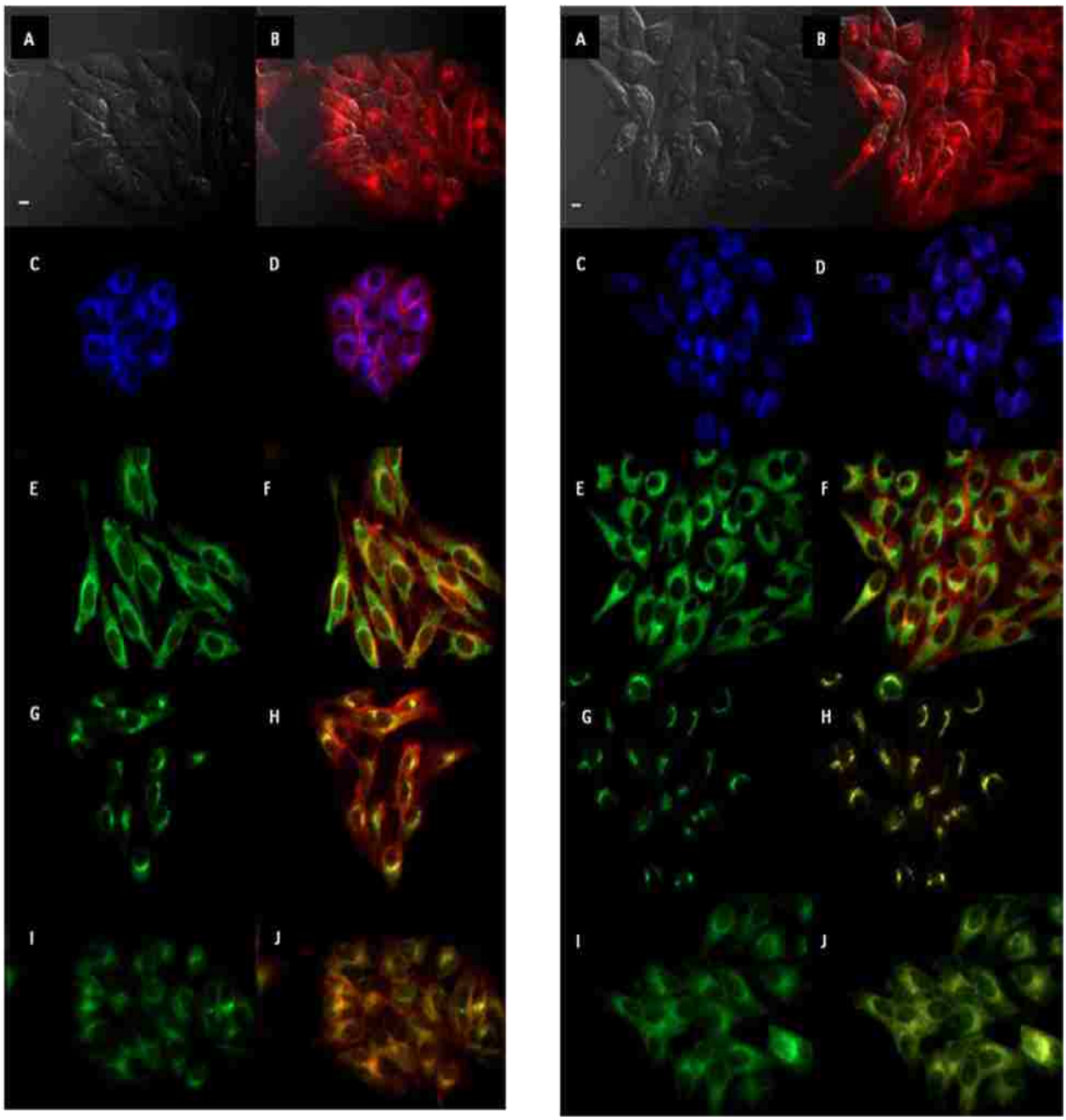

Figure 5.4. Subcellular localization of: (a) ZnPc **5.4** in HEp2 cells at 10 μM for 6 h. (A) Phase contrast, (B) Overlay of **5.4** fluorescence and phase contrast, (C) ER Tracker Blue/White fluorescence, (E) MitoTracker green fluorescence, (G) BODIPY Ceramide fluorescence, (I) LysoSensor green fluorescence, and (D, F, H, J) overlays of organelle tracers with **5.4** fluorescence. (b) Pc **5.6** in HEp2 cells at 10 μM for 6 h. (A) Phase contrast, (B) Overlay of **5.6** fluorescence and phase contrast, (C) ER Tracker Blue/White fluorescence, (E) MitoTrack green fluorescence, (G) BoDIPY Ceramide, (I) LysoSensor green fluorescence, and (D, F, H, J) overlays of organelle tracers with **5.6** fluorescence. Scale bar: 10 μm.

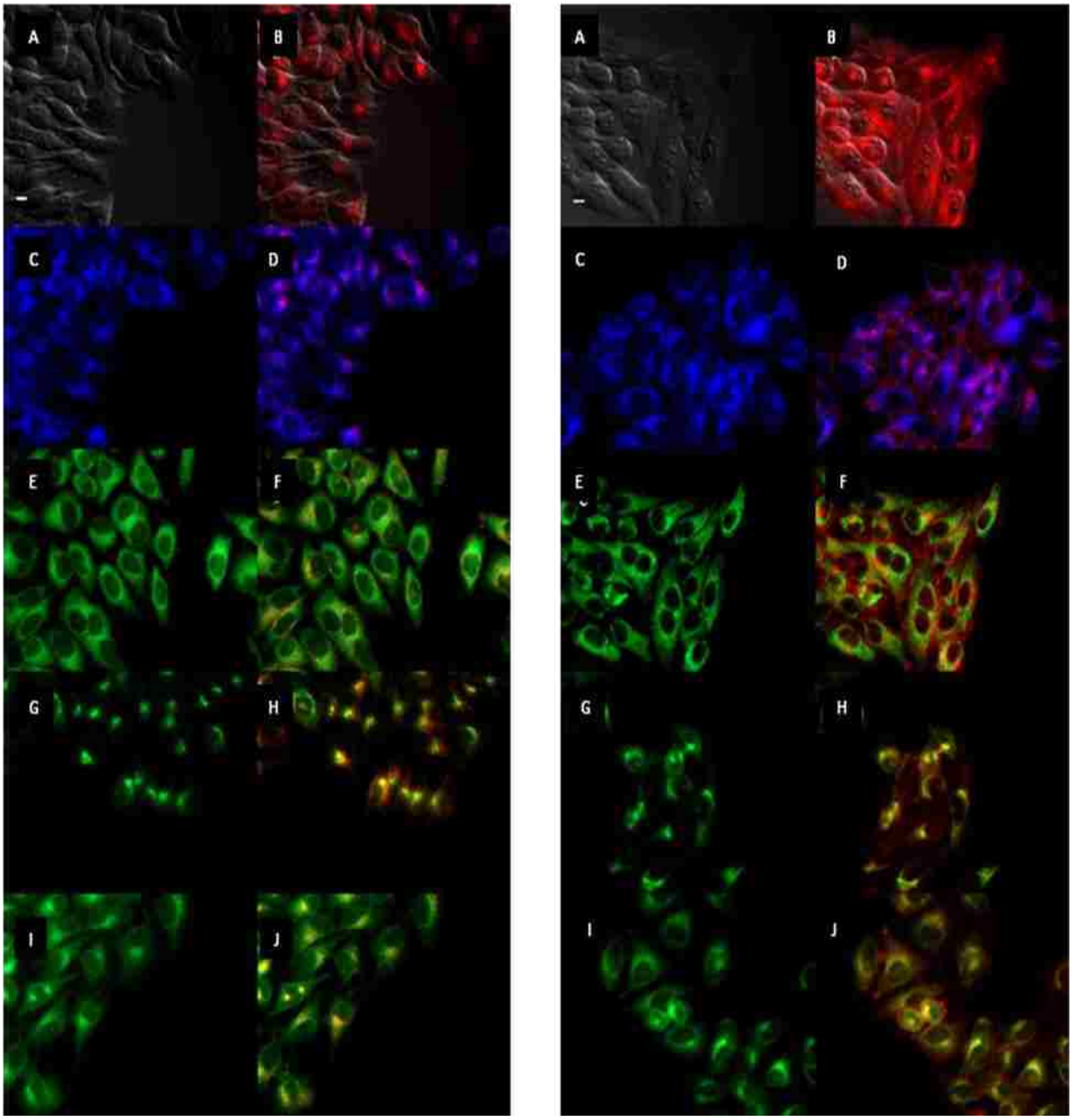

a) **b)**

Figure 5.5. Subcellular localization of: (a) Pc **5.9** in HEp2 cells at 10 μM for 6 h. (A) Phase contrast, (B) Overlay of **5.9** fluorescence and phase contrast, (C) ER Tracker Blue/White fluorescence, (E) MitoTrack green fluorescence, (G) BoDIPY Ceramide, (I) LysoSensor green fluorescence, and (D, F, H, J) overlays of organelle tracers with **5.9** fluorescence. (b) ZnPc **5.11** in HEp2 cells at 10 μM for 6 h. (A) Phase contrast, (B) Overlay of **5.11** fluorescence and phase contrast, (C) ER Tracker Blue/White fluorescence, (E) MitoTracker green fluorescence, (G) BODIPY Ceramide, fluorescence (I) LysoSensor green fluorescence, and (D, F, H, J) overlays of organelle tracers with **5.11** fluorescence. Scale bar: 10 μm.

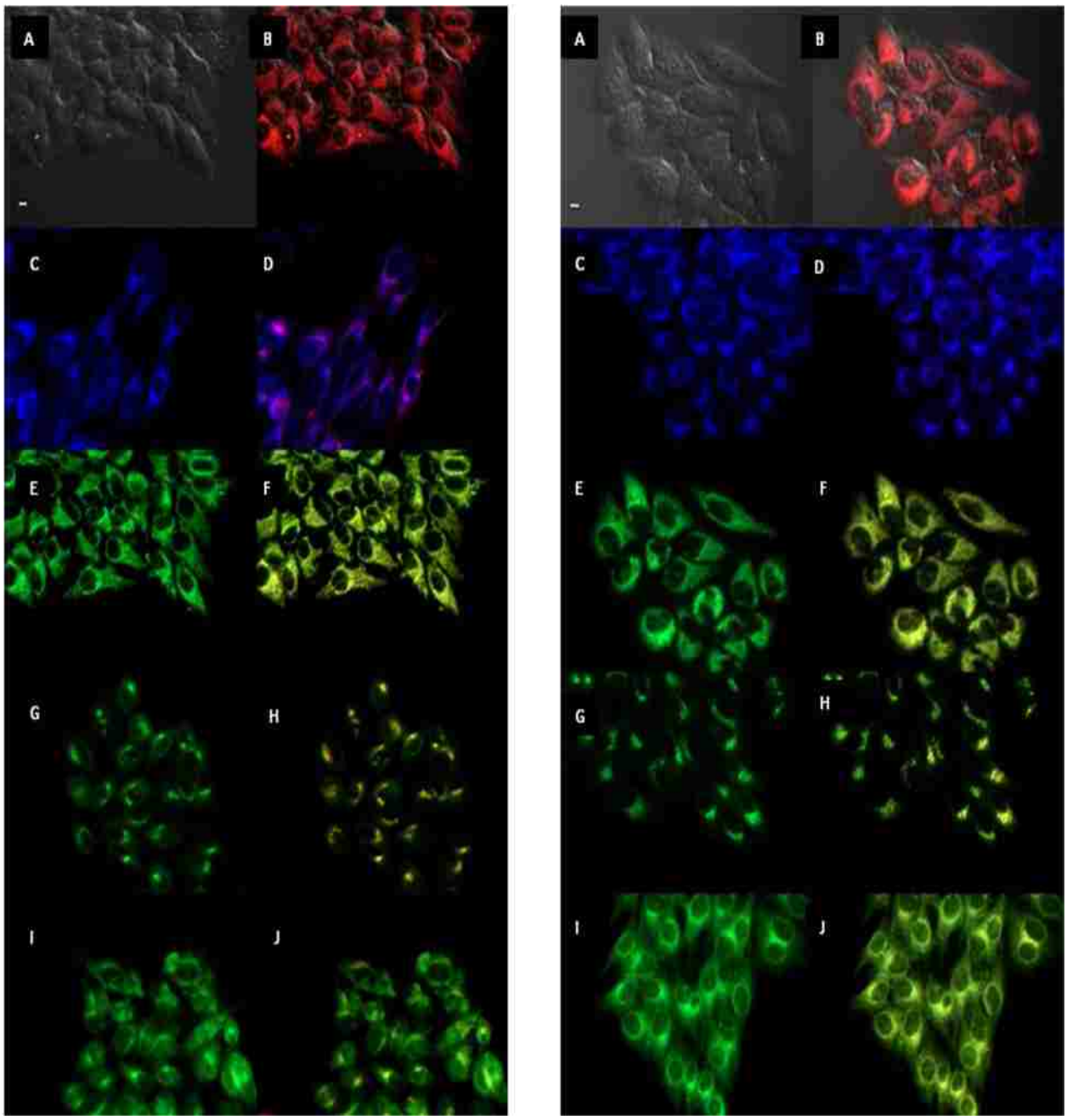

a) **b)**

Figure 5.6. Subcellular localization of: (a) Pc **5.15** in HEp2 cells at 10 μM for 6 h. (A) Phase contrast, (B) Overlay of **5.15** fluorescence and phase contrast, (C) ER Tracker Blue/White fluorescence, (E) MitoTrack green fluorescence, (G) BoDIPY Ceramide, (I) LysoSensor green fluorescence, and (D, F, H, J) overlays of organelle tracers with **5.15** fluorescence. (b) Pc **5.17** in HEp2 cells at 10 μM for 6 h. (A) Phase contrast, (B) Overlay of **5.17** fluorescence and phase contrast, (C) ER Tracker Blue/White fluorescence, (E) MitoTrack green fluorescence, (G) BoDIPY Ceramide, (I) LysoSensor green fluorescence, and (D, F, H, J) overlays of organelle tracers with **5.17** fluorescence. Scale bar: 10 μm.

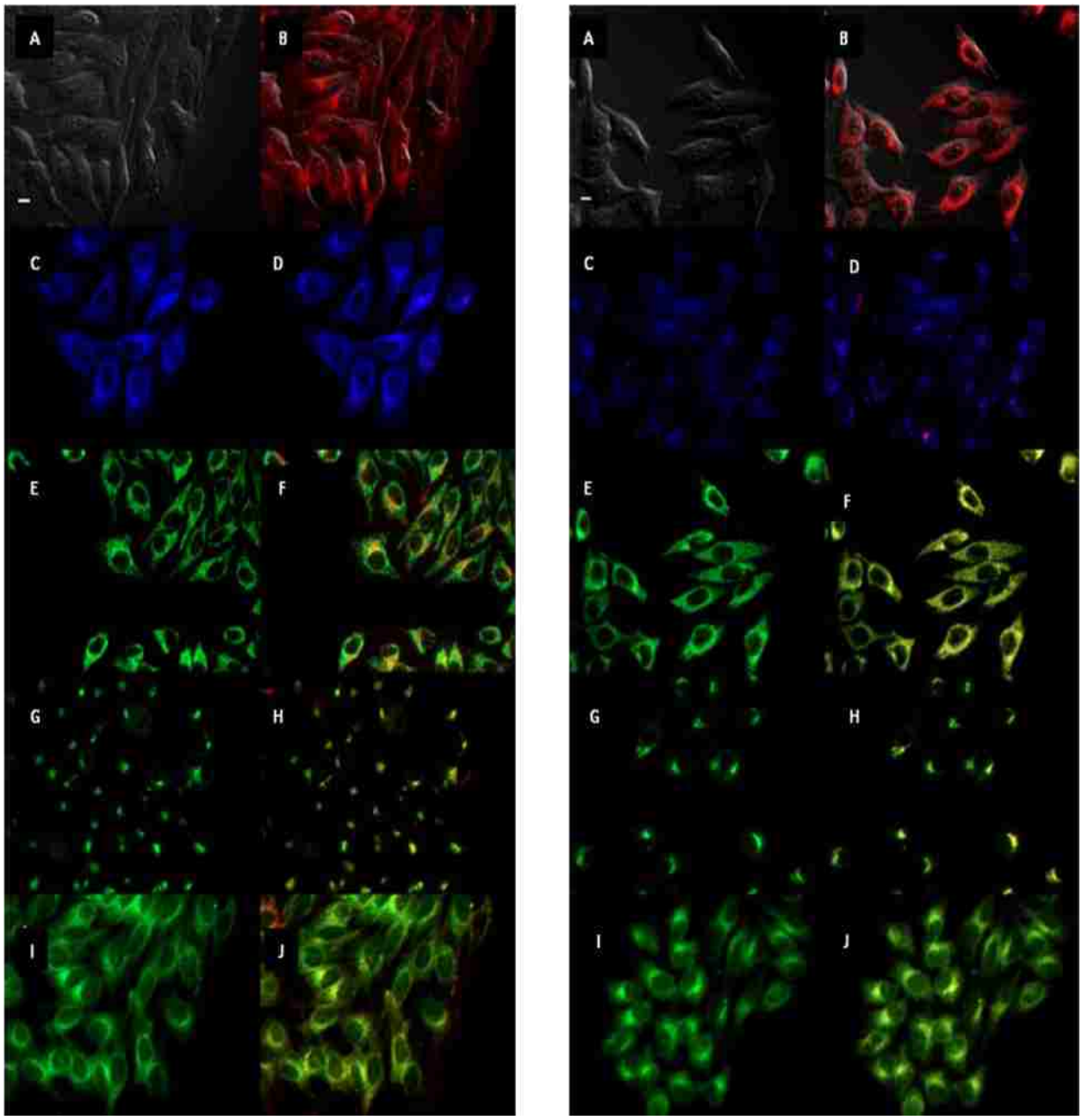

Figure 5.7. Subcellular localization of: (a) Pc **5.20** in HEp2 cells at 10 μM for 6 h. (A) Phase contrast, (B) Overlay of **5.20** fluorescence and phase contrast, (C) ER Tracker Blue/White fluorescence, (E) MitoTrack green fluorescence, (G) BoDIPY Ceramide, (I) LysoSensor green fluorescence, and (D, F, H, J) overlays of organelle tracers with **5.20** fluorescence. (b) Pc **5.22** in HEp2 cells at 10 μM for 6 h. (A) Phase contrast, (B) Overlay of **5.22** fluorescence and phase contrast, (C) ER Tracker Blue/White fluorescence, (E) MitoTrack green fluorescence, (G) BoDIPY Ceramide, (I) LysoSensor green fluorescence, and (D, F, H, J) overlays of organelle tracers with **5.22** fluorescence. Scale bar: 10 μm.

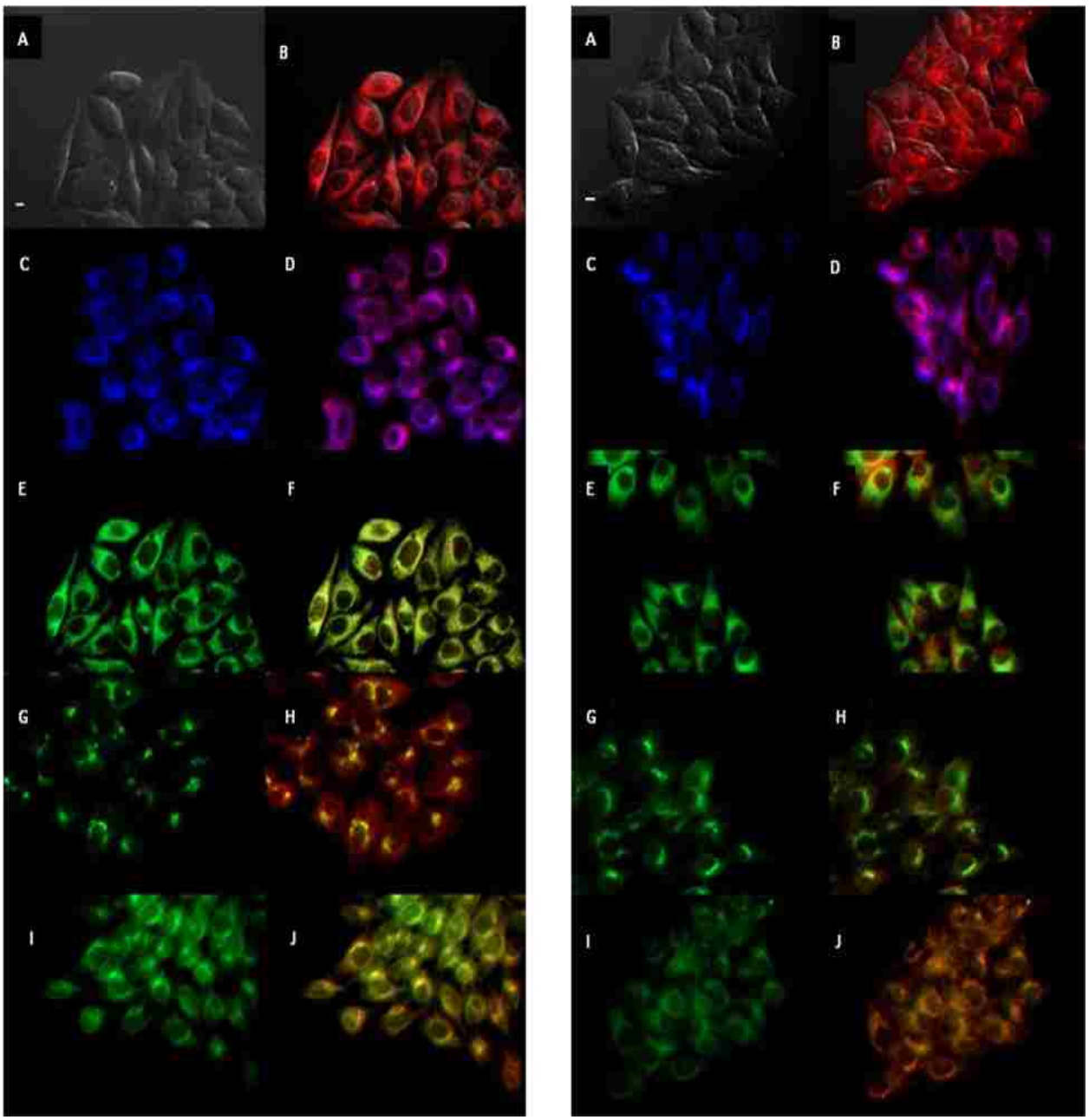

a) **b)**

Figure 5.8. Subcellular localization of: (a) ZnPc **5.27** in HEp2 cells at 10 μM for 6 h. (A) Phase contrast, (B) Overlay of **5.27** fluorescence and phase contrast, (C) ER Tracker Blue/White fluorescence, (E) MitoTracker green fluorescence, (G) BODIPY Ceramide fluorescence, (I) LysoSensor green fluorescence, and (D, F, H, J) overlays of organelle tracers with **5.27** fluorescence. (b) Pc **5.32** in HEp2 cells at 10 μM for 6 h. (A) Phase contrast, (B) Overlay of **5.32** fluorescence and phase contrast, (C) ER Tracker Blue/White fluorescence, (E) MitoTrack green fluorescence, (G) BoDIPY Ceramide, (I) LysoSensor green fluorescence, and (D, F, H, J) overlays of organelle tracers with **5.32** fluorescence. Scale bar: 10 μm.

5.2.3. Pc-Monoclonal Anti-Carcinoembryonic Antigen (AntiCEA) Conjugates

Monoclonal antibodies (mAbs) are antibodies that are made by identical immune cells that are all clones of a unique parent cell, and they have affinity for a specific substance.[40] The mAbs are artificially produced via a technique of cell fusion followed by selection; body cells are obtained from a single cell in a culture medium. Monoclonal antibody therapy is the use of mAbs to target specific cells or proteins.[41,42] Several antibodies have been approved for the treatment of cancer, either as unconjugated antibodies or for delivery of drugs to cancer cells. Some of the monoclonal antibodies that have been approved by FDA for the treatment of various types of cancer are show in Table 5.3.[40]

Table 5.3. Some of the antibodies approved by DFA for cancer treatment.

Monoclonal antibody	Target Cancer
Alemtuzumab (Campath)	Chronic lymphocytic leukemia
Bevacizumab (Avastin)	Breast cancer, colon cancer, lung cancer
Cetuximab (Erbitux)	Colon cancer, head and neck cancers
Gemtuzumab (Mylotarg)	Acute myelogenous leukemia
Ibritumomab (Zevalin)	Non-Hodgkin's lymphoma
Panitumumab (Vectibix)	Colon cancer
Rituximab (Rituxan)	Non-Hodgkin's lymphoma
Tositumomab (Bexxar)	Non-Hodgkin's lymphoma

Many factors dictate the success of targeted therapeutics: affinity and specificity of the ligand used, the density of the target molecule on the cell surface, localization of the drug within the target tissue, and the rate at which the drug molecules enter the appropriate cell compartments.[43] In Chapter 2, two small peptides with sequences LARLLT[44] and YHWYGYTPQNVI[45] are among the EGFR-targeting biomolecules, which have recently been reported as potential ligands for selective delivery of cytotoxic drugs to the target sites. The

molecules are particularly attractive due to their availability, low immunogenicity, ease of conjugation to various molecules, and reported superior EGFR-targeting ability. Monoclonal antibodies have also been used in targeted therapeutics.[46-49] Despite their large molecular weight and relatively higher cost, monoclonal antibodies have attracted interest in targeted therapeutics due to their unique specificity.

In this section, several ZnPcs were synthesized and conjugated to human carcinoembryonic antigen (antiCEA). The conjugates were then investigated in mice bearing colon tumors derived from HT-29 cell lines, as imaging agents. The CEA is most abundantly expressed extracellular marker associated with human colorectal cancer or the precursor aberrant crypti foci, and is used as serum marker of CRC in clinical medicine.[50,51] The CEA antigen is also non-internalizing and as a result was not expected to cause phototoxicity. The CEA is a large protein and therefore, cannot be internalized – it has a molecular mass of about 150 kD. The non-internalization of the CEA is important since the conjugate will be bound to the tumor surface, resulting in enhanced fluorescence. The ZnPc derivatives conjugated to monoclonal antiCEA investigated in here, are pegylated and/or cationic; this enhanced their water-solubility. Solubility in water is a key factor since all the conjugation reactions were carried out at pH 7.4 in PBS solution. Positively charged photosensitizers may also interact with negatively charged cell membranes and the targeted surfaces.[16-23]

In Chapter 2, ZnPcs with *tert*-butyl groups, which minimized aggregation, were synthesized. These groups introduced hydrophobicity to the macrocycles and thus reduced their solubility in aqueous media. The removal of the *tert*-butyl groups from the Pc macrocycles synthesized in this section resulted in enhanced solubility in aqueous medium. The synthesized ZnPcs were conjugated to the CEA via carboxylic groups. The CEA has a several amino terminal

groups that were used in the conjugation reactions. Introduction of the PEG groups enhanced the solubility of the ZnPcs and also served as spacers between the ZnPcs and the CEA.

5.2.4. Syntheses of Pcs for Conjugation to the AntiCEA

Water-soluble pegylated ZnPcs and a hexa-cationic ZnPc were synthesized for conjugation to the mAb. Water-solubility is critical since the mAb is stable in basic aqueous medium and thus conjugation was carried out in PBS. Conjugation of mAb to cationic porphyrins has been reported before.[52] The conjugation was achieved in 0.5 M bicarbonate buffer (pH = 9.2). The conjugations were performed using 20, 40 and 60 equivalents of the porphyrins to obtain an average degree of loading (DOL) of 2. DOL is the number of photosensitizer molecules per unit molecule of the mAb. A DOL of 4 was reported by Vrouentaets *et al.*[53]

The synthesis of the ZnPcs started with 3-nitrophthalonitrile or 4-nitrophthalonitrile, which reacted with either aminophenol or a diol in DMF solvent under heat to give various phthalonitriles. In Scheme 5.6, 2,3-dicyanohydroquinone was the starting reagent and served as the alcohol in the reaction. The synthetic strategies to these starting materials are shown in Schemes 5.5 – 5.7.

Phthalonitrile **5.34** was obtained via reaction of 1,4-dioxane-2,6-dione with **5.33** in 92.1% yield. Reacting tert-butyl-1,2-amino-4,7,10-trioxadodecanoate with **5.34** using coupling reagents DIEA, HOBt and TBTU, gave **5.35** in 92.2% yield. The crystal structures of phthalonitriles **5.33**, **5.35** and **5.36** are shown in Figure 5.9. The molecular structure of phthalonitrile **5.35** was grown in a mixed solvent systen of acetone/methanol (9:1) over a period of one month. The conditions favored the formation of the ester analog of the target phthalonitrile, as seen from X-ray structure (Figure 5.9b).

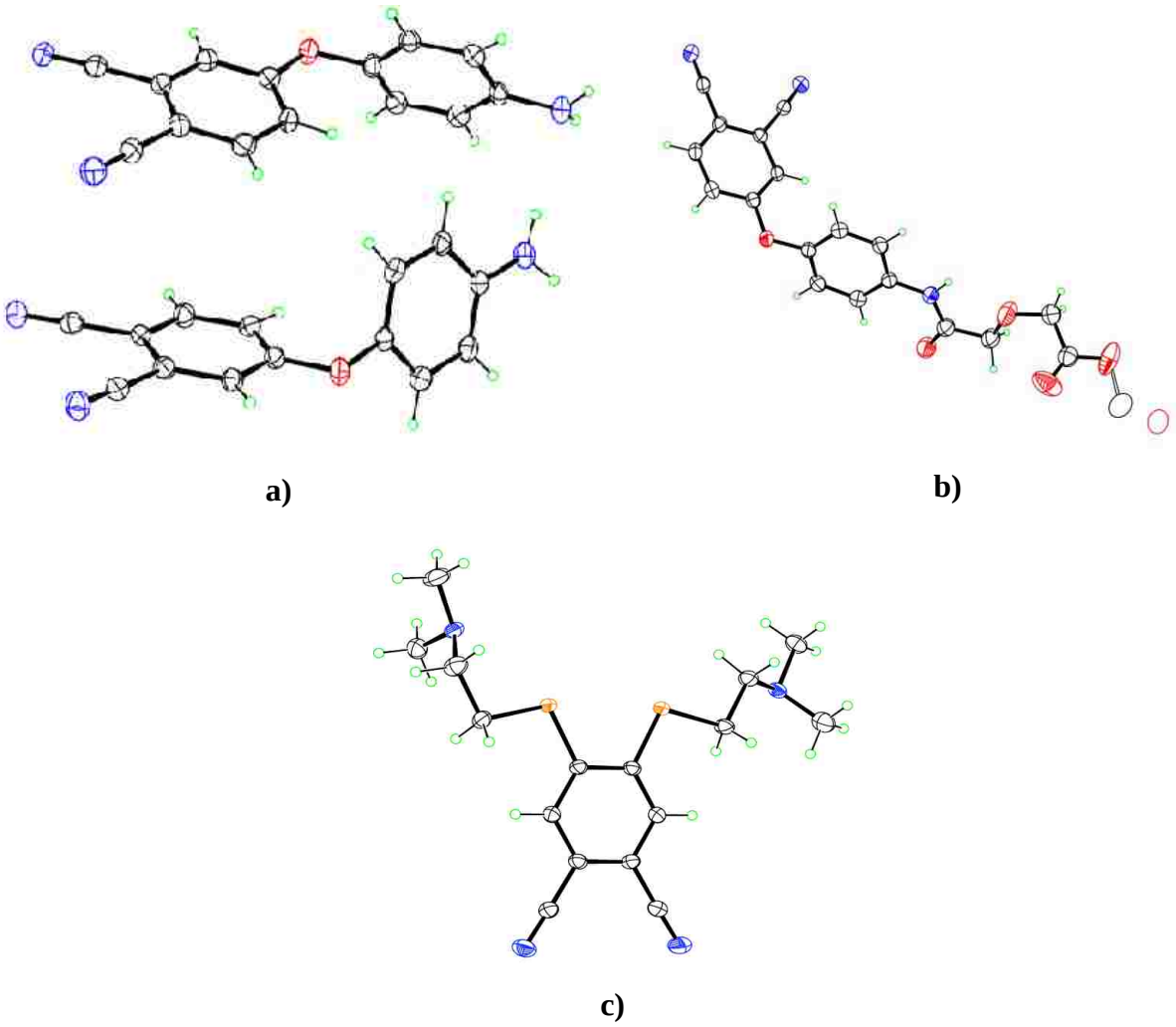

Figure 5.9. Molecular structures of phthalonitriles (a) **5.33**, (b) **5.35** and (c) **5.36** from crystal structure determinations (N atoms are blue, O atoms red, S atoms orange and H atoms green). Ellipsoids are drawn at the 50% probability level.

Synthesis of ZnPc **5.40** was achieved according to a procedure previously reported in Chapter 2. Phthalonitrile **5.35** was obtained by reacting phthalonitrile **5.34** with tert-butyl-1,2-amino-4,7,10-trioxadodecanoate using DIEA, HOBt and TBTU in DMF at 25 °C. Phthalonitrile **5.35** was reacted with 3 equiv. phthalonitrile **5.36** at 140 ºC for 5 h in DMAE and in the presence of zinc(II) acetate, and a catalytic amount of DBN. The ZnPc **5.37** was obtained in 10.1% yield. Reacting ZnPc **5.37** with iodomethane in DMF, gave **5.38** in 98.0% yield and **5.39** in quantitative yield, after TFA deprotection (Scheme 5.5).

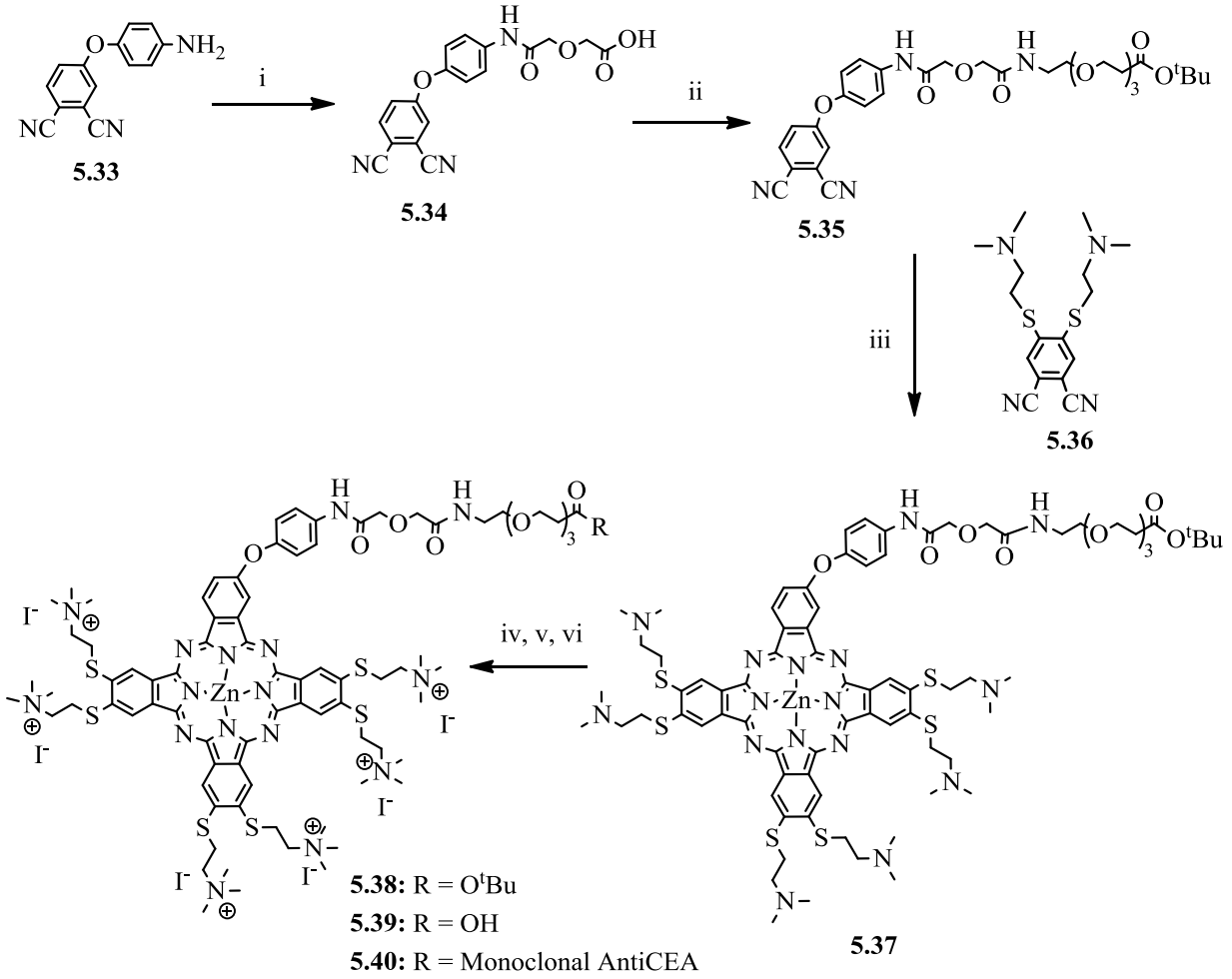

Scheme 5.5. Synthesis of Pc-antiCEA conjugate **5.40**. Conditions: (i) 1, 4-dioxane-2, 6-dione, DMF, r.t., (92.1%). (ii) tert-butyl-1,2-amino-4,7,10-trioxadodecanoate, DIEA, HOBt, TBTU, DMF, 48 h, r.t., (92.2%). (iii) phthalonitrile **5.36**, zinc acetate, DBN, DMAE, 5 h, (10.1%) (iv) iodomethane, DMF, 2 days, r.t., (98%). (v) TFA, dichloromethane, 4 h, (quantitative). (vi) DIEA, HOBt, TBTU, monoclonal antibody, DMSO/$NaHCO_3$.

Mono-pegylated phthalonitrile **5.42** was synthesized according to the literature procedure,[9] and used in macrocyclization reaction with phthalonitrile to give mono-PEG-Pc **5.43** (Scheme 5.6). Phthalonitrile **5.42** was mixed with 30 equiv. phthalonitrile in DMAE solvent, and heated at 140 ºC for 5 h in the presence of zinc(II) acetate and a catalytic amount of DBN. Purification of the crude product via column chromatography gave ZnPc **5.43** in 9.8% yield. Reacting ZnPc **5.43** with *tert*-butyl 3-(2-(2-(2-iodoethoxy)ethoxy)ethoxy)propanoate gave ZnPc **5.44** in 74.9% overall yield, after TFA deprotection.

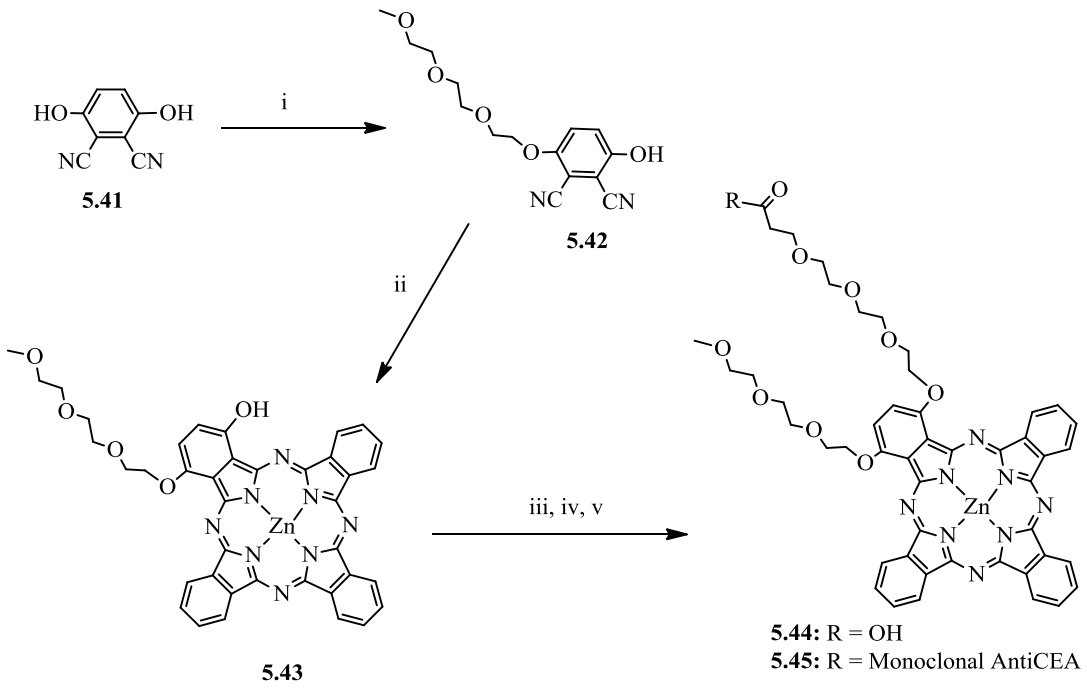

Scheme 5.6. Synthesis of Pc-antiCEA conjugate **5.45**. Conditions: (i) 1-iodo-2-(2-(2-methoxyethoxy)-ethoxy)ethane, K_2CO_3, DMF, 65 °C, 24 h (42%). (ii) phthalonitrile, zinc acetate, DBN, DMAE, 5 h (9.8%). (iii) *tert*-butyl 3-(2-(2-(2-iodoethoxy)ethoxy)ethoxy)-propanoate, K_2CO_3, DMF, 65 °C, 24 h (76.7%). (iv) TFA, dichloromethane, 4 h, (97.7%). (v) DIEA, HOBt, TBTU, monoclonal antibody, DMSO/$NaHCO_3$.

5.2.5. Conjugation of Pcs to AntiCEA

Monopegylated ZnPc **5.46** was prepared according to the procedure described earlier in Chapter 3. Coupling ZnPcs **5.39**, **5.44** and **5.46** with monoclonal antibody, antiCEA, using DIEA, HOBt and TBTU, in DMSO/$NaHCO_3$ gave Pc-conjugates **5.40**, **5.45** and **5.47** respectively, which were purified using microspin columns. The mAb was reconstituted at 2 mg/mL in 0.1 M $NaHCO_3$ solution. Then ZnPcs **5.39**, **5.44** and **5.46** (1 mg each) were dissolved in DMSO (50 µL) and DIPA (0.078 mg, 0.006 mmol) added. The mixture was stirred for 1 h, after which HOBt (0.34 mg, 0.002 mmol) and TBTU (0.59 mg, 0.002 mmol) were added and the reaction solutions stirred for 2 h. The reconstituted monoclonal antibody solution (500 µL) was added into each activated Pc solution and the solutions were kept with frequent shaking at room temperature for 1 hour. Then the solutions were kept at 4 °C for 24 h, with occasional shaking.

The crude of each antibody-Pc conjugate solution was purified by spin column chromatography (50 µL for each spin column to load, 3000 rpm, 1 min, 24 °C). The resulting solutions were combined for each Pc, to afford the blue conjugate solution (600 - 700 µL).

The PEG group on the ZnPcs significantly enhanced their solubility in organic solvents, which made their purification and characterization relatively easy. The solubility of ZnPc **5.46** in aqueous medium was relatively lower than that of ZnPc **5.44**, which made conjugation reaction relatively less successful compared with Pc-conjugate **5.47**. ZnPc **5.44** was soluble in aqueous medium, which made conjugation reaction a success (see Table 5.5). Of all the Pc-antiCEA conjugates, **5.47** was the one with the lowest UV-vis absorption, resulting in lower DOL. This can be associated to the *tert*-butyl groups on the macrocycle (which make it more hydrophobic) and it also has a single PEG compared with ZnPc **5.44**, which has two PEG groups. Reduced solubility of the ZnPc in aqueous medium will affect conjugation reaction. The ZnPc precipitate will not label the mAb. Thus, the observed result was expected.

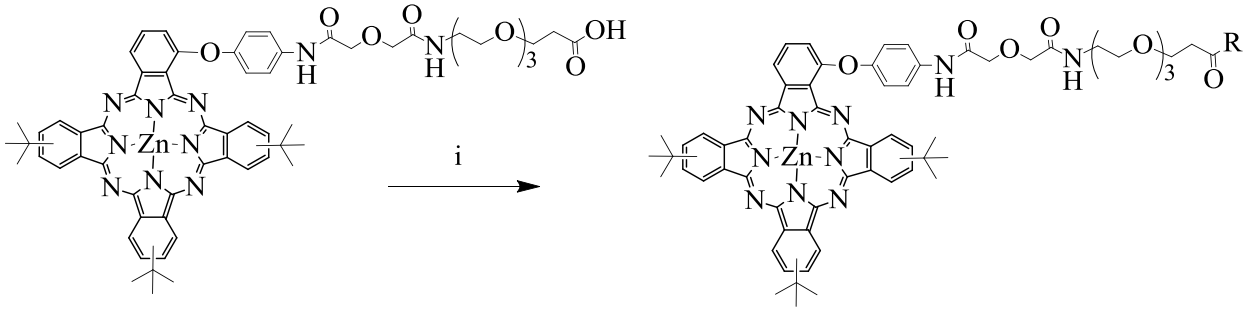

5.46 **5.47:** R = Monoclonal antiCEA

Scheme 5.7. Synthesis of Pc-antiCEA conjugate **5.47**. Conditions: (i) DIEA, HOBt, TBTU, monoclonal antibody, DMSO/$NaHCO_3$.

All the ZnPcs **5.37**, **5.38**, **5.39**, **5.43**, **5.44**, **5.45** and **5.46** were soluble in polar organic solvents, such as DMF, THF and methanol, while the cationic Pc **5.39** was water-soluble. Cationic Pc **5.39** remained aggregated in DMF, even upon sonication. Nonetheless, all Pcs remained in aqueous solution upon dilution from concentrated Pc stocks in DMF or DMSO

solvents into 0.1 M $NaHCO_3$ (final DMF or DMSO concentration of 1%) for 10 µM concentrations.

The spectroscopic properties of the ZnPcs **5.38**, **5.39**, **5.43**, **5.44** and **5.46** in DMF are summarized in Table 5.4. All ZnPcs showed strong Q absorptions and emissions in the near-IR between 679 – 686 nm in DMF, with small Stokes' shifts between 2 – 4 nm, as is characteristic of this type of macrocycle.[31-33] All the ZnPcs show a Soret absorption between 330 – 360 nm, a strong Q band between 678 – 696 nm and a vibrational band at around 620 nm, that strictly follow the Lambert-Beer law. The ZnPcs had fluorescence quantum yields in the range 0.10 – 0.29 in DMF, as expected for this type of compounds.[32,33]

Table 5.4. Spectroscopic Properties of Pcs in DMF at 25 °C.

ZnPc	Absorption (nm)	Emission[a] (nm)	Stokes' Shift	log ε ($M^{-1}cm^{-1}$)[1]	ϕ_F[b]
5.38	696	699	3	5.04	0.29
5.39	696	698	2	4.94	0.21
5.43	694	696	2	5.17	0.14
5.44	688	691	3	5.18	0.22
5.46	678	682	4	5.35	0.10

[a] Excitation at 640 nm. [b] Calculated using ZnPc (Φ_f = 0.17) as the standard in DMF.

Table 5.5. Estimated payloads (ZnPc per unit antiCEA) for various conjugates.

ZnPc	$C_{CEA}=[A_{280nm} - (0.5 \times A_{ZnPc})]/\varepsilon_{CEA}$	$C_{ZnPc} = A_{ZnPc}/\varepsilon_{ZnPc}$	C_{ZnPc}/ C_{CEA}
5.40	2.560×10^{-7}	1.918×10^{-6}	7
5.45	2.970×10^{-7}	2.816×10^{-6}	9
5.47	1.454×10^{-6}	2.199×10^{-6}	2

The concentrations for the above conjugates were obtained using samples which had been diluted five times. Therefore, the actual Pc concentrations are 3.8×10^{-5}, 5.6×10^{-5} and 4.2×10^{-5} M for Pc-antiCEA conjugates **5.40**, **5.45** and **5.47** respectively. ZnPc **5.44** (5.0×10^{-5} M) was

used as the control. The ZnPc/CEA ratio was determined by the measurements of absorbance at 280 nm to estimate the concentration of antibody and absorbance at 353 nm, 337 nm and 338 nm to estimate the concentration of Pc **5.39**, **5.44** and **5.46** respectively. The molar antibody and ZnPc concentrations were calculated by the formula $C_{CEA}=[A_{280nm} - (0.5 \times A_{ZnPc})]/\varepsilon_{CEA}$, $C_{ZnPc} = A_{ZnPc}/\varepsilon_{ZnPc}$ according to the literature;[47,52,54] with ε_{CEA} = 223,045 ($M^{-1}cm^{-1}$), $\varepsilon_{Pc\mathbf{5.46}}$ = 49,471 ($M^{-1}cm^{-1}$), $\varepsilon_{Pc\mathbf{5.39}}$ = 40040 ($M^{-1}cm^{-1}$ and $\varepsilon_{Pc\mathbf{5.44}}$ = 48784 ($M^{-1}cm^{-1}$). The extinction coefficients of the ZnPcs were determined by dissolving the non-conjugated ZnPcs in 0.1 M $NaHCO_3$ containing 0.1% DMSO.

5.2.6. Preliminary Animal Studies

The ZnPc conjugate **5.45** with Pc concentrations of 5.6×10^{-5} M for Pc-antiCEA conjugate, and ZnPc **5.44** (5.0×10^{-5} M) as a control, were used in the study. Both the conjugate and the unconjugated ZnPc were both visible in the tumor at 1 h and diffused slightly by 6 h (Figure 5.10 and 5.11 respectively). There was appreciable regional tissue retention of the Pc-CEA conjugate **5.45** in the tumor at 24 h, while Pc alone showed dissipation. At 96 h post injection, the dyes were not detectable, contrary to the observations made earlier in Chapter 3, where Pc-EFGR-L1 conjugate **3.11** was used during *in vivo* studies. Of all the Pcs prepared, **5.45** was chosen for preliminary studies in mice due to the low DOL of ZnPc **5.47** and the apparently lower fluorescence intensity of ZnPc **5.40**.

After injection of Pc-antiCEA conjugate **5.45** and Pc **5.44** into a non-tumor bearing mouse, both dyes were retained for a few hours, but diffused away within 24 hours (Figure 5.12). This result suggests that the antiCEA in Pc-antiCEA conjugate **5.45** enhances the targeting specificity after intratumoral injection. The result is in agreement with our previous observations in Chapter 3, that peptide conjugate can enhance the targeting ability of photosensitizers.

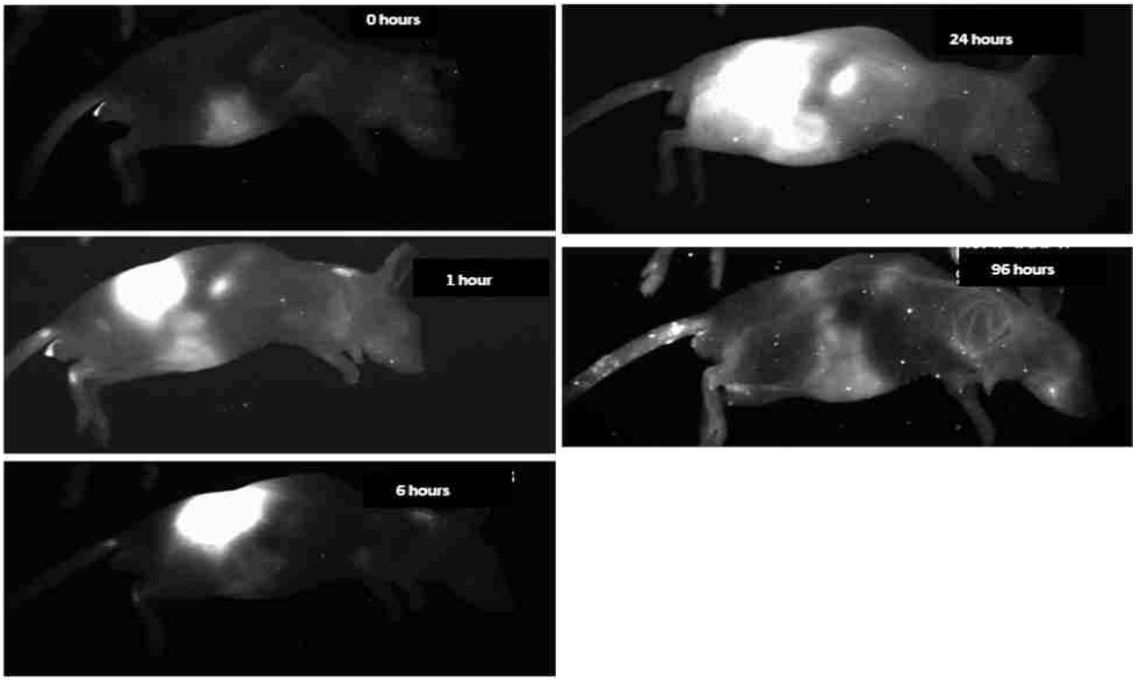

Figure 5.10. Fluorescent images (exc 630 nm/em 700 nm) of nude mice bearing subcutaneous tumor implants of HT-29 cancer cells taken at various times following intratumoral administration of Pc-antiCEA conjugate **5.45**.

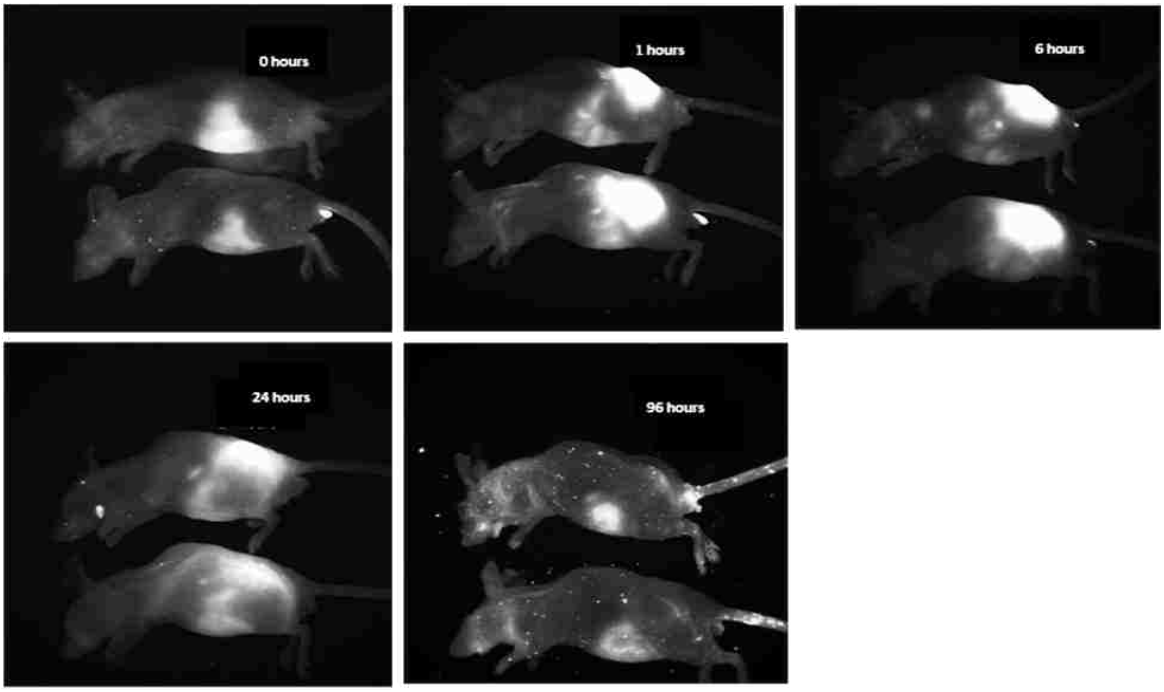

Figure 5.11. Fluorescent images (exc 630 nm/em 700 nm) of nude mice bearing subcutaneous tumor implants of HT-29 cancer cells taken at various times following intratumoral administration of Pc **5.44** alone.

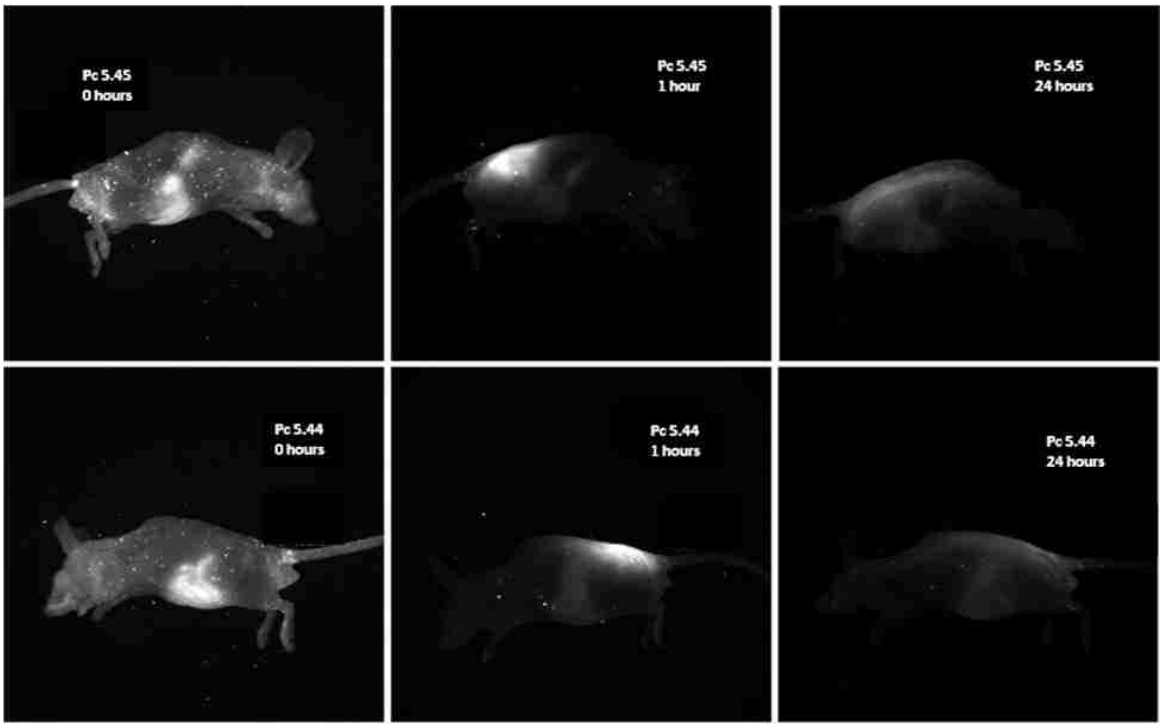

Figure 5.12. Fluorescent images (exc 630 nm/em 700 nm) of nude mice bearing no tumor implants of cancer cells, taken at various times following intratumoral administration of Pc-antiCEA conjugate **5.45** and Pc **5.44** in mice.

5.3. Conclusions

Ten dicationic ZnPcs were investigated in human carcinoma HEp2 cells for their biological properties for possible *in vivo* applications. The ZnPcs were A_3B-type, synthesized via statistical condensation of two different phthalonitriles. The Pcs with the cationic charge non-peripherally substituted on the ring were found to be more phototoxic (> 5-fold) than their peripherally substituted counterparts. ZnPc **5.27** was more phototoxic (IC_{50} = 8.7 μM at 1.5 J/cm^2) than **5.4** (IC_{50} = 10.7 μM), although their localization in the ER and favorable interaction with important biological targets made them the most phototoxic among the series. In addition, a PEG group on the macrocycle and/or the positive charges in close proximity are likely to boost phototoxicity. Markedly, the β-substituted ZcPcs **5.15** and **5.17** accumulated the most within HEp2 cells. It can be concluded that it is the position of the charge on the Pc macrocycle (α-

substitution and close proximity of charges) and the subcellular localization of the positively charged ZnPcs, and not the degree of their cellular uptake, which determine their photodynamic activity for the synthesized ZnPcs.

The antiCEA conjugate investigations have also shown that Pc-antiCEA conjugates can be used for near-IR fluorescence imaging of cancers over-expressing CEA, such as CRC. Due to the hydrophobic nature of the Pc macrocycle, two low molecular PEG linkers were required for adequate aqueous solubility and receptor targeting ability. Pc-antiCEA conjugate **5.45** had equivalent or superior tumor uptake and retention compared to uncoupled Pc **5.44** after intratumoral injection. Both dyes diffused regionally after injection and then dissipated within 24 h in non-tumor mice.

5.4. Methods and Materials

5.4.1. Syntheses

The reagents and solvents were all obtained from suppliers and used without additional purification. Antibody, mAb to Carcinoembryonic Ag Monoclonal Antibody to Human Carcinoembryonic Antigen (CEA), was obtained from Meridian Life Science Inc. (catalog # H45655M, 5.71 mg/mL, OD 280 nm). MicroSpin^{TM} G-25 Columns were bought from Amersham Biosciences. Purification of conjugates was performed on an AccuSpin Micro 17 Centrifuge (Fisher Scientific) at 25 °C. Silica chromatographic gel 60 (230×400 mesh, Sorbent Technologies), Sephadex G-100 and LH-20 (Amersham Biosciences) were used for purification of the ZnPcs. Thin-layer chromatography (TLC) for analytical purposes was carried out using polyester backed TLC plates 254 (precoated, 200 μm) from Sorbent Technologies. The NMR spectroscopy was performed using an AV-400 LIQUID Bruker spectrometer (400 MHz for ^{1}H, 100 MHz for ^{13}C). The chemical shifts were reported in δ ppm with the following deuterated

solvents as internal orientation: DMF-d_7 8.03 ppm (^{1}H), 163.15 ppm (^{13}C); CD_3COCD_3 2.04 ppm (^{1}H), 29.92 ppm (^{13}C); THF-d_8 3.58 ppm (^{1}H), 67.57 ppm (^{13}C); $CDCl_3$ 7.27 ppm (^{1}H), 77.23 ppm (^{13}C); DMSO-d_6 2.50 ppm (^{1}H), 39.51 ppm (^{13}C). MALDI-TOF mass spectra were performedd on a Bruker UltrafleXtreme (MALDI-TOF/TOF) with 4-chloro-α-cyanocinnamic acid as the matrix. The high resolution ESI mass spectra were recorded using Agilent Technologies 6210 TOF LC/MS spectrometer. The UV-vis spectra were measured on a UV-vis NIR scanning spectrophotometer; a 10 mm path length quartz cuvette was used. The stock solutions (1.0 mM, 1.0 mL each) of all the ZnPcs in HPLC grade DMF solvent were diluted by spiking 20 – 80 µL of each stock solution into DMF (10 mL) and their absorbances recorded. Emissions were recorded on a Fluorolog® - HORIBA JOBINVYON, Model LFI-3751 spectrofluorimeter. The optical densities were kept within 0.04 – 0.05 at excitation wavelengths for the solutions used in emission studies to minimize re-absorption by the photosensitizers. The experiments were performed within 4 h after solution preparation between 23-25 °C. The ZnPcs **5.1**, **5.2**, **5.12** and **5.13** were synthesized as described previously in Chapters 2 and 3.

ZnPc 5.3. To a mixture of ZnPc **5.2** (20.0 mg, 0.017 mmol) in DMF (0.4 mL) were added in the sequence: Et_3N (3.3 mg, 0.032 mmol), HOBt (4.7 mg, 0.035 mmol), 1,4-bis-Boc-triazaheptane (7 mg, 0.023 mmol), and EDCI (4.0 mg, 0.026 mmol). The mixture was stirred at 25 °C for 4 days, diluted with ethyl acetate (40 mL) and washed with water (2 × 20 mL). The organic phase was dried over anhydrous Na_2SO_4 and the solvent removed under reduced pressure. The crude product was purified by column chromatography using DCM/methanol for elution, to afford a blue solid (20.2 mg, 81.8%). ^{1}H NMR (DMSO-d_6): δ 9.33-9.03 (m, 6H, Ar-H), 8.30-8.07 (m, 5H, Ar-H), 7.84-7.44 (m, 5H, Ar-H), 7.20 (br, 1H, N-H), 6.79 (br, 1H, N-H), 4.14-3.98 (m, 4H, CH_2O), 3.53-3.50 (m, 4H, CH_2O), 3.44-3.38 (m, 12H, CH_2NH), 3.36-3.22 (m,

2H, CH_2NH), 3.00 (br, 2H, CH_2NH), 2.31-2.20 (m, 2H, CH_2CO), 1.80–1.76 (m, 27H, $C(CH_3)_3$), 1.37-1.34 (m, 18H, -$OC(CH_3)_3$). ^{13}CNMR (DMSO-d_6): δ 171.0, 170.1, 168.9, 167.4, 167.3 (C=O), 155.6, 155.3, 154.7, 152.9, 152.6, 151.5, 150.8, 150.4, 150.2, 140.2, 138.1, 137.9, 137.6, 135.8, 135.2, 133.1, 132.4, 130.6, 128.3, 127.4, 127.0, 122.5, 122.0, 121.8, 121.5, 118.9, 118.6, 117.7, 117.4, 115.8 (Ar-C), 78.5, 77.5 (-$OC(CH_3)_3$), 70.6, 70.5, 70.4, 69.6, 69.5, 68.8, 66.7 (OCH_2), 46.7, 46.2, 38.2, 36.1, 35.7, 35.6 (N-CH_2), 31.8 (Ar-$C(CH_3)_3$), 28.2, 28.0 (O-$C(CH_3)_3$). MS (MALDI-TOF) *m/z* 1455.650 $[M]^+$, calcd for $C_{77}H_{93}N_{13}O_{12}Zn$ 1455.636. The blue solid (20.2 mg, 0.014 mmol) was dissolved in a 1:1 mixture of DCM/trifluoroacetic acid (TFA) (6 mL) and stirred at 0 °C for 3 h. Solvent was removed and the residue treated with 2N NaOH (10 mL) to afford the title ZnPc as a blue solid (15.5 mg, 89.0 %). ^{1}H NMR (DMF-d_7): δ 9.59-9.07 (m, 6H, Ar-H), 8.41-8.32 (m, 4H, Ar-H), 8.12-8.06 (m, 1H, Ar-H), 7.92-7.85 (m, 2H, Ar-H), 7.60-7.53 (m, 2H, Ar-H), 6.96 (br, 1H, N-H), 4.23-4.10 (m, 4H, CH_2O), 3.57-3.28 (m, 20H, CH_2O), 2.13-2.03 (m, 2H, CH_2CO), 1.79-1.75 (m, 27H, $C(CH_3)_3$). ^{13}CNMR (DMF-d_7): δ 171.2, 171.1, 170.4, 168.8, 168.7, 157.3, 156.8, 155.9, 155.7, 155.5, 155.4, 155.0, 154.8, 154.6, 154.3, 154.2, 153.9, 153.7, 152.9, 152.7, 152.3, 152.1, 142.6, 140.1, 139.8, 137.7, 137.4, 134.7, 134.3, 131.7, 131.5, 130.6, 128.50, 128.3, 124.0, 123.6, 123.4, 123.2, 122.6, 122.4, 120.7, 120.1, 120.0, 119.8, 119.6, 119.0118.3, 117.6, 117.1 (Ar-C), 72.4, 72.13, 72.08, 71.1, 71.0, 70.9, 70.24, 70.20, 68.3, 68.0 (O-$C(CH_3)_3$), 48.9, 48.7, 39.6, 39.3, 38.7, 37.5, 37.3, 36.8 (N-CH_2), 32.7, 32.6 (m, 27H, $C(CH_3)_3$). MS (MALDI-TOF) *m/z* 1255.633 $[M]^+$, calcd for $C_{67}H_{77}N_{13}O_8Zn$ 1255.531. UV-vis (DMF): λ_{max} (log ε) 350 (5.00), 612 (4.77), 680 (5.52) nm.

ZnPc 5.4. ZnPc **5.3** (20.0 mg, 0.015 mmol), DIPA (0.015 mL, 0.107 mmol) and CH_3I (0.2 mL) were dissolved in dry DMF (0.5 mL), and the final solution stirred at 25 °C for 2 days. The solvent was removed under reduced pressure and the resulting residue purified by Sephadex

G-100 using DCM/methanol to afford a blue solid (17.2 mg, 68.3%). ^{1}H NMR (DMF-d_7): δ 9.57-9.06 (m, 7H, Ar-H), 8.38-8.18 (m, 5H, Ar-H), 7.94-7.84 (m, 3H, Ar-H), 7.61-7.54 (m, 2H, Ar-H), 4.29-4.13 (m, 8H, CH_2O), 3.62-3.44 (m, 18H, CH_2O/N-CH2/N-CH_3), 3.28 (s, 9H, N-CH_3), 2.47-2.30 (m, 2H, $COCH_2$), 1.78 (s, 27H, $C(CH_3)_3$). ^{13}C NMR (DMF-d_7): δ 172.6, 170.5, 168.8, 168.7 (C=O), 157.1, 156.4, 155.8, 155.5, 155.3, 154.5, 154.2, 154.1, 153.9, 153.8, 153.5, 152.8, 152.7, 152.3, 142.7, 140.3, 140.2, 139.9, 137.8, 137.5, 134.9, 134.4, 131.4, 130.5, 129.7, 128.3, 128.1, 123.5, 123.3, 123.2, 123.1, 122.7, 122.5, 121.9, 120.4, 120.0, 119.8, 119.7, 118.9, 117.5 (Ar-C), 72.2, 72.0, 71.1, 71.0, 67.9 (CH_2O), 64.6, 64.4, 58.6, 57.1, 54.3, 52.4 (N-CH_3), 39.6, 37.3, 36.8 (N-CH_2) 32.7, 32.6 ($C(CH_3)_3$). MS (MALDI-TOF) *m*/*z* 1493.711 $[M-I+K]^+$, 1441.654 $[M-I-CH_3+H]^+$; calcd for $C_{72}H_{89}IKN_{13}O_8Zn^+$ 1493.493, $C_{71}H_{88}IN_{13}O_8Zn^+$ 1441.522. UV–Vis (DMF): λ_{max} (log ε) 348 (4.81), 611 (4.55), 679 (5.32) nm.

ZnPc 5.5. A procedure related to that described for ZnPc **5.3** was used: ZnPc **5.1** (40.0 mg, 0.04 mmol), DMF (0.5 mL), Et_3N (5.2 mg, 0.051 mmol), HOBt (7.5 mg, 0.055 mmol), 1,4-bis-Boc-triazaheptane (15.5 mg, 0.051 mmol) and EDCI (9.8 mg, 0.051 mmol). The protected ZnPc was achieved as a blue solid (38.6 mg, 77.0%). ^{1}H N MR (DMF-d_7): δ 9.60-9.03 (m, 6H, Ar-H), 8.40-8.20 (m, 5H, Ar-H), 7.96-7.79 (m, 3H, Ar-H), 7.61–7.50 (m, 2H, Ar-H), 6.73 (br, 1H, N-H), 4.26–4.12 (m, 4H, CH_2O), 3.38–3.26 (m, 6H, CH_2NH), 3.20–3.16 (m, 2H, CH_2NH), 1.82–1.78 (m, 27H, $C(CH_3)_3$), 1.42–1.32 (m, 18H, -$OC(CH_3)_3$). ^{13}C NMR (DMF-d_7): δ 170.4, 168.6 (C=O), 157.1, 156.8, 156.5, 156.2, 155.5, 155.4, 155.3, 155.2, 155.0, 154.6, 154.4, 154.3, 154.2, 154.1, 153.5, 152.5, 152.1, 142.3, 140.0, 139.9, 139.6, 137.6, 137.5, 137.2, 135.0, 134.5, 131.7, 130.1, 129.4, 128.6, 128.4, 123.6, 123.5, 122.7, 122.5, 122.0, 120.4, 120.1, 120.0, 119.8, 119.7, 119.0, 118.9, 117.5 (Ar-C), 79.9, 78.7 (-$OC(CH_3)_3$), 72.3, 72.0 (OCH_2), 48.4, 48.2, 47.6, 40.0, 39.8, 38.4, 36.8 (N-CH_2), 32.7, 32.6 (Ar-$C(CH_3)_3$), 28.9, 28.8 (O-$C(CH_3)_3$). MS (MALDI-

TOF) *m/z* 1053.438 $[M\text{-}2Boc+H]^+$, calcd for $C_{58}H_{61}N_{12}O_4Zn$ 1053.423. The blue solid (51.6 mg, 0.044 mmol) was dissolved in 1:1 DCM/TFA (6 mL) and stirred at 0 °C for 3 h. The solvent was evaporated and the residue treated with 2N NaOH (10 mL) to obtain a blue-greenish solid (38.2 mg, 89.2 %). ^{1}H NMR (DMF-d_7): δ 9.62-9.12 (m, 7H, Ar-H), 8.63-8.31 (m, 5H, Ar-H), 7.99–7.88 (m, 3H, Ar-H), 7.65–7.58 (m, 2H, Ar-H), 4.29–4.17 (m, 4H, CH_2O), 4.01 (br, 4H, NH_2), 3.63–3.55 (m, 6H, CH_2NH), 3.38–3.35 (m, 2H, CH_2NH), 1.81 (s, 27H, $C(CH_3)_3$). ^{13}C NMR (DMF-d_7): δ 171.4, 168.6 ,168.5 (C=O), 161.2, 160.9, 160.6, 160.2, 157.1, 156.4, 155.9, 155.8, 155.6, 155.5, 154.9, 154.8, 154.7, 154.6,154.0, 153.8, 153.7, 153.6, 153.3, 152.7, 152.3, 142.8, 140.5, 140.3, 140.0, 138.0, 137.9, 137.6, 134.8, 134.3, 131.2, 130.5, 129.9, 128.1, 127.9, 123.4, 123.2, 122.9, 122.7, 122.5, 121.9, 120.3, 120.0, 119.8, 119.7, 119.6, 118.7, 117.4, 116.8 (Ar-C), 72.1, 71.8 (OCH_2), 48.4, 46.0, 37.3, 36.7 ($N\text{-}CH_2$), 32.7, 32.5 ($Ar\text{-}C(CH_3)_3$). MS (MALDI-TOF) *m/z* 1053.433 $[M+H]^+$, calcd for $C_{58}H_{61}N_{12}O_4Zn$ 1053.423. UV-vis (DMF): λ_{max} (log ε) 350 (4.66), 612 (4.42), 680 (5.19) nm.

ZnPc 5.6. A procedure related to that described for ZnPc **5.4** was used: ZnPc **5.5** (20.0 mg, 0.021 mmol), DIPA (0.015 mL, 0.107 mmol), CH_3I (0.2 mL) and dry THF (0.5 mL). The product was attained as a pale-green solid (14.7 mg, 53.3%). ^{1}H NMR (DMF-d_7): δ 9.56-9.06 (m, 6H, Ar-H), 8.36-8.24 (m, 4H, Ar-H), 7.96-7.80 (m, 4H, Ar-H), 7.58-7.51 (m, 2H, Ar-H), 4.34-4.13 (m, 8H, $CH_2O/N\text{-}CH_2$), 3.80-3.67 (m, 4H, $N\text{-}CH_2$), 3.62-3.47 (m, 6H, $N\text{-}CH_3$), 3.41-3.27 (m, 9H, $N\text{-}CH_3$), 1.79-1.71 (m, 27H, $C(CH_3)_3$). ^{13}C NMR (DMF-d_7): δ 171.3, 168.7, 168.6, 168.4, 157.2, 156.7, 155.9, 155.8, 155.7, 155.6, 155.5, 155.43, 155.36, 155.1, 155.0, 154.9, 154.8, 154.7, 154.6, 154.5, 154.1, 154.0, 153.8, 153.7, 153.6, 153.5, 153.2, 152.7, 152.63, 152.55, 152.33, 152.27, 152.2, 142.8, 140.4, 140.3, 140.0, 137.9, 137.6, 134.7, 134.3, 133.4, 132.5, 131.8, 131.4, 130.6, 129.9, 128.3, 128.0, 123.4, 123.3, 123.2, 123.0, 122.6, 122.4, 120.5,

120.0, 119.9, 119.8, 119.7, 119.6, 119.5, 118.6, 117.3 (Ar-C), 72.0, 71.9, 71.8, 71.4 (CH_2O), 66.9, 66.6, 64.9, 64.5, 58.6, 58.5, 57.1, 54.3, 52.40, 52.35 (N-CH_3), 36.8, 36.7 (N-CH_2) 32.7, 32.6 ($C(CH_3)_3$). MS (MALDI-TOF) *m/z* 1238.544 $[M\text{-}I\text{-}CH_3+2H]^+$, calcd for $C_{62}H_{71}IN_{12}O_4Zn$ 1238.406. UV–Vis (DMF): λ_{max} (log ε) 357 (4.72), 611 (4.46), 679 (5.23) nm

ZnPc 5.7. A procedure related to that described for ZnPc **5.3** was used: ZnPc **5.1** (50.0 mg, 0.05 mmol), DMF (0.8 mL), Et_3N (6.2 mg, 0.061 mmol), HOBt (9.3 mg, 0.069 mmol), aspartic acid di-*tert*-butyl ester hydrochloride (18 mg, 0.064 mmol) and EDCI (12.3 mg, 0.064 mmol). The crude was purified on a silica column chromatography eluted by DCM/methanol (98/2), to give the di-ester ZnPc as a blue solid (0.052 g, 87.1%). ^{1}H NMR (DMF-d_7): δ 10.09, 10.05 (s, 1H, N-H), 9.63-9.28 (m, 6H, Ar-H), 9.19-9.01 (m, 1H, Ar-H), 8.47-8.20 (m, 5H, Ar-H), 7.97-7.79 (m, 3H, N-H), 7.62-7.47 (m, 2H, N-H), 4.55-4.45 (m, 1H, N-H), 4.28-4.19 (m, 4H, CH_2O), 2.96-2.67 (m, 3H, CH_2), 1.81–1.77 (m, 27H, $C(CH_3)_3$), 1.45-1.36 (m, 18H, -$OC(CH_3)_3$). ^{13}C NMR (DMF-d_7): δ 170.9, 170.7, 170.4, 170.0, 168.7 (C=O), 156.8, 156.2, 155.6, 155.4, 154.5, 154.3, 154.1, 153.6, 152.5, 152.2, 142.3, 140.0,139.9, 139.6, 1137.5, 137.5, 137.2, 135.2, 134.6, 131.8, 130.2, 129.5, 128.8, 128.5, 123.7, 123.5, 123.3, 122.5, 122.3, 120.4, 120.1, 119.9, 119.7, 119.0, 117.6 (Ar-C), 82.4, 81.7 (-$OC(CH_3)_3$), 72.3, 71.9 (OCH_2), 50.4, 38.4, 36.8 (N-CH_2), 32.7, 32.6 (Ar-$C(CH_3)_3$), 28.4, 28.3 (O-$C(CH_3)_3$). MS (MALDI-TOF) *m/z* 1083.625 $[M\text{-}2C_4H_9+H]^+$, calcd for $C_{58}H_{55}N_{10}O_8Zn$ 1083.350. The solid (0.052 g, 0.044 mmol) was dissolved in 1:1 DCM/TFA (8 mL) and stirred for 4 h at 0°C. The tert-butyl group was removed as described for ZnPc **5.5** to give the product as a blue solid (34.3 mg, 82.3 %). (MALDI-TOF) *m/z* 1195.180 $[M+Na]^+$, calcd for $C_{58}H_{54}N_{10}NaO_8Zn$ 1105.332. UV-vis (DMF): λ_{max} (log ε) 349 (4.68), 612 (4.41), 679 (5.17) nm.

ZnPc 5.8. A procedure related to that described for ZnPc **5.3** was used: ZnPc **5.7** (18.4 mg, 0.017 mmol), DMF (0.5 mL), Et_3N (6.2 mg, 0.061 mmol), HOBt (5.7 mg, 0.042 mmol), *N*-Boc-2,2′-(ethylenedioxy)diethylamine (9.4 mg, 0.038 mmol) and EDCI (6.5 mg, 0.042 mmol). The crude was purified on a silica column eluted by DCM/methanol (95:5) to obtain a blue solid (13.6 mg, 51.9 %). ^{1}H NMR (DMF-d_7): δ 9.59-9.08 (m, 6H, Ar-H), 8.50-8.27 (m, 5H, Ar-H), 7.99-7.74 (m, 5H, Ar-H), 7.61-7.53 (m, 2H, Ar-H), 6.65 (br, 1H, Ar-H), 4.77–4.71 (m, 1H, NHCH(CH_2)CO), 4.28–4.16 (m, 4H, CH_2O), 3.48–3.36 (m, 14H, CH_2O), 3.31–3.16 (m, 8H, CH_2O), 2.75–2.67 (m, 2H, $CHCH_2CO$), 1.81–1.76 (m, 27H, $C(CH_3)_3$), 1.37 (s, 18H, $OC(CH_3)_3$). ^{13}C NMR (DMF-d_7): δ 171.90, 171.86, 171.35, 171.28, 170.3, 168.7, 168.6 (C=O), 157.1, 155.4, 155.3, 154.5, 153.6, 152.6, 142.4, 140.0, 137.6, 135.1, 134.6, 132.5, 131.8, 129.9, 128.7, 123.4, 122.6, 122.4, 120.1, 119.0, 117.6 (Ar-C), 78.7 ($OC(CH_3)_3$), 72.1, 71.9, 71.0, 70.95, 70.7, 70.4, 70.3 (CH_2O), 51.1 (NHCH(CH_2)CO), 41.2, 40.1, 38.4, 36.8 (CH_2), 32.7, 32.6 ($C(CH_3)_3$), 28.9 ($OC(CH_3)_3$). MS (MALDI-TOF) *m/z* 1542.669 $[M]^+$, calcd for $C_{80}H_{98}N_{14}O_{14}Zn$ 1542.668. The solid ZnPc (13.1 mg, 8.5 mmol) was dissolved in DCM/TFA (1:1) and stirred at 0°C for 3 h. The solvent was evaporated and the residue treated with 2N NaOH (10 mL) to obtain a blue solid (10.5 mg, 92.3%). ^{1}H NMR (DMF-d_7): δ 9.60-9.10 (m, 7H, Ar-H), 8.60-8.29 (m, 5H, Ar-H), 7.95-7.87 (m, 2H, Ar-H), 7.56–7.51 (m, 2H, Ar-H), 4.56 (br, 1H, NH), 4.21 (d, 9.48 Hz, 2H, CH_2O), 4.16 (d, 8.92 Hz, 2H, CH_2O), 3.75–3.35 (m, 10H, CH_2O), 3.16–2.95 (m, 9H, CH_2O), 2.90–2.80 (m, 3H, CH_2O), 2.90–2.80 (m, 3H, CH_2O), 2.62-2.47 (m, 2H, CH_2), 2.19 (br, 2H, NH_2), 1.80–1.74 (m, 27H, $C(CH_3)_3$). ^{13}C NMR (DMF-d_7): δ 171.8, 171.3, 171.2, 170.2, 168.6, 168.5, 157.7, 157.4, 155.9, 155.6, 155.5, 155.0, 154.3, 154.2, 154.1, 154.0, 153.7, 152.4, 151.7, 142.4, 140.1, 139.8, 137.7, 137.3, 134.4, 134.1, 131.7, 130.8, 128.5, 123.7, 123.4, 123.1, 122.5, 122.3, 120.1, 120.0, 119.8, 117.6, 116.7 (Ar-C), 72.0, 71.8, 71.5, 71.0, 70.5, 70.4, 70.0 (N-CH),

51.2 (NHCH(CH_2)CO), 40.9, 39.9, 39.8, 38.1, 36.8 (CH_2), 32.7, 32.6 (C(CH_3)$_3$). MS (MALDI-TOF) *m/z* 1343.610 $[M+H]^+$, calcd for $C_{70}H_{83}N_{14}O_{10}Zn$ 1343.571. UV-vis (DMF): λ_{max} (log ε) 349 (4.70), 612 (4.45), 680 (5.20) nm.

ZnPc 5.9. A procedure related to that described for ZnPc **5.4** was used: ZnPc **5.8** (20.0 mg, 0.015 mmol), DIPA (0.015 mL, 0.107 mmol), CH_3I (0.2 mL) and dry DMF (0.5 mL). The product was attained as a blue solid (17.2 mg, 68.3%). ^{1}H NMR (DMF-d_7): δ 9.57-9.33 (m, 5H, Ar-H), 9.20-9.05 (m, 1H, Ar-H), 8.52-8.28 (m, 4H, Ar-H), 7.95-7.84 (m, 4H, Ar-H), 7.61-7.52 (m, 2H, Ar-H), 4.31-4.11 (m, 4H, OCH_2), 3.93 (br, 2H, NH), 3.71-3.40 (m, 27H, OCH_2/N-CH_3), 3.33-3.29 (m, 10H, N-CH_3), 1.80-1.76 (m, 27H, C(CH_3)$_3$). MS (MALDI-TOF) *m/z* 1427.749 $[M-2I-H]^+$, calcd for $C_{76}H_{95}N_{14}O_{10}Zn^+$ 1427.665. UV–Vis (DMF): λ_{max} (log ε) 348 (4.48), 612 (4.23), 680 (5.01) nm.

ZnPc 5.10. A procedure related to that described for ZnPc **5.3** was used: ZnPc **5.7** (18.4 mg, 0.017 mmol), DMF (0.5 mL), Et_3N (6.2 mg, 0.061 mmol), HOBt (5.7 mg, 0.042 mmol), *N*-Boc-ethylenediamine (6.1 mg, 0.038 mmol) and EDCI (6.5 mg, 0.042 mmol). The mixture was stirred for 4 days at 25 °C. The solvent was evaporated and the residue treated with 2N NaOH (10 mL) to obtain a blue solid (13.4 mg, 57.8 %). ^{1}H NMR (DMF-d_7): δ 9.59-9.21 (m, 6H, Ar-H), 8.45-8.23 (m, 4H, Ar-H), 8.12-7.82 (m, 3H, Ar-H), 7.62–7.52 (m, 2H, Ar-H), 6.73-6.66 (m, 2H, Ar-H), 4.75-4.71 (m, 1H, NH), 4.28–4.18 (m, 4H, CH_2O), 3.29–3.11 (m, 8H, CH_2NH), 2.70-2.65 (m, 2H, CH_2CO), 1.81–1.77 (m, 27H, C(CH_3)$_3$), 1.41–1.34 (m, 18H, C(CH_3)$_3$). ^{13}C NMR (DMF-d_7): *δ* 172.1, 172.0, 171.5, 171.4, 170.3, 168.7, 168.6, 157.2, 157.1, 155.6, 155.4, 155.2, 154.4, 154.1, 153.7, 153.6, 152.6, 152.3, 142.3, 139.9, 139.7, 137.6, 137.2, 135.1, 134.6, 131.8, 130.1, 129.4, 128.6, 128.5, 123.5, 122.6, 122.4, 122.0, 120.1, 119.7, 119.1, 119.0, 117.7 (Ar-C), 78.8 (OC(CH_3)$_3$), 72.2, 71.9 (CH_2O), 51.3, 51.2 (NHCH(CH_2)CO), 41.0, 40.5, 40.4, 38.8, 36.8

(CH_2), 32.7, 32.6 ($C(CH_3)_3$), 28.9 ($OC(CH_3)_3$). MS (MALDI-TOF) *m/z* 1166.466 $[M\text{-}2Boc]^+$, 1189.469 $[M\text{-}2Boc+Na]^+$, 1205.444 $[M\text{-}2Boc+K]^+$, calcd for $C_{62}H_{66}N_{14}O_6Zn$ 1166.4581, $C_{62}H_{66}NaN_{14}O_6Zn$ 1189.4479, $C_{62}H_{66}KN_{14}O_6Zn$ 1206.4218 respectively. The ZnPc (13.1 mg, 0.0096 mmol) was dissolved in a mixture of DCM/TFA (1:1) at 0 °C for 3h. The solvent was evaporated and the residue treated with 2N NaOH (10 mL) to obtain a blue solid (10.1 mg, 90.1%). ^{1}H NMR (THF-d_8): δ 9.58-9.08 (m, 7H, Ar-H), 8.39-8.07 (m, 4H, Ar-H), 7.82-6.86 (m, 5H, Ar-H), 4.15-3.76 (m, 4H, CH_2O), 3.57–3.20 (m, 8H, CH_2NH), 2.28-2.13 (m, 2H, CH_2CO), 1.80–1.72 (m, 27H, $C(CH_3)_3$). ^{13}C NMR (DMF-d_7): δ 171.2, 171.0, 169.6, 168.2, 157.7, 155.8, 155.7, 155.0, 154.4, 153.9, 153.5, 151.6, 142..4, 140.1,139.8, 139.5, 137.7, 137.2, 133.4, 131.9, 130.4, 128.5, 128.3, 123.9, 123.4, 122.2, 121.9, 120.8, 120.4, 119.9, 119.8, 117.1, 116.6 (Ar-C), 71.7, 71.6 (CH_2NH), 50.7 ($NHCH(CH_2)CO$), 40.7, 40.2, 36.8, 36.7 (CH_2), 32.8, 32.7, 32.6 ($C(CH_3)_3$). MS (MALDI-TOF) *m/z* 1166.503 $[M\text{-}2Boc]^+$, calcd for $C_{62}H_{66}N_{14}O_6Zn$ 1166.4581. UV-vis (DMF): λ_{max} (log ε) 349 (4.72), 613 (4.48), 680 (5.23) nm.

ZnPc 5.11. A procedure related to that described for ZnPc **5.4** was used: ZnPc **5.10** (20.0 mg, 0.017 mmol), DIPA (0.015 mL, 0.107 mmol), CH_3I (0.2 mL) and dry THF (0.5 mL). After purification, the title ZnPc was obtained (15.2 mg, 58.9%). ^{1}H NMR (DMF-d_7): δ 9.56-8.80 (m, 10H, Ar-H), 8.38-8.24 (m, 4H, Ar-H), 7.96-7.85 (m, 3H, Ar-H), 7.62-7.54 (m, 2H, Ar-H), 7.16 (d, 8.6Hz, 1H, Ar-H), 6.90 (d, 8.2Hz, 1H, Ar-H), 4.22-4.09 (m, 4H, OCH_2), 3.38-3.29 (m, 8H, N-CH_2), 3.11-3.02 (m, 18H, N-CH_3), 1.92-1.73 (m, 27H, $C(CH_3)_3$). ^{13}C NMR (d-DMF): δ 172.8, 172.7, 171.7, 170.8, 168.9, 168.8 (C=O), 157.9, 155.9, 155.7, 155.4, 154.9, 153.9, 153.8, 153.6, 144.2, 142.9, 140.4, 140.1, 138.0, 137.7, 134.7, 134.2, 128.7, 128.1, 123.4, 123.2, 122.8, 122.7, 119.8, 119.7, 119.5, 118.4, 117.3, 115.0 (Ar-C), 72.2, 71.9, 70.5, 65.4, 64.4 (N-CH_2), 53.9, 53.6

(N-CH_3), 32.7, 32.6 ($C(CH_3)_3$). MS (MALDI-TOF) *m/z* 1209.761 $[M\text{-}3CH_3\text{-}2I]^+$, calcd for $C_{65}H_{73}N_{14}O_6Zn^+$ 1209.513. UV–Vis (DMF): λ_{max} (log ε) 348 (4.65), 612 (4.42), 679 (5.19) nm.

ZnPc 5.14. A procedure related to that described for ZnPc **5.3** was used: ZnPc **5.13** (20.0 mg, 0.017 mmol), DMF (0.4 mL), Et_3N (3.2 mg, 0.032 mmol), HOBt (4.7 mg, 0.035 mmol), 1,4-bis-Boc-triazaheptane (7 mg, 0.023 mmol) and EDCI (4.0 mg, 0.026 mmol). The crude was purified as described above to obtain a blue solid (19.7 mg, 79.6%). ^{1}H NMR (DMF-d_7): δ 9.32-8.67 (m, 8H, Ar-H), 8.35-8.30 (m, 4H, Ar-H), 8.15-8.04 (m, 2H, Ar-H), 7.94-7.82 (m, 2H, Ar-H), 7.64-7.59 (m, 2H, Ar-H), 6.90 (br, 1H, N-H), 4.39 (d, J = 13.6, 2H, CH_2O), 4.30 (d, J = 9.76, 2H, CH_2O), 3.73-3.68 (m, 4H, CH_2O), 3.62-3.56 (m, 14H, CH_2O), 3.51-3.47 (m, 2H, CH_2NH), 3.35-3.19 (m, 8H, CH_2NH), 2.47-2.42 (m, 2H, CH_2CO), 1.86–1.82 (m, 27H, $C(CH_3)_3$), 1.45-1.36 (m, 18H, -$OC(CH_3)_3$). ^{13}C NMR (DMF-d_7): δ 172.4, 171.5, 170.6, 169.2, 169.1 (C=O), 161.0, 160.4, 157.1, 156.3, 154.4, 153.9, 139.1, 138.9, 136.7, 136.3, 133.7, 128.7, 125.3, 123.5, 122.8, 122.0, 121.5, 121.1, 120.8, 120.3, 115.0, 112.8, 111.6 (Ar-C), 79.9, 78.7 (O-$C(CH_3)_3$), 72.4, 72.20, 72.16, 71.3, 71.2, 71.12, 71.06, 70.4, 68.2, 67.9 (OCH_2), 48.6, 48.3, 46.1 39.7, 38.9, 37.6, 37.5, 36.9, 36.6 (N-CH_2), 32.6 (Ar-$C(CH_3)_3$), 29.0, 28.9 (O-$C(CH_3)_3$). MS (MALDI-TOF) *m/z* 1355.693 $[M\text{-}^t Bu]^+$, 1255.650 $[M\text{-}2\ ^t Bu]^+$; calcd for $C_{72}H_{85}N_{13}O_{10}Zn$ 1355.583, $C_{67}H_{77}N_{13}O_8Zn$ 1255.531. The blue solid (19.0 mg, 0.013 mmol) was dissolved in 1:1 DCM/TFA (6 mL) and stirred at 0 °C for 3 h. The crude product was treated as described for ZnPc **5.3** above to give a blue solid (14.9 mg, 90.7 %). ^{1}H NMR (DMF-d_7): δ 9.56-8.89 (m, 8H, Ar-H), 8.39-8.31 (m, 4H, Ar-H), 8.08-7.92 (m, 2H, Ar-H), 7.55-7.51 (m, 2H, Ar-H) 4.36 (d, J = 6.88, 2H, CH_2O), 4.26 (d, J = 6.64, 2H, CH_2O), 3.56-3.25 (m, 24H, CH_2O), 2.38-2.22 (m, 2H, CH_2CO), 1.80-1.76 (m, 27H, $C(CH_3)_3$). ^{13}CNMR (DMF-d_7): δ 171.3, 170.6, 169.2, 169.1, 160.6, 160.3, 155.2, 155.1, 154.8, 154.0, 153.4, 141.5, 140.0, 139.8, 137.7, 136.5, 136.2, 135.1, 134.9, 134.7, 128.3, 125.1, 123.3,

122.8, 121.3, 120.7, 119.8, 115.0, 112.6, 111.5, 111.0 (Ar-C), 72.4, 72.2, 71.2, 71.1, 70.9, 70.3, 68.1 (O-C(CH_3)$_3$), 48.9, 48.1, 39.7, 39.3, 37.5, 37.3 (N-CH_2), 32.6 (m, 27H, C(CH_3)$_3$). MS (MALDI-TOF) *m/z* 1255.555 $[M]^+$, calcd for $C_{67}H_{77}N_{13}O_8Zn$ 1255.531. UV-VIS (DMF): λ_{max} (log ε) 351 (4.81), 612 (4.53), 677 (5.28) nm.

ZnPc 5.15. A procedure related to that described for ZnPc **5.4** was used: ZnPc **5.14** (20.0 mg, 0.015 mmol), DIPA (0.015 mL, 0.107 mmol), CH_3I (0.2 mL) and dry DMF (0.5 mL). The title ZnPc was attained as a blue solid (16.2 mg, 64.3%). ^{1}H NMR (DMF-d_7): δ 9.57-9.26 (m, 7H, Ar-H), 8.38-8.18 (m, 5H, Ar-H), 7.94-7.84 (m, 2H, Ar-H), 7.61-7.48 (m, 2H, Ar-H), 4.35-4.23 (m, 8H, CH_2O), 3.81-3.48 (m, 18H, CH_2O/N-CH2/N-CH_3), 3.46 (s, 9H, N-CH_3), 2.47-2.30 (m, 2H, $COCH_2$), 1.85-1.76 (m, 27H, C(CH_3)$_3$). ^{13}C NMR (DMF-d_7): δ 173.0, 172.6, 172.4, 170.6, 169.2, 169.1 (C=O), 160.6, 160.2, 155.1, 154.9, 154.6, 154.0, 153.9, 153.2, 141.4, 140.0, 139.9, 137.6, 137.4, 136.5, 136.2, 134.9, 134.6, 129.5, 128.7, 128.4, 125.0, 123.3, 122.8, 121.3, 121.1, 120.7, 119.8, 115.0, 112.6, 111.5 (Ar-C), 72.4, 72.2, 71.2, 71.1, 70.3, 68.0 (CH_2O), 64.6, 64.4, 58.6, 57.2, 55.9, 54.4, 52.5, 49.9, 48.0 (N-CH_3), 43.2, 39.7, 37.5, 36.8 (N-CH_2) 32.6 (C(CH_3)$_3$). MS (MALDI-TOF) *m/z* 1493.710 $[M-I+K]^+$, calcd for $C_{72}H_{89}IKN_{13}O_8Zn^+$ 1493.493. UV–Vis (DMF): λ_{max} (log ε) 351 (4.84), 610 (4.54), 677 (5.30) nm.

ZnPc 5.16. A procedure related to that described for ZnPc **5.5** was used: ZnPc **5.12** (40.0 mg, 0.04 mmol), DMF (0.5 mL), Et_3N (5.2 mg, 0.051 mmol), HOBt (7.5 mg, 0.055 mmol), 1,4-bis-Boc-triazaheptane (15.5 mg, 0.051 mmol), and EDCI (9.8 mg, 0.051 mmol). The product was obtained as a blue solid (44.4 mg, 88.6%). ^{1}H NMR (DMF-d_7): δ 9.42-9.24 (m, 6H, Ar-H), 8.78 (br, 1H, NH), 8.40-8.20 (m, 4H, Ar-H), 8.10-8.04 (m, 2H, Ar-H), 7.89-7.79 (m, 1H, Ar-H), 7.64–7.59 (m, 2H, Ar-H), 6.82-6.76 (m, 1H, N-H), 4.38 (d, J = 6.92 MHz, 2H, CH_2O), 4.29 (d, J = 9.68 MHz, 2H, CH_2O), 3.47 (br, 4H, CH_2NH), 3.38 (br, 2H, CH_2NH), 3.25 (m, 2H, CH_2NH),

1.87–1.83 (m, 27H, $C(CH_3)_3$), 1.48 (s, 9H, $-OC(CH_3)_3$), 1.41 (s, 18H, $-OC(CH_3)_3$). ^{13}CNMR (DMF-d_7): δ 170.6, 169.1 (C=O), 160.6, 160.5, 160.2, 160.1, 157.2, 156.6, 156.4, 154.8, 154.72, 154.65, 154.5, 154.3, 154.2, 154.1, 154.0, 153.9, 153.4, 152.8, 141.1, 139.8, 139.6, 137.4, 137.3, 137.2, 136.5, 136.2, 134.5, 134.3, 132.6, 129.8, 128.4, 128.3, 126.2, 125.0, 123.4, 123.3, 122.9, 122.0, 121.3, 121.1, 120.8, 120.7, 119.9, 119.7, 112.7, 111.5 (Ar-C), 80.0, 78.8 ($-OC(CH_3)_3$), 72.4, 72.1 (OCH_2), 48.5, 48.3, 47.7, 40.1, 39.9, 38.7, 38.5, 36.8 ($N-CH_2$), 32.7 ($Ar-C(CH_3)_3$), 29.0, 28.9 ($O-C(CH_3)_3$). MS (MALDI-TOF) *m/z* 1052.447 $[M-2Boc]^+$, calcd for $C_{58}H_{60}N_{12}O_4Zn$ 1052.415. The blue solid (44.4 mg, 0.035 mmol) was dissolved in DCM/TFA (1:1) and stirred at 0 °C for 3 h. The solvent was evaporated and the remaing solid treated with 2N NaOH (10 mL) to afford a blue-greenish solid (33.5 mg, 89.9 %). ^{1}H NMR (DMF-d_7): δ 9.55-9.24 (m, 7H, Ar-H), 8.97-8.89 (m, 1H, Ar-H), 8.40-8.11 (m, 4H, Ar-H), 8.07 – 8.00 (m, 1H, Ar-H), 7.92 – 7.90 (m, 1H, Ar-H), 7.65–7.50 (m, 2H, Ar-H), 4.37 (d, J = 6.88 MHz, 2H, CH_2O), 4.26 (d, J = 4.24 MHz, 2H, CH_2O), 3.47 (br, 2H, CH_2NH), 3.03–2.91 (m, 2H, CH_2NH), 1.82-1.79 (m, 27H, $C(CH_3)_3$). ^{13}C NMR (DMF-d_7): δ 171.4, 169.2 ,169.1 (C=O), 160.6, 160.5, 160.2, 159.7, 155.2, 155.1, 154.8, 154.7, 154.3, 154.1, 154.0, 153.4,153.2, 141.4, 140.0, 139.8, 137.7, 137.5, 134.9, 134.7, 128.3, 128.2, 125.0, 123.3, 123.2, 122.8, 121.2, 121.1,120.7, 119.9, 119.8, 119.3, 116.4, 112.7, 111.5 (Ar-C), 72.3, 72.1, 72.0 (OCH_2), 49.1, 48.7, 47.5, 47.0, 39.5, 38.7, 36.7 ($N-CH_2$), 32.6 ($Ar-C(CH_3)_3$). MS (MALDI-TOF) *m/z* 1052.411 $[M]^+$, calcd for $C_{58}H_{60}N_{12}O_4Zn$ 1052.415. UV-vis (DMF): λ_{max} (log ε) 351 (4.73), 609 (4.43), 676 (5.19) nm.

ZnPc 5.17. A procedure related to that described for ZnPc **5.4** was used: ZnPc **5.16** (20.0 mg, 0.021 mmol), DIPA (0.015 mL, 0.107 mmol), CH_3I (0.2 mL) and dry THF (0.5 mL). The title ZnPc was obtained as a blue-green solid (16.1 mg, 58.3%). ^{1}H NMR (DMF-d_7): δ 9.56-9.19 (m, 6H, Ar-H), 9.03-8.77 (m, 2H, Ar-H), 8.39-8.27 (m, 3H, Ar-H), 8.01-8.86 (m, 3H, Ar-H),

7.58-7.45 (m, 4H, Ar-H), 4.41-4.27 (m, 8H, CH_2O/N-CH_2), 3.92-3.82 (m, 4H, N-CH_2), 3.53 (s, 6H, N-CH_3), 3.49 (s, 9H, N-CH_3), 1.86-1.72 (m, 27H, C(CH_3)$_3$). ^{13}C NMR (DMF-d_7): δ 171.4, 169.0, 168.6, 168.9, 160.5, 160.4, 160.1, 160.0, 155.9, 155.5, 155.3, 155.2, 155.1, 154.9, 154.8, 154.3, 154.0, 153.9, 153.8, 141.6, 140.2, 140.0, 137.8, 137.7, 137.6, 136.3, 136.0, 135.2, 135.0, 128.3, 128.12, 128.07, 125.1, 123.24, 123.15, 123.0, 122.8, 122.7, 121.3, 121.1, 120.6, 119.9, 119.8, 119.7, 112.8, 111.7 (Ar-C), 72.1, 71.9 (CH_2O), 64.5, 58.7, 57.3, 54.5, 52.5 (N-CH_3), 36.7 (N-CH_2) 32.6 (C(CH_3)$_3$). MS (MALDI-TOF) *m*/*z* 1252.575 $[M-I+2H]^+$, calcd for $C_{63}H_{73}IN_{12}O_4Zn$ 1252.421. UV–Vis (DMF): λ_{max} (log ε) 351 (4.83), 610 (4.55), 676 (5.31) nm.

ZnPc 5.18. A procedure related to that described for ZnPc **5.3** was used: ZnPc **5.12** (50.0 mg, 0.05 mmol), DMF (0.8 mL), Et_3N (6.2 mg, 0.061 mmol), HOBt (9.3 mg, 0.069 mmol), aspartic acid di-*tert*-butyl ester hydrochloride (18 mg, 0.064 mmol) and EDCI (12.3 mg, 0.064 mmol). The protected ZnPc was obtained as a blue solid (0.056 g, 89.0%). ^{1}H NMR (Acetone-d_6): δ 9.86-9.68 (m, 1H, N-H), 9.37-8.57 (m, 6H, Ar-H), 8.38-7.96 (m, 6H, Ar-H), 7.92-7.56 (m, 4H, Ar-H), 4.74 (br, 1H, N-H), 4.25 (s, 4H, CH_2O), 2.82 (s, 1H, CH), 2.66 (s, 2H, CH), 1.94–1.87 (m, 27H, C(CH_3)$_3$), 1.45 (s, 18H, -OC(CH_3)$_3$). ^{13}C NMR (Acetone-d_6): δ 170.6, 170.4, 169.99, 169.95, 168.3, 168.23, 168.17 (C=O), 160.0, 159.9, 159.8, 159.4, 159.3, 159.2, 155.3, 155.1, 154.6, 154.4, 153.2, 1153.1, 153.03, 152.97, 139.4, 139.1, 139.0, 136.8, 135.9, 135.8, 135.4, 127.7, 124.3, 122.8, 122.4, 121.8, 121.1, 121.0, 120.5, 120.4, 119.5, 112.8, 112.6, 111.5 (Ar-C), 82.4, 81.7 (-OC(CH_3)$_3$), 72.4, 71.9 (OCH_2), 50.1, 50.0, 38.4, 36.6 (N-CH_2), 32.6 (Ar-C(CH_3)$_3$), 28.4, 28.2 (O-C(CH_3)$_3$). MS (MALDI-TOF) *m/z* 1194.433 $[M+H]^+$, 1138.332 $[M-C_4H_9]^+$, 1083.257 $[M-2C_4H_9+H]^+$, calcd for $C_{66}H_{70}N_{10}O_8Zn$ 1194.467, $C_{62}H_{62}N_{10}O_8Zn$ 1138.404, $C_{58}H_{55}N_{10}O_8Zn$ 1083.350. The solid (0.056 g, 0.047 mmol) was dissolved in DCM/TFA (1:1) and stirred for 4 h at 0°C. The solvent was evaporated and the precipitate treated with 2N NaOH

(10 mL) to obtaiin a blue solid (42.1 mg, 83.0 %). MS (MALDI-TOF) *m/z* 1082.7 $[M]^+$, 1105.3315 $[M+Na]^+$, calcd for $C_{58}H_{54}N_{10}O_8Zn$ 1082.34, $C_{58}H_{54}N_{10}NaO_8Zn$ 1105.7. UV-vis (DMF): λ_{max} (log ε) 351 (4.83), 610 (4.51), 677 (5.28) nm.

ZnPc 5.19. A procedure related to that described for ZnPc **5.3** was used: ZnPc **5.18** (18.4 mg, 0.017 mmol), DMF (0.5 mL), Et_3N (6.2 mg, 0.061 mmol), HOBt (5.7 mg, 0.042 mmol), *N*-Boc-2,2′-(ethylenedioxy)diethylamine (9.4 mg, 0.038 mmol) and EDCI (6.5 mg, 0.042 mmol). The product was obtained as a blue solid (13.3 mg, 50.8 %). ^{1}H NMR (DMF-d_7): δ 9.52-9.15 (m, 6H, Ar-H), 8.81-8.54 (m, 2H, Ar-H), 8.42-8.34 (m, 3H, Ar-H), 8.17-8.05 (m, 4H, Ar-H), 7.97-7.88 (m, 1H, Ar-H), 7.65–7.59 (m, 2H, Ar-H), 6.70 (br, 2H, Ar-H), 4.87 – 4.85 (m, 1H, N-H), 4.42 (d, 8.0 Hz, 2H, CH_2O), 4.33 (d, 5.96 Hz, 2H, CH_2O), 3.58–3.46 (m, 16H, CH_2O), 3.42–3.37 (m, 4H, CH_2NH), 3.25–3.19 (m, 4H, CH_2NH), 2.83–2.78 (m, 2H, CH_2CO), 1.86–1.83 (m, 27H, $C(CH_3)_3$), 1.40–1.36 (m, 18H, $OC(CH_3)_3$). ^{13}C NMR (DMF-d_7): δ 172.0, 171.4, 170.42, 170,40, 169.1, 169.0, 160.6, 160.5, 160.2, 160.1, 157.1, 154,73, 154.67, 154.4, 154.2, 154.0, 153.9, 153.4, 152.9, 141.2, 139.8, 139.6, 137.5, 137.3, 136.,5, 136.2, 134.6, 128.4, 125.1, 123.35, 123.25, 122.83, 122.79, 122.0, 121.3, 121.2, 121,1, 120.73, 120.67, 119.9, 1119.8, 112.8, 111.6 (Ar-C), 78.8 ($OC(CH_3)_3$), 72.2, 72.0, 71.1, 70.04, 70.01, 71.0, 70.8, 70.5, 70.4 (CH_2O), 51.2 ($NHCH(CH_2)CO$), 42.5, 41.2, 40.2, 38.5 (CH_2), 32.6 ($C(CH_3)_3$), 28.9 ($OC(CH_3)_3$). MS (MALDI-TOF) *m/z* 1544.802 $[M]^+$, calcd for $C_{80}H_{98}N_{14}O_{14}Zn$ 1544.669. The ZnPc (13.1 mg, 8.5 mmol) was dissolved in DCM/TFA (1:1) and stirred at 0°C for 3 h. The solvent was evaporated and the solid treated with 2N NaOH (10 mL) to give the title product (10.2 mg, 89.7%). ^{1}H NMR (DMF-d_7): δ 9.54-9.23 (m, 7H, Ar-H), 9.00-8.77 (m, 1H, Ar-H), 8.39-8.29 (m, 3H, Ar-H), 8.09-7.94 (m, 3H, Ar-H), 7.47 – 7.42 (m, 2H, Ar-H), 4.66 (br, 1H, NH), 4.33 (d, 7.36 Hz, 2H, CH_2O), 4.33 (d, 5.16 Hz, 2H, CH_2O), 3.65–3.45 (m, 8H, CH_2O), 3.25–3.14 (m, 8H, CH_2O), 3.08-3.02 (m, 2H,

CH_2NH), 2.98-2.91 (m, 2H, CH_2NH), 2.87-2.80 (m, 2H, CH_2NH), 2.72-2.58 (m, 2H, CH_2CO), 2.34 (br, 2H, NH_2), 2.13 (br, 2H, NH_2), 1.80–1.73 (m, 27H, $C(CH_3)_3$). ^{13}C NMR (DMF-d_7): δ 171.9, 171.5, 170.2, 170.17, 168.95, 168.87, 160.5, 160.0, 155.5, 155.4, 155.2, 155.1, 155.0, 154.8, 154.4, 154.1, 153.9, 153.3, 141.5, 140.0, 139.9, 137.7, 136.2, 135.2, 134.9, 132.5, 129.9, 128.5, 125.2, 123.3, 122.8, 122.7, 122.3, 122.0, 120.8, 120.1, 119.8, 113.3, 112.1 (Ar-C), 72.1, 72.0, 71.4, 71.1, 70.7, 70.52, 70.46, 70.3, 70.2, 70.1 (N-CH), 51.2 ($NHCH(CH_2)CO$), 40.6, 40.2, 40.0, 39.9, 38.0, 36.8 (CH_2), 32.6 ($C(CH_3)_3$). MS (MALDI-TOF) *m/z* 1343.588 $[M+H]^+$, 1365.575 $[M+Na]^+$, 1381.546 $[M+K]^+$ calcd for $C_{70}H_{83}N_{14}O_{10}Zn$ 1343.5708, $C_{70}H_{82}NaN_{14}O_{10}Zn$ 1365.5528, $C_{70}H_{82}KN_{14}O_{10}Zn$ 1381.5267. UV-vis (DMF): λ_{max} (log ε) 352 (4.77), 611 (4.50), 677 (5.27) nm.

ZnPc 5.20. A procedure related to that described for ZnPc **5.4** was used: ZnPc **5.19** (20.0 mg, 0.015 mmol), DIPA (0.015 mL, 0.107 mmol), CH_3I (0.2 mL) and dry DMF (0.5 mL). The ZnPc was a blue solid (16.2 mg, 64.3%). ^1H NMR (DMF-d_7): δ 9.56-9.27 (m, 7H, Ar-H), 9.06-8.83 (m, 2H, Ar-H), 8.36-8.26 (m, 4H, Ar-H), 8.13-8.06 (m, 2H, Ar-H), 7.92-7.81 (m, 1H, Ar-H), 7.52-7.44 (m, 2H, Ar-H), 4.38 (d, 8.0Hz, 2H), 4.28 (d, 6.0Hz, 2H), 3.94-3.90 (m, 5H, NH), 3.73-3.49 (m, 24H, OCH_2), 3.34-3.23 (m, 18H, $N\text{-}CH_3$), 1.78-1.64 (m, 27H, $C(CH_3)_3$). ^{13}C NMR (DMF-d_7): δ 172.2, 171.5, 170.5, 169.2 (C=O), 159.9, 159.1, 155.6, 155.1, 153.8, 141.8, 140.4, 140.2, 137.9, 136.3, 135.9, 135.2, 128.1, 124.9, 123.1, 122.9, 122.8, 121.0, 120.4, 119.7, 112.7, 111.6 (Ar-C), 72.2, 72.0, 71.0, 70.9, 70.8, 70.7, 70.4 (OCH_2), 66.2, 65.65, 65.60 ($NHCH_2$), 54.4 ($N\text{-}CH_3$), 32.6 ($C(CH_3)_3$). MS (MALDI-TOF) *m/z* 1413.828 $[M\text{-}2I\text{-}CH_3]^+$, calcd for $C_{75}H_{93}N_{14}O_{10}Zn^+$ 1413.649. UV–Vis (DMF): λ_{max} (log ε) 350 (4.51), 610 (4.26), 677 (5.01) nm.

ZnPc 5.21. A procedure related to that described for ZnPc **5.3** was used: ZnPc **5.18** (18.4 mg, 0.017 mmol), DMF (0.5 mL), Et_3N (6.2 mg, 0.061 mmol), HOBt (5.7 mg, 0.042 mmol), *N*-

Boc-ethylenediamine (6.1 mg, 0.038 mmol) and EDCI (6.5 mg, 0.042 mmol). After stirring for for 4 days at 25 °C followed by purification, the ZnPc was obtained as a blue solid (14.3 mg, 61.6 %). ^{1}H NMR (DMF-d_7): δ 9.52-9.14 (m, 6H, Ar-H), 8.80-8.33 (m, 4H, Ar-H), 8.20-8.10 (m, 3H, Ar-H), 7.65-7.61 (m, 2H, Ar-H), 6.79-6.76 (m, 2H, Ar-H) 4.83 (br, 1H, NH), 4.43 (d, 8.24 Hz, 2H, CH_2O), (d, 5.76 Hz, 2H, CH_2O), 3.39–3.25 (m, 4H, CH_2NH), 3.24–3.16 (m, 4H, CH_2NH), 2.82-2.77 (m, 2H, CH_2CO), 1.95-1.84 (m, 27H, $C(CH_3)_3$), 1.41 (s, 18H, $C(CH_3)_3$). ^{13}C NMR (DMF-d_7): δ 172.1, 171.6, 170.4, 169.1, 169.0, 160.6, 160.5, 160.2, 160.1, 157.3, 157.2, 154.7, 154.4, 154.2, 154.0, 153.9, 152.9, 141.2, 139.8, 137.5, 137.3, 136.2, 134.5, 128.4, 128.23 125.0, 123.2, 122.83, 122.79, 122.0, 121.3, 121.1, 120.7, 119.9, 119.7, 112.7, 111.6 (Ar-C), 78.91, 78.87 ($OC(CH_3)_3$), 72.3, 72.0 (CH_2O), 51.3 ($NHCH(CH_2)CO$), 41.1, 40.6, 40.5, 38.8, 36.8 (CH_2), 32.7 ($C(CH_3)_3$), 29.0 ($OC(CH_3)_3$). MS (MALDI-TOF) *m/z* 1166.471 $[M\text{-}2Boc]^+$, 1189.475 $[M\text{-}2Boc+Na]^+$, 1205.448 $[M\text{-}2Boc+K]^+$, calcd for $C_{62}H_{66}N_{14}O_6Zn$ 1166.4581, $C_{62}H_{66}N_{14}NaO_6Zn$ 1189.4479, $C_{62}H_{66}KN_{14}O_6Zn$ 1206.4218 respectively. The ZnPc (14.3 mg, 0.0105 mmol) was dissolved in DCM/TFA (1:1) at 0 °C for 3h. The solvent was evaporatedand the residue treated with 2N NaOH (10 mL) to obtaiin the title compound (11.1 mg, 91.2%). ^{1}H NMR (THF-d_8): δ 9.80-9.36 (m, 8H, Ar-H), 9.01-8.8.97 (m, 1H, Ar-H), 8.43-8.37 (m, 3H, Ar-H), 8.00–7.81 (m, 3H, Ar-H), 7.51 – 7.42 (m, 2H, Ar-H), 4.20-3.70 (m, 4H, CH_2O), 3.47–3.10 (m, 8H, CH_2NH), 2.08-1.93 (m, 2H, CH_2CO), 1.75–1.65 (m, 27H, $C(CH_3)_3$). ^{13}C NMR (DMF-d_7): δ 171.8, 171.0, 170.4, 169.8, 168.8, 161.0, 160.4, 155.4, 154.9, 154.1, 141.6, 140.0, 137.6, 136.4, 135.9, 134.9, 134.6, 128.4, 125.2, 123.3, 122.7, 121.6, 121.1, 120.7, 119.8, 112.7, 111.3 (Ar-C), 72.0, 71.5 (CH_2NH), 50.8 ($NHCH(CH_2)CO$), 41.0, 40.1, 36.7 (CH_2), 32.6, 32.3 ($C(CH_3)_3$). MS (MALDI-TOF) *m/z* 1166.534 $[M\text{-}2Boc+2H]^+$, calcd for $C_{62}H_{66}N_{14}O_6Zn$ 1166.4581. UV-vis (DMF): λ_{max} (log ε) 352 (4.73), 610 (4.44), 677 (5.19) nm.

ZnPc 5.22. A procedure related to that described for ZnPc **5.4** was used: ZnPc **5.21** (20.0 mg, 0.017 mmol), DIPA (0.015 mL, 0.107 mmol), CH_3I (0.2 mL) and dry DMF (0.5 mL). After work-up, the title compound was achieved as a blue solid (17.4 mg, 67.4%). ^{1}H NMR (DMF-d_7): δ 9.56-9.27 (m, 7H, Ar-H), 9.04-8.92 (m, 1H, Ar-H), 8.65-8.50 (m, 3H, Ar-H), 8.39-8.31 (m, 3H, Ar-H), 7.92-7.90 (m, 1H, Ar-H), 7.54-7.47 (m, 2H, Ar-H), 4.47-4.31 (m, 4H, OCH_2), 381-3.70 (m, 8H, CH_2), 3.38-3.35 (m, 18H, N-CH_3), 1.79-1.74 (m, 27H, $C(CH_3)_3$). ^{13}C NMR (Acetone-d_6): δ 172.6, 171.8, 170.9, 169.2, 155.5, 154.8, 154.0, 153.5, 153.0, 141.8, 140.3, 140.2, 137.7, 136.4, 136.0, 129.6, 128.8, 128.3, 126.2, 125.0, 123.2, 122.8, 121.1, 120.5, 119.6, 115.0, 112.8, 111.7 (Ar-C), 72.2, 72.1, 65.6 (N-CH_2), 54.0 (N-CH_3), 32.6 ($C(CH_3)_3$). MS (MALDI-TOF) *m/z* 1194.434 $[M\text{-}4CH_3\text{-}2I]^+$, calcd for $C_{64}H_{70}N_{14}O_6Zn^+$ 1194.489. UV–Vis (DMF): λ_{max} (log ε) 350 (4.55), 610 (4.25), 677 (4.99) nm.

Phthalonitrile 5.24. To a mixture of 3-nitrophthalonitrile **5.23** (2.0 g, 11.5 mmol) and *tert*-butyl 20-hydroxy-3,6,9,12,15,18-hexaoxaicosan-1-oate (4.99 g, 12.6 mmol) in THF (15 mL), K_2CO_3, (5.26 g, 40 mmol) was added in six portions every 5 min. The solution was heated at 65 °C for 6 h. The solids were removed and the product purified via silica chromatography. A mixed solvent system of DCM/methanol (199:1 → 98:2) was used for elution. The product was obtained as a brown-yellow oil (4.70 g, 78.3%). ^{1}H NMR (d-$CDCl_3$, 400 MHz): δ 7.64 (d, J = 8.1 Hz, 1H, Ar-H), 7.31 (d, J = 8.2 Hz, 1H, Ar-H), 4.27 (t, J = 4.4, 2H, OCH_2), 3.96 (s, 2H, OCH_2), 3.87 (t, 2H, J = 4.5, OCH_2), 3.70-3.58 (m, 20H, OCH_2), 1.41 (s, 9H, $C(CH_3)_3$). ^{13}C NMR ($CDCl_3$): *δ* 169.65 ($CH_2C(O)O$*t*Bu), 161.41, 134.71, 125.34, 117.55, 113.09, 104.91 (Ar-C), 116.77, 115.41, (CN), 81.49 ($C(CH_3)$, 71.11, 70.67, 70.54, 69.72, 69.21, 68.98 (OCH_2), 28.09 ($C(CH_3)_3$). MS (MALDI-TOF) *m/z* 545.2232 $[M+H+Na]^+$, calcd for, $C_{18}H_{36}NaO_9$, 519.2257; *m/z* 545.2466 $[M+H]^+$, calcd for, $C_{26}H_{37}N_2NaO_9$, 545.2475.

ZnPc 5.25. A combination of 4-*tert*-butylphthalonitrile (1.32 g, 7.16 mmol), phthalonitrile **5.24** (475.0 mg, 1.42 mmol) and zinc(II) acetate (500 mg, 2.73 mmol) was stirred in DMAE (35 mL). The solution was heated under the flow of argon and two drops of DBN were added. The reaction solution was heated for 5 h. The solvent was evaporated and the residue purified on a silica column eluted by DCM/methanol (97:3). Another silica column eluted by chloroform, and then chloroform/methanol (99:1 → 98:2) gave a blue solid (273.6 mg, 16.9%). ^{1}H NMR (DMF-d_7): δ 9.63-8.92 (m, 6H, Ar-H), 8.47-8.05 (m, 3H, Ar-H), 7.85-7.62 (m, 3H, Ar-H), 4.95-4.88 (m, 2H, CH_2O), 4.49-4.39 (m, 2H, CH_2O), 4.16-4.00 (m, 3H, CH_2O), 3.88-3.44 (m, 19H, CH_2O), 1.88–1.82 (m, 27H, $C(CH_3)_3$), 1.45, 1.38, 1.36 (s, 9H, -$OC(CH_3)_3$). ^{13}CNMR (DMF-d_7): δ 170.73, 170.66 (C=O), 158.1, 157.8, 157.4, 157.3, 157.2, 154.9, 154.8, 154.7, 154.5, 154.3, 154.1, 153.8, 153.7, 141.9, 141.8, 140.1, 139.9, 139.8, 137.9, 137.5, 137.2, 136.7, 137.2, 134.0, 131.6, 131.30, 131.26, 130.5, 128.9, 128.4, 126.9, 126.7, 126.4, 123.6, 123.4, 123.3, 122.9, 120.2, 120.1, 119.8, 119.7, 118.7, 117.0, 116.3, 114.8, 114.7, 114.6, 104.6 (Ar-C), 81.73, 81.68 (-$OC(CH_3)_3$), 72.1, 71.9, 71.7, 71.5, 71.44, 71.36, 71.3, 71.2, 70.9, 70.4, 70.0, 69.9, 69.62, 69.56, 68.9 (OCH_2), 52.1, 45.9, 36.8 (N-CH_2), 32.8, 32.7 (Ar-$C(CH_3)_3$), 28.6 (O-$C(CH_3)_3$). MS (MALDI-TOF) *m/z* 1139.675 $[M+H]^+$, calcd for $C_{62}H_{75}N_8O_9Zn$ 1138.495. The protected ZnPc (273.6 mg, 0.240 mmol) was dissolved in DCM/TFA (1:1) and the solution was stirred at 0 °C for 3 h. The solvent was removed and the resulting residue treated with 2 N NaOH (15 mL). The product was extracted using 5:1, DCM/methanol (20 mL × 4) and the organic phase washed with water (20 mL × 2) and dried over anhydrous sodium sulfate. The solvent was removed under reduced pressure to afford the title ZnPc as a blue solid (243.7 mg, 93.7 %). ^{1}HNMR (DMF-d_7): δ 9.59-9.11 (m, 6H, Ar-H), 8.40-8.34 (m, 3H, Ar-H), 8.19-7.70 (m, 3H, Ar-H), 5.00-4.94 (m, 2H, CH_2O), 4.60-4.43 (m, 2H, CH_2O), 4.19-4.06 (m, 2H, CH_2O), 3.90-3.04

(m, 16H, CH_2O), 1.83–1.78 (m, 27H, $C(CH_3)_3$). ^{13}CNMR (DMF-d_7): δ 170.6 (C=O), 157.5, 157.1, 156.8, 155.9, 155.3, 155.0, 154.5, 153.8, 153.6, 142.5, 140.5, 140.2, 140.0, 138.3, 137.9, 137.6, 136.2, 132.5, 131.4, 130.4, 128.9, 128.5, 128.1, 127.2, 127.0, 123.9, 123.6, 123.1, 122.8, 120.7, 120.0, 119.8, 119.7, 119.5, 116.5, 116.1, 113.9 (Ar-C), 72.5, 72.0, 71.7, 71.5, 71.3, 71.2, 71.0, 70.5, 70.2, 69.7, 69.6, 68.9, 68.6 (OCH_2), 52.1, 46.2, 36.8, 36.7 (N-CH_2), 32.7, 32.6 (Ar-$C(CH_3)_3$). MS (MALDI-TOF) *m/z* 1083.444 $[M+H]^+$, calcd for $C_{58}H_{67}N_8O_9Zn$ 1083.432. UV-vis (DMF): λ_{max} (log ε) 345 (4.77), 613 (4.57), 681 (5.34) nm.

ZnPc 5.26. A procedure related to that described for ZnPc **5.3** was used: ZnPc **5.25** (20.0 mg, 0.018 mmol), DMF (0.4 mL), Et_3N (3.3 mg, 0.032 mmol), HOBt (4.7 mg, 0.035 mmol), 1,4-bis-Boc-triazaheptane (7.0 mg, 0.023 mmol) and EDCI (4.0 mg, 0.026 mmol). After work-up and purification the ZnPc was achieved as a blue solid (16.1 mg, 63.6%). ^{1}H NMR (DMF-d_7): δ 9.54-9.20 (m, 5H, Ar-H), 9.06-8.84 (m, 1H, Ar-H), 8.47-8.35 (m, 3H, Ar-H), 7.82-7.76 (m, 2H, Ar-H), 6.76-6.70 (m, 1H, Ar-H), 4.96-4.92 (m, 2H, $COCH_2O$), 4.58-4.44 (m, 2H, CH_2O), 4.19-4.10 (m, 1H, CH_2O), 4.07-3.09 (m, 1H, CH_2O), 3.88-3.72 (m, 5H, CH_2O), 3.60-3.43 (m, 17H, CH_2O), 3.34-3.28 (m, 6H, CH_2NH), 3.20-3.18 (m, 2H, CH_2NH), 1.86-1.82 (m, 27H, $C(CH_3)_3$), 1.46-1.39 (m, 18H, -$OC(CH_3)_3$). ^{13}C NMR (DMF-d_7): *δ* 170.7, 175.1, 156.4, 154.8, 154.0, 139.8, 137.5, 131.8, 128.5, 123.4, 119.8, 116.4, 114.9, 114.7 (Ar-C), 79.9, 78.7 (O-$C(CH_3)_3$), 72.0, 71.71, 71.66, 71.5, 71.4, 71.3, 71.2, 71.0, 70.4, 69.9 (CH_2O), 48.4, 48.2, 44.3 40.1, 39.9, 38.4, 36.8 (N-CH_2), 32.6 (Ar-$C(CH_3)_3$), 29.0, 28.8 (O-$C(CH_3)_3$). MS (MALDI-TOF) *m/z* 1367.708 $[M]^+$, 1207.655 $[M\text{-}2^tBu+K]^+$; calcd for $C_{72}H_{93}N_{11}O_{12}Zn$ 1367.630, $C_{62}H_{78}KN_{11}O_8Zn$ 1207.496. The blue solid (16.1 mg, 0.0118 mmol) was dissolved in a 1:1 mixture of DCM/TFA (6 mL) and stirred at 0 °C for 3 h. The solvent was evaporated and the residue treated with 2N NaOH (10 mL) to give a blue solid (12.5 mg, 91.0 %). ^{1}H NMR (DMF-d_7): δ 9.56-8.95 (m, 7H, Ar-H),

8.52-8.31 (m, 3H, Ar-H), 8.13-8.03 (m, 1H, Ar-H), 7.83-7.70 (m, 1H, Ar-H), 5.02-4.83 (m, 2H, $COCH_2O$), 4.59-4.35 (m, 2H, CH_2O), 4.19-4.00 (m, 2H, CH_2O), 3.92-3.00 (m, 22H, CH_2O), 1.79 (s, 27H, $C(CH_3)_3$). ^{13}C NMR (DMF-d_7): δ 171.2, 170.9, 170.3, 157.3, 155.0, 154.4, 154.1, 154.0, 142.2, 140.3, 140.1, 138.0, 137.7, 131.6, 129.0, 128.3, 126.9, 123.6, 123.3, 119.8, 116.5, 115.0, 114.7 (Ar-C), 71.9, 71.6, 71.4, 71.3, 71.2, 71.1, 70.8, 70.6, 70.1, 69.6 (CH_2O), 49.1, 48.0, 47.5, 47.0, 46.6, 46.3, 45.9, 45.8, 44.6, 44.3, 39.6, 38.8, 36.8 (N-CH_2), 32.6 (Ar-$C(CH_3)_3$). MS (MALDI-TOF) *m/z* 1167.520 $[M]^+$, calcd for $C_{62}H_{77}N_{11}O_8Zn$ 1167.525. UV-vis (DMF): λ_{max} (log ε) 346 (4.77), 615 (4.55), 683 (5.31) nm.

ZnPc 5.27. A procedure related to that described for ZnPc **5.4** was used: ZnPc **5.26** (20.0 mg, 0.017 mmol), DIPA (0.015 mL, 0.107 mmol), CH_3I (0.2 mL) and dry DMF (0.5 mL). The title compound was obtained as a blue solid (17.4 mg, 67.4%). ^1H NMR (DMF-d_7): δ 9.57-9.34 (m, 6H, Ar-H), 9.13-8.99 (m, 1H, Ar-H), 8.38-8.18 (m, 3H, Ar-H), 8.20-8.09 (m, 1H, Ar-H), 7.88-7.72 (m, 1H, Ar-H), 5.03-4.94 (m, 2H, $COCH_2$), 4.65-4.36 (m, 2H, CH_2O),4.15-3.51 (m, 28H, CH_2O/N-CH2/N-CH_3), 3.43 (s, 9H, N-CH_3), 1.83-1.79 (m, 27H, $C(CH_3)_3$). ^{13}C NMR (DMF-d_7): δ 171.7, 170.5 (C=O), 157.5, 157.4, 155.1, 155.0, 154.8, 154.5, 154.1, 154.0, 142.3, 142.2, 142.1, 140.4, 140.0, 138.0, 137.7, 131.7, 128.4, 126.9, 123.6, 123.3, 119.9, 119.8, 116.5, 115.0, 114.8 (Ar-C), 72.1, 72.0, 71.8, 71.7, 71.4, 71.2, 71.0, 70.7, 70.5, 70.2 (CH_2O), 64.5, 54.5, 53.5, 52.5, 52.2, 51.4, 48.2 (N-CH_3), 43.3, 43.2, 36.8 (N-CH_2) 32.7, 32.6 ($C(CH_3)_3$). MS (MALDI-TOF) *m*/z 1404.705 $[M-I+2H+K]^+$; calcd for $C_{67}H_{90}IKN_{11}O_8Zn^+$ 1404.495. UV–Vis (DMF): λ_{max} (log ε) 347 (4.75), 615 (4.51), 682 (5.28) nm.

Phthalonitrile 5.29. A procedure related to that described for ZnPc **5.24** was used: 4-nitrophthalonitrile **5.28** (2.0 g, 11.5 mmol), *tert*-butyl 20-hydroxy-3,6,9,12,15,18-hexaoxaicosan-1-oate (4.99 g, 12.6 mmol), THF (15 mL) and K_2CO_3, (5.26 g, 40 mmol). The resulting crude

was purified on a silica column eluted by DCM/methanol (98:2), to give brown oil (4.87 g, 81.2%). ^{1}H NMR (d-$CDCl_3$, 400 MHz): δ 7.64 (d, J = 8.8 Hz, 1H, Ar-H), 7.24 (s, 1H, Ar-H), 7.18 (d, J = 8.8 Hz, 1H, Ar-H), 4.15 (t, J = 3.5, 2H, OCH_2), 3.91 (s, 2H, OCH_2), 3.79 (t, 2H, J = 3.7, OCH_2), 3.60-3.50 (m, 20H, OCH_2), 1.36 (s, 9H, $C(CH_3)_3$). ^{13}C NMR ($CDCl_3$): *δ* 169.48 ($CH_2C(O)O^tBu$), 161.95, 135.13, 119.81, 119.56, 117.01, 106.97 (Ar-C), 115.64, 115.20, (CN), 81.30 ($C(CH_3)$, 70.71, 70.50, 70.37, 70.29, 70.05 (OCH_2), 28.12 ($C(CH_3)_3$). MS (MALDI-TOF) *m/z* 545.2473 $[M+H+Na]^+$, calcd for, $C_{26}H_{37}N_2NaO_9$, 545.2475.

ZnPc 5.30. A mixture of 4-*tert*-butylphthalonitrile (385 mg, 2.09 mmol), phthalonitrile **5.29** (273.4 mg, 0.69 mmol) and zinc(II) acetate (254.7 mg, 1.4 mmol) were stirred in DMAE (35 mL). The solution was heated under a flow of argon in the presence of DBN. The reaction was treated as ZnPc **5.25** to give blue solid (121.6 mg, 15.5%). ^{1}HNMR (DMF-d_7): δ 9.59-8.92 (m, 7H, Ar-H), 8.47-8.35 (m, 3H, Ar-H), 7.88-7.78 (m, 2H, Ar-H), 4.74-4.58 (m, 2H, CH_2O), 4.19-4.00 (m, 4H, CH_2O), 3.87-3.57 (m, 18H, CH_2O), 1.83–1.75 (m, 27H, $C(CH_3)_3$), 1.42- 1.38 (s, 9H, $-OC(CH_3)_3$). ^{13}CNMR (DMF-d_7): δ 170.7 (C=O), 158.4, 158.1, 155.0, 154.9, 154.8, 154.6, 154.4, 154.2, 154.0, 142.8, 141.8, 140.0, 137.6, 133.5, 132.9, 132.5, 132.2, 131.7, 131.3, 130.4, 128.9, 128.4, 124.8, 123.9, 123.33, 123.25, 122.9, 120.8, 120.2, 119.9, 119.2, 118.9, 109.4, 107.4, 104.2 (Ar-C), 81.7 ($-OC(CH_3)_3$), 71.74, 71.69, 71.5, 71.4, 71.33, 71.30, 70.8, 70.2, 69.8, 69.61, 69.57, 69.0 (OCH_2), 52.1, 47.4, 45.5, 36.8 ($N-CH_2$), 32.6 ($Ar-C(CH_3)_3$), 28.5 ($O-C(CH_3)_3$). MS (MALDI-TOF) *m/z* 1138.454 $[M]^+$, 1082.448.454 $[M-C_4H_9]^+$, calcd for $C_{62}H_{74}N_8O_9Zn$ 1138.487, $C_{58}H_{66}N_8O_9Zn$ 1082.424. The solid (113.0 mg, 0.119 mmol) was dissolved in DCM/TFA (1:1) and stirred at 0 °C for 3 hours. The solvent was evaporated and the solid treated with 2N NaOH (10 mL) to obtain a blue solid (94.7 mg, 93.7 %) was obtained. ^{1}HNMR (DMF-d_7): δ 9.59-9.09 (m, 7H, Ar-H), 8.36-8.24 (m, 3H, Ar-H), 7.89-7.70 (m, 2H, Ar-

H), 4.56-4.46 (m, 2H, CH_2O), 3.90-3.04 (m, 24H, CH_2O), 1.83–1.78 (m, 27H, $C(CH_3)_3$). ^{13}CNMR (DMF-d_7): δ 171.8 (C=O), 159.6, 158.2, 157.9, 157.1, 155.2, 155.0, 154.9, 154.6, 154.1, 154.0, 153.8, 153.6, 142.2, 141.9, 140.2, 141.1, 140.0, 137.8, 137.6, 134.4, 133.4, 133.0, 132.5, 131.6, 131.4 130.8, 130.4, 128.9, 128.4, 128.3, 128.1, 128.0, 126.3, 124.7, 124.6, 123.9, 123.2, 122.8, 120.7, 120.0, 119.9, 119.8, 119.1, 115.0, 107.5, 107.4, 107.2 (Ar-C), 71.7, 71.6, 71.5, 71.4, 71.3, 71.2, 71.0, 70.7, 70.5, 70.1, 69.8, 69.5, 68.9 (OCH_2), 52.1, 47.4, 46.1, 40.9, 36.8, 36.5 (N-CH_2), 32.6 (Ar-$C(CH_3)_3$). MS (MALDI-TOF) *m/z* 1083.428 $[M+H]^+$, calcd for $C_{58}H_{67}N_8O_9Zn$ 1083.432. UV-vis (DMF): λ_{max} (log ε) 351 (4.65), 609 (4.38), 676 (5.14) nm.

ZnPc 5.31. A procedure related to that described for ZnPc **5.3** was used: ZnPc **5.30** (20.0 mg, 0.018 mmol), DMF (0.4 mL), Et_3N (3.2 mg, 0.032 mmol), HOBt (4.7 mg, 0.035 mmol), 1,4-bis-Boc-triazaheptane (7.0 mg, 0.023 mmol), and EDCI (4.0 mg, 0.026 mmol). The ZnPc was obtained as a blue solid (17.1 mg, 65.6%). ^{1}H NMR (DMF-d_7): δ 9.58-9.52 (m, 3H, Ar-H), 9.46-9.22 (m, 4H, Ar-H), 8.96-8.88 (m, 1H, Ar-H), 8.45-8.38 (m, 3H, Ar-H), 7.82-7.76 (m, 2H, Ar-H), 6.76-6.70 (m, 1H, Ar-H), 4.73-4.70 (m, 2H, $COCH_2O$), 4.49-4.44 (m, 2H, CH_2O), 3.89-3.82 (m, 4H, CH_2O), 3.77-3.72 (m, 2H, CH_2O), 3.69-3.58 (m, 14H, CH_2O), 3.35-3.28 (m, 6H, CH_2NH), 3.20-3.18 (m, 2H, CH_2NH), 1.82-1.80 (m, 27H, $C(CH_3)_3$), 1.45-1.36 (m, 18H, -$OC(CH_3)_3$). ^{13}CNMR (DMF-d_7): *δ* 170.7, 162.2, 157.1, 156.5, 154.9, 154.8, 154.7, 154.3, 154.2, 141.7, 139.9, 137.5, 133.4, 132.8, 132.1, 131.4, 130.4, 128.4, 123.4, 120.8, 119.9, 119.8, 119.2, 115.0, 113.3, 107.4, 107.2 (Ar-C), 79.9, 78.7 (O-$C(CH_3)_3$), 71.74, 71.68, 71.51, 71.48, 71.41, 71.37, 71.34, 71.30, 71.1, 70.8, 69.6 (OCH_2), 48.4, 48.2, 48.0, 47.6, 47.4, 46.1 40.9, 40.1, 39.9, 38.4, 36.8 (N-CH_2), 32.6 (Ar-$C(CH_3)_3$), 29.0, 28.8 (O-$C(CH_3)_3$). MS (MALDI-TOF) *m/z* 1267.606 $[M-^tBu]^+$, calcd for $C_{67}H_{85}N_{11}O_{10}Zn$ 1267.577. The solid (17.1 mg, 0.013 mmol) was dissolved in DCM/TFA (1:1) and stirred at 0 °C for 3 h. The solvent was evaporated and the

residue treated with 2N NaOH (10 mL) to give a blue solid (13.5 mg, 92.8 %). ^{1}H NMR (DMF-d_7): δ 9.60-9.25 (m, 7H, Ar-H), 9.15-8.91 (m, 1H, Ar-H), 8.52-8.31 (m, 3H, Ar-H), 7.89-7.73 (m, 1H, Ar-H), 4.74-4.63 (m, 2H, $COCH_2O$), 4.19-4.05 (m, 3H, CH_2O), 3.92-3.45 (m, 29H, CH_2O), 3.29-3.10 (m, 6H, CH_2NH) 1.80 (s, 27H, $C(CH_3)_3$). ^{13}C NMR (DMF-d_7): δ 171.6, 162.1, 160.2, 159.7, 155.0, 154.6, 154.4, 154.1, 153.9, 141.9, 140.1, 137.7, 133.1, 128.2, 124.7, 123.3, 119.8, 119.1, 107.2 (Ar-C), 71.72, 71.67, 71.6, 71.4, 71.3, 71.2, 71.0, 70.7, 69.6 (OCH_2), 49.0, 46.5, 38.4, 37.4, 36.7 (N-CH_2), 32.6 (Ar-$C(CH_3)_3$). MS (MALDI-TOF) *m/z* 1167.531 $[M]^+$, calcd for $C_{62}H_{77}N_{11}O_8Zn$ 1167.525. UV-vis (DMF): λ_{max} (log ε) 352 (4.90), 611 (4.61), 678 (5.35) nm.

ZnPc 5.32. A procedure related to that described for ZnPc **5.4** was used: ZnPc **5.31** (20.0 mg, 0.017 mmol), DIPA (0.015 mL, 0.107 mmol), CH_3I (0.2 mL) and dry DMF (0.5 mL). A blue solid was obtained (16.2 mg, 62.8%). ^{1}H NMR (DMF-d_7): δ 9.57-9.34 (m, 7H, Ar-H), 9.03-8.99 (m, 1H, Ar-H), 8.38-8.18 (m, 4H, Ar-H), 7.84-7.82 (m, 1H, N-H), 4.80-4.70 (m, 2H, $COCH_2$), 4.35 (br, 2H, CH_2O),4.15-3.51 (m, 28H, CH_2O/N-CH2/N-CH_3), 3.37 (s, 9H, N-CH_3), 1.85-1.79 (m, 27H, $C(CH_3)_3$). ^{13}C NMR (DMF-d_7): δ 171.7 (C=O), 162.0, 155.0, 154.5, 154.3, 153.9, 151.2, 142.1, 140.2, 137.7, 133.2, 128.3, 128.1, 124.6, 123.2, 119.7, 119.0, 107.5, 107.3, 107.1 (Ar-C), 71.8, 71.7, 71.4, 71.3, 71.2, 71.1, 71.0, 70.7, 69.6 (CH_2O), 64.3, 58.6, 57.2, 55.9, 54.3, 52.4, 47.9 (N-CH_3), 43.2, 36.7 (N-CH_2) 32.6 ($C(CH_3)_3$). MS (MALDI-TOF) *m*/z 1493.721 $[M]^+$, 1404.681 $[M\text{-}I\text{-}H+K]^+$; calcd for $C_{67}H_{89}I_2N_{11}O_8Zn^+$ 1493.428, $C_{67}H_{88}IKN_{11}O_8Zn^+$ 1404.479. UV−Vis (DMF): λ_{max} (log ε) 351 (4.81), 610 (4.50), 677 (5.26) nm.

5.4.2. Syntheses of Pcs and Their AntiCEA Bioconjugates

***tert*-Butyl-12-iodo-4,7,10-trioxadodecanoate.** A slurry of *p*-TsCl (0.38 g, 2.0 mmol) and pyridine (0.35 mL) was mechanically stirred in a three-neck, N_2 flushed flask. The temperature was maintained at 5 °C (ice-cold water bath), while *tert*-Butyl-12-hydroxy-4,7,10-

trioxadodecanoate (0.5 g, 1.8 mmol) was slowly added from an addition funnel. After the addition was complete, the mixture was stirred for 15 minutes. The mixture was poured into ice-cold water (10 mL) and washed with DCM (10 mL). The organic layer was washed with ice-cold 6N HCl (3 × 5 mL) and reduced to minimum under reduced pressure. The tosylate obtained was used without further purification.[32] To a solution of the above tosylate (700.0 mg, 1.62 mmol) in dry acetone (10 mL) was added NaI (300.0 mg, 2.0 mmol) and the reaction heated (65 °C) for 20 h. On cooling to room temperature, the reaction mixture was filtered under vacuum and washed with acetone. The filtrate was concentrated and the residue dissolved in 20.0 mL of DCM. The solution was successively washed with 1N sodium thiosulfate solution and brine, and dried over anhydrous sodium sulfate. The solvent was removed under vacuum and the product obtained as a light yellow oil (623.8 mg, 99.2 %).[9]

Phthalonitrile 5.33. A mixture of 4-nitrophthalonitrile (1 g, 5.8 mmol) and 4-aminophenol (0.7 g, 6.4 mmol) was dissolved in DMF (15 mL) and heated to 63°C. Potassium carbonate, K_2CO_3 (2.63 g, 20 mmol) was added into solution in six portions after every five minutes. The reaction mixture was stirred 4 h under argon at the same temperature. It was left to cool to room temperature and poured into ice-cold water (500 mL). This was then filtered and the crude product (brown) purified using a silica column eluted with DCM/methanol (98:2). The solvent was removed to give a yellow solid (1.0 g, 73.3%), mp 130 - 131°C. ^{1}H NMR (d-CD_2Cl_2, 400 MHz): δ 7.70 (d, J = 8.6 Hz, 1H, Ar-H), 7.23 (t, J = 8.8 Hz, 2H, Ar-H), 6.87 (d, J = 7.8 Hz, 2H, Ar-H), 6.73 (d, J = 7.8, 2H, H-Ar), 3.86 (br, 2H, NH_2). ^{13}C NMR (d-$CDCl_3$, 100 MHz): δ 162.89, 145.32, 144.96, 135.36, 121.71, 120.98, 120.82, 117.31, 116.16, 115.84, 115.40, 107.96 (Ar-C, CN). MS (MALDI-TOF) *m/z* 236.0813 $[M+H]^+$, calcd for, $C_{14}H_9N_3O$, 23.0818.

Phthalonitrile 5.34. A mixture of **Pn 5.33** (0.5 g, 2.13 mmol) and 1,4-dioxane-2,6-dione (0.275 g, 2.37 mmol) was dissolved in DMF (1.5 mL) and stirred overnight at 25 °C. Then water (5.0 mL) was added to the solution to precipitate the product. The solid was centrifuged and washed with water and hexane. The solid was dried under vacuum for 2 days to afford the pure yellow solid (688.7 mg, 92.1%), mp 176 – 177 °C). ^{1}H NMR (CD_3COCD_3, 400 MHz): δ 9.68 (br, 1H, NH), 8.01 (d, *J* = 8.76 Hz, 1H, Ar-H), 7.86 (d, *J* = 9.00 Hz, 2H, Ar-H), 7.60 (d, *J* = 2.52 Hz, 1H, Ar-H), 7.42 (dd, J = 2.60 Hz, 1H, Ar-H), 7.20 (d, *J* = 9.00 Hz, 2H, Ar-H), 4.37 (s, 2H, CH_2O), 4.27 (s, 2H, CH_2O). ^{13}C NMR (CD_3COCD_3, 100 MHz): δ 172.4, 168.8 (CO), 163.0, 150.6, 137.3, 136.9, 122.8, 122.5, 122.3, 122.0, 118.3, 109.5 (Ar-H), 116.5, 116.1 (CN), 72.5, 69.7 (CH_2O). MS (MALDI-TOF) *m/z* 352.0800 $[M+H]^+$, calcd for, **$C_{18}H_{14}N_3O_5$, 352.0933**.

Phthalonitrile 5.35. Phthalonitrile **5.34** (0.25 g, 0.712 mmol) was dissolved in DMF (8 mL). Et_3N (90 mg, 0.912 mmol, 122.4 µL, 1 h), HOBt (102.4 mg, 0.757 mmol, 2 h) and tert-butyl-12-amino-4,7,10-trioxadodecanoate (240.3 mg, 0.868 mmol) were added to the reaction solution and the solution was stirred for 20 min. EDCI (117.9 mg, 0.757 mmol) was added to the reaction solution in one portion. The reaction solution was stirred for 3 days at 25 °C. The reaction solution was diluted using ethyl acetate (20 mL) and the organic solution washed subsequently with water (30 mL × 2). The organic layer was dried over anhydrous sodium sulfate. The solvent was evaporated and the crude was purified by silica column eluted by DCM/chloroform (4:1), and then DCM/methanol (98:2) to afford yellowish oil (400.6 mg, 92.2%). ^{1}H NMR (CD_3COCD_3, 400 MHz): δ 10.10 (br, 1H, NH), 8.02 (d, *J* = 8.76 Hz, 1H, Ar-H), 7.88 (d, *J* = 8.96 Hz, 2H, Ar-H), 7.59 (d, *J* = 2.52 Hz, 1H, Ar-H), 7.44 – 7.40 (m, 1H, Ar-H), 7.19 (d, *J* = 8.96 Hz, 2H, Ar-H), 4.21 (d, *J* = 3.24, 2H, CH_2O), 3.65 (t, *J* = 6.36, 2H, CH_2O), 3.57 – 3.53 (m, 10H, CH_2O), 3.45 (t, *J* = 5.52, 2H, CH_2O), 2.43 (d, *J* = 6.32, 2H, CH_2O), 1.42 (s, 9H,

$C(CH_3)_3$). ^{13}C NMR (CD_3COCD_3, 100 MHz): δ 171.3, 170.3, 168.7 (C=O), 163.0, 150.6, 137.6, 136.9, 128.2, 125.4, 122.8, 122.5, 122.4, 122.0, 120.1, 118.3, 110.3, 109.5 (Ar-H), 116.5, 116.1 (CN), 80.5 (CO), 72.6, 72.2, 71.1, 71.0, 70.2, 67.6 (CH_2O), 39.6, 37.0 (CH_2), 28.3 ($C(CH_3)_3$). MS (MALDI-TOF) *m/z* 633.2551 $[M+Na]^+$, calcd for **$C_{31}H_{38}N_4NaO_9$ 610.2536**.

ZnPc 5.37. A mixture of **5.36** (1002.39 mg, 3.0 mmol), phthalonitrile **5.35** (610.26 mg, 1.0 mmol) and zinc acetate (254.7 mg, 1.4 mmol) were mixed together in DMAE (10.0 mL). The solution was heated under the flow of argon, and two drops of DBN were added to the reaction solution. The reaction solution was further heateed at 135 °C for 5 hours. After the reaction, the solvent was removed under vacuum. The residue was purified by column chromatography (neutral alumina, 10 cm, loaded by chloroform) with the elution of mixed solvents of chloroform/DCM (95:5). A second column (sephadex G-100) eluted by DCM gave the title compound as a green solid, dried at 85 °C under vacuum overnight (50.8 mg, 10.1%). ^1H NMR (d-DMF, 400 MHz): δ 9.25 – 8.83 (m, 9H, Ar-H), 8.25 – 8.22 (m, 1H, Ar-H), 7.89 – 7.54 (m, 3H, Ar-H), 4.34 (s, 2H, OCH_2), 4.26 (s, 2H, OCH_2), 3.65 – 3.57 (m, 12H, OCH_2), 3.40 – 3.37 (m, 4H, OCH_2), 3.03 – 2.99 (m, 12H, SCH_2), 2.69 – 2.65 (m, 2H, CH_2), 2.56 – 2.45 (m, 36H, NCH_2), 2.33 – 2.29 (m, 12H, NCH_2), 1.43 – 1.41 (m, 9H, Boc- $C(CH_3)_3$). MS (MALDI-TOF) *m/z* peak at 1621.551 $(M-t\text{Bu}+H)^+$, calcd for **$C_{75}H_{96}N_{16}O_9S_6Zn$ 1621.519**. UV-vis (DMF): λ_{max} (log ε) 371 (4.70), 631 (4.38), 701 (5.09) nm.

ZnPc 5.38 (40 mg, 0.0239 mmol) was then dissolved and stirred in DCM (1 mL) and CH_3I (2 mL) at 25 °C for 48 h. The solvent was removed under reduced pressure. The residue was washed with hexanes several times. The residue was purified on C18 column (40-75 μm) eluted by methanol/water (40:60 → 100:0) to give a green solid (20.3 mg, 33.7%). ^1H NMR (DMF-d_7, 400 MHz): δ 9.56 – 9.28 (m, 6H, Ar-H), 8.37 – 8.32 (m, 1H, Ar-H), 7.95 – 7.81 (m,

4H, Ar-H), 7.55 – 7.51 (m, 2H, Ar-H), 4.39 – 4.20 (m, 24H, OCH_2/NCH_3), 4.26 (s, 4H, OCH_2), 3.68 – 3.57 (m, 68H, OCH_2/NCH_3), 2.48 – 2.45 (m, 2H, CH_2), 1.46 – 1.41 (m, 9H, Boc-$C(CH_3)_3$). UV-vis (DMF): λ_{max} (log ε) 376 (4.68), 625 (4.31), 696 (5.04) nm.

ZnPc 5.39. The Pc **5.38** was dissolved in a mixture of DCM/TFA (3 mL/3 mL) and the solution was stirred at 0 °C for 4 h. After the reaction, the solvent was removed using nitrogen gas. The resulting residue was dissolved in acetone, cold ethyl ether added to precipitate the product and then centrifuged to afford green solid in quantitative yield. ^{1}H NMR (DMSO-d_6, 400 MHz): δ 9.51 – 9.35 (m, 6H, Ar-H), 8.37 – 8.32 (m, 1H, Ar-H), 8.10 – 7.96 (m, 4H, Ar-H), 7.54 – 7.51 (m, 2H, Ar-H), 4.39 – 4.25 (m, 24H, OCH_2/NCH_3), 3.81 (s, 4H, OCH_2), 3.72 – 3.57 (m, 68H, OCH_2/NCH_3), 2.55 – 2.52 (m, 2H, CH_2). UV-vis (DMF): λ_{max} (log ε) 378 (4.58), 625 (4.22), 696 (4.94) nm.

ZnPc 5.40. The monoclonal antibody was reconstituted at 2 mg/mL in 0.1 M $NaHCO_3$ solution. Pc **5.39** (1 mg, 0.0005 mmol) was dissolved in DMSO (50 µL). DIEA (0.078 mg, 0.006 mmol), HOBt (0.34 mg, 0.002 mmol) and TBTU (0.59 mg, 0.002 mmol) were added to the DMSO solvent and the reaction solution was stirred for 2 min. The reconstituted monoclonal antibody solution (500 µL) was added into the activated phthalocyanine solution and the combined solution was kept with shaking frequently at 25 ℃ for 1 hour. Then the solution was kept at 4 °C overnight. The crude antibody-Pc conjugate solution was purified by spin column chromatography (50 µL for each spin column to load, 750 rcf, 1 min, 24 °C). The resulting solution was combined together to afford the blue conjugate solution (600 µL).

ZnPc 5.43. A mixture of phthalonitrile **5.42** (75.0 mg, 0.24 mmol), phthalonitrile (885.0 mg, 6.60 mmol), and zinc acetate (348.6 mg, 1.9 mmol) were mixed together in DMAE (10.0 mL). The solution was heated at 140 °C under the flow of argon, and one drop of DBN was

added to the reaction solution. The reaction solution was further heated at 140 °C for 5 hours. After the reaction, the solvent was removed under vacuum. The residue was filtered under gravity and purified by silica column chromatography with the elution of DCM/THF (3:1). The product was eluted by acetone and concentrated to give a blue-green solid. Another silica column eluted by DCM/ethyl acetate (1:2) gave the product as a green solid (17.8 mg, 9.8%). ^{1}H NMR (DMF-d_7): δ 9.32 - 9.02 (m, 6H, Ar-H), 8.29-8.12 (m, 6H, Ar-H), 7.82-7.42 (m, 2H, Ar-H), 6.99 (br, 1H, OH), 5.11-4.97 (m, 2H, OCH_2), 4.45-4.42 (m, 2H, OCH_2), 4.12 (t, J = 4.76, 2H, OCH_2), 3.68 (t, J = 3.52, 2H, OCH_2), 3.48 (t, J = 4.68, 2H, OCH_2), 3.30-3.27 (s, 3H, OCH_3). ^{13}C NMR (DMF-d_7, 100 MHz): δ 154.4, 153.9, 152.9, 150.7, 139.3, 138.0, 130.3, 130.2, 129.4, 126.7, 123.8, 123.5, 123.4, 123.2, 123.0, 119.7, 117.7 (Ar-C), 72.9, 72.1, 71.7, 71.4 (OCH_2), 59.1 (OCH_3). MS (MALDI-TOF) *m/z* peak at **755.225** $(M+H)^+$, calcd for **$C_{39}H_{31}N_8O_5Zn$ 755.171**. UV-vis (DMF): λ_{max} (log ε) 342 (4.71), 628 (4.49), 694 (5.19) nm.

ZnPc 5.44. A mixture of Pc **5.43** (9.0 mg, 0.012 mmol) and *tert*-Butyl-12-iodo-4,7,10-trioxadodecanoate (6.6 mg, 0.017 mmol) were mixed together in DMF (5.0 mL). The solution was heated at 70 °C, and K_2CO_3 (25.0 mg, 1.8 mmol) was added to the reaction solution. The reaction solution was heated for 5-6 hours. After the reaction, the solvent was removed under reduced pressure. The residue was dissolved in ethyl acetate (10 mL), washed with water (10 mL) and dried to obtain a blue solid. The solid was purified by column chromatography with the elution of DCM/methanol (95:5) to give a blue solid (9.2 mg, 76.7 %). ^{1}H NMR (DMF-d_7): δ 9.40-9.35 (m, 6H, Ar-H), 8.26-8.20 (m, 6H, Ar-H), 7.62 (s, 2H, Ar-H), 4.94 (t, J = 4.52, 4H, OCH_2), 4.46 (t, J = 4.56, 4H, OCH_2), 4.10 (t, J = 4.28, 4H, OCH_2), 3.84-3.81 (m, 4H, OCH_2), 3.67-3.62 (m, 6H, OCH_2), 3.58-3.54 (m, 4H, OCH_2), 3.24 (s, 3H, OCH_3), 2.42 (t, J = 6.24, 2H, CH_2), 1.39 (s, 9H, ^{t}Bu-$C(CH_3)_3$). ^{13}C NMR (DMF-d_7): δ 171.7 (C=O), 154.5, 154.3, 153.8,

151.55, 151.8, 139.9, 139.6, 130.3, 130.2, 128.7, 128.4, 123.9, 123.4, 117.3 (Ar-C), 80.8 (C=O), 72.8, 72.0, 71.6, 71.4, 71.3, 71.2, 70.8, 67.7 (OCH_2), 59.0 (OCH_3), 37.2 (CH_2), 28.5 ($C(CH_3)_3$). MS (MALDI-TOF) *m/z* peak at **1015.376** $(M+H)^+$, **959.318** $(M-^tBu+H)^+$, calcd for **$C_{52}H_{55}N_8O_{10}Zn$ 1014.325**, **$C_{48}H_{47}N_8O_{10}Zn$ 959.271**. The above product (9.2 mg, 9.1 mmol) was subjected to DCM/TFA (1:1, 5 mL) treatment for 4 h to remove the tert-butyl protecting group. After the reaction, the solvent was removed under reduced pressure (at 65 °C). The residue was dissolved in DCM (1.0 mL), treated with cold diethyl ether (10 mL) and centrifuged to obtain a blue solid. The solid was dried under vacuum for two days to give a blue solid (8.5 mg, 97.7 %). ^1H NMR (DMF-d_7): δ 9.39 (s, 6H, Ar-H), 8.23(s, 6H, Ar-H), 7.62 (s, 2H, Ar-H), 4.96 (br, 4H, OCH_2), 4.47 (s, 4H, OCH_2), 4.10 (t, J = 4.72, 4H, OCH_2), 3.85-3.81 (m, 4H, OCH_2), 3.76-3.62 (m, 6H, OCH_2), 3.60-3.56 (m, 2H, OCH_2), 3.47-3.44 (m, 2H, OCH_2), 3.24 (s, 3H, OCH_3), 2.54 (t, J = 6.28, 2H, CH_2). ^{13}C NMR (DMF-d_7): δ 173.7 (C=O), 154.4, 139.8, 139.6, 130.2, 123.8, 123.5, 117.2 (Ar-C), 83.5 (C=O), 73.5, 72.8, 71.92, 71.89, 71.63, 71.61, 71.5, 71.4, 71.3, 71.2, 70.7, 67.7, 66.6 (OCH_2), 59.0 (OCH_3), 51.9 (CH_2). MS (MALDI-TOF) *m/z* peak at **959.449** $(M+H)^+$, **981.441** $(M+Na)^+$; calcd for **$C_{48}H_{47}N_8O_{10}Zn$ 959.271**, **$C_{48}H_{47}N_8NaO_{10}Zn$ 981.253**. UV-vis (DMF): λ_{max} (log ε) 335 (4.57), 619 (4.42), 688 (5.18) nm.

ZnPc 5.45. The monoclonal antibody was reconstituted at 2 mg/mL in 0.1 M $NaHCO_3$ solution. Pc **5.44** (1 mg, 0.001 mmol) was dissolved in DMSO (50 µL). DIEA (0.078 mg, 0.006 mmol. 1.1 µL), HOBt (0.34 mg, 0.002 mmol) and TBTU (0.59 mg, 0.002 mmol) were added to the DMSO solvent. The reaction solution was stirred for 2 h and added the monoclonal antiCEA as described for conjugate **5.40** above. The crude antibody-Pc conjugate solution was purified by spin column chromatography (50 µL for each spin column to load, 750 rcf (3000 rpm), 1 min, 24 °C). The resulting solution was combined to afford the blue conjugate solution (600 µL).

ZnPc 5.47. The monoclonal antibody was reconstituted at 2 mg/mL in 0.1 M $NaHCO_3$ solution. Pc **5.46** (1 mg, 0.001 mmol) was dissolved in DMSO (50 µL). DIEA (0.078 mg, 0.006 mmol. 1.1 µL), HOBt (0.34 mg, 0.002 mmol) and TBTU (0.59 mg, 0.002 mmol) were added to the DMSO solvent. The reaction solution was stirred for 2 h and added the monoclonal antiCEA as described for conjugate **5.40** above. The crude antibody-Pc conjugate solution was purified by spin column chromatography (50 µL for each spin column to load, 750 rcf (8000 rpm), 1 min, 24 °C). The resulting solution was combined to afford the blue conjugate solution (700 µL).

5.4.3. Cell Studies

The human carcinoma HEp2 cells used in this study were kept in a 50:50 mixture of DMEM:AMEM (Invitrogen) complemented with 5% FBS (Invitrogen), Primocin antibiotic (Invitrogen) and 5% CO_2 at 37 ^{o}C. To sustain subconfluent stocks, the cells had to be subcultured twice weekly. The cells used in all the studies were from the 4^{th} to 15^{th} passage.

Time-Dependent Cellular Uptake: The incubation of the human carcinoma HEp2 cells involved 7500 cells per well in a Costar 96-well plate and permitted to grow for 48 h. Each ZnPc stock solution was prepared in DMSO at 32 mM and then diluted to 20 µM in medium (a 2X stock). Finally, a concentration of 10 µM with a maximum DMSO concentration of 1% was achieved via dilution into the 96-well plate. The cellular uptake was permitted to go on for 0, 1, 2, 4, 8, 12 and 24 h, after which it was halted. This was achieved by removing the loading medium and washing the wells with PBS. The concentration of each compound was obtained using standard curves via intrinsic fluorescence. The fluorescence was measured using a BMG FLUOstar plate reader with a 355 nm excitation and a 650 nm emission filter. The cells were measured and their uptake expressed in nM compound concentration per unit cell, following a CyQuant cell proliferation assay (Invitrogen).

Dark Cytotoxicity: The plating of HEp2 cells was achieved as described above. The ZnPcs were diluted to a final concentration of 400 µM in medium. Two-fold serial dilutions to 50 µM were prepared and the cells were incubated overnight. The cell toxicity was calculated using Promega's Cell Titer Blue Viability assay according to the manufacturer's directions. Cells that were not treated were considered 100% viable, while those treated with 0.2% saponin were considered to be nonviable (0% viability). The dose-response curves were used to calculate IC_{50} values for each ZnPc.

Phototoxicity: The plating of HEp2 cells was achieved as described above. The ZnPc concentrations ranged between 6.25-100 µM. Following overnight loading, 50 mM HEPES pH 7.2 replaced the initial medium. A NewPort light system with a 175 W halogen lamp was used to irradiate the cells for 20 min. The light was filtered through a water filter to provide approximately 1.5 J/cm^2 light dose required. The culture was kept on a 5 ^oC Echotherm chilling/heating plate (Torrey Pines Scientific, Inc.) to keep the cells cool. Subsequent to the light exposure, the plate was incubated overnight and the cell viability calculated as described for the dark cytotoxicity.

Microscopy: The incubation of the cells was done in a glass bottom 6-well plate (MatTek) and permitted to grow for 48 h. The cells were then exposed to 10 µM of each ZnPc for 6 h. Tracers for different organelles were used at the shown concentrations: LysoSensor Green 50 nM, MitoTracker Green 250 nM, ER Tracker Blue/white 100 nM, and BODIPY FL C5 ceramide 1 µM. The cells were incubated concurrently with ZnPcs and then diluted with tracers for 30 min before washing them 3 times using PBS. A Leica DMRXA microscope with a 40× NA 0.8dip objective lens and DAPI, GFP and Texas Red filter cubes (Chroma Technologies) was used to acquire microscopy images as described in Chapter 2.

5.4.4. Methods for Mouse Imaging

Nude mice were subcutaneously implanted on either side of the upper thigh with 1 x 10^6 HT-29 colon cancer cells suspended in DMEM media: Matrigel 4:1 (v/v). Tumors were allowed to establish until visible (approximately 100 cm^3). One additional mouse had no implanted tumor but was used to evaluate the kinetics of tissue uptake, in addition to the retention of the Pc or PcCEA in normal subcutaneous tissue. Mice were anesthetized using isoflurane to effect, and imaged for 20 seconds at 630 nm excitation/700 nm emission in a Kodak In Vivo FX imager to obtain a background image (0 hours), then given an intratumor administration of 80 µL of 100 µM phthalocyanine only (Pc **5.44**) on the right flank or ZnPc coupled with antiCEA (Pc-antiCEA **5.45**) in the left flank. Mice were then returned to their boxes and re-imaged at times of 1, 6, 24 and 96 hours.

5.5. References

1. Baron ED, Malbasa CL, Santo-Domingo D, Fu, P.; Miller, J. D.; Hanneman, K. K.; Hsia, A. H.; Oleinick, N. L.; Colussi, V. C.; Cooper, K. D. *Lasers Surg. Med.* **2010**, *42* (10), 728–735.
2. Kinsella, T. J.; Baron, E. D.; Colussi, V. C.; Cooper, K. D.; Hoppel, C. L.; Ingalls, S. T.; Kenney, M. E.; Li, X.; Oleinick, N. L.; Stevens, S. R.; Remick, S. C. *Front. Oncol.* **2011**, *1* (14), 1-6.
3. Sokolov, V. V.; Chissov, V. I.; Yakubovskya, R.I.; Aristarkhova, E.I.; Filonenko, E.V.; Belous, T.A.; Vorozhtsov, G. N.; Zharkova, N. N.; Smirnov, V. V.; Zhitkova, M. B. *Proceedings of SPIE (Photochemistry: Photodynamic Therapy and Other Modalities).* **1996**, *2625*, 281-287.
4. Gijsens, A.; Derycke, A.; Missiaen, L.; De Vos, D.; Huwyler, J.; Eberle, A.; de Witte, P. *Int. J. Cancer.* **2002**, *101*, 78-85.
5. Arnida; Nishiyama, N.; Kanayama, N.; Jang, W-D.; Yamasaki, Y.; Kataoka, K. *J. Controlled Release* **2006**, *115* (2), 208-215.
6. Suzuki, T.; Oishi, M.; Nagasaki, Y. *J. Photopolym. Sci. Tec.* **2009**, *22* (4), 547-550.
7. Durmus, M.; Ayhan, M. M.; Gürek, A. G.; Ahsen, V. *Dyes and Pigments* **2008**, *77*, 570-577.
8. Bai, M.; Lo, P-C.; Ye, J.; Wu, C.; Fong, W-P.; Ng; Dennis, K. P. *Org. Biomol. Chem.* **2011**, *9* (20), 7028-7032.

9. Li, H.; Fronczek, F. R.; Vicente, M. G. H. *Tetra. Lett.* **2011**, *52*, 6675-6678.

10. Hamblin, M. R.; Miller, J. L.; Rizvi, I.; Loew, H. G.; Hasan, T. *Br. J. Cancer* **2003**, *89*, 937-943.

11. Rovers, J. P.; Saarnak, A. E.; de Jode, M.; Sterenborg, H. J.; Terpstra, O. T.; Grahn, M. F. *Photochem. Photobiol.* **2000**, *71*, 211-217.

12. Krueger, T.; Altermatt, H. J.; Mettler, D.; Scholl, B.; Magnusson, L.; Ris, H. B. *Lasers Surg. Med.* **2003**, *32*, 61-68.

13. Fang, J.; Sawa, T.; Akaike, T.; Greish, K.; Maeda, H. *Int. J. Cancer* **2004**, 109, 1-8.

14. Savellano, M. D.; Hasan, T. *Photochem. Photobiol.* **2003**, *77*, 431-439.

15. Ichikawa, K.; Hikita, T.; Maeda, N.; Takeuchi, Y.; Namba, Y.; Oku, N. *Biol. Pharm. Bull.* **2004**, *27*, 443-444.

16. Wöhrle, D.; Iskander, N.; Graschew, G.; Sinn, H.; Friedrich, E. A.; Maier-Borst, W.; Stern, J.; Schlag, P. *Photochem. Photobiol.* **1990**, *51*, 351-356.

17. Ball, D. J.; Mayhew, S.; Wood, S. R.; Griffiths, J.; Vernon, D. I.; Brown, S. B. *Photochem. Photobiol.* **1999**, *69*, 390–396.

18. Duan, W.; Lo, P-C.; Duan, L.; Fong, W-P.; Ng; Dennis, K. P. *Bioorg. Med. Chem.* **2010**, *18*, 2672-2677.

19. Dummin, H.; Cernay, T.; Zimmermann, H. W. *J. Photochem. Photobiol. B: Biol.* **1997**, *37*, 219-229.

20. Li, H.; Jensen, T. J.; Fronczek, F. R.; Vicente, M. G. H. *J. Med. Chem.* **2008**, *51* (3), 502-511.

21. Marino, J.; Garcia, M. C. V.; Dicelio, L. E.; Roguin, L. P.; Awruch, J. *Eur. J. Med. Chem.* **2010**, *45* (9), 4129-4139.

22. Chen, Z.; Zhou, S.; Chen, J.; Deng, Y.; Luo, Z.; Chen, H.; Hamblin, M. R.; Huang, M. *Chem. Med. Chem.* **2010**, *5* (6), 890-898.

23. Durmus, M.; Ahsen, V. *J. Inorg. Biochem.* **2010**, *104* (3), 297-309.

24. Minnock, A.; Vernon, D. I.; Schofield, J.; Griffiths, J.; Parish, J. H.; Brown, S. B. *J. Photochem. Photobiol. B: Biol.* **1996**, *32*, 159-164.

25. Mantareva, V.; Kussovski, V.; Angelov, I.; Wohrle, D.; Dimitrov, R.; Popova, E.; Dimitrov, S. *Photochem. Photobiol. Sci.* **2011**, *10*, 91-102.

26. Tempesti, T. C.; Alvarez, M. G.; Durantini, E. N. *Dyes and Pigments* **2011**, *91*, 6-12.

27. Ongarora, B. G.; Hu, X.; Verberne-Sutton, D.; Garno, J. C.; Vicente, M. G. *J. Theranostics* **2012**, *2* (9), 850-870.

28. Sibrian-Vazquez, M.; Jensen, T. J.; Vicente, M. G. H. *J. Photochem. Photobiol B: Biol.* **2007**, *86*, 9-21.

29. Sehgal, I.; Sibrian-Vazquez, M.; Vicente, M. G. H. *J. Med. Chem.* **2008**, *51*, 6014-6020.

30. Warnecke, A.; Kratz, F. *Bioconj. Chem.* **2003**, *14*, 377-387.

31. Hofman, J-W.; van Zeeland, F.; Turker, S.; Talsma, H.; Lambrechts, S. A. G.; Sakharov, D. V.; Hennink, W. E.; van Nostrum, C. F. *J. Med. Chem.* **2007**, *50*, 1485-1494.

32. Zorlu, Y.; Dumoulin, F.; Durmuş, M.; Ahsen, V. *Tetrahedron* **2010**, *66* (17), 3248-3258.

33. Masilela, N.; Nyokong, T. *Dyes and Pigments* **2010**, *84* (3), 242-248.

34. Jensen, T. J.; Vicente, M. G. H.; Luguya, R.; Norton, J.; Fronczek, F. R.; Smith, K. M. *J. Photochem. Photobiol. B: Biol.* **2010**, *100* (2), 100-111.

35. Kessel, D.; Luguya, R.; Vicente, M. G. H. *Photochem. Photobiol.* **2003**, *78*, 431-435.

36. Sibrian-Vazquez, M.; Jensen, T. J.; Fronczek, F. R.; Hammer, R. P.; Vicente, M. G. H. *Bioconj. Chem.* **2005**, *16* (4), 852-863.

37. Sibrian-Vazquez, M.; Ortiz, J.; Nesterova, I. V.; Fernández-Lázaro, F.; Sastre-Santos, A.; Soper, S. A.; Vicente, M. G. H. *Bioconj. Chem.* **2007**, *18*, 410-420.

38. Rao, R. V.; Hermel, E.; Castro-Obregon, S.; del Rio, G.; Ellerby, L. M.; Ellerby, H. M.; Bredesen, D. E. *J. Biol. Chem.* **2001**, *276* (36), 33869-33874.

39. Groenendyk, J.; Michalak, M. *Acta Biochim. Pol*. **2005**, *52*, 381-395.

40. Jadiya, S. S. *Int. J. Pharm.* **2012**, *2* (3), 679-686.

41. Chames, P.; Regenmortel, M. V.; Weiss, E.; Baty, D. *British Journal of Pharmacology* **2009**, *157*, 220-233.

42. Scott, A. M.; Allison, J. P.; Wolchok, J. D. *Cancer Immunity* **2012**, 12, 14.

43. Rihova, B. *Folia Microbiol.* **1995**, *40* (4), 367-384.

44. Song, S.; Liu, D.; Peng, J.; Deng, H.; Guo, Y.; Xu, L. X.; Miller, A. D.; Xu, Y. *FASEB J.* **2009**, *23*, 1396-1404.

45. Li, Z.; Zhao, R.; Wu, X.; Sun, Y.; Yao, M.; Li, J.; Xu, Y.; Gu, J. *FASEB J.* **2005**, *19*, 1978-1985.

46. Vrouenraets, M. B.; Visser, G. W. M.; Stewart, F. A.; Stigter, M.; Oppelaar, H.; Postmus, P. E.; Snow, G. B.; van Dongen, G. A. M. S. *Cancer Research* **1999**, *59* (7), 1505-1513.

47. Carcenac, M.; Larroque, C.; Langlois, R.; van Lier, J. E.; Artus, J.-C.; Pelegrin, A. *Photochem. Photobiol.* **1999**, *70* (6), 930-936.

48. Xu, P.; Chen, J.; Chen, Z.; Zhou, S.; Hu, P.; Chen, X.; Huang, M. *PLoS ONE* **2012**, *7* (5), e37051.

49. Stuchinskaya, T.; Moreno, M.; Cook, M. J.; Edwards, D. R.; Russell, D. A. *Photochemical & photobiological sciences: Official journal of the European Photochemistry Association and the European Society for Photobiology* **2011**, *10* (5), 822-831.

50. Su, B.-B.; Shi, H.; Wan, J. *World J. Gastroenterol.* **2012**, *18* (17), 2121-2126

51. Goldstein, M. J.; Mitchell, E. P. *Cancer Invest.* **2005**, *23* (4), 338-351.

52. Hudson, R.; Carcenac, M.; Smith, K.; Madden, L.; Clarke, O. J.; Pelegrin, A.; Greenman, J.; Boyle, R. W. *Br. J. Cancer* **2005**, *92*, 1442-1449.

53. Vrouenraets, M. B.; Visser, G. W. M.; Stewart, F. A.; Stigter, M.; Oppelaar, H.; Postmus, P. E.; Snow, G. B.; van Dongen, G. A. M. S. *Cancer Res.* **1999**, *59*, 1505.

54. Kaushal, S.; McElroy, M. K.; Luiken, G. A.; Talamini, M. A.; Moossa, A. R.; Hoffman, R. M.; Bouvet, M. *J. Gastrointest. Surg.* **2008**, *12*, 1938-1950.

APPENDIX A: CHARACTERIZATION DATA FOR COMPOUNDS IN CHAPTER 2

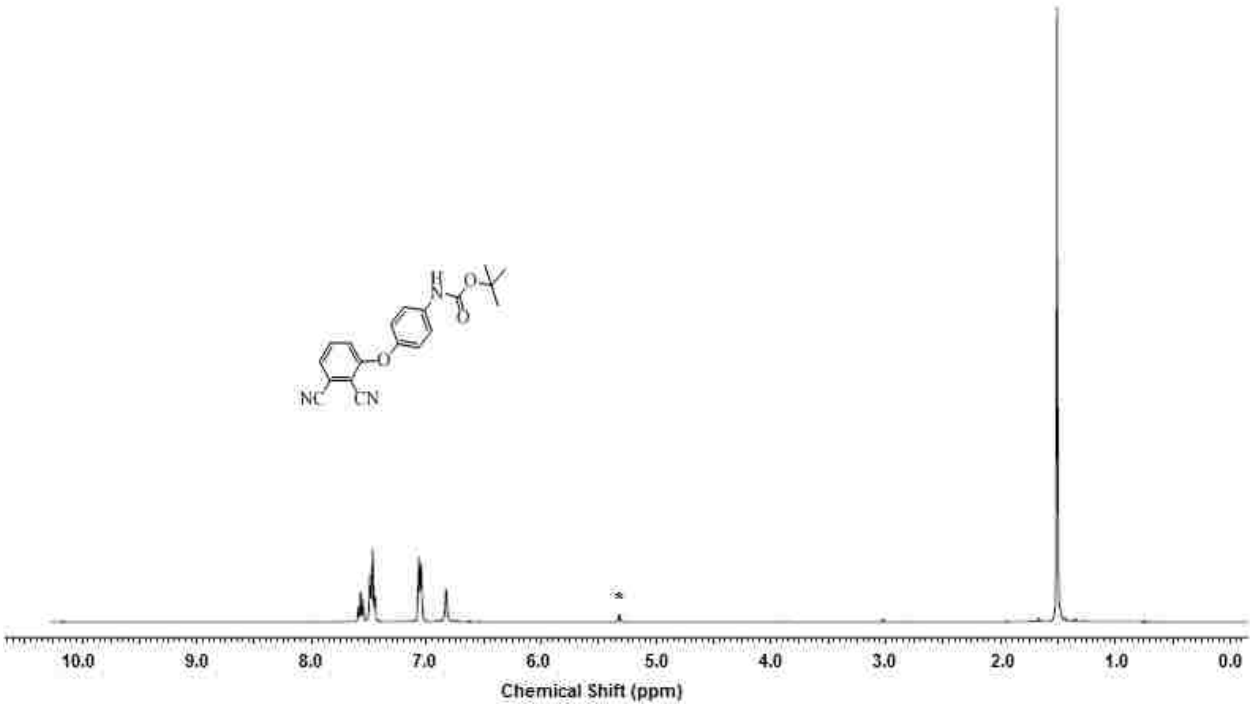

Figure A.1: ^{1}H NMR spectrum of phthalonitrile **2.3** in d-DCM at 400 MHz (*denotes solvents).

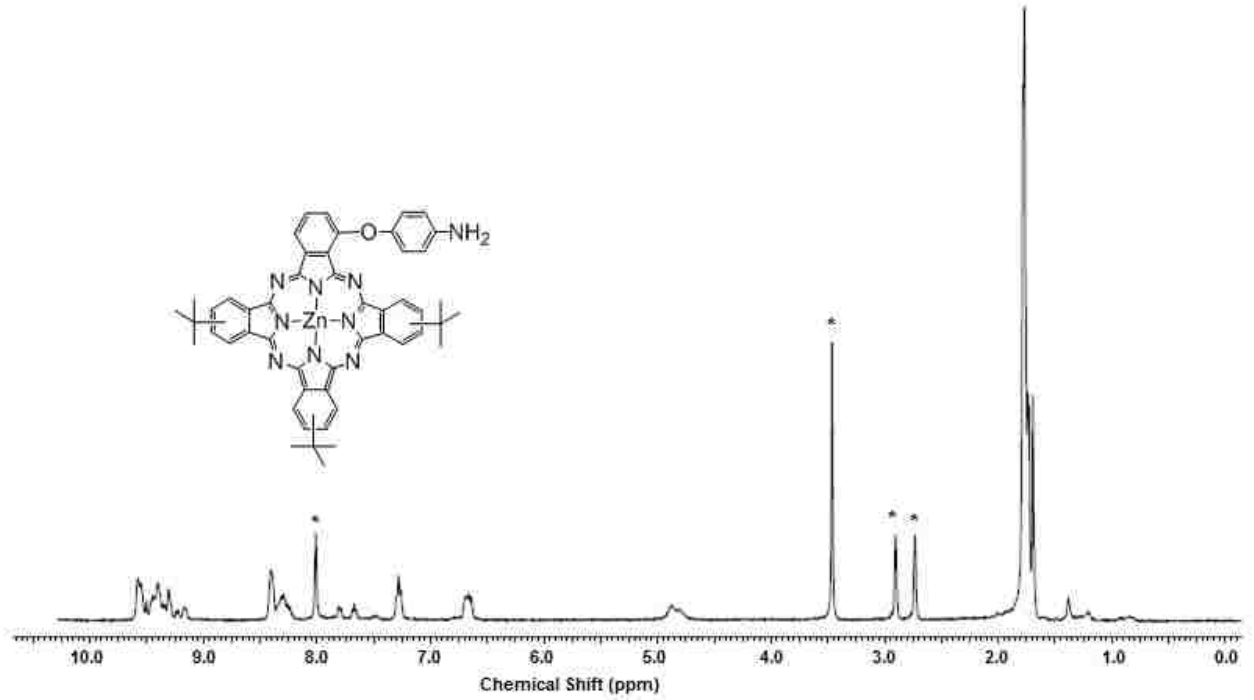

Figure A.2: ^{1}H NMR spectrum of ZnPc **2.4** in d-DMF at 400 MHz (*denotes solvents).

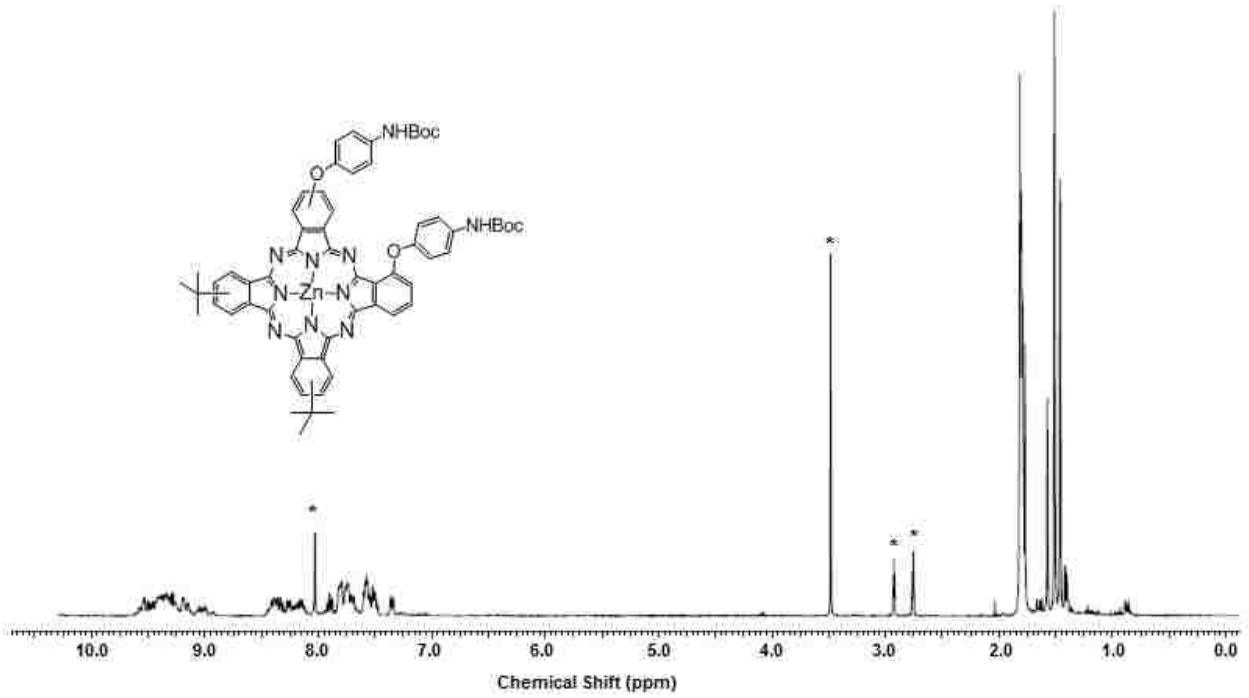

Figure A.3: ^{1}H NMR spectrum of N-Boc protected ZnPc **2.6** in d-DMF at 400 MHz (*denotes solvents).

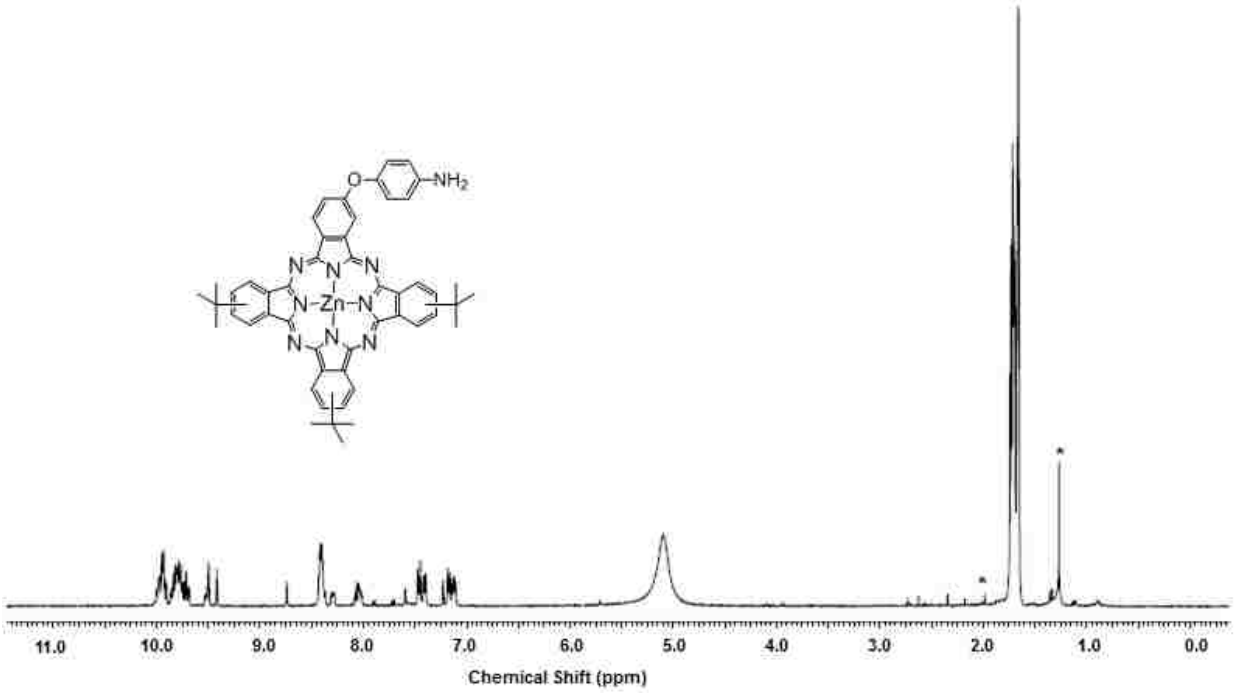

Figure A.4: ^{1}H NMR spectrum of ZnPc **2.11** in d-acetone at 400 MHz (*denotes solvents).

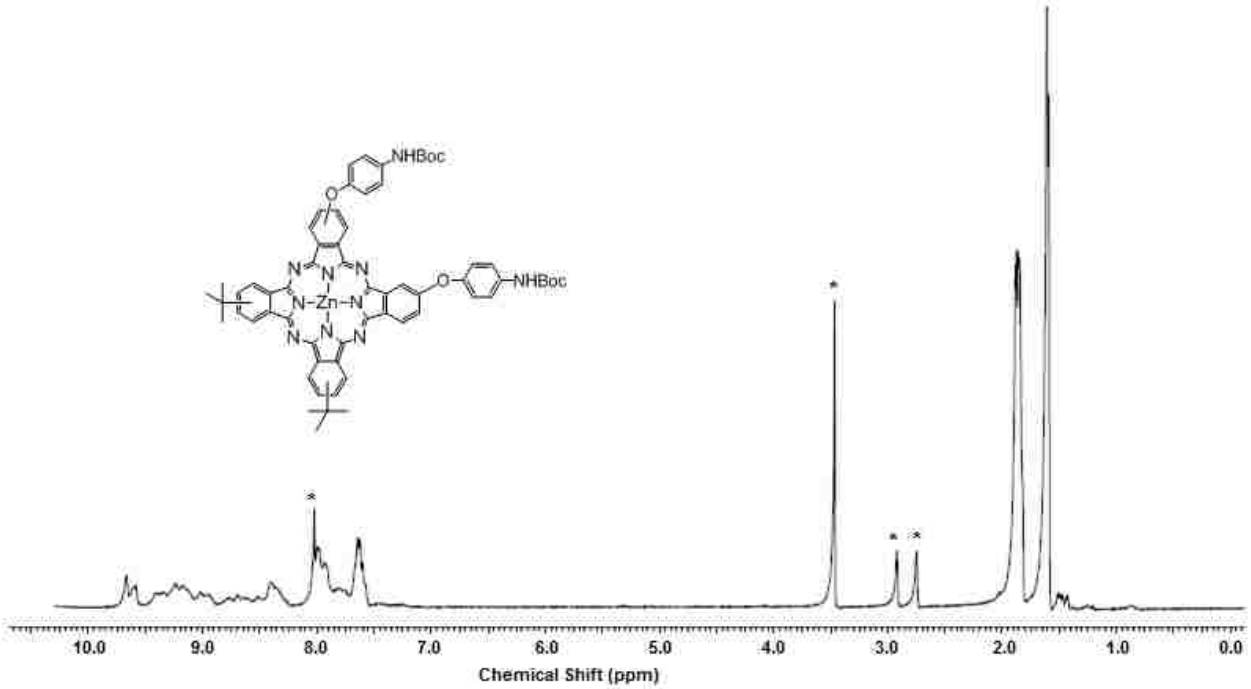

Figure A.5: ^{1}H NMR spectrum of N-Boc protected ZnPc **2.13** in d-DMF at 400 MHz (*denotes solvents).

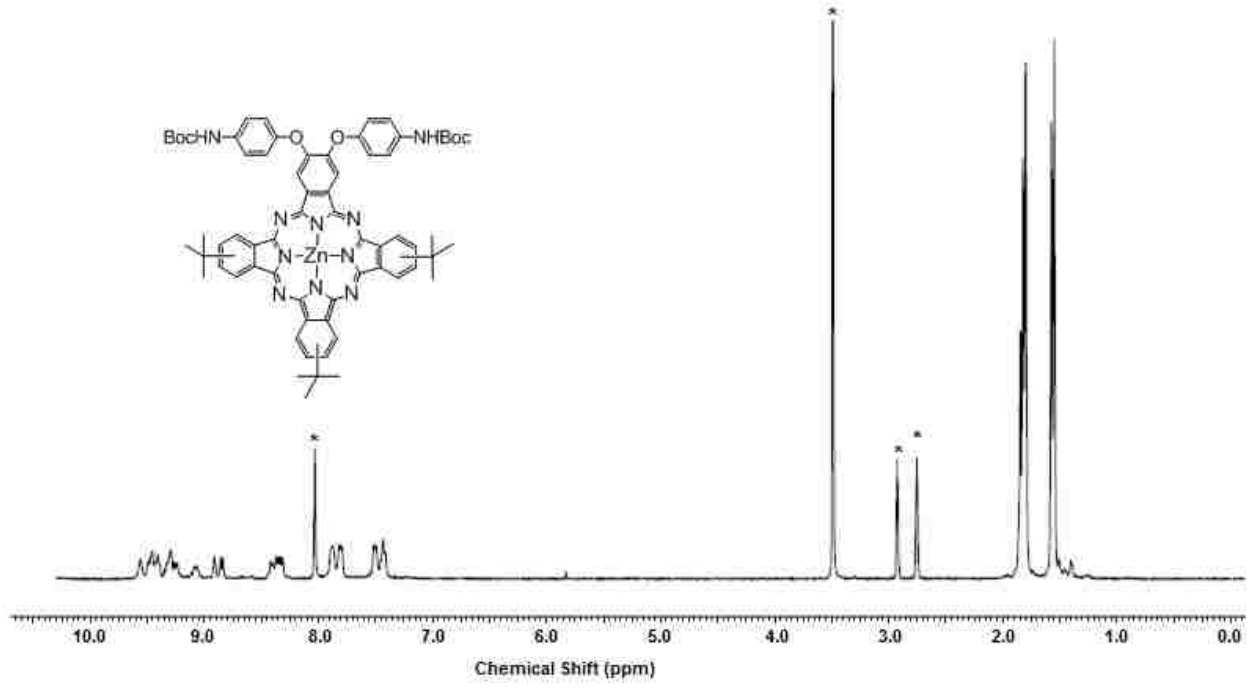

Figure A.6: ^{1}H NMR spectrum of N-Boc protected ZnPc **2.19** in d-DMF at 400 MHz (*denotes solvents).

APPENDIX B: BIOLOGICAL DATA FOR COMPOUNDS IN CHAPTER 3

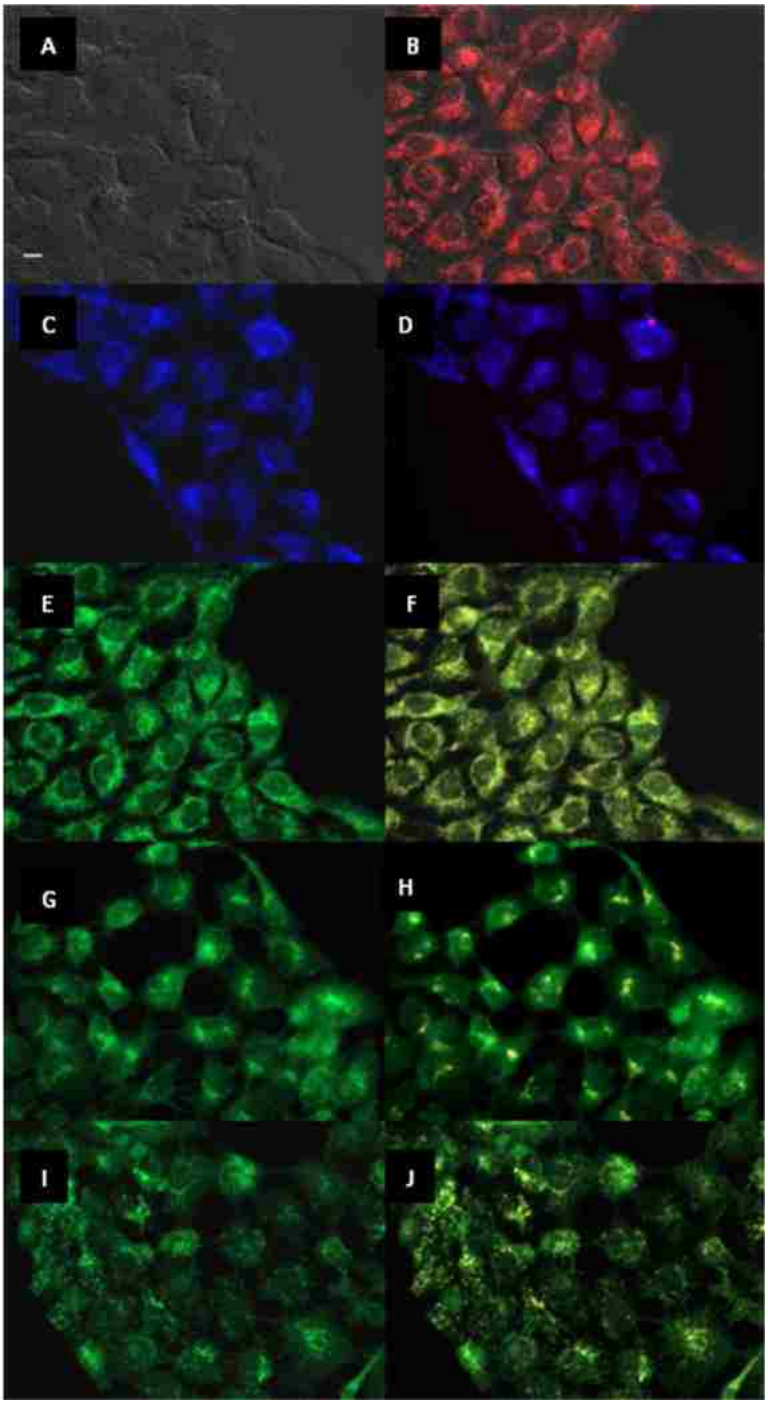

Figure B.1. Subcellular localization of Pc **3.4** in A431 cells at 10 μM for 6 h. (a) Phase contrast, (b) Overlay of **3.4** fluorescence and phase contrast, (c) ER Tracker Blue/White fluorescence, (e) MitoTrack green fluorescence, (g) BoDIPY Ceramide, (i) LysoSensor green fluorescence, and (d, f, h, j) overlays of organelle tracers with **3.4** fluorescence. Scale bar: 10 μm.

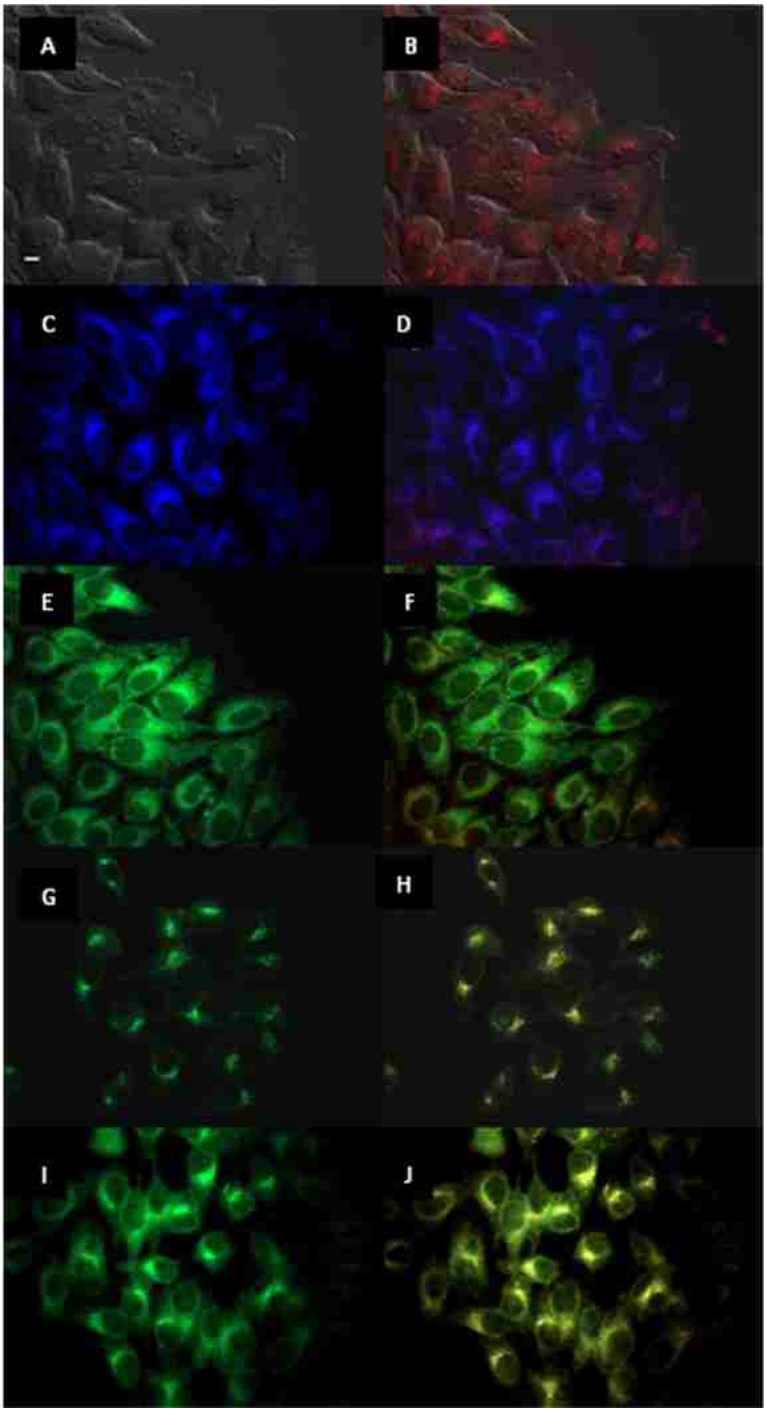

Figure B.2. Subcellular localization of Pc **3.4** in HEp2 cells at 10 μM for 6 h. (a) Phase contrast, (b) Overlay of **3.4** fluorescence and phase contrast, (c) ER Tracker Blue/White fluorescence, (e) MitoTrack green fluorescence, (g) BoDIPY Ceramide, (i) LysoSensor green fluorescence, and (d, f, h, j) overlays of organelle tracers with **3.4** fluorescence. Scale bar: 10 μm.

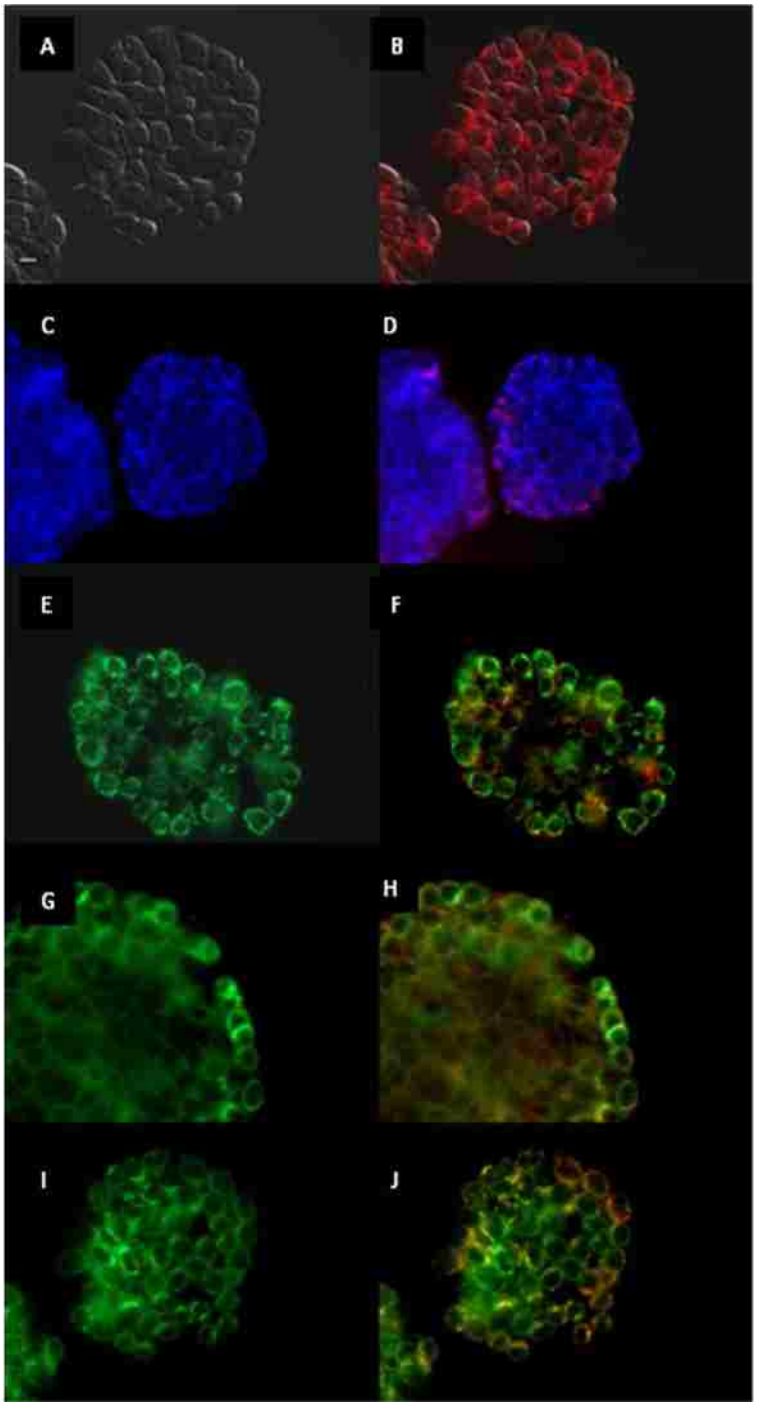

Figure B.3. Subcellular localization of Pc **3.4** in HT-29 cells at 10 μM for 6 h. (a) Phase contrast, (b) Overlay of **3.4** fluorescence and phase contrast, (c) ER Tracker Blue/White fluorescence, (e) MitoTrack green fluorescence, (g) BoDIPY Ceramide, (i) LysoSensor green fluorescence, and (d, f, h, j) overlays of organelle tracers with **3.4** fluorescence. Scale bar: 10 μm.

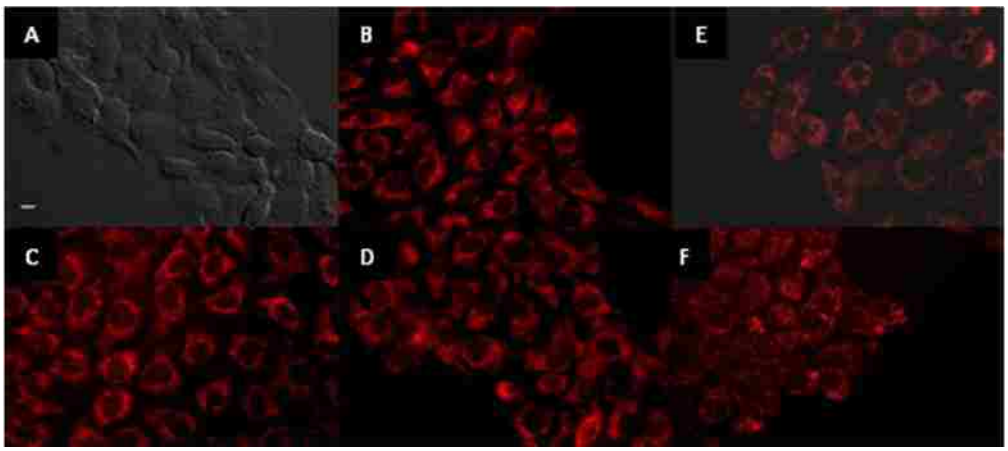

Figure B.4. Subcellular fluorescence of Pcs in A431 cells at 10 µM for 6 h. (a) Phase contrast, (b) Pc **3.4**, (c) Pc **3.9**, (d) Pc **3.6**, (e) Pc **3.5**, (f) Pc **3.11**. Scale bar: 10 µm.

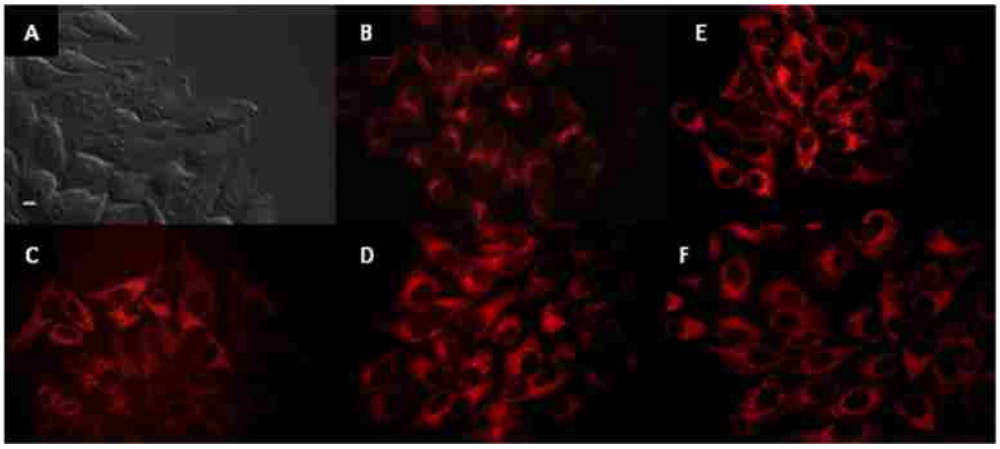

Figure B.5. Subcellular fluorescence of Pcs in HEp2 cells at 10 µM for 6 h. (a) Phase contrast, (b) Pc **3.4**, (c) Pc **3.9**, (d) Pc **3.6**, (e) Pc **3.5**, (f) Pc **3.11**. Scale bar: 10 µm.

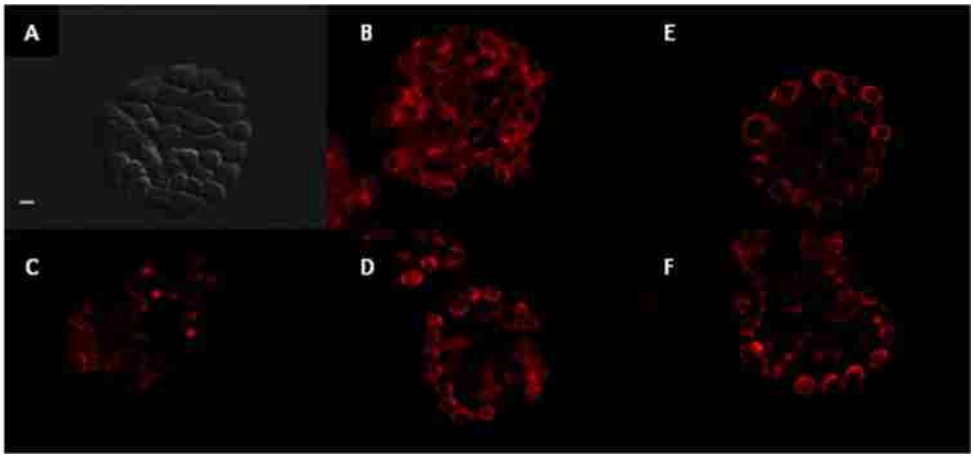

Figure B.6. Subcellular fluorescence of Pcs in HT-29 cells at 10 µM for 6 h. (a) Phase contrast, (b) Pc **3.4**, (c) Pc **3.9**, (d) Pc **3.6**, (e) Pc **3.5**, (f) Pc **3.11**. Scale bar: 10 µm.

APPENDIX C: CHARACTERIZATION DATA FOR COMPOUNDS IN CHAPTER 4

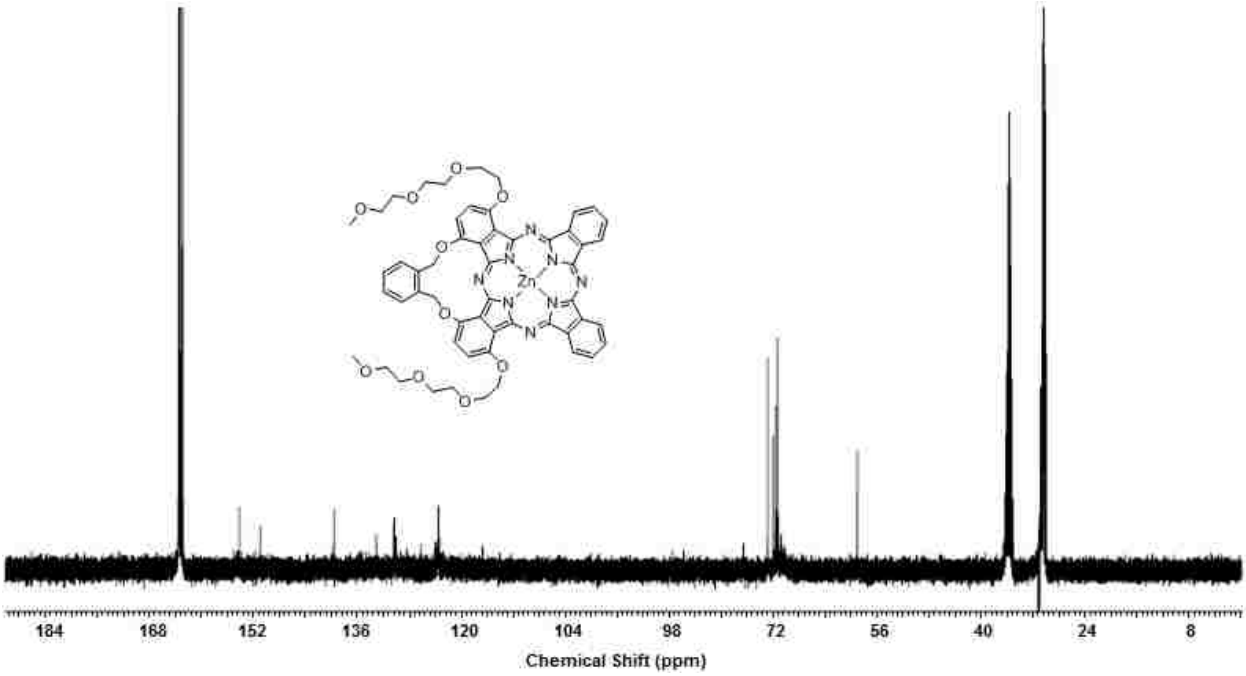

Figure C.1. ^{13}C NMR spectrum of ZnPc **4.10** in d-DMF at 100 MHz (*denotes solvents).

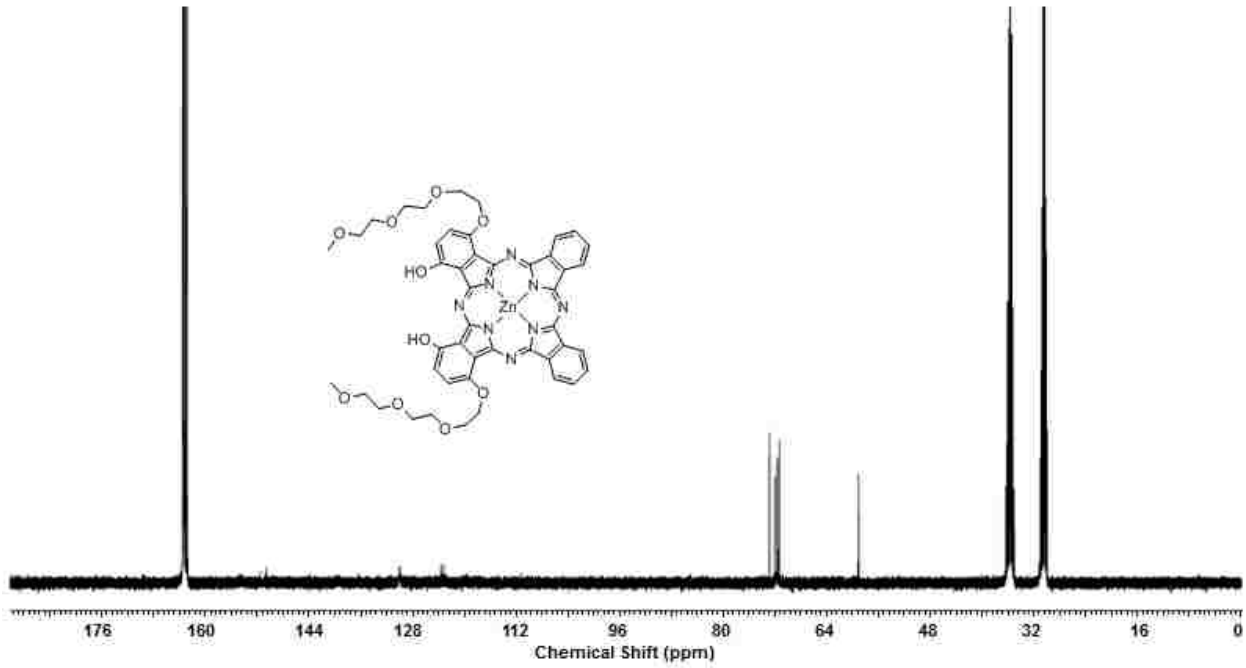

Figure C.2. ^{13}C NMR spectrum of ZnPc **4.12** in d-DMF at 100 MHz (*denotes solvents).

APPENDIX D: CHARACTERIZATION DATA FOR COMPOUNDS IN CHAPTER 5

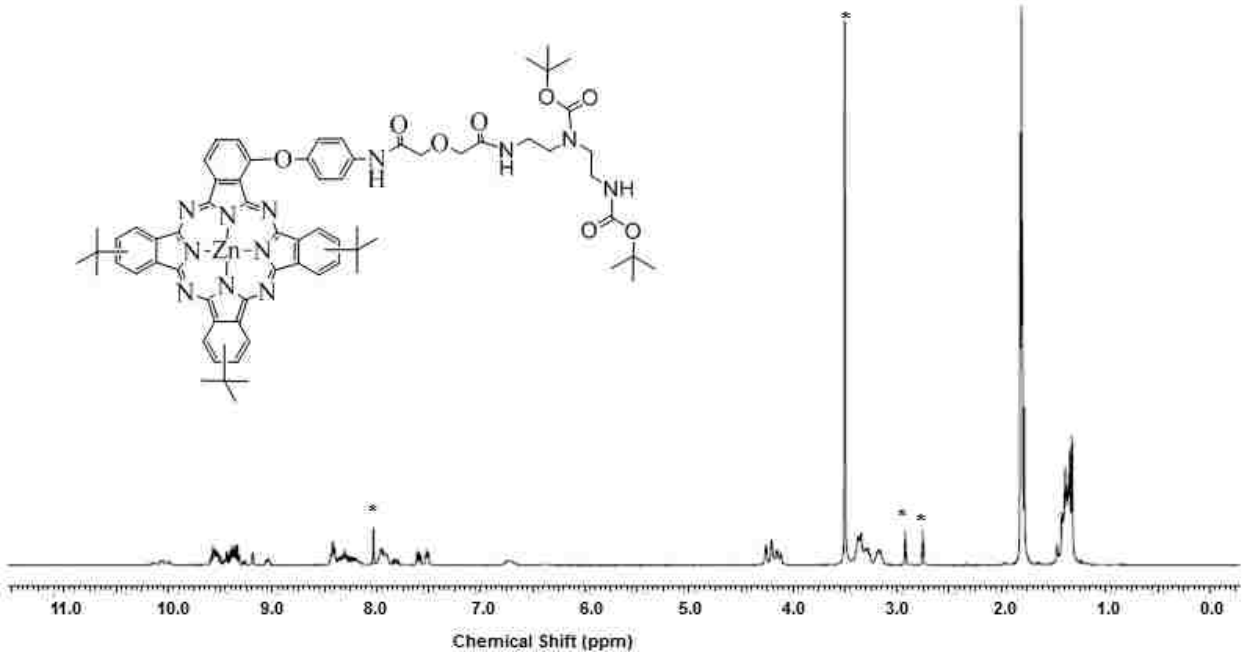

Figure D.1. ^{1}H NMR spectrum of N-Boc protected **5.5** in d-DMF at 400 MHz (*denotes solvents).

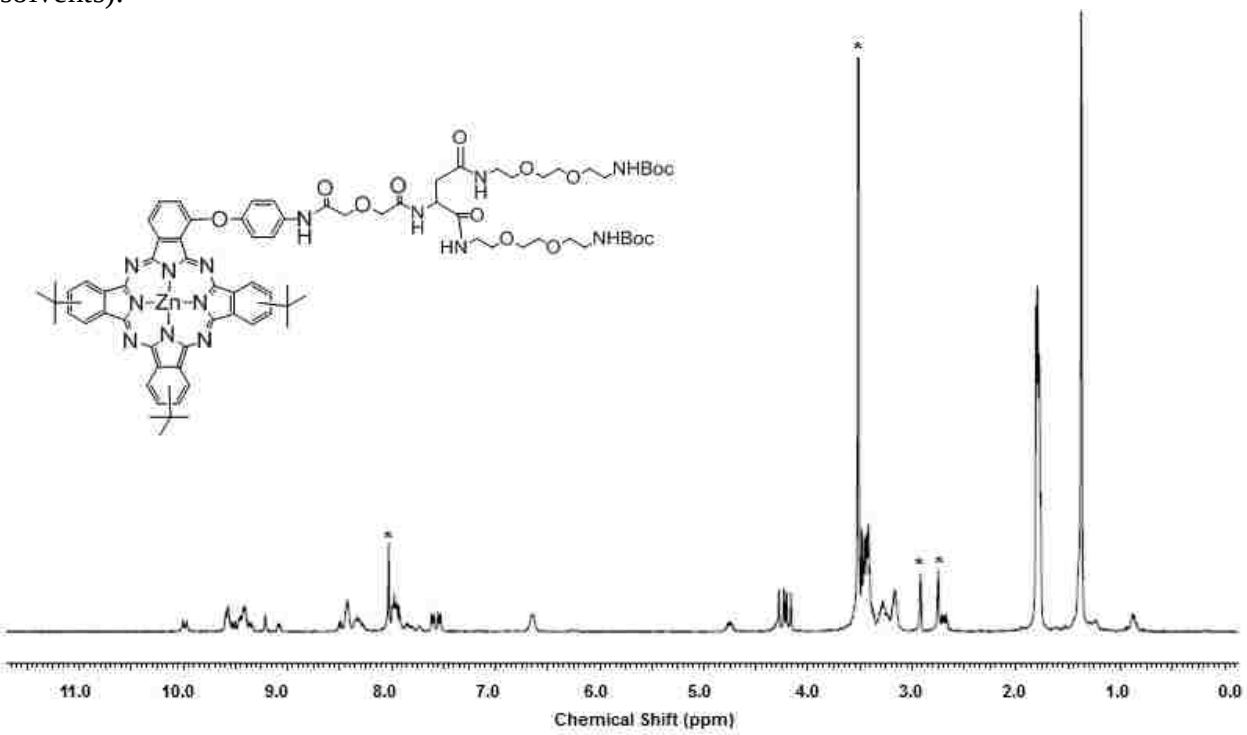

Figure D.2. ^{1}H NMR spectrum of N-Boc protected **5.8** in d-DMF at 400 MHz (*denotes solvents).

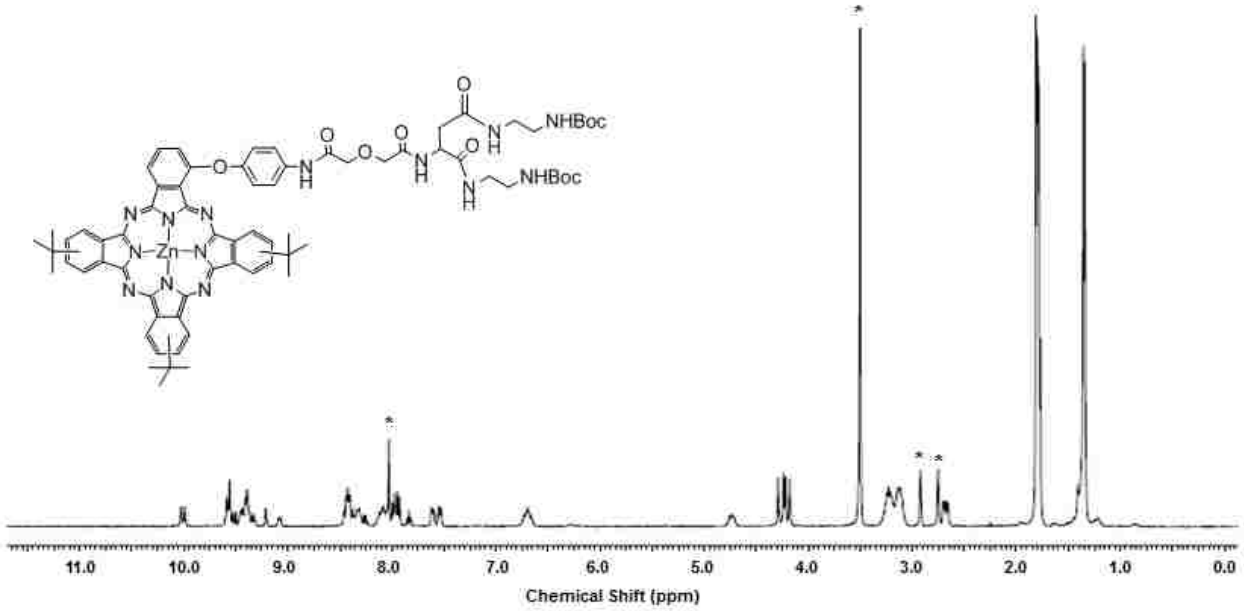

Figure D.3. [1]H NMR spectrum of N-Boc protected **5.10** in d-DMF at 400 MHz (*denotes solvents).

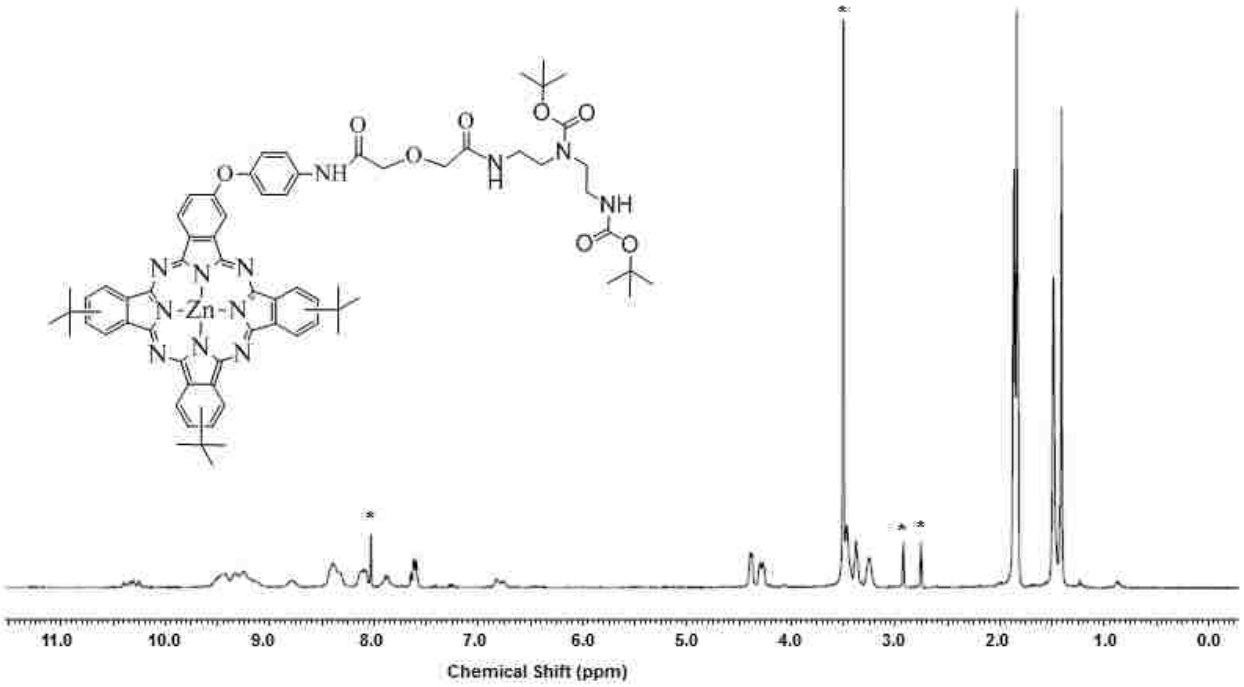

Figure D.4. [1]H NMR spectrum of N-Boc protected **5.16** in d-DMF at 400 MHz (*denotes solvents).

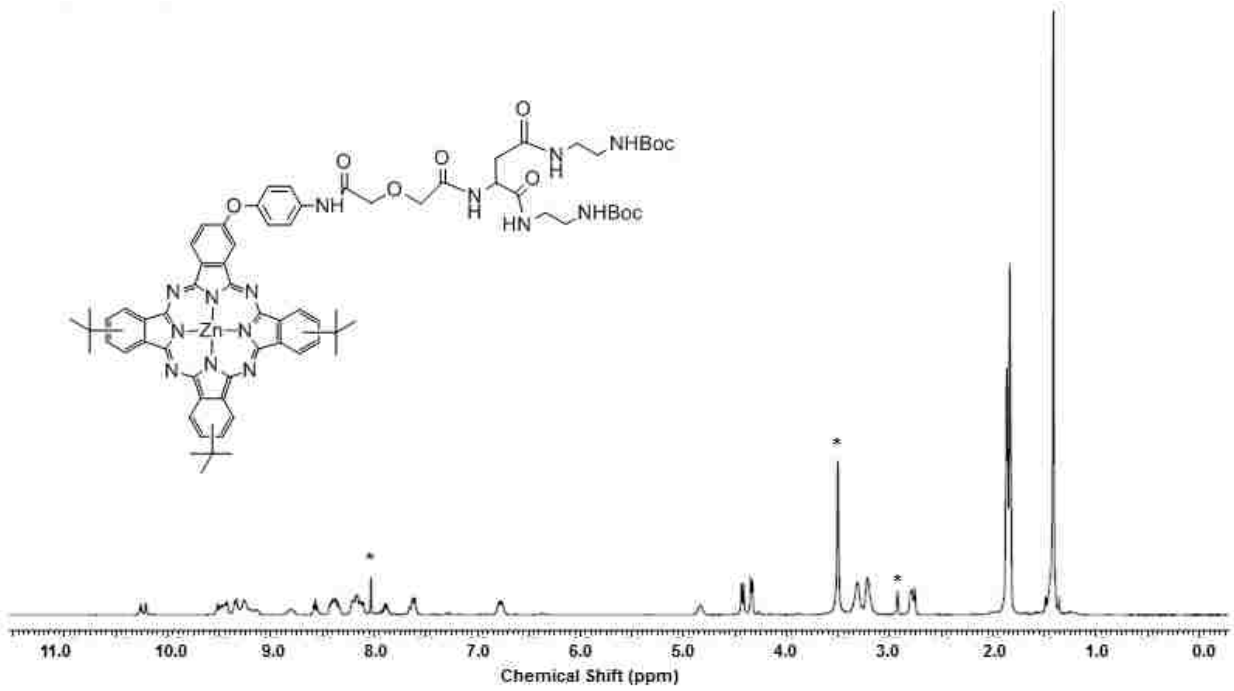

Figure D.5. ^{1}H NMR spectrum of N-Boc protected **5.21** in d-DMF at 400 MHz (*denotes solvents).

APPENDIX E: LETTERS OF PERMISSION

Re: Reprint Permission Inbox x

Print all

Theranostics Publishing Team 3:39 AM (31 minutes ago)

to me

Dear Benson G. Ongarora,

Thanks for your email. Permission is granted to re-use the article in your dissertation with citation and credit of the original source.

Ongarora BG, Hu X, Verberne-Sutton SD, Garno JC, Vicente MGH. Syntheses and Photodynamic Activity of Pegylated Cationic Zn(II)-Phthalocyanines in HEp2 Cells. Theranostics 2012; 2(9):850-870. Available from http://www.thno.org/v02p0850.htm.

Kind regards,
THNO Publishing Team
Theranostics
http://www.thno.org

CONTRACTS-COPYRIGHT (shared) Sep 12

to Benson

Dear Benson

The Royal Society of Chemistry (RSC) hereby grants permission for the use of your paper(s) specified below in the printed and microfilm version of your thesis. You may also make available the PDF version of your paper(s) that the RSC sent to the corresponding author(s) of your paper(s) upon publication of the paper(s) in the following ways: in your thesis via any website that your university may have for the deposition of theses, via your university's Intranet or via your own personal website. We are however unable to grant you permission to include the PDF version of the paper(s) on its own in your institutional repository. The Royal Society of Chemistry is a signatory to the STM Guidelines on Permissions (available on request).

Please note that if the material specified below or any part of it appears with credit or acknowledgement to a third party then you must also secure permission from that third party before reproducing that material.

Please ensure that the thesis states the following:

Reproduced by permission of The Royal Society of Chemistry

and include a link to the paper on the Royal Society of Chemistry's website.

Please ensure that your co-authors are aware that you are including the paper in your thesis.

Regards

Gill Cockhead
Publishing Contracts & Copyright Executive

Gill Cockhead (Mrs), Publishing Contracts & Copyright Executive
Royal Society of Chemistry, Thomas Graham House
Science Park, Milton Road, Cambridge CB4 0WF, UK
Tel +44 (0) 1223 432134, Fax +44 (0) 1223 423623
http://www.rsc.org

Title: Phthalocyanine–Peptide Conjugates for Epidermal Growth Factor Receptor Targeting

Author: Benson G. Ongarora, Krystal R. Fontenot, Xiaoke Hu, Inder Sehgal, Seetharama D. Satyanarayana-Jois, and M. Graça H. Vicente

Publication: Journal of Medicinal Chemistry

Publisher: American Chemical Society

Date: Apr 1, 2012

PERMISSION/LICENSE IS GRANTED FOR YOUR ORDER AT NO CHARGE

This type of permission/license, instead of the standard Terms & Conditions, is sent to you because no fee is being charged for your order. Please note the following:

- Permission is granted for your request in both print and electronic formats, and translations.
- If figures and/or tables were requested, they may be adapted or used in part.
- Please print this page for your records and send a copy of it to your publisher/graduate school.
- Appropriate credit for the requested material should be given as follows: "Reprinted (adapted) with permission from (COMPLETE REFERENCE CITATION). Copyright (YEAR) American Chemical Society." Insert appropriate information in place of the capitalized words.
- One-time permission is granted only for the use specified in your request. No additional uses are granted (such as derivative works or other editions). For any other uses, please submit a new request.

VITA

Benson G. Ongarora was born in Kisii, Kenya, to Mr. Peter Ongarora Omari and Mrs. Margaret Bitutu Ongarora. He attended Geteri Primary School from 1988-1995. He then enrolled at Moi Gesusu – High School for his secondary school education. He attended Moi University – Kenya, from 2001 – 2005, and earned his Bachelors of Science in chemistry in December of 2005. In Fall 2008, he was granted an opportunity to join Graduate School Doctoral program at Louisiana State University (LSU) in the Department of Chemistry. He joined Prof. M. Graça H. Vicente research group in the Spring of 2009. Benson is currently a candidate for the Doctor of Philosophy in organic chemistry, which will be awarded to him during the December 2012 Commencement at LSU, Baton Rouge, Louisiana.